

Posttranslational Oxidative Modification of SOD1 in Neurodegeneration

By

Xueping Chen

A Thesis submitted to the Faculty of Graduate Studies of

The University of Manitoba

In partial fulfillment of the requirements of the degree of

DOCTOR OF PHILOSOPHY

Department of Human Anatomy and Cell Science

University of Manitoba

Winnipeg, Manitoba

Copyright © 2012 by Xueping Chen

Abstract

Converging evidence indicates that SOD1 aggregation is a common feature of mutant SOD1 (mSOD1)-linked FALS, and seems to be directly related to the gain-of-function toxic property. However, the mechanisms of protein aggregation are not fully understood. To study the contribution of modification on cysteine residues in SOD1 aggregation, we systematically examined the redox state of SOD1 cysteine residues in the G37R transgenic mouse at different stages of ALS and under oxidative stress induced by H₂O₂. Our data showed that under normal circumstances, cysteine 111 in SOD1 is free. Under oxidative stress, it is prone to oxidative modification by providing the thiolate anion (S⁻). With the progression of ALS, increased levels of oxidative insults facilitated the oxidation of thiol groups of cysteine residues. Human mutant SOD1 could generate an upper shifted band in SDS-PAGE, which turned out to be a Cys111-peroxidized SOD1 species. We also found that at different stages of ALS, accumulated oxidative stress facilitated the aggregates formation, which were not mediated by disulfide bond. The oxidative modification of cysteine 111 may promote the formation of disulfide bond-independent SOD1 aggregates.

In addition, we investigated the correlation between nitrosative stress and S-nitrosylation of protein disulfide isomerase (PDI) in the mechanism of aggregates formation. Our data showed that up-regulated inducible nitric oxide synthase (iNOS) generated high levels of nitric oxide (NO), which induced S-nitrosylation of PDI with the progression of ALS in the spinal cords of mSOD1 transgenic mice. This correlation was confirmed by treating SH-SY5Y cells with NO donor SNOC to trigger the formation of

S-nitrosylated PDI (SNO-PDI). When mSOD1 was overexpressed in SH-SY5Y cells, iNOS expression was up-regulated, NO generation was increased consequently. Furthermore, both SNO-PDI and mSOD1 aggregates were detected in these cells. Blocking NO generation with NOS inhibitor N-nitro-L-arginine (NNA) attenuated the S-nitrosylation of PDI; the formation of mSOD1 aggregates was inhibited as well. We conclude that NO-mediated S-nitrosylation of PDI is highly linked to the accumulation of mSOD1 aggregates in ALS.

To study the nitrosative stress-induced protein aggregation in cerebral ischemia, we systematically examined the iNOS expression, and consequently NO generation in cultured astrocytes following oxygen glucose deprivation (OGD)/reperfusion. Our data showed that the up-regulation of iNOS expression was highly associated with NO-mediated S-nitrosylation of PDI, and this S-nitrosylation of PDI was correlated with the formation of ubiquitinated-protein aggregates, seeing as the levels of SNO-PDI were parallel to the aggregates formation. Furthermore, pharmacological inhibition of NO generation with iNOS specific inhibitor 1400W significantly inhibited S-nitrosylation of PDI; the formation of ubiquitinated-protein aggregates was suppressed by 1400W as well in cultured astrocytes following OGD/reperfusion. Interestingly, these aggregates were co-localized with SOD1. We conclude that S-nitrosylation of PDI can contribute to the SOD1-linked protein ubiquitination and aggregation in cerebral ischemia.

Acknowledgements

There are many people I would like to thank for their support and guidance over the past few years. First and foremost, I have to thank my parents, Dami Chen and Liangyu Mao. Without their patience, understanding and extreme sacrifice, this thesis would not have been possible. Their love is the source of my strength. I would like to take the chance to tell them how much their support and encouragement meant to me, and with their love, I am forever grateful and blessed.

To my ex-husband, Changming, I extend my thanks for what he has brought to my life. During my PhD training, we were going through a lot of happiness and sadness. We got married and then divorced. He taught me what life should be.

I would like to thank my supervisor, Dr Jiming Kong for his full patience and unconditional support. Within the research field, he helped me build knowledge and essential skills in research and teaching; outside the lab, he treated me like a family member, I feel emotionally supported in dealing with difficulties. He is truly an exceptional scientist, teacher, mentor, and friend to me.

I am truly fortunate to have an incredible committee. To Dr. Maria E. Vrontakis, Dr. Fiona Parkinson and Dr. Keding Cheng, I also extend my deepest gratitude. I am tremendously grateful for the guidance and support from them. Without their efforts and kindness, this work would not have been done and I certainly would not have been in the position to do it.

I greatly appreciated the help from other professors; special thanks go to Dr. Thomas Klönisch, the departmental head, for his leadership and enthusiasm in supporting the students' wellbeing, Dr. Xin-min Li for his insightful and provocative questions, which helped me rethink the ways of doing things, and Dr Xiaozhong Qiu for his patience in teaching me laboratory techniques.

I want to thank all the professors of the Anatomy Department including, Dr. Vriend, Dr. Hugo Bergen, Dr. Hombach-Klönisch, Dr. Hassan Marzban — their dedication and professionalism in teaching anatomy inspired me so much.

Many thanks go out to all my friends in the lab and department — Lin, Teng, Jiequn, Leilanie, Chen, Jacqueline, Kelly, Nadin, Jennifer, Ruoyang, Junhui and Handi. They did so many things for me, from solving technical issues to providing personal support. They have enriched my life and made these past few years an enjoyable time of my life that I would truly cherish.

Last, but certainly not least, I want to thank all the people in Department of Human Anatomy and Cell Science. It was a wonderful place to work and they are very dedicated people. I gained so much from it.

Dedication

For my parents, who offered me unconditional love and support throughout the course of this thesis.

Table of Content

Abstract	i
Acknowledgements	iii
Dedication	v
List of Figures	xii
List of Tables	xiv
Abbreviations	xv
Chapter 1. Introduction	1
1.1 Amyotrophic lateral sclerosis (ALS)	1
1.1.1 Clinical Features	2
1.1.2 Pathogenic mechanisms	3
1.1.2.a Genetic factors	4
1.1.2.b Oxidative stress	7
1.1.2.c Protein misfolding and aggregation	9
1.1.2.d ER stress	10
1.1.2.e Mitochondrial dysfunction	11
1.1.2.f Non-cell autonomous effect and neuroinflammation	13
1.1.2.g Excitotoxicity	15
1.1.2.h Axonal transport defects	17
1.1.2.i Dysregulated RNA processing	18
1.1.3 Animal models of ALS	19
1.1.3.a SOD1 mutant transgenic mouse models	19
1.1.3.b SOD1 wild-type transgenic mouse models	20
1.1.4 Vulnerability of motor neurons in ALS	20
1.1.5 Emerging targets in ALS therapeutics	21
1.1.5.a Anti-glutamatergic agents	21

1.1.5.b Drugs targeting protein misfolding and accumulation.....	22
1.1.5.c RNA targets.....	22
1.1.5.d Mitochondrial targets.....	22
1.1.5.e Neurotrophic factors.....	23
1.1.5.f Stem-cell therapy.....	23
1.1.5.g Muscle-directed therapies.....	24
1.2 Copper/zinc superoxide dismutase (SOD1).....	25
1.2.1 Function of SOD1.....	25
1.2.2 Structure of SOD1.....	25
1.2.3 Genetic variants of SOD1 in ALS.....	26
1.2.4 SOD1 gene expression in ALS.....	27
1.2.5 Mutant SOD1 in ALS-a toxic gain of function.....	27
1.2.6 Subcellular distribution of mSOD1.....	28
1.2.6.a mSOD1 in mitochondria.....	28
1.2.6.b mSOD1 in ER.....	29
1.2.6.c mSOD1 in Golgi apparatus and secretory pathway.....	29
1.2.7 Extracellular mSOD1 in the non-cell-autonomous pathology.....	30
1.2.8 SOD1 aggregation-a toxic property.....	30
1.2.9 Formation of SOD1 aggregates.....	32
1.2.9.a SOD1 mutations facilitate loss of metals.....	32
1.2.9.b SOD1 mutations facilitate partial unfolding or monomerization of apo-SOD1	33
1.2.9.c SOD1 mutations increase the susceptibility to disulfide reduction.....	34
1.2.9.d SOD1 can form aggregates with or without intermolecular disulfide bonds.....	34
1.2.10 Oxidative stress in SOD1 aggregates formation.....	36
1.2.11 Oxidative modification of Cys111 in SOD1 aggregates.....	37
1.2.12 Oxidative modification of wild-type SOD1 in aggregates formation.....	39
1.3 Protein disulfide isomerase (PDI).....	40
1.3.1 Structure of PDI.....	41
1.3.2 Function of PDI.....	42
1.3.3 Subcellular distribution of PDI.....	43

1.3.4 PDI in the neurodegenerative diseases	44
1.3.5 ER stress and the UPR in ALS.....	44
1.3.6 PDI in ALS.....	47
1.3.7 NO-mediated nitrosative stress in ALS.....	48
1.3.8 S-nitrosylation of PDI in ALS.....	49
1.4 Cerebral ischemia	51
1.4.1 The involvement of iNOS in cerebral ischemia.....	51
1.4.2 The involvement of NO in cerebral ischemia	53
1.4.3 The involvement of PDI in ischemic injury.....	54
1.4.4 The involvement of protein aggregation in cerebral ischemia.....	56
Chapter 2. Hypotheses and Aims.....	58
2.1 Hypotheses	58
Chapter 3. Oxidative modification of cysteine 111 promotes disulfide bond-independent aggregation of SOD1	62
3.1 Introduction	62
3.2 Materials and Methods	64
3.2.1 Construction of Expression Vectors.....	64
3.2.2 Cell Culture, Transfection, and Antibodies.....	65
3.2.3 Transgenic Mice.....	66
3.2.4 Detection of Accessible SOD1 Cysteines in Tissue and Cell Lysates	67
3.2.5 Chemical Cross-linking	67
3.2.6 Western Blotting Analysis.....	68
3.2.7 Statistical analysis	68
3.3 Results	69
3.3.1 Cysteine 111 residue of SOD1 existed in sulfhydryl state (-SH) under normal circumstance.	69
3.3.2 Human mutant SOD1 cysteine residues exhibited decreased accessibility to MalPEG modification accompanied with appearance of an additional upper band under increased oxidative stress.....	70
3.3.4 Cys111-peroxidized SOD1 was increased with the progression of the disease.....	71

3.3.5 Oxidative stress induced by H ₂ O ₂ promoted the formation of disulfide bond-independent SOD1 multimers both in wild-type and G37R transgenic mice, which increased with disease progression	72
3.3.6 C111S mutation inhibited the formation of aggregation in mutant SOD1.	73
3.4 Discussion	73

Chapter 4. S-Nitrosylated Protein Disulphide Isomerase Links

Mutant SOD1 aggregates in Amyotrophic Lateral Sclerosis.. 87

4.1 Introduction	87
4.2 Materials and methods.....	90
4.2.1 Transgenic Mice.....	90
4.2.2 Plasmids, Cell Culture and Transfection.....	92
4.2.3 Inclusion quantification and Subcellular fractionation.....	92
4.2.4 Measurement of NO - level.....	93
4.2.5 Biotin-switch assay for detection of S-nitrosylated PDI.....	94
4.2.6 Preparation of S-Nitrosocysteine (SNOC) and N-nitro-L-arginine (NNA).....	94
4.2.7 Immunoblotting.....	95
4.2.8 Statistics	95
4.3 Results	96
4.3.1 iNOS protein levels were up-regulated in the spinal cords of mutant SOD1 transgenic mice and increased with disease progression.	96
4.3.2 NO concentrations were increased in the spinal cords of mutant SOD1 transgenic mice and the NO production was up-regulated during disease progression.....	97
4.3.3 PDI was increased and S-nitrosylated in the spinal cords of mutant transgenic mice, and up-regulation and S-nitrosylation of PDI developed as disease progresses	97
4.3.4 Mutant SOD1 induced up-regulation of iNOS expression and NO generation.	99
4.3.5 Exposure of SH-SY5Y cells to SNOC triggered the SNO-PDI formation. Expression of mutant SOD1 ^{G93A} in SH-SY5Y cells induced the SNO-PDI formation, which was blocked by the NOS inhibitor NNA.....	100
4.3.6 SNOC promoted and NNA suppressed the mutant SOD1 aggregates formation in	

transfected SH-SY5Y cells	101
4.4 Discussion	102
Chapter 5. SOD1-linked ubiquitination and aggregation in astrocytes following OGD/reperfusion: a role of NO-mediated S-nitrosylation of protein disulfide isomerase in hypoxic/ischemic injury.....	120
5.1 Introduction	120
5.2 Materials and methods.....	123
5.2.1 Primary astrocyte culture	123
5.2.2 OGD/reperfusion and 1400W treatment.....	124
5.2.3 Measurement of NO level.....	124
5.2.4 Western blot and immunoprecipitation	125
5.2.5 Biotin-switch assay for detection of SNO-PDI.....	126
5.2.6 Subcellular fractionation.....	126
5.2.7 Double-immunofluorescence staining of ubiquitin and SOD1.....	127
5.2.8 Statistics	128
5.3 Results	128
5.3.1 OGD/reperfusion induces NO formation and iNOS protein expression	128
5.3.2 PDI and SOD1 are up-regulated after OGD/reperfusion treatment, and they were binding to each other.....	129
5.3.3 PDI is S-nitrosylated in astrocytes following OGD/reperfusion; this S-nitrosylation of PDI is blocked by iNOS inhibitor 1400W.....	130
5.3.4 OGD/reperfusion triggers formation of detergent/salt-insoluble ubiquitinated-protein aggregates, which is blocked by iNOS inhibitor 1400W.....	132
5.3.5 OGD/reperfusion induces re-distribution of ubiquitinated-protein, and co-localization of ubiquitin with SOD1 protein.....	133
5.4 Discussion	134
Chapter 6. Discussion and Significance	147
6.1 Oxidative modification of SOD1 in protein aggregate formation in ALS	147

6.2 S-nitrosylated modification of PDI in protein aggregates formation in ALS.....	151
6.3 S-nitrosylated modification of PDI in ubiquitinated-protein aggregates formation in cerebral ischemia	154
6.4 Limitations and strengths	160
6.4.1 Limitations	160
6.4.2 Strengths	162
6.5 Conclusions	164
6.6 Future directions.....	165
Reference	167

List of Figures

Fig. 3.1 MalPEG modification is cysteine 111 specific.....	79
Fig. 3.2 Oxidation by H ₂ O ₂ decreased the MalPEG modification and increased Cys 111-peroxidation in G37R spinal cord extract (n = 3).	80
Fig. 3.3 MalPEG modification of G37R transgenic mice spinal cord decreased, but reciprocally the Cys111-peroxidation increased dependent with ALS progress (n = 3).	82
Fig. 3.4 Oxidation by H ₂ O ₂ increased SOD1 multimers in G37R transgenic mice spinal cord extract, and the SOD1 multimers was increased dependent with ALS progress (n = 3).	84
Fig. 4.1 iNOS protein levels in the spinal cords of non-transgenic and SOD1 transgenic mice	111
Fig. 4.2 The changes of NO levels in the spinal cords of non-transgenic and SOD1 transgenic mice	113
Fig. 4.3 Total PDI and SNO-PDI levels in the spinal cords of non-transgenic and SOD1 transgenic mice.....	114
Fig. 0.4 The iNOS expression and NO generation in SH-SY5Y cells expressing SOD1wt or mutant SOD1G93A.....	117
Fig. 0.5 Exogenous NO donor and mutant SOD1G93A expression induce S-nitrosylation of PDI in SH-SY5Y cells.....	119
Fig. 0.6 The effect of SNOC and NNA on the SOD1 aggregates formation in transfected SH-SY5Y cells.....	120
Fig. 5.1 Effect of OGD/reperfusion treatment on NO production and iNOS protein production.	141
Fig. 5.2 Expressions of PDI and SOD1 protein and their correlations in cultured astrocytes following OGD/reperfusion.....	142
Fig. 5.3 S-nitrosylation of PDI in cultured astrocytes following OGD/reperfusion	143

Fig. 5.4 The formation of detergent/salt-insoluble ubiquitinated-protein aggregates following OGD/reperfusion, and the inhibition effect of 1400W.....	145
Fig. 5.5 The distribution of ubiquitin-conjugated proteins and localization of ubiquitin and SOD1 in cultured astrocytes following OGD/reperfusion by using immunostaining.....	146

List of Tables

Table 1.1 Genetic causes of FALS.....	6
---------------------------------------	---

Abbreviations

ATP	Adenosine triphosphate
AD	Alzheimer's disease
A β	Amyloid- β
ALS	Amyotrophic Lateral Sclerosis
ANG	Angiogenin
ARE	Antioxidant response element
ASK1	Apoptosis signal-regulating kinase 1
BACE1	Beta-site APP-cleaving enzyme 1
BBB	Blood-brain barrier
BDNF	Brain-derived neurotrophic factor
<i>C. elegans</i>	<i>Caenorhabditis elegans</i>
CNS	Central nervous system
CSF	Cerebrospinal fluid
ChgA	Chromagranin A
cGMP	Cyclic guanosine monophosphate
CaBP	Cytosolic calcium-binding proteins
DSG	Disuccinimidyl glutarate
DB	Double-blind
DS	Down syndrome
ER	Endoplasmic reticulum
ERAD	Endoplasmic-reticulum-associated protein degradation

Ecs	Endothelial cells
eNOS	Endothelial NOS
ERMCC	ER mitochondria calcium cycle
Ero1	ER oxidoreductin 1
EAAT2	Excitatory amino acid transporter 2
ERK1/2	extracellular signal-regulated kinase 1/2
FALS	Familial Amyotrophic Lateral Sclerosis
FUS	Fusion in sarcoma
Grp78	Glucose-related protein 78
GRX2	Glutaredoxin 2
GAPDH	Glyceraldehyde 3-phosphate dehydrogenas
HSF1	Heat shock factor protein1
HSPs	Heat shock proteins
HMW	High molecular weight
HIF-1 α	Hypoxia-inducible factor-1 α
Bip/Grp78	Immunoglobulin heavy chain binding protein/glucose-regulated protein 78
iNOS	Inducible NOS
IP3R	Inositol 1,4,5-trsphosphate receptor
IRE1	Inositol-requiring kinase-1
IGF-1	Insulin-like growth factor 1
IL-1 β	Interleukin-1 β
Il-6	Interleukin-6
IMS	Intermembrane space

JNK	Jun N-terminal Kinase
LPS	Lipopolysaccharide
LUM	Lower motor neuron
MMP-9	Matrix metalloproteinase 9
MGF	Mechanogrowth factor
MMTS	Methyl methane thiosulphonate
miR	MicroRNA
MCAO	Middle cerebral artery occlusion
MalPEG	Mono-methyl polyethylene glycol 5'000 2-maleimidoethyl ether
mSOD1	Mutant SOD1
NKCC1	Na ⁺ -K ⁺ -Cl ⁻ cotransporter isoform 1
NF	Neurofilaments
nNOS	Neuronal NOS
NGF	Neurotrophic growth factor
NO	Nitric oxide
NMDA	N-methyl-D-aspartate
NOS	NO synthase
NRF-2	Nuclear factor-erythroid 2 p45-related factor 2
OPTN	Optineurin
OGD	Oxygen and glucose deprivation
PERK	Pancreatic ER kinase
PDI	Parkinson's disease

PTEN	Phosphatase and tensin homolog deleted on chromosome 10
PLS	Primary lateral sclerosis
PMA	Progressive muscular atrophy
PDI	Protein-disulfide isomerase
Rac1	Ras-related C3 botulinum toxin substrate 1
ROS	Reactive oxygen species
sGC	Soluble guanylate cyclase
SALS	Sporadic Amyotrophic Lateral Sclerosis
SOD1	Superoxide Dismutase-1
TARDBP	TAR DNA binding protein
TCEP	Tris (2-carboxyethyl) phosphine
TNF- α	Tumor Necrosis Factor- α
Trk	Tyrosine kinase receptor
UPS	Ubiquitin-proteasome system
UPR	Unfolding protein response
UMN	Upper motor neuron
VEGF	Vascular endothelial growth factor
VAPB	Vesicle-associated membrane protein/synaptobrevin-associated protein B
VDAC1	Voltage-dependent anion channel 1
AMPA	α -amino-3-hydroxy-5-methyl-4-isoxazolepropionic acid

Chapter 1. Introduction

1.1 Amyotrophic lateral sclerosis (ALS)

ALS is a rapidly progressive and fatal neurodegenerative disease that mainly affects pyramidal upper motor neurons in the motor cortex and lower motor neurons in the brainstem and spinal cord. This leads to a loss of control of voluntary muscle movement and increased muscular paralysis; and this progressive failure of neuromuscular system usually culminates in death from respiratory failure. Most of the ALS cases are sporadic (SALS). Only 5-10% are familial (FALS), with a Mendelian pattern of inheritance. Approximately 2.16 per 100,000 individuals have ALS in Western nations [1]. There are a few clusters of increased incidence, such as in the Kii peninsula and Guam. The clinical features of ALS are reflected by the name of the disease, “Amyotrophic” denotes the atrophy of muscle fibres and loss of muscle mass; “Lateral” refers to the lateral and anterior corticospinal tracts that run down both sides of the spinal cord; and “Sclerosis” refers to the hardening of the nerve tracts and the scar tissue that remains following nerve degeneration. The pathogenesis of the disease is not fully understood. Until very recently, it was widely accepted that ALS resulted from a complex interaction of endogenous factors (mostly genetic predisposition and age) and exogenous factors (lifestyle/diet and environmental exposures). Now, the most plausible mechanisms are thought to be genetic factors, oxidative stress, protein aggregation, endoplasmic reticulum (ER) stress, mitochondrial dysfunction, non-cell autonomous effects, excitotoxicity, as well as impairments in axonal transport and RNA processing.

1.1.1 Clinical Features

The hallmark of clinical manifestations of ALS is the combination of upper and lower motor neuron signs and symptoms. There are four main presentations of ALS, which include: (1) limb-onset ALS with a combination of upper and lower motor neuron (UMN and LMN) signs in the limbs; (2) bulbar-onset ALS, manifesting with speech and swallowing difficulties, and developing limb features later in the course of the disease; (3) the primary lateral sclerosis (PLS), which is a pure UMN syndrome, with no LMN features; and (4) progressive muscular atrophy (PMA), which presents with pure LMN involvement, in the absence of UMN and bulbar features. About 70% percent of patients have the limb-onset, spinal form of the disease. Specifically, the presentations of UMN disturbance involving the limbs include spasticity, weakness, and brisk deep tendon reflexes, while the LMN limb disturbances include fasciculations, wasting, and weakness. Normally, the first symptoms of the limb-onset form of ALS form are focal muscle weakness in either the upper limbs (cervical-onset) or lower limbs (lumbar-onset). The muscle atrophy in hands, forearms, shoulders or proximal thigh or distal foot can be identified in early body examinations. The onset is usually asymmetrical, though the other limbs will progressively be involved, and symptoms will develop into spasticity affecting both the gait and dexterity of the individual. Mostly, the spinal ALS patients will progress to bulbar symptoms and respiratory failure within 3-5 years. About 25% of patients have bulbar onset, which is more common in women and older individuals [2,3]. Specifically, bulbar UMN dysfunction leads to spastic dysarthria, characterized by slow, laboured, and distorted speech, often with a nasal quality, and emotional lability, characterized by uncontrolled laughing or crying [4]. The jaw jerk and gag reflexes can

be pathologically brisk. Bulbar LMN dysfunction results in tongue wasting, weakness, and fasciculations, accompanied by flaccid dysarthria and dysphagia. The lower part of face becomes weakened and patients have difficulties in closing the lips, and this also contributes to excessive drooling. Mostly, these patients will develop limb-weakening symptoms by 1-2 years after the initial onset and die from respiratory failure with 2-3 years. The progress of bulbar-onset form is slightly quicker than the spinal-onset form. About 5% of patients have initial trunk or respiratory involvement, subsequent spreading to involve other regions [5,6].

ALS was traditionally considered to be a pure motor disorder. This concept is now obsolete. It is now considered to be a multisystem neurodegenerative disease. Evidence has suggested that the sensory and spino-cerebellar pathways are involved, as well as neuronal groups within the substantia nigra and the hippocampal dentate granule layers. In addition, pathological findings suggest that sympathetic and parasympathetic neurones, Onuf's nucleus, peripheral sensory nerves and oculomotor nuclei are also involved [7]. However, for the majority of patients, the motor neuron systems tend to be affected earliest and most severely. Cognitive dysfunction, including subtle subclinical cognitive defects and frontal lobe dysfunction, can be identified in up to half of ALS patients with detailed neuropsychological testing [8,9].

1.1.2 Pathogenic mechanisms

ALS is a heterogeneous disease, in which a variety of relatively distinct initiating factors are linked to the clinical manifestations. A major breakthrough in ALS research came in 1993, with the discovery that approximately 10-20% of the FALS were caused

by the mutations in *SOD1* gene. Up until recently, over 150 mutations spreading throughout the gene have been identified, and the disease-linked mutant SOD1 proteins promote motor neurons degeneration through a toxic gain of function. The first SOD1 rodent model was created in 1994; these mice develop hindlimb paralysis and motor neuronal degeneration, so they provide invaluable tools for studying the molecular mechanisms of ALS. Taken together, ALS is a multifactorial disease, and some or perhaps all, of the initiating factors will trigger a common cascade of downstream processes, finally resulting in neuronal dysfunction.

1.1.2.a Genetic factors

Approximately 90-95% of ALS cases are sporadic, while 5-10% of ALS cases are familial and usually of autosomal dominant inheritance [10]. Intensive genetic approaches to FALS have successfully identified diverse ALS-causing genes (Table 1). Mutations to these genes are applicable not only to the minority of cases that carry FALS, but also to SALS. The involvement of genetic factors in pathogenesis of SALS implies that genetic contribution is particularly important to the mechanisms of ALS. Of the known genes, mutations in *SOD1* (encodes for superoxide dismutase-1) [11], *TARDBP* [12,13,14,15] (encodes for TAR DNA binding protein), *FUS* [16] (encoding fusion in sarcoma), *ANG* [17] (encodes angiogenin, ribonuclease, RNase A family) and *OPTN* [18] (encodes optineurin) cause a typical clinical ALS phenotype. Mutations in *SOD1* uniformly cause toxicity in cells not by loss but rather by gain of function. TDP43 and FUS are both multifunctional proteins with striking structural and functional similarities. They contain RNA/DNA-binding motifs, and their potential actions include

transcriptional regulation, mRNA processing and micro RNA biogenesis. Mutations in *SOD1* account for 20% of FALS and 5% of apparently sporadic ALS, whereas mutations in *TARDBP* (5%), *FUS* (5%), and *ANG* are less common [19]. Most recently, an expansion of the GGGGCC hexanucleotide repeat in the non-coding of C9ORF72 was reported to account for nearly 50% of FALS cases in Finland, more than one-third of FALS in other European populations. This lesion is also the strongest genetic risk factor in SALS [20,21]. All these gene mutations described so far have provided important clues about the underlying molecular mechanisms in the disease.

Table 1.1 Genetic causes of FALS

Genetic subtype	Chromosomal locus	Gene	Onset/ Inheritance	Phenotype
ALS1	21q22	Superoxide dismutase 1 (SOD1)	Adult/AD	Variable
ALS2	2q33	Alsin (<i>ALS2</i>)	Juvenile/AR	Predominant UMN, slow progression
ALS3	18q21	Unknown	Adult/AD	Typical
ALS4	9q34	Senataxin (<i>SETX</i>)	Juvenile/AD	LMN predominant, slow progression
ALS5	15q15–q21	Spatacsin (<i>SPG11</i>)	Juvenile/AR	Variable phenotype, spasticity, with distal amyotrophy
ALS6	16p11.2	Fused in sarcoma (<i>FUS</i>)	Adult/AD	Typical, juvenile variant
ALS7	20ptel–p13	Unknown	Adult/AD	Typical
ALS8	20q13.3	Vesicle-associated membrane protein-associated protein B (<i>VAPB</i>)	Adult/AD	LMN predominant with tremor and dysautonomia
ALS9	14q11.2	Angiogenin (<i>ANG</i>)	Adult/AD	Typical
ALS10	1p36.2	TAR DNA-binding protein (<i>TARDBP</i>)	Adult/AD	Typical
ALS11	6q21	Polyphosphoinositide phosphatase (<i>FIG4</i>)	Adult/AD	ALS or PLS syndrome, apparent sporadic occurrence
ALS12	10p13	Optineurin (<i>OPTN</i>)	Adult/AD and AR	FALS symmetric slow progression (AD) Typical, more rapidly progressive than the dominant form (AR)
ALS–dementia–PD	17q21	Microtubule-associated protein tau (<i>MAPT</i>)	Adult/AD	Typical, associated with dementia and Parkinson’s symptoms
ALS–FTD	9p13.3	σ Non-opioid receptor 1 (<i>SIGMAR1</i>)	Adult/AD Juvenile/AR	Typical, associated with fronto-temporal dementia
ALS–FTD	9q21–q22	Chromosome 9 open reading frame 72 (<i>C9ORF72</i>)	Adult/AD	Typical, associated with fronto-temporal

1.1.2.b Oxidative stress

Oxidative stress plays a primary role in the pathogenesis of ALS, especially in 20% FALS caused by mutations in *SOD1* gene. The *SOD1* gene encodes a major antioxidant protein called superoxide dismutase (SOD1), an enzyme that neutralizes supercharged oxygen molecules [22]. All of these ALS-causing SOD1 mutations act in a dominant fashion; only one copy of the mutant gene is sufficient to cause ALS [23]. The most frequent mutation in United States is A4V (<http://alsod1.iop.kcl.ac.uk/>). The most studied ALS transgenic mouse model is G93A. Furthermore, many disease-associated mutations do not affect its dismutase enzymatic activity, and SOD1-knockout mice do not develop ALS. Mutant SOD1 (mSOD1) is still capable of causing motor neuron degeneration even under an enzymatically inactive state due to depletion of copper loading [24]. mSOD1 may cause oxidative stress by a mechanism beyond its catalytic activity. Research shows that mSOD1 can directly increase oxidative stress by binding Ras-related C3 botulinum toxin substrate 1 (Rac1), and locking Rac1 into its active state in the NOX complex, resulting in prolongation of reactive oxygen species (ROS) generation [25]. Oxidative stress is one of the most plausible mechanisms that induce the neurotoxicity, either through primary stress within motor neurons or through secondary toxicity from surrounding glial cells. Oxidative stress causes molecular damage that can seriously alter the cell membranes and other structures such as proteins, lipids, lipoproteins, and DNA. Elevated levels of oxidative insults to proteins [26], lipids [27], and DNA [28] have been investigated in post-mortem tissue from SOD1-associated FALS and SALS cases. In addition, elevation of markers for free radical damage was observed in the biosamples from ALS patients, such as cerebrospinal fluid (CSF), serum and urine. RNA species

were also exposed to oxidative damage in ALS patients and mSOD1 transgenic mouse models [29]. Interestingly, the SOD1 protein itself is particularly susceptible to oxidative posttranslational modification [30]. Oxidative stress arises from an imbalance between the productions of ROS and a biological system's ability to detoxify the reactive intermediates. The accumulation of oxidative stress during aging may be an initial factor that erodes the ability to cope with toxic insults. The presence of disease-causing mutations turns this imbalance into a vicious circle of cellular injury that culminates in neuronal death and neurodegeneration in later life [31]. In this vicious circle, oxidative stress interacts with, and potentially exacerbates, other pathophysiological processes. All these processes act together and trigger a devastating cascade that contributes to motor neuron degeneration, including protein aggregation, ER stress, excitotoxicity, mitochondrial impairment and alteration in signaling from astrocytes and microglia [32]. The effect of alleviating oxidative stress can potentially ameliorate multiple facets of pathobiology in motor neuron degeneration, the converse is also true. Overexpression of nuclear factor-erythroid 2 p45-related factor 2 (NRF-2) in mSOD1 transgenic mouse astrocytes delays disease onset and increases life span, mostly likely by preventing oxidative stress generated from astrocytes [33]. NRF-2 is a transcription factor that binds and upregulates the antioxidant response element (ARE) gene, thus improving antioxidant status [34]. Mitochondrial dysfunction in activated astrocytes triggers oxidative stress. Incubation of mSOD1 astrocytes with the mitochondrial-specific antioxidants ubiquinone and carboxy-proxyl nitroxide reduces superoxide levels and protects motor neurons from cell death *in vitro* [35]. Edaravone, a free radical scavenger used to treat cerebral ischemia, inhibits SOD1 misfolding/aggregation, and reduces lipid

peroxides and hydroxyl radicals in mSOD1 mice, thereby linking SOD1 aggregation and oxidative stress [36].

1.1.2.c Protein misfolding and aggregation

The accumulation of misfolded protein and protein aggregates is a pathological hallmark of many neurodegenerative diseases, including ALS [37]. The compact or skein-like ubiquitinated inclusions are TDP-43 positive, and they are unique features in both SALS and the syndrome seen in patients with TDP-43 mutations [12]. Furthermore, the TDP-43 mutant rodent model develops clinical syndromes similar to human ALS; these models presents a typical accumulation of ubiquinated aggregates in specific neuronal populations in cortical and anterior horn cells [38]. In addition to TDP-43, in patients with FUS-related FALS, the cytoplasmic inclusions containing the mutant FUS protein have also been identified [39]. In SOD1-associated FALS, the neurofilament-rich hyaline conglomerate inclusions are observed in motor neurons [40]. The mutations in *SOD1* can affect the protein dimer structure, leading to a “misfolded” conformation. Under pathological conditions, these misfolded proteins can develop into aggregates, which in turn trigger a toxic cascade that leads to neuronal degeneration. Using a specific antibody against misfolded SOD1 to treat mSOD1 mice can extend survival by 6 days, suggesting that neutralization of misfolded SOD1 can delay disease progression [41]. However, overexpression of chromogranin A (ChgA), a glycoprotein that interacts with mutant SOD1, accelerates disease onset in mSOD1 mice and increases misfolded SOD1 level, indicating that ChgA stabilizes misfolded SOD1 and increases its neurotoxicity [42]. Interestingly, cytoplasmic protein aggregates can translocate from one cultured cell

to another, and be secreted into the cell medium [43]. Even the spinal cord homogenates derived from mSOD1 mouse can seed further aggregates formation in a prion-like fashion [44]. If this finding could be proved *in vivo*, it could provide explanation to the rapid progression and prion-like clinical spread of ALS. The recent identification of aberrant wild-type SOD1 conformation under oxidative stress in both SALS and FALS patients suggests a possible common mechanism between SALS and SOD1-associated FALS. In the mouse model with wild-type SOD1 overexpression, the additional expression of mSOD1 accelerates aggregates formation and disease onset, and shortens survival [45].

1.1.2.d ER stress

ER consists of a complex reticular membranous net work, which mediates protein synthesis, protein secretory, posttranslational processing, and newly synthesized membrane folding [46]. It also contains large stores of calcium [47], which plays a critical role in cellular signaling and ER mitochondria calcium cycle (ERMCC). This is crucial to maintaining the coupling of energy metabolism in mitochondria and protein processing in the ER [48]. In ALS, ER stress can be triggered by accumulation of misfolded mSOD1 [49]. A localization of mSOD1 and a deposit of amorphous or granular material in the ER lumen in post-mortem lumbar spinal cord of ALS patients, indicate an accumulation of misfolded mSOD1 in ER stress [50]. Furthermore, mSOD1 was found to be co-localized with different ER marker such as ER tracker [51], glucose-related protein 78 (Grp 78) [52] and calnexin [53], suggesting a retention of cytosolic mSOD1 in the ER. Protein-disulfide isomerase (PDI), one of the ER-resident

chaperones, is activated and co-localized with mSOD1 inclusion in mSOD1 mice and in SALS patients [54]. The decreased ER calcium content in hypoglossal motor neurons of mSOD1 mice indicated the involvement of ER calcium in ALS [55]. Thapsigargin, which disturbs the ER calcium homeostasis, leads to an increased die-back in motor neurons compared to cortical and striatal neurons [56]. Protein misfolding can elicit the ER stress response pathway, which activates the unfolding protein response (UPR) system, including recognition the aberrant proteins by ER-resident chaperones that correct protein folding [57]. The most common ER-resident chaperones include Grp78, Grp58, PDI, calnexin and calreticulin. Grp78 is up-regulated in spinal cord tissue of SALS patients [58]. PDI, the UPR marker, is increased in the spinal cord of mSOD1 rodent and post-mortem spinal cord samples of ALS patients [59]. Knockdown of PDI in Neuro2a cells expressing mSOD1 leads to an increase of inclusion-positive cells, while overexpression of PDI in NSC-34 cells expressing mSOD1 results in a decreased inclusion formation and SDS-insoluble mSOD1 amount [60]. The upregulation of Grp78 and PDI enhances their ability to bind to misfolded protein and assist their folding. However, due to prolonged ER stress, the UPR is perturbed and become insufficient to deal with the stress conditions, and then apoptotic cell death will be initiated. Arimoclomol, a new drug in phase III trial for ALS, can delay disease progression by stimulating the UPR pathway through the activation of heat shock factor protein 1 (HSF1) [61]. Inhibiting the UPR pathway by crossing mSOD1 mice with pancreatic ER kinase haploinsufficiency (PERK^{+/-}) mice dramatically accelerates mSOD1 aggregates formation, and reduces disease duration by approximately 18% [62].

1.1.2.e Mitochondrial dysfunction

The morphological abnormalities, including mitochondrial swelling and vacuolation, are found in both ALS patients and rodent models of ALS [63,64]. Aggregated, swollen, vacuolated, or fragmented mitochondria are also observed in primary motor neurons and NSC-34 cells (a murine motor neuronal cell line) [65]. Abnormal mitochondrial morphology is tightly associated with mitochondrial dysfunction. Mitochondrial membrane potential maintenance is reliant on the activity of the four complexes of the electron transport chain. The reduced activity of complexes of the electron transport chain, especially complex I and IV, has been observed in tissues obtained from ALS patients and animal models. This is associated with consistent abnormality in mitochondrial respiratory function [66,67]. A decreased activity of complex I in mitochondrial fractions and the mitochondrial depolarization have also been observed in neuroblastoma cells overexpressing mSOD1 [68]. Impaired ATP synthesis [69] and reduced mitochondrial Ca^{2+} buffering [70] in cells expressing mSOD1 also indicate the involvement of mitochondrial dysfunction in the pathogenesis of ALS. ATP generation is decreased and intracellular Ca^{2+} homeostasis is impaired in neuronal cells of mSOD1 mice as well as in cell lines expressing mSOD1. The Ca^{2+} buffering capacity is significantly decreased in mitochondrial fractions from mSOD1 mice, making motor neurons susceptible to Ca^{2+} overload. The increased oxidative and/or nitrosative stress also causes damages to mitochondrial proteins, lipids, and DNA [71]. The nonspecific accumulation of mSOD1 aggregates at the mitochondrial surface and in the intermembrane space might compromise the function of mSOD1 [72,73]. Overexpression of glutaredoxin 2 (GRX2), a thiol-disulphide oxidoreductase in mitochondrial, reduces the mitochondrial mSOD1 aggregation and fragmentation [74]. The aberrant association between mSOD1 and

mitochondrial proteins also lead to impaired electron transport chain functioning, shortage of ATP, increased ROS formation and Ca^{2+} dysregulation. For example, mSOD1 binds to voltage-dependent anion channel 1 (VDAC1), a multifunctional mitochondrial protein in the transport of ions and small molecules including Ca^{2+} , ATP/ADP and NADH [75]. The binding of mSOD1 to VDAC1 reduces VDAC1-mediated ADP transport, which will limit ATP synthesis. VDAC1 interacts with pro- and anti-apoptotic proteins of the Bcl-2 family [76]. VDAC1 also plays a part in the physical link between mitochondria and the ER Ca^{2+} -release channel inositol 1,4,5-trisphosphate receptor (IP_3R) [77]. Abnormal interaction between VDAC1 and mSOD1 causes the ER-mitochondrial uncoupling, disrupts ER-mitochondria calcium exchange, and limits the ATP generation. Genetic disruption of the *VDAC1* gene in mSOD1 mice accelerates disease onset and reduces life span of mice [75,78]. The mitochondrial abnormalities in motor neurons are through cell-autonomous and non-cell autonomous mechanisms. Co-culturing astrocytes expressing mSOD1 with motor neurons reduces mitochondrial membrane potential and increases intramitochondrial Ca^{2+} [79]. Similarly, astrocytes from mSOD1 rats have mitochondrial defects that can influence motor neuron survival. Muscle mitochondria from mSOD1 mice are vacuolated, lose inner membrane potential, and release more Ca^{2+} [80]. Olesoxime, a compound that can potentially stabilize mitochondrial structures by binding to components of mitochondrial permeability transition pores, has shown some positive effects in mSOD1 mice; it is currently in a phase III clinical trial for ALS [81].

1.1.2.f Non-cell autonomous effect and neuroinflammation

Various non-neuronal cell types contribute to motor neuron survival and disease

course in ALS, including microglia, astrocytes, Schwann cells, T lymphocytes and skeletal muscles cells. Chimeric mouse models provide us with a good demonstration of non-cell autonomous death mechanisms in ALS [82]. The presence of mSOD1 in non-neuronal cells induces ALS-type pathology in wild-type motor neurons; in contrast, the presence of wild-type non-neuronal cells ameliorates the mutant phenotype and extends motor neuron survival. In the presence of mSOD1-expressing glia, both wild-type and mSOD1 neurons develop signs of neurodegeneration [83]. Widespread microglial activation in the brains of living ALS patients has recently been identified, and this activation correlates well with the severity of upper motor neuron damage [84]. Activated microglia release a huge number of pro-inflammatory cytokines, ROS, chemokines, mitogenic factors, neurotoxic molecules, which can lead to further neuronal dysfunction and cell death [85]. However, recent study demonstrates that removal of myeloid precursor cells, which are responsible for microglia proliferation in microgliosis, does not affect motor neuron degeneration [86]. This result indicates that the detrimental role of microglia is highly associated with mSOD1 expression in microglia. Microglia expressing mSOD1 release higher levels of tumor necrosis factor- α (TNF- α) and Interleukin-6 (Il-6) when stimulated with lipopolysaccharide (LPS) compared to wild-type microglia [87]. Co-culturing mSOD1-expressing microglia with motor neurons reduces survival rates of the motor neurons [88]. If mSOD1 expression in microglia/macrophages is selectively reduced by using the Cre-Lox system, the disease progression in several mSOD1 mice is sharply slowed down [89,90]. Similarly, replacing mutant microglia/macrophage with wild-type microglia/macrophage via bone marrow transplantation slows disease progression in mSOD1 mice [91]. Extracellular mSOD1

released from damaged neurons can activate microglia *in vitro* through CD14 [92]. Activation of astrocytes is also common in ALS patients and almost all animal models of ALS. When wild-type motor neurons are co-cultured with mSOD1-expressing astrocytes, neuronal cell death occurs [35,79]. Astrocytes expressing mSOD1 secrete mediators that lower the expression of GluR2 glutamate receptor subunit, and this leads to more Ca²⁺ permeable AMPA receptor in motor neurons. Without mSOD1-expression in astrocytes, motor neurons don't have the same effect [93]. Astrocytes expressing mSOD1 also release factors into the culture media to induce motor neuron apoptosis, one of toxic factors is neurotrophic growth factor (NGF) [94,95]. Furthermore, mSOD1 expressing in astrocytes triggers mitochondrial dysfunction and oxidative stress in neighbouring motor neurons. Attempts to alter oxidative stress levels in astrocytes through the ARE/NRF-2 pathway have successfully protected neighbouring neurons *in vitro*, and extended the survival of mSOD1 mice [33]. Glial cell is becoming an interesting therapeutic target in order to delay disease progression. Astrocytes replacement, bone marrow transplants, and transplantation of healthy glial precursor cells can prolong the survival time in mSOD1 mice [96,97,98]. mSOD1 expression in skeletal muscles leads to pathological alterations and induces pre-symptomatic sign of ALS. Skeletal-muscle-restricted expression of mSOD1 causes motor neuron degeneration suggests that mSOD1 toxicity is transmissible between muscles and neurons [99]. Injection of mechanogrowth factor (MGF) cDNA in mSOD1 mice muscles can improve motor neuron survival [100].

1.1.2.g Excitotoxicity

Glutamate is the main excitatory neurotransmitter in the CNS. Glutamate exerts its

effect by binding to ionotropic N-methyl-D-aspartate (NMDA) receptors and α -amino-3-hydroxy-5-methyl-4-isoxazolepropionic acid (AMPA) receptors on the postsynaptic membrane [101]. The levels of glutamate are elevated in CSF from ALS patients [102]. Glutamate released from spinal cord nerve terminals is increased, and this is highly correlated with the increased glutamate-containing vesicles at the presynaptic membrane [103]. Excitatory amino acid transporter 2 (EAAT2), the glutamate reuptake transporter is downregulated in mSOD1 mice as ALS progresses [104]. Transplantation-based astrocyte replacement is neuroprotective in mSOD1 mice, seeing as EAAT2 level increases and mSOD1 mice survival extends [96]. Furthermore, motor neurons are especially susceptible to AMPA-mediated excitotoxicity; these features include low expression of calcium-buffering proteins and GluR2, a subunit of the AMPA receptor complex responsible for the calcium permeability. The alteration of electrophysiological properties is implicated in ALS pathology. Postnatal day 4 motor neurons and interneurons of mSOD1 mice are intrinsically hyper-excitable, which coincides with early motor defects in mouse pups [105]. Riluzole, an antagonist of glutamate neurotransmission, is the only FDA-approved drug for ALS treatment [106]. It can prolong median survival of ALS patients by 2-3 months. However, other antiglutamate agents, including lamotigine, gabapentin, topiramate, verapamil, and nimodipine, has not been effective. One possible explanation is that riluzole has multiple potential neuroprotective effects, including activation of G-protein-dependent signal transduction cascades, inhibition of tyrosine phosphorylation, and inhibition of neuronal sodium channels [107]. Recent study using methionine sulfoxamine to inhibit the glutamate synthetase in mSOD1 mice shows a reduction of glutamate level by 30% and

an extension of survival by 8% compared with the control group [108].

1.1.2.h Axonal transport defects

Defects in anterograde and retrograde axonal transport are observed in both mSOD1 mice and ALS patients [109,110]. Accumulations of neurofilaments (NF) indicate the defects in anterograde transport. The build up of synaptic vesicles in motor neurons expressing mSOD1 points to the defects in retrograde transport [103]. Furthermore, mSOD1 expression inhibits fast retrograde transport mediated by the dynein/dynactin complex, and promotes retrograde transport of stress/cell-death pathway proteins such as p75NTR, caspase 8, and Jun N-terminal Kinase (JNK). However, mSOD1 suppresses retrograde transport of prosurvival proteins such as phosphorylated tyrosine kinase receptor (Trk) and extracellular signal-regulated kinase 1/2 (ERK1/2) [111]. Misfolded wild-type SOD1 can inhibit fast kinesin-based anterograde transport via a p38-dependent pathway. This finding, combined with the identification of misfolded SOD1 in SALS patients, suggests that axonal transport inhibition could be a unifying mechanism in ALS [45]. Evidence demonstrates that the pathological changes in motor axons and nerve terminals appear to precede motor neuron degeneration and clinical symptoms, supporting the concept that ALS is a dying-back axonopathy [112,113]. The defects in anterograde axonal transport and mitochondrial dysfunction may work together to cause energy depletion specifically in the distal axon [110]. The accumulation of insoluble complexes results in insufficient maintenance of the distal axon, which inhibits retrograde axonal transport and confers selective damage to motor neurons, possibly by preventing the delivery of target-derived neurotrophic factors back to the cell body.

1.1.2.i Dysregulated RNA processing

The identification RNA binding protein TDP-43 in cytoplasmic aggregates of ALS and the mutations in the *TARDBP* and *FUS* gene in ALS suggest a role of RNA processing in ALS [13,114] [115]. Fibroblast cell lines derived from patients with *TARDBP*-associated ALS exhibit the loss of TDP-43 nuclear expression and widespread changes in RNA splicing. Overexpressing TDP-43 in mice leads to a dramatic disruption of gene expression, including those in the chromatin assembly pathway, indicating the involvement of TDP-43 in transcriptional regulation [116]. Similarly, silencing TDP-43 expression with antisense oligonucleotides in adult mouse striatum alters the expression levels of 601 mRNA transcripts and changes the splicing patterns of 965 mRNA transcripts [117]. The increased level of oxidized mRNA disrupts the protein translation and contributes to motor neuron injury. mSOD1 can modulate the stability of mRNA encoding the neurofilament light chain [118,119]. The identification of the biomarker of RNA oxidation within motor neurons in human ALS and mSOD1 mice also confirms the dysregulated RNA processing in ALS [118,120,121]. The unexpected roles of microRNA (miRNAs or miR) have been uncovered. miRNAs repress translation or promote mRNA degradation by bind to complementary sequences on target mRNA transcripts and its target sites locate in the three untranslated regions (3'UTR) of the mRNA [122]. Both TDP43 and FUS proteins could interact specifically with the Drosha protein, which catalyzes the initial cleavage and plays a crucial role in miRNA bioogenesis [123]. miR206, expressed uniquely in skeletal muscles, delays ALS progression and promotes regeneration of neuromuscular synapses in mSOD1 mice. Loss of miR-206 accelerates disease progression and muscle atrophy, and leads to kyphosis, paralysis and death [124].

1.1.3 Animal models of ALS

A large number of animal models have a progressive motor phenotype that is reminiscent of what occurs in ALS patients to some extent, so they are of great value to delineate potential pathogenic mechanisms. SOD1 models are the most widely used animal models of ALS. The identification of other causative genes, such as *TARDBP*, *FUS*, and *VAPB*, also leads to the creation of various mouse models with these gene expression [125]. Other models in various species such as rat, dog, zebrafish, drosophila and *Caenorhabditis elegans* (*C. elegans*) were also developed. These animal models all have different advantages for experimental manipulation [126].

1.1.3.a SOD1 mutant transgenic mouse models

Up to date, there are 12 different human SOD1 mutations expressed in the mouse, including 9 missense and 3 terminally truncated variants [127]. SOD1^{G93A} (B6SJL-Tg(SOD1-G93A)1Gur/J) became the most widely used mouse strain. The overexpressed human SOD1^{G93A} is 20-fold higher than the normal mRNA levels of mouse endogenous SOD1 [128]. Pathologically, peripheral denervation occurs as early as 25 days [129] and neuromuscular junctions degenerate around 47 days [130]. Proximal axonal loss is evident by 80 days and correlates with motor impairment. The severe 50% dropout of lower motor neurons is prominent around 100 days [131]. SOD1^{G37R} transgenic mice exhibited the earliest detectable locomotor deficits at eight months in terms; this results in a margin of 3-4 months to evaluate the experimental therapies [132]. Transgenic mice with low-level expression of human and murine mutation equivalents, SOD1^{G85R} mice are characterized by late disease onset, aggressive disease progression

and short disease duration. SOD1^{G86R} mice harbour a point mutated gene in mouse endogenously, and develop fatal motor neuron degeneration in early life. A series of ALS transgenic mouse models expressing C-terminally truncated versions have been developed, including SOD1^{L126X} and SOD1^{G127X}. These mouse models of ALS are characterized by late onset and rapidly progress to death [133]. However, a spontaneous SOD1 mouse mutant exists, and this mice expressing active endogenous SOD1^{E77K} are phenotypically normal at one year [134]. One speculation is that multicopy SOD1 transgenes might be one prerequisite for disease in mice. The other speculation is that murine SOD1 lacks Cys111 which may be an important mediator of toxicity [135,136]. Therefore only the severe destabilizing mutation SOD1G^{86R} is disease-related.

1.1.3.b SOD1 wild-type transgenic mouse models

Down syndrome (DS), which is characterized by triplication of at least 200-300 genes on the distal long arm of chromosome 21, has increased gene dosage of wild-type SOD1 (SOD1^{WT}). Transgenic mice overexpressing human SOD1^{WT} were created as a model of DS. Axonal loss, vacuolar pathology and motor neuron degeneration have been observed in the spinal cords of aged SOD1^{WT} mice. These mice experience impaired regeneration after peripheral nerve injury [137] and prolonged subclinical motor neuron degeneration, termed a multi-system axonopathy [138].

1.1.4 Vulnerability of motor neurons in ALS

The motor neurons have cell body diameters between 30-80 micrometres; the axons of motor neurons can be more than a metre in length. These important properties have

implications for high reliance on intracellular cytoskeleton and axonal transport, high metabolic demands, and efficient regulation of mRNA distribution. The high energy demands for proper neuronal function and axonal transport highly rely on highly functional mitochondria, which predisposes the cells to oxidative damage and calcium overload [139]. The motor neurons of sporadic ALS patients express various proportions of GluR2 mRNA lacking A-to-I conversion at the Q/R site. Under normal conditions, the majority of neurons express only Q/R site-edited GluR2. If A-to-I conversions at the Q/R site are incomplete in pathological conditions, neurons become easily excitable due to an increase in Ca^{2+} influx through AMPA receptors [140]. Motor neurons express lower levels of cytosolic calcium-binding proteins (CaBP) compared to other neuronal populations [141,142]. These features make motor neurons more vulnerable to excitotoxicity and dysregulation of intracellular calcium homeostasis. Motor neurons also have a reduced capacity for heat shock response and chaperone activity, and increased sensitivity to ER stress [143]. The identification of the fast fatigue-resistant motor neurons in the spinal cord, which differ from the vulnerable spinal cord motor neurons, provides a strategy of boosting intrinsic neuroprotective defense mechanisms. For example, the surviving motor neurons exhibit upregulation of specific genes that promote cell survival [144].

1.1.5 Emerging targets in ALS therapeutics

The studies over the past five years have tested potential targets that would hopefully translate into meaningful therapeutics for ALS patients.

1.1.5.a Anti-glutamatergic agents

The EAAT glutamate transporter on astrocytes acts to inactivate the buildup of excitotoxic levels of synaptic glutamate. Ceftriaxone, a β -lactam antibiotic, can stimulate EAAT expression and increase astrocyte-mediated glutamate transport [145]. A double-blind (DB), randomized, placebo-controlled phase III trial investigating intravenous ceftriaxone in ALS patients is underway across the USA and Canada.

1.1.5.b Drugs targeting protein misfolding and accumulation

Heat shock proteins (HSPs) act as molecular chaperones that aid in restoring normal structure and function of damaged proteins, or degrading abnormal proteins. Arimoclomol, an oral compound, can enhance the expression of *HSPA4* and *HSP90AA1*, which encode HSP70 and HSP90 proteins, respectively [146]. Arimoclomol is effective in mSOD1 mice by extending survival 22% [147], and it is now being investigated in an adaptive, DB, randomized, placebo-controlled phase II/III trial. Vaccination with mSOD1 protein and passive immunization with antibodies against SOD1 can extend lifespans of mSOD1 mice in preclinical studies.

1.1.5.c RNA targets

Using antisense oligonucleotide and small inhibitory RNA molecules to neutralize the mutant mRNA slowed disease progression and increased survival in mSOD1 mice [148,149,150]. A phase I human trial in the USA using intrathecally administered antisense SOD1 oligonucleotides to SOD1-associated FALS patients is underway.

1.1.5.d Mitochondrial targets

A newer agent targeting mitochondrial function is olesoxime (previously TRO19622); it can modulate the mitochondrial permeability and reduce mitochondrial cytochrome C release after neuronal apoptosis is induced. The benefit of olesoxime has been identified in mSOD1 mice [81]. It is now in a phase II/III trial as an add-on therapy to riluzole. Dexpramipexole has neuroprotective effects, seeing it can inhibit oxidative stress and improve mitochondrial function [151]. Dexpramipexole is currently in a large, international, phase III study.

1.1.5.e Neurotrophic factors

Brain-derived neurotrophic factor (BDNF) improved survival and retarded loss of pulmonary function in ALS patients in a phase I through phase II study. BDNF did not show a significant effect on survival in the phase III trial, but post hoc analyses showed significant benefit in a certain subset of ALS patients [152]. Vascular endothelial growth factor (VEGF) can delay disease progression and increase survival in two mSOD1 rodent models of ALS [153,154]. A human study of intracerebroventricularly administered VEGF is in progress in a phase I/II trial.

1.1.5.f Stem-cell therapy

Although the ethical impediment is the first concern of stem cell trials, stem cell implantation therapy can benefit ALS patients through an independent effect of cytoprotection. Stem cells can differentiate directly into non-neuronal cells and protect motor neurons by releasing specific growth factors or expressing enzymes or transporters to detoxify the local environment. A Spanish study of a phase I/II clinical trial, in which

mesenchymal stem cells were injected into the thoracic spinal cord of nine ALS patients, found no serious adverse effects [155]. Another non-randomized study of ten ALS patients transplanted autologous CD133⁺ bone marrow stem cells into the frontal motor cortex. This procedure turned out to be safe and well-tolerated. A survival benefit was also confirmed [156]. Autologous bone marrow stem cells were transplanted into the rostral cervical cord of 13 patients with bulbar ALS, and no adverse effects were observed and nine patients showed notable improvement [157].

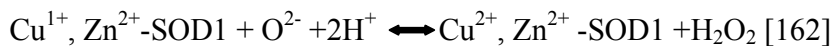
1.1.5.g Muscle-directed therapies

Respiratory failure, the lethal complication of ALS, results from progressive weakness of the diaphragm. Diaphragm pacing with laparoscopically placed electrodes is safe and it can slow respiratory decline in ALS patients. ACE-031 is a promising investigational drug that inhibits GDF-8 and other factors. In a phase Ib trial, this drug is well tolerated, and it can increase lean muscle mass and volume [158]. CK-2017357 is another similar investigational drug that selectively activates fast skeletal muscle troponin complex by increasing the calcium sensitivity. A randomized, DB, placebo-controlled, phase II clinical trial showed that this drug was well-tolerated, and there was a dose-dependent improvement in fatigue, strength, and pulmonary function. Reticulon 4 is a protein found in skeletal and neurons. Reticulon 4 expression in the skeletal muscles and neurons of ALS patients is concordant with disease severity [159], and genetic removal of reticulon 4 extends mSOD1 mice survival [160]. GSK1223249 is a humanized monoclonal antibody against reticulon 4; its safety and pharmacodynamics is currently being investigated in an international phase I trial.

1.2 Copper/zinc superoxide dismutase (SOD1)

1.2.1 Function of SOD1

The function of SOD1 is to catalyze the dismutation of superoxide radical (O_2^-) to dioxygen (O_2) and hydrogen peroxide (H_2O_2). SOD1, the most important antioxidant enzyme, acts as a scavenger of superoxide through a two-step reaction involving reduction and reoxidation of the copper ion at its active site [161].



1.2.2 Structure of SOD1

The human *SOD1* gene is located on the chromosome 21q22.11, and codes for the monomeric SOD1 polypeptide, which has 153 amino acids, with molecular weight 16 kDa. The human SOD1 is a 32 kDa homodimeric metalloenzyme. It is composed of two identical subunits. A copper and zinc ion are embedded in each unit. Each of the two subunits consists of a main β -barrel, which is composed of eight antiparallel β -strands arranged in a "Greek-key motif". This Greek-key motif and the hydrophobic dimer interface are essential for the structural stability of SOD1. Each of the subunits contains active sites; a copper-binding site (binding residues: His46, His48, His63 and His120) and a zinc-binding site (binding residues: His63, His71, His80 and Asp83). The copper ion is the more solvent exposed metal and it is the catalytic site where the substrate/product/reaction intermediate is likely to bind during the enzymatic reaction. The binding of zinc is not essential for the catalytic reaction. However, the binding of zinc confers high protein stability to SOD1. For the optimally fast catalysis, the substrate

of superoxide is electrostatically guided through a channel from the protein surface to the active site. This channel is formed by two external loops. The first loop, also known as the zinc loop, tethers the dimer interface with the zinc active site and contains a disulfide bond that aids structural stability. The second loop, also known as electrostatic loop, contains charged residues that contribute to guiding the negatively charged superoxide substrate toward the copper catalytic site. Four posttranslational events are required for obtaining the mature, correctly folded and enzymatically active form of SOD1; they are copper and zinc binding, disulfide bond formation, and dimerization [163,164,165].

Human SOD1 has four cysteine residues: Cys 6, Cys 57, Cys 111 and Cys 146. Cys 57 and Cys 146 are conserved, forming the intramolecular disulfide bond [166]. Disulfide bond formation stabilizes protein structure through lowering entropy of the unfolded polypeptide chain. Cys 6 and Cys 111 are free, existing in a thiol group state (-SH). Cys 6 is buried within the interior of the β -barrel, and it is solute-inaccessible in the native, folded conformation. Cys 111 is on the surface, near the dimer interface, and it is solute-accessible and reactive. Cysteine residues in the active sites of the protein build up intracellular antioxidant defenses through the thiol functional group [167].

1.2.3 Genetic variants of SOD1 in ALS

In 1993, Rosen first reported that mutations in *SOD1* are involved in ALS using classical linkage analysis [11]. Approximately 12-23% FALS cases are caused by mutations in *SOD1* gene [168]. *SOD1* exonic mutations have occasionally been described in SALS patients. *SOD1* mutations account for 1-2% SALS cases [169]. More than 150 mutations of *SOD1* have been identified in 68 of the 153 codons, spreading over all five

exons [170].

1.2.4 SOD1 gene expression in ALS

The results of studies of SOD1 expression in ALS is conflicting [171,172,173]. The latest study demonstrated that SOD1 mRNA level is increased in the brain stem and spinal cord, which are typically affected in ALS, but not in other areas that are not associated with motor neuron degeneration [174]. Increased SOD1 mRNA level has also been detected in lymphocytes from SALS patients compared to healthy people. However, the SOD1 protein expression in SALS patients and healthy people detected by western blot showed similar level in both lymphocytes and affected nervous areas [175]. Histopathological analysis showed an increased protein level in the spinal cords of SALS patients compared to healthy people. These contradictory results indicate that mutant SOD1 protein is misfolded or becomes aggregates, which would probably precipitate the insoluble fraction and become undetectable. Normally, the soluble supernatant fraction is applied to western blot. Several studies have demonstrated the presence of proteinaceous inclusions bodies containing SOD1 in motor neurons of SALS patients. [45,176,177]. The insoluble mSOD1 aggregation is a pathological hallmark of SOD1-associated FALS [178]. In mSOD1 mice, the insoluble SOD1 aggregates accumulation occurs before the onset of paralysis and increases as the mice develop ALS-like symptoms [179]. A shared pathological trait is suggested in both familial and sporadic cases.

1.2.5 Mutant SOD1 in ALS-a toxic gain of function

The rodent models expressing active as well as inactive forms of mSOD1 develop

comparable disease pathologies similar to that of human patients [180,181,182]. Furthermore, SOD1 gene knock-out mice do not develop motor neuron degeneration [183]. Knock-out mouse endogenous SOD1 in mice expressing dismutase inactive hSOD1^{G85R} does not affect disease progression [184]. Increasing wild-type hSOD1 expression, accompanied by chronic elevation of dismutase activity [133], either has no effect on disease course [184]. Taken together, these experiments suggest that the toxicity of mSOD1 is not mediated by the loss of dismutase activity, but rather by a toxic gain of function. Not only motor neurons are affected by mSOD1; studies also indicate that mSOD1 expressing in neighboring glial cells is involved in motor neurons degeneration.

1.2.6 Subcellular distribution of mSOD1

By using live-cell imaging of EGFP-fused SOD1, SOD1 is found to be distributed evenly in the cytosol. By using digitonin in the presence of ATP to wash out soluble cytosolic protein, the mild membrane perforation unveiled vesicular or punctuate locations of SOD1 in mitochondria, lysosomes, ER, and trans-Golgi network [185]. mSOD1 interacts with several “ accompanying proteins” such as VDAC1 and Bcl-2 , resulting in abnormal subcellular localization.

1.2.6.a mSOD1 in mitochondria

Distinct from wild-type SOD1, mSOD1 induces morphological change and subsequently impairs mitochondrial function. mSOD1 in mitochondria affects their role as calcium buffers and disrupts the calcium homeostasis [186]. Blocking Ca²⁺ entry into mitochondria protects cultured motor neurons against glutamate-induced neuronal injury

[187]. misfolded mSOD1 damages mitochondria by its deposition onto the cytoplasmic side of the outer membrane of spinal cord mitochondria [188]. The involvement of mitochondrial-mediated apoptosis in mSOD1-associated ALS has been uncovered [189,190]. mSOD1 disrupts the axonal transport of mitochondria along microtubules and mitochondrial dynamics in ALS [191]. Destabilization of mSOD1 is associated with its increased binding to the intermembrane space (IMS) and elevated ROS production in the IMS [192,193]. This IMS-targeted mSOD1 causes neuronal toxicity, neurite mitochondrial fragmentation and impaired mitochondrial dynamics [194].

1.2.6.b mSOD1 in ER

Several studies have demonstrated the precisely localization of mSOD1 in ER by using immunoelectron microscopy [195,196]. The ER localization of SOD1 was confirmed by sucrose density-gradient ultracentrifugation and floating ultracentrifugation using an iodixanol cushion and high-salt wash [185]. SOD1 was co-localized with Derlin-1 in ER by immunocytochemistry. Derlin-1, is an ERAD-linked protein. It takes part in the endoplasmic-reticulum-associated protein degradation (ERAD) pathway, which targets aberrant proteins in the ER for ubiquitination and degradation. mSOD1 interacts with Derlin-1 and leads to ER-stress-induced apoptosis signal-regulating kinase 1 (ASK1) activation, apoptosis and disease progression [197]. Study shows that immunoglobulin heavy chain binding protein/glucose-regulated protein 78 (Bip/Grp78), an ER resident chaperone, co-localized with mSOD1 and induced ER stress [198]. The interaction between mSOD1 and Bip/Grp78 led to the entry of mSOD1 into ER [195].

1.2.6.c mSOD1 in Golgi apparatus and secretory pathway

In ALS patients, the fragmented Golgi apparatus are observed in the motor neurons. Early studies showed that wild-type SOD1 can be secreted from thymus-derived epithelial and fibroblast cells as well as cultured astrocytes [199]. Both wild-type SOD1 and mSOD1 secretions involved brefeldin-A sensitive transport, indicating an ER-Golgi transduction pathway [200]. The presence of mSOD1 in the ER-Golgi system was also confirmed by immunisolating the organelle. Both *in vivo* and *in vitro* studies showed that mSOD1 interacted with neurosecretory proteins, such as ChgA and ChgB, and this interaction promoted the secretion of mSOD1 [196].

1.2.7 Extracellular mSOD1 in the non-cell-autonomous pathology

mSOD1 expression in glial cell greatly affects the survival of motor neurons and ALS disease progression. Molecules that secreted by mSOD1-expressing astrocytes are toxic only to motor neurons [201,202,203]. Furthermore, mSOD1-expressing microglia produces higher levels of toxic mediators, such as superoxide and nitrite, but lower level of growth factors, such as insulin-like growth factor 1 (IGF-1) [204]. Externally applied recombinant mSOD1 into the culture media led to microglia activation and motor neuron degeneration. This toxicity of extracellular mSOD1 was mediated by CD14 on the microglia [196]. Misfolded SOD1 was detectable in the CSF from FALS patients [205,206].

1.2.8 SOD1 aggregation-a toxic property

The misfolding and aggregation of SOD1 species is related to the toxicity of mSOD1. Several studies have demonstrated that eight FALS-linked SOD1 mutants (in

transgenic mouse models) and 13 FALS-linked SOD1 mutants (in cell culture models) exhibit great potential to form aggregates [181,207,208,209]. SOD1 mutations alter SOD1's solubility and make it more prone to aggregates. Normally, the mSOD1 aggregates have two destinies: one is to be helped by protein chaperones and the other is to be degraded by ubiquitin-proteasome proteins. The presence of Hsp70, Hsp40, Hsp27 and $\alpha\beta$ -crystallin and increased interaction between mSOD1 and Hsp70 indicate the sequestration of housekeeping Hsp proteins into mSOD1 aggregates, which reduces the available amount of Hsp proteins to fulfill their cytoprotective functions. Neutralizing the toxicity of mSOD1 aggregates by over-expressing Hsp70 can significantly reduce aggregates formation and prolong the survival of primary motor neurons derived from mSOD1 mice [210]. Similarly, overexpression of Hsp40 and Hsp27 in cell lines or cultured primary motor neurons can also decrease aggregates formation and apoptosis. mSOD1 aggregates are intensely immunoreactive with ubiquitin antibodies, and mSOD1 is selectively ubiquitinated by dorfin, the RING finger-type E3 ubiquitin ligase [211]. Overexpression of dorfin in neuronal cells neutralizes the toxic effects of mSOD1 and reduces the level of mSOD1 aggregates. These mSOD1 aggregates inhibit the ubiquitin-proteasome protein degradation system, by sticking in the proteasome and leading to the proteasome dysfunction [212]. The characteristic of mSOD1 aggregates include insolubility and bulkiness, which leads to obstruction the essential components in axonal transport, including neurotrophic factors [213]. For example, the intracerebroventricular delivery of VEGF is significantly reduced in the mSOD1 rat model [214]. The high molecular-weight SDS-resistant mSOD1 aggregates are highly related to the spinal cord mitochondria in mSOD1 mice [215]. These aggregates can

interact with Bcl-2, an anti-apoptotic protein. This interaction converts Bcl-2 into a pro-apoptotic protein. [216]. Research also demonstrates that increased aggregation propensity of SOD1 is associated with decreased survival of ALS patients [217,218].

1.2.9 Formation of SOD1 aggregates

The identification of Bunina and Lewy body-like hyaline inclusions in motor neurons of FALS and SALS patients highly indicates the involvement of SOD1 in the protein aggregates formation, and these protein aggregates are strongly immunoreactive to SOD1 [219]. It is important to recognize the role of intracellular regulation of SOD1 stability in the molecular mechanism of FALS pathology. The factors, including improper metallation of the protein, genetic mutations, and loss of disulfide bond and posttranslational modification, drive SOD1 to acquire propensity to misfold, and favor the reduced SOD1 monomers to convert into oligomeric and aggregated species with toxic properties.

1.2.9.a SOD1 mutations facilitate loss of metals

Holo-form of SOD1 is very stable with its melting temperature, T_m , around 90°C; however, removing a copper ion or zinc ion from holo-SOD1 decreases T_m to ~70°C or 60°C, respectively. Studies demonstrate that the deficiency of the copper-bond drives SOD1 molecule to form aggregates through oxidation of the histidine residues into 2-oxohistidine [220]. Mutations of SOD1 promote the aggregates formation by facilitating the removal of metals from SOD1 and by increasing the reduction of SOD1's intra-molecular disulfide bond. ALS mutations result in enhanced aggregates formation at

pH 5; this effect is most pronounced with metal-binding-region mutants. H80R mutant is nearly devoid of metals, forming aggregates in high yield with a longer lag time at pH 5. G85R and D125H, the metal-binding region mutants, also generate a significantly greater yield of aggregates at pH 5 than wild-type SOD1 [221]. Other mutations, such as H46R and S134N, lead to demetallation-induced conformational changes in SOD1 proteins and create a new protein-protein interaction site [222]. Mutations, like A4V and I113T, result in alteration of the subunit orientation in solution [223]. Demetallation-mediated monomerization is considered a step leading to formation of misfolded intermediates in the aggregation pathway [224].

1.2.9.b SOD1 mutations facilitate partial unfolding or monomerization of apo-SOD1

Most of the mutant apo-SOD1s are significantly destabilized [225]. Only a few types of mutations, such as H46R and D124V, have increased stability. These mutations are incidentally associated with relatively milder symptoms [226,227]. Many ALS-associated SOD1 mutations are indicated to provoke dramatic destabilization and conformational changes. The instability of apo mSOD1, especially in the metal-deficient state, is considered to be a “common denominator” for the increased propensity of mSOD1 aggregates. Apo-SOD1 bearing these mutations undergoes partial unfolding while the corresponding protein without these mutations remains stably folded [228]. While apo-SOD1 is predominantly dimeric, mutations may facilitate the unfolding of apo-SOD1 and result in dimer dissociation, and the consequently monomerization of apo SOD1 is an obligatory step in SOD1 aggregation. Nonetheless the unfolded SOD1 was detected by a specific antibody, raised against 4-20, 57-72, and 131-153 of an SOD1

amino acid sequence. This antibody also detected the SOD1-positive inclusions in motor neurons of the spinal cord from 29 SALS and 8 FALS patients [176].

1.2.9.c SOD1 mutations increase the susceptibility to disulfide reduction

Study has demonstrated that treatment with Tris (2-carboxyethyl) phosphine (TCEP) to SOD1, a hydrosoluble reagent to protect sulfhydryls or cleave disulfide bridges, leads to loss of the disulfide bond and converts SOD1 to a form capable of forming aggregates. The C146R mutation, forms aggregates in the absence of TCEP [228]. Furthermore, many mSOD1s have a greater tendency to form aggregates when incubating with TCEP compared with wild-type SOD1. Similarly, many mSOD1s, such as A4V, G93A and G85R, have an increased susceptibility of the Cys57-146 disulfide bond to reduction [229]. Several studies have demonstrated that reduction of the disulfide bond resulted in apo SOD1 to dissociate into monomers. Mutations, such as A4V and G93A, have been described as destabilizing both zinc-containing and metal-free SOD1 whose intramolecular disulfide bond is reduced [230]. Taken together, these results indicate that cleavage of the disulfide bridges can trigger aggregates formation from metalated SOD1. The disulfide-reduced monomer is considered to be the common aggregation-prone, neurotoxic mediator of mSOD1 [231].

1.2.9.d SOD1 can form aggregates with or without intermolecular disulfide bonds

The formation of disulfide bond is mediated by oxidation of the thiol groups of cysteine residues. There is an intra-molecular disulfide bond between Cys57 and 146 in the natively folded holo-SOD1. Previous studies have established that detergent-insoluble

mSOD1 aggregates accumulated in spinal cords of mSOD1 mice are extensively cross-linked by disulfide bonds, because they are detectable in SDS-PAGE without use of reducing agents [136,232,233]. Studies found that disulfide bond formation between mSOD1 proteins could either trigger oligomerization or facilitate the bonding force to stabilize aggregates structures [234,235]. One study states that the formation of disulfide-linked multimers does not need the involvement of the non-conserved cysteine residues, Cys6 and 111, while the conserved cysteine residues (Cys57 and 146) take a part in the multimerization of apo SOD1 upon oxidative stress [236]. However, recent studies indicate that an aberrant intermolecular disulfide bond between Cys 6 and 111 of mSOD1 is crucial for the formation of high molecular weight aggregates in cells [235]. Among the identified mutations of SOD1, mutations of cysteine residues at either position 6 or 146, such as C6F, C6G, and C146R, still causes FALS. In addition, all of the truncated SOD1 proteins which have cysteine residues at position 6, 57, and 111 but lack Cys146 are still associated with FALS [233]. The role of cysteine residues in modulating the mSOD1 aggregates is likely to involve other mechanisms rather than disulfide cross-linking. When the FALS-associated SOD1 cysteine mutant (C6F, C6G, and C146R) were expressed in cell lines, the mSOD1 aggregates were detected, indicating that loss of any single cysteine residue does not block aggregates formation [162,168,237]. *In vitro* study further confirmed aggregates formation *per se* does not depend on the formation of intermolecular disulfide bonds. SOD1 proteins, containing or lacking free cysteines, form amyloid-like aggregates in the high presence of TCEP [228]. Previously, the oligomeric form of mSOD1 was thought to be a noxious mSOD1 species because inhibition of the formation of disulfide-linked oligomers results in decreased mitochondrial mSOD1

aggregates. However, introducing the C111S does not decrease the mSOD1 mitochondrial localization [238]. These results suggest that the disulfide bond formation involving Cys111 is not needed to elicit mitochondrial defects [72]. The mSOD1 lacking the native intramolecular disulfide bond is the major component of the insoluble SOD1 aggregates [239]. The reduction of the conserved intramolecular disulfide in most of the mSOD1 molecules constituting inclusions indicates the involvement of posttranslational modification of SOD1 polypeptides in the formation of pathological aggregates.

1.2.10 Oxidative stress in SOD1 aggregates formation

Aggregation process is strongly sensitive to the redox conditions of the environment, and oxidative stress produces a shift in the cellular environment [240]. Oxidative stress is indicated further to augment the SOD1 aggregates formation in cell culture model. High molecular weight (HMW) complexes and insoluble SOD1 species become more evident when the neuronal cells expressing mSOD1 are exposed to increasing concentration of H_2O_2 [241]. Actually, H_2O_2 is a product as well as a substrate of SOD1. When bovine SOD1 is incubated with H_2O_2 , it will lead to oxidation of His¹¹⁸ to 2-oxohistidines and inactivation of the enzyme [242]. When H_2O_2 is too excessive, it will result in oxidation of almost all cysteine and histidine residues, fragmentation and aggregation of SOD1 [243,244]. When SOD1 is co-incubated with bicarbonate and H_2O_2 , it will induce bicarbonate radical anion formation, resulting in SOD1 oligomerization [245]. The discrete aggregates containing mSOD1 are detectable when *C. elegans* is challenged with paraquat, a herbicide used to generate oxidative stress [246]. The SOD1 aggregates are much more specific to the spinal cord, because the accumulation of mSOD1 aggregates in

the spinal cord is identified in both mSOD1 mice and FALS patients [247]. This mSOD1 aggregates is detectable only in spinal cord of symptomatic animal, but not in brain or liver [233]. Spinal cord exhibits higher oxidative stress relative to other tissues [248]. SOD1 is delivered to the nerve terminus at a slow rate about 0.5~2 mm/day [249]. Because the axon of the motor neuron is about a metre long, it will take one or two years for the SOD1 protein to reach the nerve terminus. During this process, there will be an increased chance of oxidative insult to SOD1, especially to the mSOD1, possibly facilitating the oxidation of thiol groups of the cysteine residues [250]. Reversible oxidation of the thiol group of cysteine to disulfide (-S-S-) or sulfenic acid (-SOH) is accomplished by thiol compounds, such as DTT, 2-ME, glutathione, or thioredoxin. The extensive oxidation to sulfinic acid (-SO₂H) or sulfonic acid (-SO₃H) is not reduced by these thiols under physiological conditions [251]. Take peroxiredoxin (Prx) for example, the thiol group of one cysteine residue of Prx is oxidized to sulfinic acid (-SO₂H) by incubating with an excess of H₂O₂ [252]. The thiol group of Cys146 in SOD1 can be irreversibly oxidized to sulfonic acid (-SO₃H); this oxidative modification was found in the brains of patients with Alzheimers' disease and Parkinsons' disease. Oxidation at Cys146 affected the stability of SOD1 protein, which is associated with the SOD1-immunoreactive senile plaques and neurofibrillary tangles in patients with Alzheimers' disease [253]. Taken together, the oxidative modification at cysteine residues plays an important role in the physiological SOD1 aggregate formation.

1.2.11 Oxidative modification of Cys111 in SOD1 aggregates

An intermolecular disulfide bond between Cys57 and Cys146 contributes to the high

stability of SOD1 protein. This disulfide bond is highly conserved in various organisms, including yeast, plants, flies, fishes and mammals [254]. However, the other two cysteines, Cys6 and Cys111, are free, not conserved. Yeast, fungi, and plants don't have free cysteines. In these organisms position 6 is Ala and position 111 is Ser. More evolved organisms, such as flies, fishes, and mammals, including the Japanese monkey, only have one free cysteine at position 6. Human, great apes (chimpanzee and orangutan) are the only species that have two free cysteine residues, Cys6 and Cys111 [255]. Free cysteines are highly reactive, and the reactivity of free cysteine is highly dependent on its molecular location. In the crystal structures of human SOD1, Cys6 is packed tightly within the interior of β -barrel, and Cys111 is located in the Greek-key loop near the dimer interface. Study shows that Cys111 is modified with persulfide (-S-SH-) in human SOD1 isolated from erythrocytes [256]. Cys111 is also heavily glutathionylated in human tissue [257], and this modified enzyme constitutes nearly 50% of the pool of SOD1 in freshly drawn erythrocytes. Glutathionylation of Cys111 induces structural rearrangements and modulates stability of both wild-type SOD1 and mSOD1 [258]. Moreover, glutaredoxin2, which specifically reduces protein-glutathione mixed disulfides to protein thiols, strongly prevents the mSOD1 aggregates formation and improves cell viability in cultured cells [259]. Cys111 can also bind to other ligands such as glutathione, thioredoxins, or other molecules. mSOD1 has higher affinity for copper than wild-type SOD1, which is strictly mediated by Cys111 [260]. C111S dramatically attenuates this affinity and increase protein stability. When the cells expressing combined mSOD1 (the C111S mutation with the A4V, G93A, and C146R FALS mutations), the SOD1 aggregates formation is significantly reduced. This finding indicates that Cys111 should be a potentially crucial

residue in promoting aggregates formation [234]. Furthermore, Cys111 was found to be selectively oxidized to sulfinic acid (-SO₂H) and sulfonic acid (-SO₃H), even under air oxidation. By using the specific antibody, raised against a synthesized peptide containing Cys111- SO₃H, the presence of oxidized SOD1 was detectable in the spinal cords of mSOD1 mice [261]. Cys111 of mSOD1 is labile to be oxidized by endogenous agents, including H₂O₂ and nitrosoglutathione, which is the first step for the substantial protein monomerization.

1.2.12 Oxidative modification of wild-type SOD1 in aggregates formation

Prevailing evidence indicates that mutation-mediated conformational changes lead to SOD1 misfolding and subsequent aggregation [262]. Since the FALS and SALS are clinically and neuropathologically similar, this similarity implies that the pathogenesis of ALS must converge on a common pathogenic pathway and/or some similar toxic factors. Wild-type SOD1 is proposed as the common link between SALS and FALS, seeing as the SOD1 is specifically modifiable with a chemical agent, the modified SOD1 was found in both FALS and SALS [263]. The aberrant covalent modifications or defects in the normal posttranslational modifications of wild-type SOD1 can induce conformational changes which is similar to the structural features of SOD1-associated FALS [264]. *In vitro* studies have shown that exposure to mildly oxidizing reagents, such as H₂O₂, copper chloride, ascorbic acid, peroxyxynitrite and oxidized glutathione SOD1, will trigger both the wild-type SOD1 and mSOD1 to form aggregates [265,266]. High concentrations of these oxidizing reagents can cause copper and zinc ions loss and disulfide bond reduction, which results in inactive SOD1 monomers [224]. These monomers are the basic

structural units that form aberrant aggregates. Motor neurons from spinal cord-derived cell culture were selectively vulnerable to oxidized wild-type SOD1, reminiscent of the selective vulnerability of motor neurons to mSOD1 proteins [267]. Wild-type SOD1 acquired toxic properties through oxidation and that the aberrantly modified wild-type SOD1 and mSOD1 may share similar structural features. One specific antibody raised against a peptide epitope that is normally buried in the native homodimer interface of SOD1, can recognize monomeric or misfolded forms of SOD1. This antibody can detect wild-type SOD1 when it is oxidized *in vitro* by copper chloride and ascorbic acid. It can also detect mSOD1 in the spinal cords of several different mSOD1 mice [268]. Another monoclonal antibody C4F6, raised against the apo-SOD1 G93A antigen, recognized multiple FALS-linked mSOD1 and the oxidized wild-type SOD1 [269]. Specifically, the thiol group of Cys111 encoding in exon 4 is fully and irreversibly oxidized to sulfonic acid (-SO₃H). Both Cys111 oxidation and G93A mutagenesis induce the formation of a conformational epitope. Oxidized wild-type SOD1 shares the same neurotoxic mechanism with FALS-linked mSOD1, it is believed that conformational abnormalities and posttranslational modifications in wild-type SOD1 contribute to SALS pathogenesis. It is plausible that oxidized SOD1, especially Cys111 oxidative modification, leads to the aberrant toxic protein species.

1.3 Protein disulfide isomerase (PDI)

PDI is the first folding catalyst ever reported, which is located in the ER in high concentration with a classic KDEL-ER retrieval motif [270]. PDI is able to catalyze disulfide bond formation, breakage, and rearrangement in all nonnative protein and peptide substrates [271]. The mechanism of how it escapes the ER is unclear, but more

recent studies indicate that it is a marker for the release of intracellular contents from damaged cells [272]. Its role in disulfide bond formation is the most important cellular function [273]. Disulfide bonds are the covalent linkages formed between the thiol groups of cysteine residues, and normally they function to stabilize protein structures. Disulfide bond formation is one of the important rate-limiting steps in protein folding. Seeing as a protein can have none, some, or all of its cysteine residues in disulfide state, this gives 10 different intramolecular thiol/disulfide redox states for a protein with four cysteine residues, such as SOD1. During the process of protein folding, there are two distinct pathways, one is cycle of reduction-oxidation, and the other is direct isomerization. PDI is able to catalyze both of these two pathways, and furthermore, independent of its catalytic function, it exhibits chaperone activity by inhibition the aggregation of unfolded/misfolded protein [274].

1.3.1 Structure of PDI

Human PDI has 491 amino acids in its mature form. It is a 57-kDa protein that mainly resides in the ER of eukaryotic cells. It has four distinct domains; *a*, *b*, *b'*, and *a'*, plus the acidic C-terminal extension *c* and the 19-amino-acid interdomain linker *x* (between the *b'* and *a'* domains) [275]. The catalytic domain *a* and *a'* share 36.8% of the same identity with each other and each contains a Cys-Gly-His-Cys (CGHC) active-site sequence, which is responsible for the oxido-reductase activity. The non-catalytic domain *b* and *b'* have only 19.3% of the same identity and *b'* domain provides the principle binding site of PDI [276]. The ability of *b'* domain to bind substrates explains its essential role in the efficient isomerization reaction. The *b'* domain is also required for

the reported chaperone functions of PDI [277]. The cationic *c* domain is not essential for the catalytic activity and ends with a C-terminal ER-retention signal. It stabilizes the functional conformation of PDI under extreme condition. The catalytic domains of PDI and thioredoxin share a high degree of sequence homology. PDI is considered to be the Trx family of proteins, which is characterized by the ability to catalyze the thiol-disulfide exchange reactions in the ER, also known as the PDI family. Proteins of this family share a common motif in their active sites (Cys-X-X-Cys, CXXC, where X refers to any amino acid) [278]. The N-terminal cysteine residue in this motif has high reactivity at physiological pH, partially due to its location on the surface of the protein. For example, ERp57, another ER housekeeping enzyme, has the active-site residues WCGHC, which are the same as those of PDI [279]. Each family member has distinct substrate specificities [280]. ERp57 is involved in the oxidative folding of glycoproteins [281,282], while PDI is associated with both glycosylated and nonglycosylated proteins [283]. The PDI family proteins have redox properties, ranging from strongly reducing to strong oxidizing. Therefore, they are equipped to perform specialized roles in a variety of cellular processes.

1.3.2 Function of PDI

PDI is essential for the cell survival with its important cellular functions. Efficiently knockdown PDI expression is highly linked to cytotoxic effects [284]. The fully knockout cells and animals of PDI are not reported, indicating that such knockout is not viable. The knockout of ERp57 in mice is also non-viable [285]. Knockout either of the PDI family members AGR2/Hag2 [286] or ERdj5 [287] increases the ER stress and

produces specific defects in mucin production and salivary gland function. The important function of PDI is required for a number of proteins that fold in the ER. There are three basic reactions that are involved in the intra- or intermolecular disulfide-bond formations: oxidation, reduction and isomerization. PDI can catalyze all these reactions [288]. For example, in eukaryotic cells, only the reduced PDI interacts with its oxidase ER oxidoreductin 1 (Ero1) [289] or peroxiredoxin4 [290]. Hence, it is elusive how PDI distinguishes its substrates or selectively binds to the same substrate at different stages in the protein-folding pathway [291]. In addition to its function to modulate the thiol/disulfide exchanges, PDI also has molecular chaperone activity. This chaperone activity requires full-length PDI, which temporarily binds with unfolded protein or peptide substrates or folding intermediates through hydrophobic interactions [292]. For example, reduced PDI exposes smaller hydrophobic area and suppresses the aggregation of GAPDH folding intermediates [293]. This redox-regulated chaperone can unfold the cholera toxin A1 subunit as well [294]. Therefore, PDI is characterized as the redox-regulated chaperone in the ER, and it plays a critical part in protecting against neurodegeneration induced by oxidative stress and/or protein misfolding [295].

1.3.3 Subcellular distribution of PDI

Beside ER-residence, PDI also has non-ER locations, including in the nucleus, extracellular matrix and on the cell surface. Take the location of cell surface for example, PDI mediates the adhesion, secretion and aggregation of platelet [296], participates in the activation of HIV virus fusion [297], and facilitates infection of HeLa cells with mouse polyoma virus [298] and dengue virus [299]. In addition, both PDI and ERp57

interact with misfolded prion protein on the cell surface, which is crucial for prion accumulation and cell-to-cell transmission. PDI also leaks into the cytoplasm triggered by ER stress. The location of other cellular compartment indicates the wide range of biological functions of PDI.

1.3.4 PDI in the neurodegenerative diseases

PDI plays a critical role in the pathogenesis of neurodegenerative diseases, which are highly associated with accumulation of misfolded proteins within neurons, cellular toxicity, dysfunction, and cell death. PDI suppresses the synphilin-1 aggregation in neuroblastoma cells [300]. PDI also inhibits the α -synuclein aggregation in the cell free *in vitro* system [301]. Accumulation and aggregation of α -synuclein in neuronal cells are characteristic features of many neurodegenerative diseases known as synucleinopathies [302]. PDI is co-localized with torsinA in the ubiquitin-positive inclusions in the transgenic mouse model of dystonia [303]. PDI is also found in the inclusions and neurofibrillary tangles in the brain tissues from patients with Alzheimer's disease (AD) [304]. The hypoxia-ischemia injury in neuronal cells [305] and cardiomyocyte cells [306] is attenuated by PDI up-regulation. Taken together, with the enzymatic and chaperone activities, PDI could protect against protein misfolding and protein aggregation.

1.3.5 ER stress and the UPR in ALS

ER is the cellular organelle for newly synthesized secretory and membrane proteins. The lumen of ER contains molecular chaperones, quality control factors and folding enzymes that assist in the protein folding and trafficking [307]. However, it is estimated

that about 30% newly synthesized proteins are rapidly degraded, partially due to improper protein folding. This fast buildup of misfolded protein overwhelms the secretory ability of the ER, resulting in misfolded protein accumulation [308]. The situation will become worse if the ER environment is perturbed, including alterations in calcium levels, redox state, and failure to posttranslationally modify secretory proteins. Physiologically, ER stress is triggered by the mutated protein synthesis, the absence of cofactors, and a drastic increase in the amount of otherwise normal cargo proteins during cell differentiation [309]. In response to ER stress, the cell activates signaling cascades that attempt to cope with the altered conditions and restore the favourable folding environment. This molecular transduction system is known as UPR, which monitors the protein-folding capacity and the cell signal of the ER. It also help to prevent accumulation of unproductive and potentially toxic protein products [310]. The basic responses include transcriptional induction of chaperone genes to promote protein folding and activation the ERAD pathway to retro-translocate the misfolded proteins from the ER for proteasome-dependent degradation [311]. Recently, ER stress and UPR are implicated in a variety of diseases associated with the accumulation of aggregated proteins, such as, diabetes, tumour development, autoimmune disorders, viral infection, and neurodegenerative diseases, including ALS [231]. UPR is activated both in mSOD1 mice and human SALS patients [58]. UPR activation in motor neurons from mSOD1 mice occurs as early as postnatal day 5, long before ALS-symptom-onset. This finding indicates that ER stress occurs specifically in the motor neurons, and it occurs prior to the activation of other disease-associated mechanisms [143]. The mSOD1 interacts with Derilin-1, causing dysregulation of ERAD and leading to ER stress-induced ASK1

activation, apoptosis, and disease progression [197]. In addition, genetic ablation of ASK1, an ER-stress-activated transcription factor X-box-binding protein-1, significantly inhibits UPR activation and slows disease progression in mSOD1 mice [312]. Genetic ablation of Xbp1, an important modulator of the UPR, increases autophagy in motor neurons and delays disease onset and prolongs the survival of mSOD1 mice [313]. Treatment with salubrinal in mSOD1 mice, a small molecule inhibitor of ER stress, significantly delays disease progression [143]. ER stress is one of possible mechanisms of mSOD1-mediated toxicity. The presence of the up-regulation of Bip/Grp78 in mSOD1 over-expressing COS7 cells indicates that UPR is activated [51]. Caspase 12, another ER-associated molecule, is up-regulated and cleaved during the disease progression in mSOD1 mice [314]. Furthermore, the activation of ER-associated transcription factors is also observed in end-stage mSOD1 mice [53]. The UPR sensors, such as inositol-requiring kinase-1 (IRE1), pancreatic ER kinase (PERK) and activating transcription factor 6 (ATF6), exhibited increased expression in the spinal cords from SALS patients [58]. Crossed G85R mSOD1/PERK^{+/-} mice have an accelerated disease onset and shortened disease duration and lifespan, probably due to the loss-of-function mutation of PERK mediated by PERK^{+/-} [62]. Overexpression mSOD1 in neuro2a neuroblastoma cells induces ER stress, including phosphorylation of PERK, eIF2 α , and JNK, nuclear translocation of ATF6, XBP1 mRNA splicing, and caspase 12 activation. Treating the cell expressing mSOD1 with salubrinal suppresses the mSOD1-mediated aggregation process and cell death [315]. Mutation in the vesicle-associated membrane protein/synaptobrevin-associated protein B (VAPB) is implicated in late-onset ALS. VAPB is associated with intracellular membranes, such as ER lumens. VAPB mutation

disrupts the UPR and resulting in accumulation of misfolded proteins in the ER [316].

1.3.6 PDI in ALS

The expression of PDI is up-regulated in the spinal cord of mSOD1 mice at the pre-symptomatic, symptomatic, and end stages of ALS disease [54,58,192,317]. PDI expression is up-regulated in the spinal cords and cerebrospinal fluid (CSF) in SALS patients, compared to non-neurological controls [58]. PDI co-localizes with inclusions in motor neurons of mSOD1 mice and human ALS patients. PDI also collocates with VAPB inclusions in a *Drosophila melanogaster* model [318]. The up-regulation of PDI and recruiting of PDI to aggregated protein indicate that PDI protects against forming the mutant protein aggregates in ALS. Bacitracin, the broad disulphide isomerase inhibitor, dramatically increases the inclusions formation in NSC-34 cells expressing mSOD1. Overexpression of PDI in neuroblastoma cells suppresses the levels of insoluble mSOD1 and decreases inclusion formation and apoptotic cell death [54]. Interestingly, a small molecule that shares the same active site as PDI efficiently inhibits mSOD1 aggregation and inclusion formation [60]. Not only the expression, but the subcellular redistribution of PDI is also indicated in ALS. Varieties of integral ER membrane proteins, which belong to the reticulon family, can modulate PDI distribution [319]. Overexpression of reticulon leads to an alteration of PDI localization, from the normal ER evenly residence to a less homogenous punctuated pattern. Genetic ablation of the reticulon-4A, B protein leads to disease progress acceleration, probably by preventing the reticulon-mediated PDI redistribution [320]. However, the up-regulation of PDI expression can not provide a beneficial effect in ALS progression. In Parkinson's disease (PD) and AD, the

posttranslational modification of PDI by NO-mediated S-nitrosylation of the cysteine residues at the critical active site leads to inhibition of the enzymatic activity of PDI.

1.3.7 NO-mediated nitrosative stress in ALS

Nitric oxide (NO) plays an important role in the pathogenesis of ALS. NO is a gaseous free radical and has multiple effects. At a low or moderate level, NO plays a vital role in normal signal transduction; at a high level it can induce energy depletion-induced necrosis, apoptosis, and ER stress [321]. NO is derived from the terminal nitrogen atom of L-arginine through the catalytic activity of NO synthase (NOS), including two constitutive forms-neuronal NOS (nNOS) and endothelial NOS (eNOS), and the third subtype-inducible NOS (iNOS), which is induced by inflammatory stimuli. In the CNS, iNOS is induced mainly in microglia and astrocytes under pathological conditions [322]. Once iNOS expression is induced, it generates moderate to high levels of NO chronically, without any requirements for further activation [323]. In ALS, one characteristic pathological feature is the activation of microglia and astrocytes, which is associated with NO generation. In the spinal cords of mSOD1 mice, the nNOS-positive motor neuron depleted while iNOS-positive activated glial cells increased. This is correlated with up-regulation of NO generation [324]. Furthermore, the increased levels of NO in the spinal cords of mSOD1 mice are believed to be produced by iNOS located in astrocytes, which are activated by pro-inflammatory cytokines or oxidative stress through NF- κ b, JAK/STAT, and HIF-1 [325]. Reactive astrocytes are immunostaining-positive with iNOS antibody in the spinal cords of mSOD1 mice [326] and ALS patients [327]. Study indicates that iNOS mRNA, protein, and enzyme activity are up-regulated in the spinal

cords and brainstem of mSOD1 mice [328]. The up-regulation of iNOS in the spinal cords of mSOD1 mice has been observed by several other studies [329,330]. Pharmacological inhibition of iNOS with 1400W, a highly selective inhibitor of iNOS, leads to delayed disease onset and extended survival of mSOD1 mice [331]. Genetic deletion of iNOS gene significantly extends the life span of mSOD1 mice [326]. High levels of iNOS expression in glia results in excessive NO generation, which can induce neuronal depolarization, glutamate release, and neuronal death by inhibiting the mitochondrial cytochrome oxidase [332]. Additionally, NO can exert its neurotoxic by reacting with cysteine thiols of target proteins to form S-nitrosothiols. This modification is termed “S-nitrosylation”. S-nitrosylation is a covalent reaction that transferring NO to the thiol groups of cysteine residues of proteins. S-nitrosylation affects many cellular processes by altering both protein-to-protein interactions and protein function. NO-mediated S-nitrosylation of many proteins has been linked to neuronal death in many neurodegenerative diseases; those proteins include matrix metalloproteinase 9 (MMP-9), parkin, and glyceraldehyde 3-phosphate dehydrogenase (GAPDH) [333,334]. Cerebral ischemia promotes S-nitrosylation of MMP-9, stimulating its activity and resulting in the formation of stable sulfinic or sulfonic acid derivatives [335]. S-nitrosylation of parkin suppresses its E3-ubiquitin-ligase activity, inhibits its protective function, and promotes the cytotoxicity [336]. Study demonstrated that in PD and AD, NO-mediated S-nitrosylation of PDI plays a key role in the disease pathogenesis [300]. S-nitrosylation of PDI inhibits its function, which leads to the increase of polyubiquitinated proteins and accumulation of misfolded proteins.

1.3.8 S-nitrosylation of PDI in ALS

The NO-mediated nitrosative stress can induce ER stress, which induces UPR to upregulate the ER-resident chaperones to ameliorate the accumulation of misfolded/unfolded proteins. The molecular mechanism of NO-induced ER stress is yet to be determined. Also yet to be determined is how NO-mediated ER stress promotes accumulation of misfolded proteins in the neurodegeneration process. S-nitrosylation of PDI may provide some of the answers to those issues. In PD, excessive generation of NO can lead to S-nitrosylation of PDI, inhibiting its isomerase and chaperone function in protein refolding, resulting in defective protein folding and accumulation of misfolded and polyubiquitinated proteins, such as synphilin [300]. The molecular basis of S-nitrosylation of PDI may also apply to the pathophysiology of ALS. In ALS, mSOD1 inclusions and misfolded mSOD1 aggregates are highly associated with the disease. Furthermore, high molecular weight mSOD1 complexes have been identified within the ER. Inhibition of PDI activity by using bacitracin promotes the formation of mSOD1 aggregates in neuronal cells. PDI co-localizes with intracellular aggregates of mSOD1. ER stress and UPR have also been observed in both mSOD1 mice and ALS patients. The up-regulation of iNOS results in increased generation of NO in ALS. Interestingly, S-nitrosothiol levels were found to be abnormal in the spinal cords of mSOD1 mice. Combining the evidence together, it is rational to propose that S-nitrosylation of PDI is involved in mSOD1 aggregation in ALS. Under normal circumstance, PDI provides the first line of defense to correct protein misfolding, and mSOD1 could be the protein substrates of PDI [306]. However, under conditions of severe nitrosative stress triggered by excessive NO, PDI is S-nitrosylated, and this posttranslational modification of PDI affects its activity to correct mSOD1 misfolding in ER. Lastly, the misfolded mSOD1

accumulates in the ER and triggers ER stress and neurodegeneration.

1.4 Cerebral ischemia

Ischemic stroke is the second most common cause of death after ischemic heart disease. Ischemic stroke is a major cause of disability worldwide. The brain only accounts for 2% of the whole body weight in humans. Meanwhile, the human brain consumes up to 25% of all oxygen for the body, indicating that it requires a large and continuous supply of oxygen and glucose to maintain normal function and viability. In the animal model of ischemia, the concentration of brain glucose, glycogen, adenosine triphosphate (ATP) and phosphocreatine decrease immediately after the onset of ischemia, and nearly completely deplete within 10-12 minutes of ischemia [337]. It is well-accepted that the depletion of tissue energy reserves is rapidly followed by acidosis, glutamate-mediated excitotoxicity, free radical production, oxidative stress [338]. The biosynthesis of NO is a key factor in the pathophysiological response of brain ischemia [339]. Furthermore, the generation of NO can trigger a cascade of free radical reactions, resulting in modifications of cerebral plasticity and increasing blood-brain barrier (BBB) permeability, which may contribute to the progression of brain ischemia [340,341].

1.4.1 The involvement of iNOS in cerebral ischemia

After experimental cerebral ischemia, all three isoforms of NOS are up-regulated. Their patterns of expression differ both temporally and spatially. In a rat ischemic model, the nNOS-positive neurons increased as early as 15 min, and expression lasted for 24 h. The eNOS expression in cerebral vessels of the ischemic core peaked at 24 h [342], and NO generated from this source has a neuroprotective effect, by increasing the blood flow

in the penumbra area during the early stages of brain ischemia [343]. The iNOS expression is induced in glia cells in both experimental cerebral ischemia and human stroke [344,345], and this induction occurs later than nNOS and eNOS. The activity of iNOS following the transient ischemia increased gradually over time, and reached maximal levels after 24 h in stratum and 48 h in the cortex. The induction of iNOS mRNA expression is also associated with the duration of ischemia [346,347]. iNOS immunoreactivity is located in polymorphonuclear neutrophils, in astrocytes and in microglia. iNOS is expressed *in vitro* models of brain ischemia. However, the mechanisms of iNOS expression after brain ischemia are not fully elucidated. Pro-inflammatory cytokines are known to induce the iNOS expression. The levels of interleukin-1 β (IL-1 β) and TNF α increase significantly within a few hours of ischemia [348], and these cytokines trigger transcriptional activation of the iNOS gene [349]. Exogenously injecting IL-1 β into the cerebral ventricles directly induces iNOS expression along the injection tract. Hypoxia-inducible factor-1 α (HIF-1 α), containing a hypoxia response element in the gene promoter activates the iNOS gene following ischemia [350]. Studies show that NO produced by de novo iNOS expression contributes to the brain ischemic damage [351]. Selective iNOS inhibitors, such as aminoguanidine or 1400W, are able to reduce the infarct volume by 30-40%, which is associated with the improved neurological deficits produced by the infarct [352,353]. Antisense oligodeoxynucleotide to iNOS also has protective effects against brain-ischemia-induced injury [354]. The iNOS knockout animals show a significant reduction in infarct volume (-30%) and have better neurological outcome than wild-type littermates [355,356]. Many drugs or compounds that elicit neuroprotection against hypoxia/ischemia-induced

oxidative brain injury are shown to have the effect of inhibiting iNOS expression [357,358,359,360].

1.4.2 The involvement of NO in cerebral ischemia

NO and its further oxidation products are generally implicated in brain ischemia pathology. NO generated during ischemia can strengthen the lipid peroxidant activity, cause lesions of the cellular barrier, and further result in necrosis or apoptosis of neurons. In addition, it can reduce the vasoconstrictor response to arterial hypocapnia, damage the vascular endothelial cells, enhance the BBB permeability, suppress protein synthesis, and damage DNA structure [361]. NO is involved in the neurotoxicity of glutamate, abnormality of mitochondrial energy metabolism and impairment of antioxidant status in rat primary cultured neurons [321]. This may relate to the mechanisms of neurodegeneration and enhancement of apoptosis mediated by nitrosative stress [362]. For example, NO/NOS signaling system can trigger amyloid- β ($A\beta$) production through the beta-site APP-cleaving enzyme 1 (BACE1) pathway during and after acute focal brain ischemia in aged rats, and $A\beta$ stimulates ROS generation and mitochondria activity alteration, leading to apoptosis [363]. Over the last decade, more and more studies have demonstrated that NO can bind to the heme of soluble guanylate cyclase (sGC) and convert guanosine triphosphate to cyclic guanosine monophosphate (cGMP). This effect of NO is mediated through a chemical modification of cysteine residues, named S-nitrosylation, which plays pervasive roles in modulating protein functions. For example, in a rat model of brain ischemic injury, brain ischemia facilitates the S-nitrosylation of PTEN (phosphatase and tensin homolog deleted on chromosome 10). AMT, a specific

inhibitor of iNOS, suppresses S-nitrosylation of PTEN, indicating that endogenously generated NO is linked to S-nitrosylation of PTEN in transient global ischemia [364]. In cultured endothelial cells (ECs), acute hypoxia transiently up-regulates the NO generation through eNOS activation. By using biotin-switch assay coupled with 2-dimensional electrophoresis (2-DE), 11 proteins are found to have increased S-nitrosylation under hypoxia, including PDI [365].

1.4.3 The involvement of PDI in ischemic injury

Ischemic stress plays a key role in the pathogenesis of heart disease, stroke, diabetes, and cancer [366,367]. PDI is identified as a hypoxic-induced protein in both *in vitro* and *in vivo* models. PDI's mRNA level and protein level are enhanced in endothelial cells from human aortic and pulmonary artery [368,369]. Chronic hypoxic exposure induces the up-regulation of endothelial PDI, which protects cells against apoptosis and increases the cellular migration, adhesion, and tubular formation, and helps to improve coronary blood flow and protects the myocardium against infarction [370]. Up-regulation of PDI specifically in endothelial cells enhanced their ability to tolerate hypoxia [371]. In patients with myocardial infarction, PDI was up-regulated in the viable peri-infarct myocardial region with presence of heart failure, which significantly decreased the cardiomyocyte apoptotic rate and biventricular dilatation [372]. In the mice model of ischemic injury *in vivo*, adenoviral-mediated PDI overexpression prevents adverse cardiac remodeling and cardiomyocyte apoptosis. This protective action of PDI is believed to be due to its ability to relieve unfolded protein accumulation and its function to activate the SOD activity [306]. Induction of PDI expression in HL1 cells (the cardiomyocyte cell

line) confers protection from hypoxic-induced apoptosis. This anti-apoptotic effect of PDI is mediated by its action of increasing SOD2 activity by 80 %. SOD1 is considered to be a target of the anti-apoptotic action of PDI [372]. To fight against oxidative and nitrosative stress, several stress proteins are up-regulated to exert adaptive neuroprotection, including PDI. Overexpressing PDI in neurons protects cells against hypoxic/ischemic-induced cell death [373]. Overexpression of PDI in neuroblastoma SK-N-MC cells results in attenuation of the cell viability loss induced by hypoxia [374]. In an *in vitro* model of gerbils, PDI is up-regulated in response to transient forebrain ischemia in astrocytes and CA1 pyramidal cells [375]. It is believed that multiple causes of ER stress occur in neurons following cerebral ischemia/reperfusion, including depletion of ER Ca^{2+} , protein aggregation, decreased protein degradation, and accumulation of lipid peroxidation products in ER and Golgi structures [376]. Ischemic stress can drastically alter the workload of the ER and trigger UPR to adjust the folding capacity of the ER. The UPR is involved in the transcriptional activation of ER stress-related genes, including oxidoreductases, ubiquitin, and the PDI family. PDI facilitates the appropriate protein folding and prevent the protein misfolding during stress. It is plausible that PDI dysfunction will lead to accumulation of unfolded/misfolded protein. In the liver of diabetic rodents, the redox state of PDI is altered, shifting to its most reduced form. This affected PDI's functional ability, resulting in accumulation of misfolded protein in the ER lumen [377]. In the mice model of diabetes induced by streptozotocin, the redox state of PDI changes dramatically, and the oxidized PDI portion is markedly reduced by 60% [306]. In cultured ECs cells, S-nitrosylation of PDI is increased under acute hypoxia, with increased NO generation through eNOS activation

[365]. S-nitrosylation of PDI is involved in protein misfolding and aggregation in several neurodegenerative diseases. It is reasonable to hypothesize that NO-mediated S-nitrosylation of PDI is involved in cerebral ischemia, and it is associated with protein aggregates formation in hypoxic/ischemic brain injury.

1.4.4 The involvement of protein aggregation in cerebral ischemia

Ischemic/reperfusion caused accumulation of ubiquitin-conjugated protein aggregates and aggregate-associated organelles following forebrain ischemia [378,379]. Protein aggregation in the subcellular fractions is likely to cause multiple organelle failure and delayed neuronal death after cerebral ischemia through several mechanisms [380]. This protein aggregation is virtually an irreversible process, which is associated with the irreversible aggregation of translational components. This translational complex components include chaperones and protein folding enzymes, such as heat-shock cognate protein 70 (HSC70) and co-chaperone Hdj1 [381,382]. The proteasomes are disassembled and aggregated after an episode of brain ischemia, which leads to proteasomes dysfunction. The ubiquitinated-proteins are too numerous to be degraded and are trapped into the aggregates after brain ischemia [7]. These ubiquitinated-protein aggregates and stress granules converge in CA1 neurons after reperfusion may contribute to sustained translation arrest and vulnerability of CA1 pyramidal neurons [383]. In the cell cultured model of stroke, the formation of ubiquitinated-protein aggregates was accompanied by decreased proteasome activity. Blocking the $\text{Na}^+ - \text{K}^+ - \text{Cl}^-$ cotransporter isoform 1 (NKCC1) activity attenuates the aggregates formation and preserves proteasome function following OGD/reperfusion [384]. When cell are stressed, some

newly synthesized protein will folded and some already synthesized protein will unfolded, thus forming two types of denatured protein without normal spacious structures [385]. To protect the cells against death and maintain their function, the denatured or aggregated proteins should be rescued or eliminated. Chaperones and ubiquitin proteasome system are involved in these processes, and the proteasome is trapped by protein aggregation and results in its dysfunction [386,387]. Further study also demonstrates that proteasome is inactivated, resulting from protein aggregation after brain ischemia [7]. Chaperones assist protein folding under both physiological and stress conditions [388], and assemble or disassemble protein complexes to suppress protein aggregation [389,390]. For example, overexpressing the chaperone Hsp70 in hippocampal CA1 neurons reduces the protein aggregation formation, and increases neuronal survival [391]. Ischemic preconditioning can prevent protein aggregation after cerebral ischemia [392]. This beneficial effect is mediated by the induction of chaperone Hsp70 expression in CA1 neurons [393].

Chapter 2. Hypotheses and Aims

2.1 Hypotheses

The overall hypothesis of this thesis was that oxidative/nitrosative stress-induced posttranslational modifications of proteins contribute to the protein aggregates formation. Specifically, it was hypothesized that: (1) Oxidative modification of Cys111 promotes the formation of disulfide bond-independent mSOD1 aggregates; (2) S-nitrosylated modification of PDI contributes to the mSOD1 aggregates formation in ALS; and (3) NO-mediated S-nitrosylation of PDI is associated with SOD1-linked ubiquitination and aggregation in cultured astrocytes following OGD/reperfusion.

2.2 Rationales and Specific Aims:

Rationale and Specific aim 1: The SOD1 aggregation and oxidative stress are associated with the pathogenesis of ALS. Oxidative stress is believed to further augment the SOD1 aggregates formation, and HMW complexes and insoluble SOD1 species become more evident when the cultured neuronal cells expressing mSOD1 are exposed to increasing concentration of H₂O₂. Given the biochemical characteristics of SOD1, when SOD1 is travelling along the spinal cord, the most affected tissue in ALS, the chance of oxidative insults to SOD1 increases dramatically, especially to the mSOD1. Cys111 locates in the Greek-key loop near the dimer interface, facilitating the oxidative modification of thiol groups of the cysteine residues. Various studies have demonstrated that Cys111 would be a potentially crucial residue in provoking SOD1 aggregates formation. Furthermore, using specific antibody against Cys111-SO₃H, the presence of Cys111-peroxidized-SOD1 was detectable in the spinal cords of mSOD1 mice. The

project was designed to:

Determine the redox state of SOD1 cysteine residues in the G37R transgenic mice during the progression of ALS and under oxidative stress induced by H₂O₂ (Chapter 3).

Determine the formation of HMW complexes of SOD1 and the oxidative modification of Cys111 during the progression of ALS (Chapter 3).

Establish the correlation between oxidative modification of Cys111 and the formation of mSOD1 aggregates in ALS (Chapter 3).

Rationale and Specific Aim 2:

The involvement of oxidative/nitrosative stress is implicated in the pathophysiology of ALS. One of the free radicals, NO, increases due to the up-regulation of iNOS expression, and NO can exert its neurotoxic effects by S-nitrosylation of proteins. S-nitrosylation of PDI was identified in PD, resulting in functional inhibition and aggregates accumulation. In ALS, PDI expression is up-regulated in the spinal cords of mSOD1 mice, as well as in the spinal cords and CSF of SALS patients. PDI co-localizes with mSOD1-positive inclusions in ALS. Up-regulation of PDI expression does not improve disease progression. It's probably due to NO-mediated S-nitrosylation of PDI, which compromises the protective effect of PDI defending against protein misfolding. Since mSOD1 interacts with PDI, dysfunction of PDI due to S-nitrosylation will promote the accumulation of the misfolded mSOD1 in the ER, trigger ER stress and

neurodegeneration. The project was designed to:

Determine the changes in iNOS expression and the NO generation during the progression of ALS (Chapter 4).

Determine the level of S-nitrosylated PDI during the progression of ALS (Chapter 4).

Establish the correlation between S-nitrosylation of PDI and the formation of mSOD1 aggregates in ALS (Chapter 4).

Rationale and Specific aim 3:

NO produced by de novo iNOS expression is believed to contribute to the cerebral ischemic damage. The role of NO in the mechanism of neurotoxicity after ischemic injury is not fully understood. Neurotoxicity of NO can be mediated through S-nitrosylation, which plays a pervasive role by modulating protein activity and cellular function. PDI is identified as a hypoxic-induced protein. Chronic hypoxic exposure induces the up-regulation of PDI, which enhances the ability of cells to tolerate hypoxia. The protective action of PDI is partially based on its ability to relieve unfolded/misfolded protein accumulation and its function to enhance the SOD activity. However, the accumulation of ubiquitin-conjugated protein aggregates is implicated in cerebral ischemia, and protein aggregation in the subcellular fractions is likely to cause multiple organelle failure and delayed neuronal death through several mechanisms. One of the mechanisms is assumed to be the S-nitrosylation of PDI. The excessive NO generation in

cerebral ischemia may promote the S-nitrosylation of PDI. Dysfunction of PDI due to S-nitrosylation may be associated with protein misfolding and aggregation. The project was designed to:

Determine the changes of iNOS expression and the NO generation in cultured astrocytes following OGD/reperfusion (Chapter 5).

Determine the changes of S-nitrosylation of PDI in cultured astrocytes following OGD/reperfusion (Chapter 5).

Establish the correlation between S-nitrosylation of PDI and the formation SOD1-linked ubiquitinated-protein aggregates in cerebral ischemia (Chapter 5).

Chapter 3. Oxidative modification of cysteine 111 promotes disulfide bond-independent aggregation of SOD1

3.1 Introduction

Amyotrophic lateral sclerosis (ALS) is an adult-onset neurodegenerative disease characterized by selective loss of motor neurons in the spinal cord, brain stem, and motor cortex leading to muscle weakness, atrophy and progressive paralysis [394,395,396]. Approximately 5-10% of ALS cases are inherited (autosomal dominant), and 90-95% of all cases are sporadic ALS [396]. About 20~25% of the familial cases are caused by mutations in the gene encoding copper-zinc superoxide (SOD1) [396,397]. To date, more than 150 mutations spanning all five exons of the *SOD1* gene have been reported in familial ALS (www.alsod.org). Strong evidence shows that the mutant SOD1 enzymes cause motor neuron degeneration by a gain of toxic properties, rather than a loss of its superoxide dismutation function. Transgenic mice expressing mutant SOD1^{G93A} or SOD1^{G37R} developed the motor neuron disease despite an elevation in SOD1 activity levels [397,398]. In addition, SOD1 knockout mice did not show any ALS symptoms [183]. However the nature of the gain-of-function toxicities in mutant SOD1 proteins is not clear.

Oxidative stress and aggregation of SOD1 are hallmark features of SOD1-linked ALS [184,399], and oxidation of SOD1 could lead to a toxic gain-of-function [264]. Studies show that mildly oxidizing reagents, including hydrogen peroxide [242,400], copper chloride, ascorbic acid [220,224], peroxynitrite [265] and oxidized glutathione SOD1 [266] are able to trigger aggregation of both wild-type SOD1 and mutant SOD1. In

fact, the main product of SOD1 catalytic reaction, hydrogen peroxide, has been shown to be a potent aggregation reagent for the SOD1 protein [242,400]. Wild-type SOD1 has been shown to exhibit aggregation after oxidation, and the oxidized wild-type SOD1 gains properties like FALS mutant SOD1s [267]. However, when compared with their wild-type counterpart, most mutant SOD1s are more susceptible to oxidation-induced aggregation [401]. These findings suggest that oxidized SOD1 may be a causing factor in triggering SOD1 aggregation and acquiring a toxic gain-of-function.

How does oxidative modification contribute to SOD1 aggregation? Previous studies suggested that disulfide bond formation between cysteine residues of SOD1 initiate the SOD1 aggregation [402,403,404]. However, other studies have shown that high molecular weight SOD1 complexes are present in cell and mouse models under completely reducing condition, which suggests that disulfide bonds may not be the only structures that mediate the formation of SOD1 aggregates [45,261,405,406]. Karch and colleagues also pointed out that the mechanism of SOD1 aggregation did not appear to require extensive intermolecular disulfide linkages between cysteine residues [406]. In the present study, we systematically examined the redox state of SOD1 cysteine residues by detecting their reactivity with MalPEG in the G37R transgenic mouse model at different stages of the disease, and under oxidative stress which can be reconstituted by inducing the H₂O₂ to the tissue lysates. Here we show that with the progression of the disease, increased levels of oxidative insult facilitated the oxidation of thiol groups of cysteine residues. We also detected the formation of SOD1 multimer at different stages of the disease. We also show that the formation of aggregates was not mediated by disulfide bonds. Under physiological conditions, cysteine 111 was free, but was prone to oxidative

modification by providing thiolate anion (S⁻). This oxidative modification of cysteine 111 may promote disulfide bond-independent aggregation of SOD1.

3.2 Materials and Methods

3.2.1 Construction of Expression Vectors

Entire wild-type human SOD1 gene was cloned by RT-PCR from total RNA extracted from wild-type human SOD1 transgenic mouse, and subcloned into pcDNA3.1 between the *Bam*HI/*Xho*I sites (pcDNA3.1-hSOD1). Mutations were introduced into pcDNA3-hSOD1 with a QuickChange site directed mutagenesis kit (Stratagene, La Jolla, CA). Primers pairs for each mutant were as follows:

5'-CTGCTGACAAAGATGCTGTGGCCGATGTGTC-3';		reverse
5'-GACACATCGGCCACAGCATCTTTGTCAGCAG-3';	G37R:	forward
5'-GTGGGGAAGCATTAAAAGACTGACTGAAGGCC-3';		reverse
5'-GGCCTTCAGTCAGTCTTTTAATGCTTCCCCAC-3';	C6S:	forward
5'-CGAAGGCCGTGTCCGTGCTGAAGGGC-3';		reverse
5'-GCCCTTCAGCACGGACACGGCCTTCG-3';	C57S:	forward
5'-GATAATACAGCAGGCTCTACCAGTGCAGGTCC-3';		reverse
5'-GGACCTGCACTGGTAGAGCCTGCTGTATTATC-3';	C111S:	forward
5'-CTCAGGAGACCATTCCATCATTGGCCGCAC-3';		reverse
5'-GTGCGGCCAATGATGGAATGGTCTCCTGAG-3';	C146S:	forward
5'-GGAAGTCGTTTGGCTTCTGGTGTAATTGGGATCG-3';		reverse
5'-CGATCCCAATTACACCAGAAGCCAAACGACTTCC-3'.		

Multiple mutants were introduced by repeatedly applying the mutagenesis kit to produce the required mutations.

All the plasmid constructions were verified by automated sequencing.

3.2.2 Cell Culture, Transfection, and Antibodies

PC12 cells, a line derived from a pheochromocytoma of the rat adrenal medulla, were maintained in Dulbecco's modified Eagle's/F-12 medium supplemented with 10% horse serum, 5% fetal calf serum, 4 mM L-glutamine, 5 units/ml penicillin, and 50 µg/ml streptomycin, at 37 °C in an atmosphere of 5% CO₂ in air. The adherent HEK293 cell line was maintained routinely in DMEM (Sigma-Aldrich, St. Louis, MO) supplemented with 10% fetal calf serum and 1% (v/v) penicillin/ streptomycin solution (Penicillin 1,000 IU, Streptomycin 10,000 mg/mL, Invitrogen Corp., Carlsbad, CA) at 37°C in a humidified incubator with a 5% CO₂ atmosphere. Transfections for transient expression of each vector (1.5 µg of DNA/3 × 10⁵ cells) were performed using Lipofectamine 2000 reagent (Invitrogen) according to the manufacturer's instructions. After a 4h incubation period with transfection reagents, cells were shifted with normal growth medium and cultured for 48 h. Primary antibodies were as follows: rabbit polyclonal anti-SOD1 antibody (Santa Cruz Biotechnology), mouse monoclonal anti-β-actin antibody (Sigma), and the specific rabbit polyclonal antibody against Cys111-peroxidized SOD1 (anti-C111ox-SOD1) [261]. Secondary antibodies used for regular immunoblots were anti-rabbit or anti-mouse IgG conjugated with horseradish peroxidase (Amersham Pharmacia Biotech). Cells were scraped off the plate in culture medium, collected by centrifugation, washed in PBS, and resuspended in 60 µl of PBS containing a protease inhibitor mixture (Sigma). Cell suspension was subjected to three freeze/thaw cycles in liquid nitrogen and centrifuged at 20000 × g for 10 min at 4 °C and supernatants were

collected for analysis.

3.2.3 Transgenic Mice

B6.Cg-Transgenic (SOD1*G37R) 42Dpr/J mutant SOD1 transgenic mice and wild-type mice were obtained from the Jackson Laboratory. Mice were genotyped by PCR with the following sense and antisense primers: 5'-CATCAGCCCTAATCCATCTGA-3', 5'-CGCGACTAACAATCAAAGTGA-3'. Disease course was monitored by a temporal profile of body weight and hindlimb extension reflex once a week using both male and female mice. Briefly, mice were suspended by the tail and the extent of hindlimb extension was evaluated as follows: a score of 3 corresponds to normal extension, 2 corresponds to the extension of only one hindlimb and 1 corresponds to absence of hindlimb extension reflex. Disease onset was determined as the time when mice reached their peak body weight before the denervation-induced muscle atrophy and weight loss. End-stage was defined as the time at which the mouse could not right itself within 30 s when placed on its side. An endpoint was frequently used for SOD1 mutant mice and was consistent with the requirements of the Animal Care and Use Committee of the University of Manitoba. Five-month-old mice were pre-symptomatic, disease-onset occurred when mice were 10 months old, and 12-month-old mice were considered symptomatic mice. The use and maintenance of the mice described here were performed in accordance with the Guide of Care and Use of Experimental Animals of the Canadian Council on Animal Care. Mice tissues were collected and homogenized in 10 volumes of lysis buffer consisting of 1% (w/v) Triton X-100, 50 mM Tris-HCl, Ph 7.4, 300 mM NaCl, 5 mM EDTA, 0.02% (w/v) sodium azide,

10 mM iodoacetamide, 1 mM PMSF and 2 µg/ml leupeptin. Homogenates were centrifuged at $20000 \times g$ for 30 min at 4 °C and supernatants were collected for analysis. Protein concentration was measured by the BCA method as described by the manufacturer (Pierce).

3.2.4 Detection of Accessible SOD1 Cysteines in Tissue and Cell Lysates

Soluble tissue lysates containing a total of 10 µg protein from transgenic mice at different stages of ALS were modified with MalPEG (mono-methyl polyethylene glycol 5'000 2-maleimidoethyl ether, Sigma) as previously described [240]. MalPEG modification is a sensitive method of detecting sulfhydryl group oxidation in specific proteins in a Western blot format. Once MalPEG forms a covalent bond with protein, the MalPEG-protein conjugate can be detected as a band shift by Western analysis. Equal volume samples were incubated for 20 minutes in the presence of variable amounts of H₂O₂ at 25 °C. Then 3 mM MalPEG was added to the above solution for 1 h at 25 °C. The same modification with MalPEG was also applied to cell lysates. The addition of MalPEG to accessible cysteines increases the subunit mass of SOD1 by 5 kDa/modification. The reaction was competitively terminated by 5% β-mercaptoethanol and ran on 15% SDS-PAGE. SOD1 reacting with MalPEG was quantified as MalPEG SOD1 immunoreactivity per total SOD1 immunoreactivity.

3.2.5 Chemical Cross-linking

The chemical cross-linking was performed as previously published [407]. Briefly, the supernatants of cell lysates (protein concentration adjusted to 2 µg/µl with lysis buffer

were incubated with disuccinimidyl glutarate (DSG, Pierce, 1mM final concentration) for 1 h at room temperature. DSG is a water-insoluble homobifunctional N-hydroxysuccinimide ester (NHS-ester) crosslinker often used for conjugating ligands to cell-surface receptors. It is the simplest and most commonly used reactive group for crosslinking and labeling protein and peptides. DSG can react with primary amines on the N-termini of peptides and the ϵ -amine of lysine residues, forming a stable, covalent amide bond and releasing the NHS groups. The reaction was stopped by adding Tris (pH 7.5, 50 mM final concentration). The reaction mixtures were boiled with 6 × SDS-PAGE loading buffer, resolved by 15% SDS-PAGE followed by Western blotting.

3.2.6 Western Blotting Analysis

Supernatants containing a total of 10 μ g protein were loaded on 15% sodium dodecyl sulphate polyacrylamide gel (SDS-PAGE) for electrophoresis and then transferred to the PVDF membrane. Membranes were blocked with 5% (w/v) milk in TBS-T buffer (10 mM Tris-HCl, pH 7.5, 150 mM NaCl, 0.05% Tween-20) for 1h and incubated with antibodies against SOD1 for 2 h at room temperature. Blots were washed three times in TBS buffer and then incubated with the appropriate secondary antibodies for 1h at room temperature. Peroxidase activity was visualized with the Enhanced Chemiluminescent Substrate (PerkinElmer USA) according to the manufacturer's instructions. Chemiluminescent signals were captured on autoradiography and were used to assess protein content.

3.2.7 Statistical analysis

Signals on films were quantified using Quantity One Analysis Software (Bio-Rad). The results were expressed as means \pm SE. Statistical significance of differences among means (more than 2) were determined by analysis of variance (one-way ANOVA) with post hoc comparison of more than 2 means by the *Bonferroni* method using SPSS13.0 software. Student's *t*-tests were also carried out for statistical analysis of the difference between 2 means. Specifically, the intensity of MalPEG modified SOD1 from 10 month old mice were compared with 5 month old mice. Values of $P < 0.05$ were considered significant.

3.3 Results

3.3.1 Cysteine 111 residue of SOD1 existed in sulfhydryl state (-SH) under normal circumstance.

MalPEG, an alkylating agent linked with 5 kDa PEG, easily reacts with sulfhydryl groups of cysteine residues and causes a 5 kDa increase in molecular weight per one modification on SDS-PAGE. The oxidized sulfur atom of cysteine residues cannot be modified by MalPEG. To study the human SOD1 cysteine residues reactivity with MalPEG, we mutated human SOD1 in each of its four cysteine residues and tested the accessibility of these mutations to MalPEG modification. In human SOD1, Cys57 and Cys146 form disulfide bond, but Cys6 and Cys111 are free. Serine was chosen as a substitute for cysteine as a conservative mutation. When plasmids carried various human SOD1 genes were transfected into PC12 cells, the human SOD1 protein were expressed in the cells. Since the PC12 is a cell line derived from a pheochromocytoma of the rat adrenal medulla, we could detect two SOD1 species, the human SOD1 (the upper band)

and the rat endogenous SOD1 (the lower band). Seeing as the rat endogenous SOD1 has serine at position 111, the control group without any transfections showed no migration (Fig. 3-1). In this way, human SOD1, the upper band, could be separated from the rat endogenous SOD1 in PC12 cells. After transfection, cells were lysed and the supernatants were modified by MalPEG. This was followed by reducing SDS-PAGE and Western blotting. When Cys111 was mutated to serine, it became unmodifiable by MalPEG, while the other cysteine-residue-mutated SOD1s behaved just like wild-type SOD1, which could be dramatically modified by MalPEG (Fig. 3-1). This result indicates that Cys111 is a primary site of MalPEG modification. Although Cys6 is also a free cysteine, Cys6 was less reactive to MalPEG, probably because Cys6 exists in a β -sheet and is buried within the SOD1 molecule.

3.3.2 Human mutant SOD1 cysteine residues exhibited decreased accessibility to MalPEG modification accompanied with appearance of an additional upper band under increased oxidative stress.

To determine the reactivity of cysteine residues in human mutant SOD1 from G37R transgenic mice with MalPEG under oxidative stress induced by H_2O_2 , we treated the lysates of G37R transgenic mice spinal cord with variable amounts of H_2O_2 for 20 minutes. As shown in Fig. 3-2a, the labeling of MalPEG was decreased with the increased concentration of H_2O_2 . In addition, human mutant SOD1 generated an additional upper band when incubated with H_2O_2 . It was strongly suggested that this upper shift band in reducing SDS-PAGE was a Cys111-peroxidized SOD1 subunit, containing sulfinic acid ($-SO_2H$) or sulfonic acid ($-SO_3H$) [261]. To confirm this, the

G37R extracts were treated with H₂O₂ and immuno-detected by an anti-C111ox-SOD1 antibody, which specifically recognizes oxidized SOD1 [261]. As expected, the upper band increased in abundance with the increase of the concentration of H₂O₂ (Fig. 3-2b). The extraction process could cause the secondary air oxidation during sample preparation, and thus the Cys111-peroxidized SOD1 band appeared before H₂O₂ treatment. The antibody also detected a 25 kDa band, which was thought to be non-specific because it was also detected in non-transgenic mice (Fig. 3-3b). These results indicated that the sulfhydryl group (-SH) of Cys111 in human SOD1 was oxidized, and thus less accessible to MalPEG modification under oxidative stress.

3.3.3 Mutant SOD1 was oxidized and the accessibility to MalPEG modification was decreased with the progression of the disease.

We compared the redox state of SOD1 cysteine residues in transgenic mouse at different stages of the disease by using MalPEG modification. At the onset stage (10 m) of the disease in the G37R mice, SOD1 (MP) 2, which reveals SOD1 modified with two MalPEG molecules, was significantly reduced (Fig. 3-3a). The percentage of MalPEG modified-SOD1 in total human SOD1 was reduced as compared to the pre-symptomatic stage (5 m). The reduction was statistically significant (Fig. 3-3a). By contrast, in wild-type SOD1 transgenic mice, neither the intensity of the MalPEG modified-band nor the percentage of MalPEG-modified SOD1 in total human SOD1 (Fig. 3-3a) showed a significant change between these two stages.

3.3.4 Cys111-peroxidized SOD1 was increased with the progression of the disease.

Next, we examined the involvement of Cys111-peroxidized SOD1 in the G37R mouse model of ALS. To prevent secondary oxidation of thiol group during sample preparation, the spinal cords were homogenized in lysate buffer containing iodoacetamide (IA). As shown in Fig. 3-3b, although the Cys111-peroxidized SOD1 was not detected in young G37R transgenic mice spinal cord (2 m), the level of Cys111-peroxidized SOD1 increased with the progression of the disease, and peaked at the end stage of the disease (13 m).

3.3.5 Oxidative stress induced by H₂O₂ promoted the formation of disulfide bond-independent SOD1 multimers both in wild-type and G37R transgenic mice, which increased with disease progression

Oxidative stress can be reconstituted by introducing H₂O₂ to the tissue lysates. The spinal cord lysates of WT SOD1 transgenic and G37R transgenic mice were incubated with H₂O₂, and then subjected to reducing SDS-PAGE and Western-blotting. SOD1 bands in the high molecular weight (HMW) region increased with the increased concentration of H₂O₂ from 0 to 1 mM, in both wild-type and mutant SOD1. However, the increase of HMW in G37R mutant was significantly higher than in wild-type SOD1 (Fig. 3-4a). Seeing as all the samples were treated with the reductant β -ME before being loaded onto the gel, these HMW bands were thought to be irreversibly cross-linked SOD1 multimers instead of inter-molecular disulfide bond-dependent multimers. Next, we examined the formation of SOD1 multimers at different disease stages of ALS. The formation of SOD1 multimer was increased in G37R transgenic mice as the disease progressed, while wild-type SOD1 did not show any multimer formation (Fig. 3-4b). The

multimer bands are still present on SDS-PAGE gels under completely reducing conditions, suggesting that the increase in the abundance of SOD1 multimers was not a consequence of disulfide cross-linking.

3.3.6 C111S mutation inhibited the formation of aggregation in mutant SOD1.

Given the critical role of oxidative modification of sulfhydryl group (SH) of cysteine 111 in SOD1 aggregation, we hypothesized that mutation in C111S would prevent SOD1 from forming HMW complexes. We transfected HEK293 cells with pcDNA3 plasmids coding for wild-type SOD1 and various SOD1 mutants, harvested cells 48 h after transfection, and incubated the fresh lysates with an amino-reactive bi-functional cross-linker, DSG. Only a single band corresponding to monomeric SOD1 was observed in the absence of DSG for both wild-type and mutant SOD1s. In the presence of DSG, species corresponding to both monomeric and dimeric SOD1 were detected in all SOD1s tested, indicating that SOD1 molecules were covalently cross-linked to stabilize the dimeric state. However, although DSG-treated G37R and G93A mutants formed HMW complexes, C111S and wild-type SOD1 did not form an appreciable fraction of HMW complexes. In addition, the fraction of HMW complexes was significantly reduced in cells transfected with G93A/C111S combined mutation (Fig. 3-5), which indicated that C111S mutation inhibited the ability of G93A mutant SOD1 to form aggregates and that cysteine 111 was required for the formation of aggregation.

3.4 Discussion

It is well-established that SOD1 aggregation is a common property of mutant SOD1 linked to fALS. What is not understood, however, are the mechanisms by which this

aggregation occurs. Our results demonstrate that oxidative modification of cysteine 111 is required for the formation of SOD1 aggregates.

Human SOD1 has four cysteine residues — cysteine 6, cysteine 57, cysteine 111 and cysteine 146. An intramolecular bond between cysteine 57 and cysteine 146 is found in the natively folded SOD1 holoenzyme. This intramolecular disulfide bond is conserved, and contributes to the highly stability of SOD1. In addition, the formation of this intramolecular disulfide bond make cysteine 57 and cysteine 146 lose their integrity. Compared to cysteine 57 and cysteine 146, cysteine 6 and cysteine 111 are intact and not conserved [402]. Mouse and rat SOD1 possess only three cysteine residues in total (equivalent to position 6, 57 and 146 in the human SOD1) and the codon 111 encodes a serine. In human SOD1, cysteine 111 is located in the Greek key loop near the dimer interface and is highly reactive. Reversible oxidation of cysteine to disulfide (-S-S-) or sulfenic acid (-SOH) is readily accomplished by thiols, such as DTT, 2-ME or glutathione, while oxidation to sulfinic acid (-SO₂H) or sulfonic acid (-SO₃H) is not reduced by these thiols under physiological conditions [403]. Our results show that mouse endogenous SOD1 from non-transgenic mice (data not shown) and rat endogenous SOD1 cannot be modified with MalPEG. Under normal circumstances cysteine 111 of WT human SOD1 exists in sulfhydryl state, while other cysteine residues exists in a disulfide (-S-S-) state. C111S mutation therefore leads to inaccessibility of MalPEG modification (Fig. 1). The SOD (MP) 1 indicates that one cysteine residue of human SOD1 is modified by MalPEG. This happens because human SOD1 expressed in PC12 cells has the full capacity to form intramolecular disulfide bonds, while intermolecular disulfide bonds can not be imitated. Therefore, the SOD (MP) 2, which likely represents

SOD1 dimer that has an intermolecular disulfide bond between SOD1 molecules, can not be detected as shown in Fig. 3-1. This result indicates that the sulfhydryl group (-SH) of cysteine 111 in human SOD1 is the main source for alkylation: the sulfhydryl group (-SH) of cysteine 111 in human SOD1 can provide thiolate anion (S-) for the oxidative modification. Our *in vitro* study also reveals that, under oxidative stress, cysteine residues in mutant SOD1 exhibit decreased accessibility to modification by MalPEG (Fig. 3-2a) because of an increased level of Cys111-peroxidized SOD1 (Fig. 3-2b). Since MalPEG is a sensitive way of detecting protein sulfhydryl group (-SH), the decreased accessibility to MalPEG modification suggests that, under oxidative stress, the sulfhydryl group (-SH) of cysteine residues is reversibly oxidized to thiolate anion (S-). Using the specific anti-C111ox-SOD1 antibody, we demonstrate that, under oxidative stress the thiolate anion (S-) is further oxidized to irreversible sulfinic acid (-SO₂H) or sulfonic acid (-SO₃H). Importantly, similar oxidative modifications of SOD1 exist in the progression of ALS. Cysteine residues of G37R mutant SOD1 is less accessible to MalPEG modification as the disease progresses (Fig. 3-3a). When exposed to H₂O₂, the G37R mutant SOD1 can be oxidized to sulfinic acid (-SO₂H) and sulfonic acid (-SO₃H) (Fig. 3-3b) as detected by the specific anti-C111ox-SOD1 antibody [261]. In addition, the oxidative modification of cysteine 111 is increased with the progression of the disease, along with the accumulated oxidative stress. Our results thus provide direct evidence that, of all the cysteines, cysteine 111 is the most sensitive to oxidative stress. Interestingly, oxidized SOD1 (Cys111-peroxidized SOD1) and mutant SOD1 are conformationally similar, and oxidized SOD1 is present in SALS spinal cord tissues. Both G93A mutation and cysteine 111 sulfonic acid moiety (-SO₃H) can induce the formation of the

conformational epitope, which could be detected in SALS spinal cord tissues [45]. Oxidative stress induced by H₂O₂ has been shown to promote the formation of non-native oligomers and decrease detergent solubility of mutant SOD1s [408]. The discrete aggregates containing mutant SOD1 in a *C. elegans* model is also present when challenged with an oxidative stress inducer [409]. These results are consistent with our findings that the SOD1 multimer formation is increased under the H₂O₂-induced oxidative stress both in wild-type and G37R transgenic mice (Fig. 4a). The amount of multimers in G37R mutant SOD1 is much higher than in wild-type SOD1, This suggests that it is much easier to form aggregates under oxidative stress in mutant SOD1 than in wild-type SOD1. It also suggests that wild-type SOD1 can be induced to form aggregates under oxidative insults (Fig. 4a). In the G37R SOD1 transgenic mice, the levels of this multimers start to increase from the onset of ALS symptoms, while there are no detectable SOD1 multimers in the wild-type SOD1 transgenic mice in any disease stages (Fig. 3-4b).

Previous studies indicate that the formation of disulfide bond mediated by cysteine residues can initiate oligomerization or provide the major bonding force to stabilized aggregate structures [234,236]. These observations support the idea that adventitious oxidation of thiols to disulfide leads to SOD1 multimerization and aggregation of the mutant protein [234]. However, recent studies suggest that the role of cysteine residues in SOD1 in modulating the SOD1 aggregation likely involves mechanisms other than disulfide crossing linking [237,239]. Our results show that the high molecular weight multimers induced by oxidative stress are not mediated by disulfide bond (Fig. 3-4). These multimers are SDS-resistant complexes and remain intact after being boiled in

Laemelli's sample buffer (typically containing 0.1–2.0% SDS and 5% β -mercaptoethanol). Other studies have also identified high molecular weight structures in denaturing SDS-PAGE in tissues from G93A mutant transgenic mice [410,411]. The SOD1 SDS-resistant complexes seen in SDS-PAGE generally range in size from dimers up to small oligomers (Fig. 3-4). A recent study has suggested that these SOD1-containing oligomers may be held together with covalent bonds and contain covalently modified SOD1 proteins [263]. Our results also suggest that the SOD1 SDS-resistant complexes could be a posttranslationally modified SOD1 species that is covalently linked by mechanisms other than disulfide linkages. Recently, Fujiwara et al reported that cysteine 111 is a primary target for oxidative modification and that oxidatively modified SOD1 accumulates in pathologic structures in G93A mutant SOD1 transgenic mice [261].

Our data supports the idea that oxidative modification of cysteine 111 promotes the formation of the disulfide bond-independent aggregation of SOD1. When cysteine 111 is mutated to serine, the mutant SOD1 fails to aggregate and behaves like wild-type SOD1. When C111S mutation is combined with G93A FALS mutations, the formation of HMW complexes decreases dramatically compared to the single G93A mutation (Fig. 3-5). Similar reductions in SOD1 aggregates are reported when C111S mutation is combined with A4V or C146R [403]. Studies also suggest that cysteine residues mediate the mutant SOD1 accumulation in the mitochondrial fraction; cysteine 111 is a key mediator of injury to mitochondria [240]. It has been reported that mutant SOD1 can accumulate in an aggregated state in the mitochondria of motor neurons in the spinal cord of mutant transgenic mice [412]. Since mitochondria is implicated in the production of oxidative

stress and is a target of ROS [413], it is tempting to speculate that mitochondria are the primary site for SOD1 oxidation.

It is interesting that the mouse SOD1, lacking of cysteine 111, is able to develop an ALS-like disease marked by hind-limb paralysis when the G86R mutant (corresponding to the G85R mutant of human SOD1) is overexpressed in mice [414]. This may be due to different protein species as mouse and human SOD1 proteins differ in sequence at 27 positions. The conformational change of mouse SOD1 due to exogenous genetic modification can trigger the instability of the protein. However, the spontaneous SOD1 mouse mutant is not disease-related, seeing as the mice expressing active endogenous SOD1^{E77K} are phenotypically normal at one year. The G86R mutant is a severe destabilizing mutation that affects the conformational structure of SOD1. It is possible that that cysteine 111 may not mediate all aspects of toxicity of mutant SOD1.

Fig. 3.1 MalPEG modification is cysteine 111 specific

PC12 cells were transfected with pcDNA3 plasmids coding for wild-type SOD1 or the indicated mutant SOD1s. Cell lysate from PC12 cells without any transfections was used as control. After 48 h of culture, the cell lysates were collected and equal volumes of lysates were subjected to reducing SDS-PAGE and Western blotting with an anti-SOD1 antibody. Transient transfection elicited high expression levels of human SOD1s. All the human SOD1s could be modified by MalPEG, except the C111S mutation. The percentage of MalPEG-modified-SOD1 was estimated by quantifying the immunoreactivity of SOD1 (MP) per human SOD1 maintaining unmodified. Three independent experiments were performed. Bonferroni's Multiple Comparison Post-Test isolated C111S groups that differed from the other groups ($*p < 0.001$).

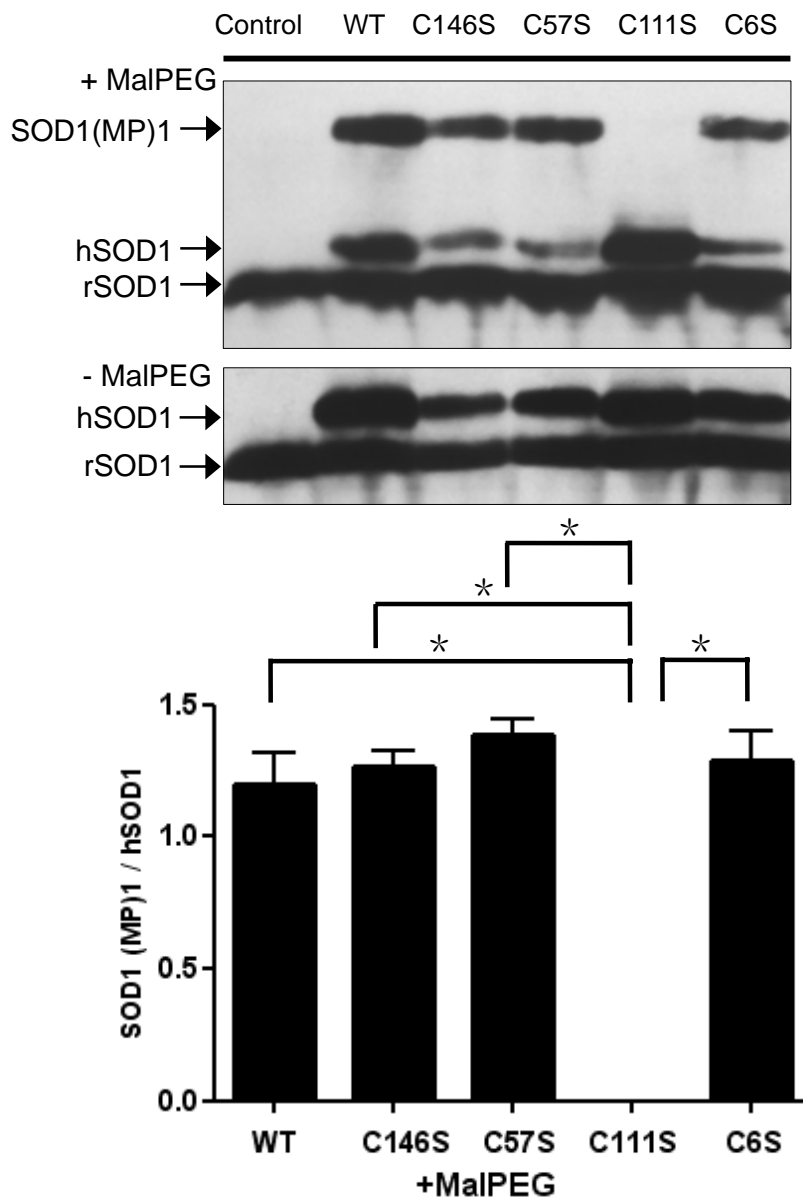
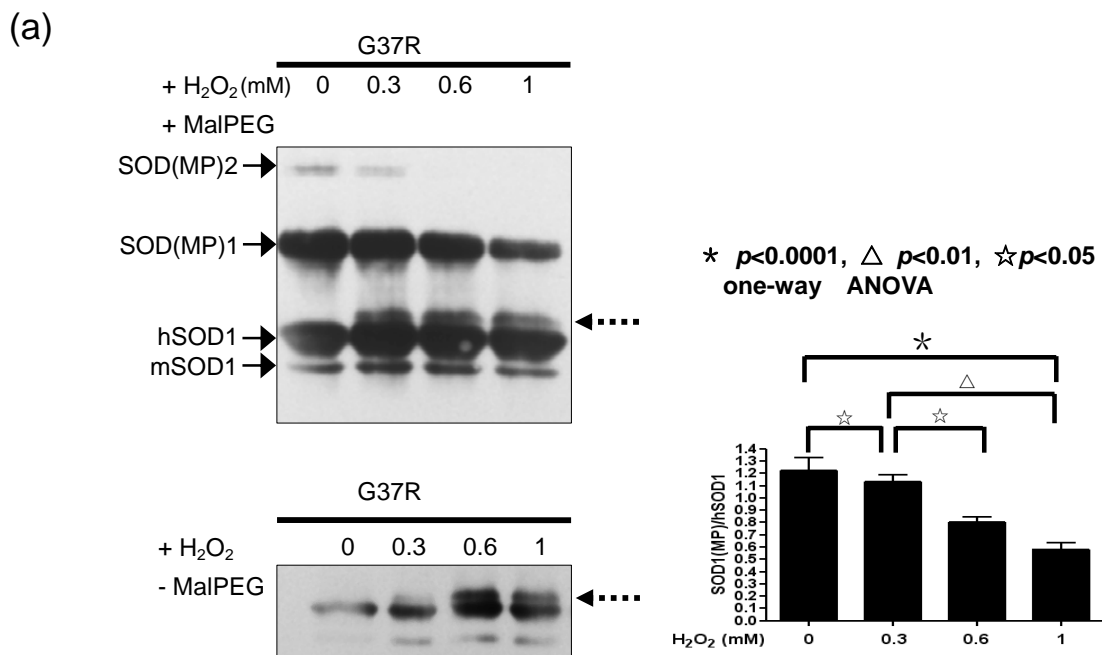
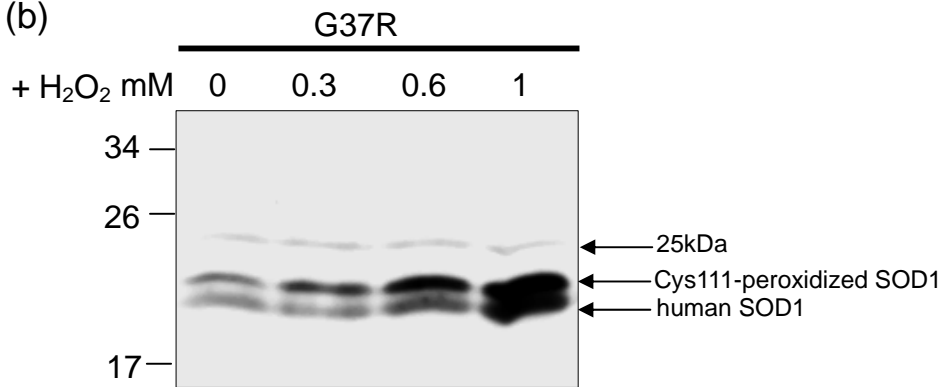


Fig. 3.2 Oxidation by H₂O₂ decreased the MalPEG modification and increased Cys 111-peroxidation in G37R spinal cord extract (n = 3).

(a) Increased oxidative stress induced by H₂O₂ decreased the MalPEG modification in G37R spinal cord extract. Equal volumes of lysates with a total of 10 µg protein from spinal cords of G37R transgenic mice and non-transgenic mice were incubated with variable concentrations of H₂O₂ as indicated for 20 minutes, and then exposed to 3mM MalPEG for 1h. The percentage of MalPEG-modified-SOD1 was estimated by quantifying the immunoreactivity of SOD1 (MP) per total human SOD1. Bonferroni's Multiple Comparison Post-Test isolated pairs of treatments that significantly differed from each other ($p < 0.05$). The arrowheads with broken lines indicate the additional upper band. (b) Cys111-peroxidized SOD1 is increased in abundance with the enhanced exposure to H₂O₂. By using anti-C111ox-SOD1, the G37R mutant SOD1 transgenic mice spinal cord extracts were detected. Equal volume lysates with 10 µg of total protein from spinal cords of G37R transgenic mice were incubated with variable concentrations of H₂O₂ for 20 minutes. Quantification of the Cys111-peroxidized SOD1 levels normalized to 25 kD band, which was used as a loading control. Three independent experiments were performed and data representing these experiments were analyzed in triplicate. Bonferroni's Multiple Comparison Post-Test isolated pairs of treatments that significantly differed from each other ($p < 0.001$).



(b)



* $p < 0.0001$
one-way ANOVA

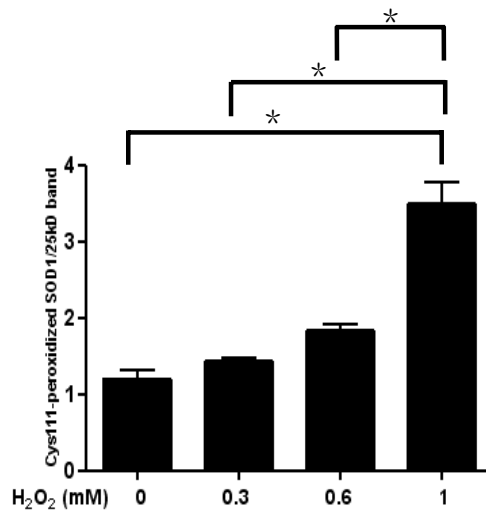
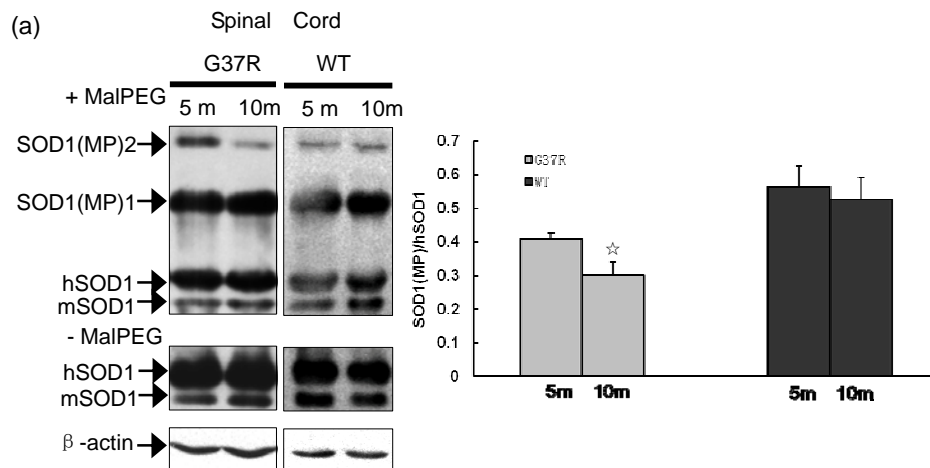
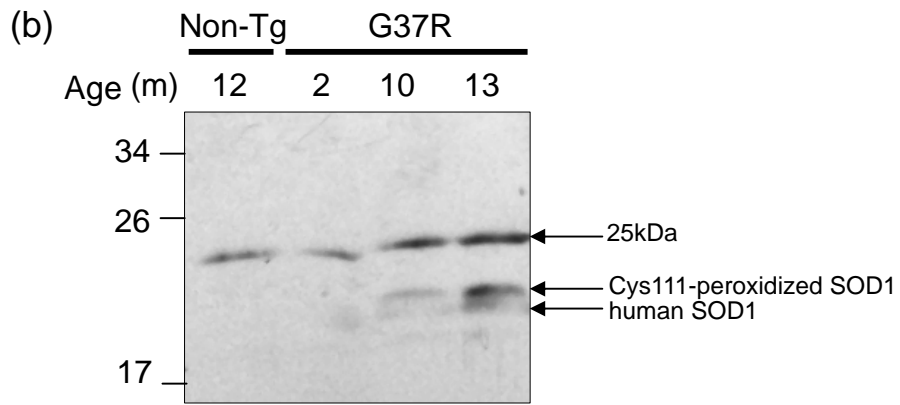


Fig. 3.3 MalPEG modification of G37R transgenic mice spinal cord decreased, but reciprocally the Cys111-peroxidation increased dependent with ALS progress (n = 3).

(a) MalPEG modification of G37R transgenic mice spinal cord is lower than that of wild-type SOD1 transgenic mice. The MalPEG modification of G37R transgenic mice decreased, which is dependent on ALS progression. Soluble tissue lysates were obtained from spinal cords of G37R and wild-type SOD1 transgenic mice at different stages of ALS (m = age in months). Lysates were incubated with 3mM MalPEG for 1 h and subjected to reducing SDS-PAGE (10 μ g/lane) followed by Western blotting with an anti-SOD1 antibody. Levels of MalPEG-modified-SOD1 decreased in the spinal cords of G37R SOD1 transgenic mice whose disease had already progressed, while there were no significant changes of MalPEG modified-SOD1 in the wild-type SOD1 transgenic mice at different stages. The percentage of MalPEG-modified-SOD1 was estimated by quantifying the immunoreactivity of SOD1 (MP) per total human SOD1. Results shown of mean ratio \pm SD, $\star p < 0.05$. (b) The Cys111-peroxidation was increased in abundance with the progression of the disease. The spinal cord extracts of the G37R mutant SOD1 transgenic mice at different stages were applied to Western blot by using the anti-C111ox-SOD1. The spinal cord extractions from non-transgenic (Non-Tg) mice were used as control. Equal volumes of lysates with a total of 10 μ g protein from spinal cords of G37R transgenic mice were applied to 15% SDS/PAGE. Quantification of the Cys111-peroxidized SOD1 levels normalized to 25 kD band. Five independent experiments were performed and data representing these experiments were analyzed in triplicate. Bonferroni's Multiple Comparison Post-Test isolated pairs of different stages that significantly differed from each other.





* $p < 0.0001$, ☆ $p < 0.05$
one-way ANOVA

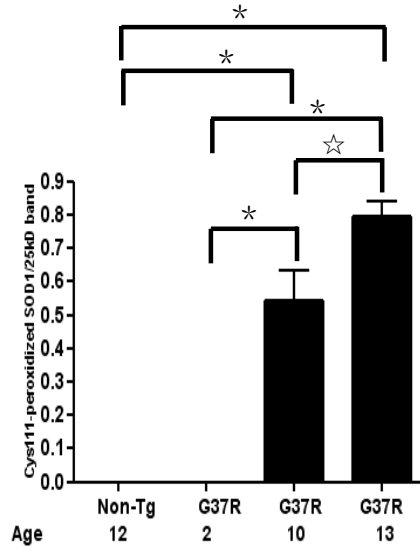
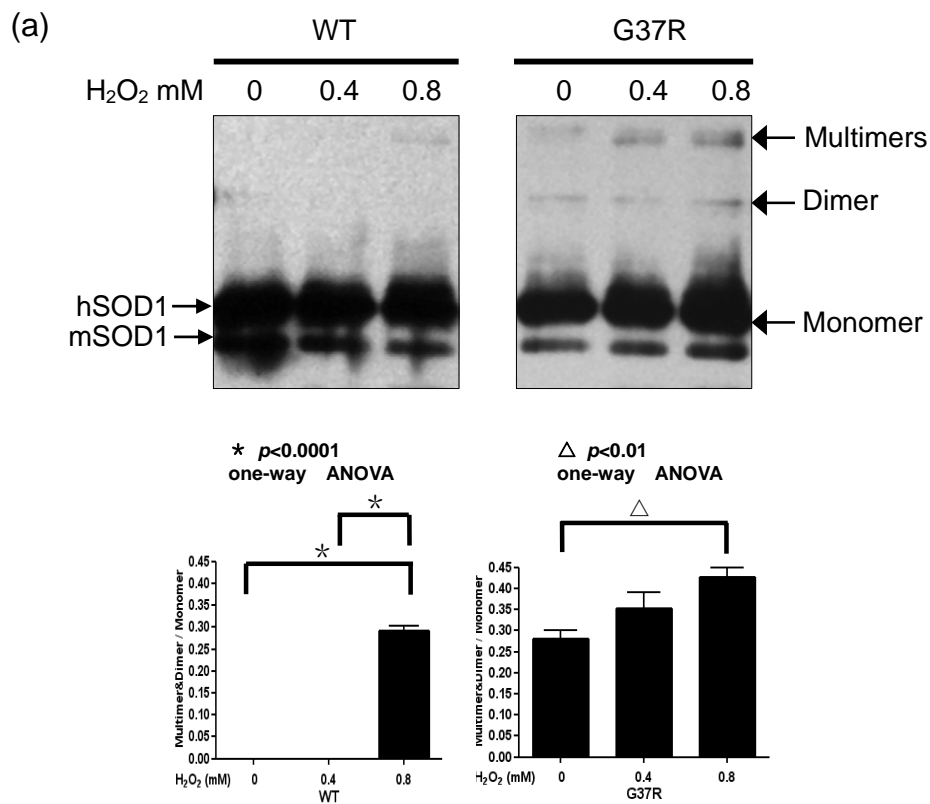


Fig. 3.4 Oxidation by H₂O₂ increased SOD1 multimers in G37R transgenic mice spinal cord extract, and the SOD1 multimers was increased dependent with ALS progress (n = 3).

(a) H₂O₂-induced SOD1 multimer formation was increased in G37R transgenic mice. After stimulation 20-min with 0-1 mM H₂O₂, tissue lysates with a total of 10 µg protein were boiled for 5 minutes in Laemmli sample buffer (with 5% β-ME) before being loaded on 15% SDS-PAGE. After electrophoresis, the protein bands were detected with Western blotting analysis. Band intensity value of SOD1 dimer and multimer were normalized with SOD1 monomer. Bonferroni's Multiple Comparison Post-Test isolated pairs of treatments that significantly differed from each other. (b) The formation of SOD1 multimers was increased with the progression of the disease. Soluble tissue lysates were obtained from spinal cords of G37R and wild-type SOD1 transgenic mice at different stages. Lysates (10 µg/lane) were boiled for 5 minutes in Laemmli sample buffer (with 5% β-ME) and then 15% SDS-PAGE and Western blotting with an anti-SOD1 antibody followed. Levels of SOD1 multimers were increased in the spinal cords of G37R mutant SOD1 transgenic mice as ALS progressed while there were no appearances of SOD1 multimers in the wild-type SOD1 transgenic mice at different stages. SOD1 dimer and multimer intensities were normalized with SOD1 monomer. Three independent experiments were performed and data representing these experiments were analyzed in triplicate. Bonferroni's Multiple Comparison Post-Test isolated pairs of different stages that significantly differed from each other.



(b)

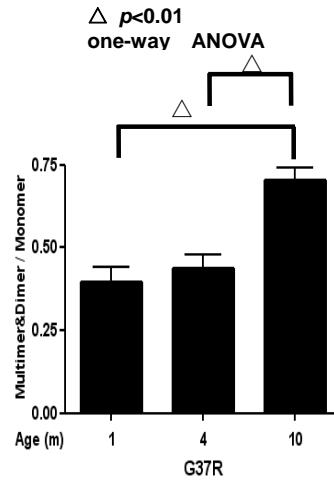
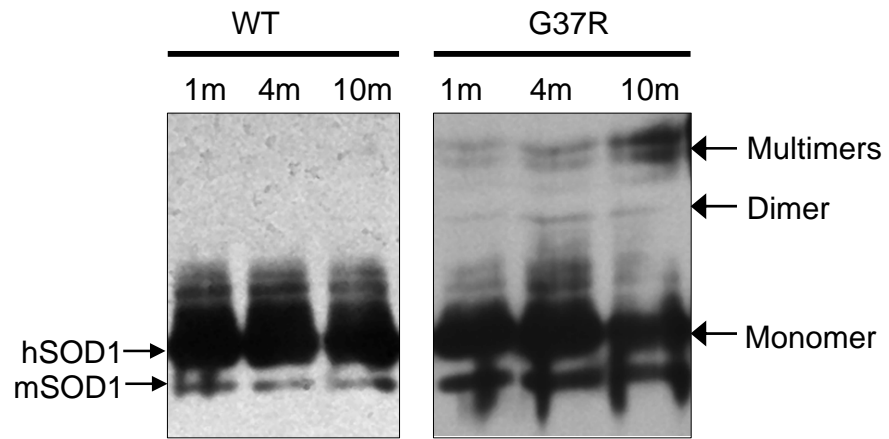
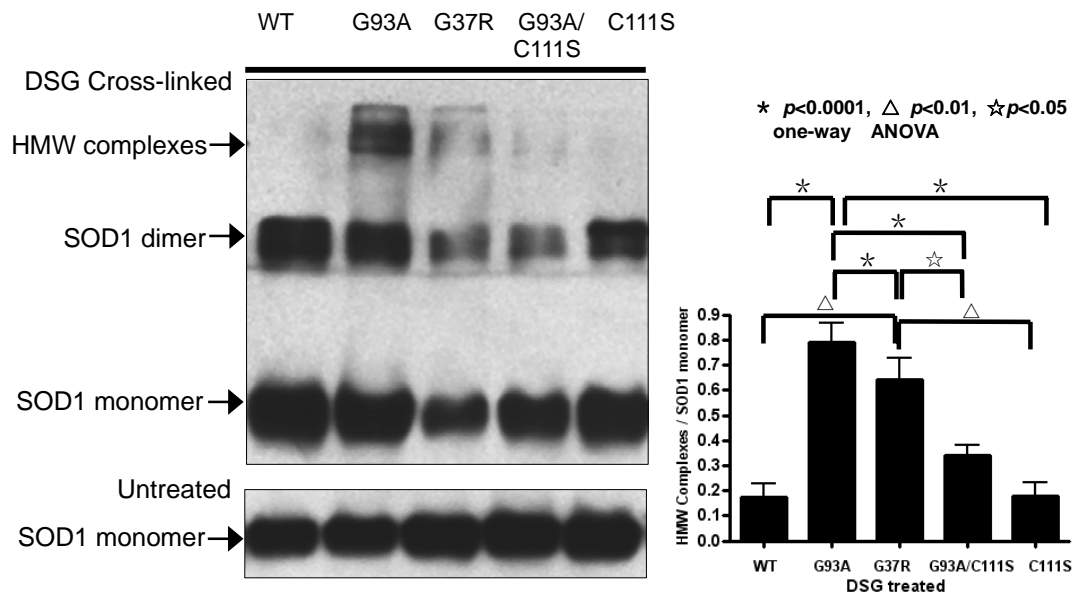


Fig. 3-5 G93A/C111S combined mutation form less HMW complexes compared with G93A mutation. Fresh HEK293 cell lysates containing wild-type or various mutants were incubated with the cross-linker DSG for 60 min before the reaction was quenched with Tris. The reaction mixtures were resolved in 15% SDS-PAGE and blotted with an anti-SOD1 antibody. After cross-linking, wild-type SOD1 migrated as both monomer and dimer; so did C111S mutant. G93A and G37R mutants showed formation of HMW complexes in addition to monomeric and dimeric forms. G93A/C111S-combined mutation significantly decreased the formation of HMW complexes. As the control in SDS-PAGE, all human SOD1s ran as monomers in the absence of DSG. Quantification of HMW complexes levels normalized to SOD1 monomer without DSG treatment represented the total SOD1 expression in transfected cells. Five independent experiments were performed. Bonferroni's Multiple Comparison Post-Test isolated pairs of different stages that significantly differed from each other.



Chapter 4. S-Nitrosylated Protein Disulphide Isomerase Links Mutant SOD1 aggregates in Amyotrophic Lateral Sclerosis

4.1 Introduction

Mutations in the Cu, Zn-superoxide dismutase (SOD1) gene have been identified as a possible cause of a subset of familial amyotrophic lateral sclerosis (FALS) [11,415], an adult-onset neurodegenerative disease characterized by degeneration of motor neurons in the spinal cord, brainstem, and motor cortex. Aggregates of misfolded mutant SOD1 are commonly associated with this disease, as seen at post-mortem examination. SOD1 is an intracellular homodimeric metalloprotein that forms a stable intra-subunit disulfide bond. Several factors are involved to drive SOD1 to acquire the propensity to misfold, and favor the disulfide-reduced SOD1 monomers to convert into oligomeric and aggregated species with toxic properties [165,224,416]. These factors include improper metallation of the protein, genetic mutations, and loss of disulfide bond and posttranslational modification. There are four cysteine residues in SOD1, located at amino acids 6, 57, 111, and 146. The formation of disulfide bonds is mediated by oxidation of the thiol groups of cysteine residues. Previous studies have established that detergent-insoluble mutant SOD1 aggregates accumulated in the spinal cords of mutant SOD1 transgenic mice are extensively cross-linked by disulfide bonds [136,232,233]. In vitro cell culture models also demonstrated that disulfide bond formation between mutant SOD1 proteins could either trigger oligomerization or facilitate the bonding force to stabilize aggregates' structures [234,235]. Furthermore, in both cell culture and mouse models, the mutant SOD1 lacking the native intramolecular disulfide bond is the major component of the insoluble SOD1 aggregates [239]. Indeed, the disulfide-reduced subunits of SOD1 are

susceptible to disulfide-linked multimerization upon oxidative stress, indicating that the regulation of disulfide-bond formation can affect the formation of SOD1 aggregates.

Although wild-type SOD1 is found predominantly in the cytoplasm, the accumulation of mutant SOD1 aggregates is observed at the mitochondrial surface and in the intermembrane space (IMS) of mitochondria. Studies demonstrate that this IMS-targeted mutant SOD1 causes neurite mitochondrial fragmentation, impaired mitochondrial dynamics, and neuronal toxicity [194]. This aberrant deposition of mutant SOD1 in mitochondria contributes to ALS pathogenesis [72,73]. Overexpression of glutaredoxin 2 (GRX2), a thiol-disulphide oxidoreductase located in mitochondria, reduces the mitochondrial fragmentation and mutant SOD1 aggregation, and protects its metabolic activity [74]. Furthermore, mutant SOD1 forms monomers or insoluble high molecular weight multimers within the endoplasmic reticulum (ER) [53]. Studies have shown that protein disulfide isomerase (PDI) was associated with mutant SOD1 inclusions in mutant SOD1 transgenic mice and in a motor neuronal cell line, seeing as pharmacological inhibition of PDI enzymatic activity increased the present of mutant SOD1 inclusions [54].

PDI is an enzyme critical for proper protein folding in the ER. PDI can introduce disulfide bonds into proteins (oxidation), break disulfide bonds (reduction), and catalyze thiol/disulfide exchange (isomerisation), thus facilitating disulfide bond formation, reaction rearrangements, and structural stability [417]. In many neurodegenerative disorders and cerebral ischemia, the accumulation of protein aggregates results in ER dysfunction [418,419], but up-regulation of PDI represents an adaptive response, which may offer neuroprotection by promoting protein refolding [373,420]. Uehara and

colleagues [421] demonstrate that in Parkinson's disease and related disorders, nitric oxide (NO)-mediated S-nitrosylation of PDI inhibits PDI function, leads to dysregulated protein folding within the ER, and consequently results in ER stress and neuronal cell death. S-nitrosylation is an important biological reaction of NO that involves the covalent addition of NO to thiol groups of cysteine residues of proteins to form S-nitrosothiols (RSNOs). This selective posttranslational modification can affect many cellular processes and regulate protein function, stability, localization, and protein-protein interactions. [333].

Seeing as nitrosative stress is linked with excessive glutamate receptor activation, excitotoxicity, and oxidative stress; NO is believed to play a key pathogenic role in neurodegenerative disorders [422,423]. These processes are key events in neurodegenerative diseases including ALS [424]. Increased levels of NO is linked to the toxicity of mutant SOD1 in neuroblastoma cells [425]. In the vicious cycle of ALS pathogenesis, inflammatory response is a pathological hallmark of ALS [426], which is characterized by the accumulation of huge numbers of activated astrocytes and microglia cells [427,428]. Additionally, ALS-linked mutant SOD1 expression in glia cells contributes to the motor neuronal death and affects disease progression of ALS. Accumulating evidence has indicated that the perturbation of the crosstalk between glial cells and neurons is associated with motor neuron degeneration [94,429,430]. Also, the mechanism of inflammatory-activated glia killing neurons is mediated by high levels of inducible NO synthase (iNOS) expression in glia [431,432]. The resulting high levels of NO can induce various damaging consequences, including S-nitrosylation of PDI. In the current study, we examined whether or not iNOS expression was correlated with

NO-mediated S-nitrosylation of PDI. We further detected an association between S-nitrosylation of PDI and accumulation of mutant SOD1 aggregates in ALS. We report here that an age-dependent expression of iNOS and formation of S-nitrosylated PDI (SNO-PDI) *in vivo* were detected in the spinal cords of mutant SOD1 transgenic mice. *In vitro*, we also found a dosage-dependent formation of SNO-PDI in SH-SY5Y cells with the treatment of NO donor S-nitrosocysteine (SNOC). Mutant SOD1^{G93A} expression in SH-SY5Y cells promotes iNOS expression and consequently NO generation, which leads to S-nitrosylation of PDI as well. Blocking NO generation with NOS inhibitor N-nitro-l-arginine (NNA) significantly attenuates formation of SNO-PDI and mutant SOD1 aggregates in an *in vitro* ALS cell model. Our elucidation of an NO-mediated pathway to dysfunction of PDI by S-nitrosylation provides a mechanistic link between free radical production and abnormal protein accumulation in ALS.

4.2 Materials and methods

4.2.1 Transgenic Mice

The mutant SOD1 transgenic mice (B6.Cg-Tg(SOD1-G93A)1Gur/J and B6.Cg-Tg(SOD1-G37R)42Dpr/J) and the wild-type SOD1 transgenic mice (B6.Cg-Tg(SOD1)2Gur/J) were obtained from the Jackson Laboratory. Inbred male mice between 1 and 13 months of age were used for this experiment. Mice were genotyped by PCR with the following sense and antisense primers: 5'-CATCAGCCCTAATCCATC-3', 5'-CGCGACTAACAATCAAAG-3'. During the past decade, the field of ALS research was largely built on the use of this transgenic mouse model. By multifolded-overexpression of the mutant gene, the transgenic mouse develops motor

deficits and ultimately dies from respiratory failure. Since the measurement of disease progression varied widely between laboratories, guidelines for preclinical animal research in ALS/MND were developed to improve the methodology of animal research [433]. Disease onset was determined as the time when mice reached their peak body weight before the denervation-induced muscle atrophy and weight loss [434]. Studies have established a high degree of correlation between the age at which Rotarod performance declines and the initial loss of body weight [435]. Indeed, peak body weight before weight loss is the earliest observable measure that defines the disease onset initiating before any observable motor performance decline, including grip strength, Rotarod performance, and cage activity [436,437]. End-stage was defined as the time at which a mouse could not right itself within 30 s when placed on its side. This is an endpoint frequently used for mutant SOD1 transgenic mice and one that was consistent with the requirements of the Animal Care and Use Committee of the University of Manitoba. One-month-old G93A mutant transgenic mice were considered pre-symptomatic; disease onset occurred when these mice were 3 months old, and disease end-stage occurred when these mice were 6 months old. Five-month-old G37R mutant transgenic mice were pre-symptomatic; disease-onset occurred when these mice were 10 months old, and disease end-stage occurred when these mice were 13 months old. The use and maintenance of the mice described here were performed in accordance with the Guide of Care and Use of Experimental Animals of the Canadian Council on Animal Care. Mice tissues were collected and homogenized in 10 volumes of lysis buffer consisting of 1% (w/v) Triton X-100, 50 mM Tris-HCl, Ph 7.4, 300 mM NaCl, 5 mM EDTA, 0.02% (w/v) sodium azide, 10 mM iodoacetamide, 1mM PMSF and 2 µg/ml leupeptin. Homogenates

were centrifuged at $20000 \times g$ for 30 min at 4°C . Supernatants are collected for analysis. Protein concentration was measured by the BCA method as described by the manufacturer (Pierce).

4.2.2 Plasmids, Cell Culture and Transfection

G93A and WT SOD1 constructs tagged with EGFP were constructed in the same manner as those previously reported [438]. Briefly, the SOD1^{WT} template for PCR amplification uses the following primers: 5'-GCGCGCGTCGACAAGCATGGC-3' (forward), 5'-GCGCGCGTCGACGCTTGGGCGATCCCAAT-3' (reverse). Primers were designed to introduce a *SalI* site to allow subcloning into pEGFP-N1 (Clontech, Palo Alto, CA) and to remove the SOD1 translation stop codon. Additional mutant SOD1^{G93A} plasmid was generated via site-directed mutagenesis of the SOD1^{WT} template using the Quik Change kit (Stratagene, La Jolla, CA), with the use of the following primers: G93A: 5'-CTGCTGACAAAGATGCTGTGGCCGATGTGTC-3' (forward) and 5'-GACACATCGGCCACAGCATCTTTGTCAGCAG-3' (reverse). All the plasmid constructions were verified by automated sequencing. SH-SY5Y human neuroblastoma cells were maintained in Dulbecco's modified Eagle's/F-12 (1:1) medium, supplemented with 10% fetal calf serum, 2 mM L-glutamine, 100 IU/ml penicillin, and 100 $\mu\text{g}/\text{ml}$ streptomycin, at 37°C in an atmosphere of 5% CO_2 in air. 80% confluent cells were transfected with the indicated plasmids using Lipofectamine (Invitrogen) following the manufacturer's instructions. Cells were analyzed 48h after transfection.

4.2.3 Inclusion quantification and Subcellular fractionation

SH-SY5Y cells were transiently transfected with the indicated plasmids carrying various SOD1s tagged with EGFP. Aggregate-positive cells were counted as a percentage of total EGFP-positive cell transfectants. If an EGFP-positive cell had one or many aggregates, the aggregates score was one. Harvested cells were lysed in 50 mM Tris-HCl, pH 7.5, containing 150 mM NaCl, 0.1% sodium dodecyl sulphate, 1% triton X-100, and 1% protease inhibitors. Lysates were centrifuged at $1,000 \times g$ for 10 min. The cleared lysates were centrifuged at 25,000 for 50 min to obtain the supernatant and pellet fractions. Protein from the resulting supernatants (soluble fraction) and the pellets (insoluble fraction) after 15 s sonication in RIPA buffer without sodium deoxycholate were analyzed by Western blot.

4.2.4 Measurement of NO - level.

Spinal cord lysates (30 mL) were collected and incubated with an equal volume of Griess reagent for 20 min at room temperature (RT) [439]. The concentration of nitrite (NO_2), which is formed by the spontaneous oxidation of NO under physiological condition, was determined by measuring the absorbance at 540 nm. The value was normalized to the protein concentration of lysates. The NO formed by the cells was determined by the Griess reaction with a minor change. Briefly, 40 μl cell culture fluid, 10 μl NADPH and 40 μl basal solution (0.03 M PBS, 1.25 mM glucose-6-phosphate, 400 U/L glucose-6-phosphate dehydrogenase, 200 U/L nitrate reductase) were incubated in a 96-well microtiter plate for 45 min at RT. Next, 50 μl Griess reagent was added, and the solutions were incubated for 20 min at RT. Finally, the absorbance of the samples was measured at 540 nm. NO_2 concentrations were calculated from a standard curve of

Sodium nitrite (NaNO_2).

4.2.5 Biotin-switch assay for detection of S-nitrosylated PDI

Briefly, mouse spinal cord tissue extracts and cell lysates were prepared in HENC buffers (250 mM Hepes pH 7.5, 1 mM EDTA, 0.1 mM neocuproine, 0.4% CHAPS). Typically 1 mg of cell lysates and up to 2 mg of tissue extracts was used. The blocking buffer (2.5% SDS, 20 mM methyl methane thiosulphonate [MMTS] in HEN buffer) were mixed with the samples and incubated for 30 min at 50°C to block free thiol groups. After removing excess MMTS by acetone precipitation, nitrosothiols were reduced to thiols with 1 mM ascorbate. The newly formed thiols were then linked with the sulfhydryl-specific biotinylation reagent *N*-[6-(biotinamido)hexyl]-3'-(2'-pyridyldithio)propionamide (Biotin-HPDP). The biotinylated proteins were pulled down with Streptavidin-agarose beads. Western blot analysis was performed to detect the amount of PDI remaining in the samples [60].

4.2.6 Preparation of S-Nitrosocysteine (SNOC) and N-nitro-L-arginine (NNA)

SNOC is a NO donor that can spontaneously decompose to generate NO. SNOC decays quickly within a half-life in the range of 2-3 minutes. A 100 mM stock of SNOC was produced immediately before each use from a mixture of 100 mM L-cysteine and 100 mM NaNO_2 by acidification with 5% (v/v) with 10 N HCl. The solution turned from clear to rose-coloured after completion of the reaction. It was applied within minutes of its synthesis. After synthesis, stocks of SNOC were left at room temperature for several days to degrade fully to “old SNOC” for use as a control. NNA is an irreversible inhibitor

of constitutive nitric oxide synthase (nNOS) and a reversible inhibitor of inducible nitric oxide synthase (iNOS). A 5 mM stock NNA was prepared by dissolving 1.096 g NNA in 1 L warmed saline and infused through a 0.22- μ m syringe tip filter. NNA (100 μ M) was added to plates 1h before the transfection.

4.2.7 Immunoblotting

Protein samples (20 μ g) were loaded on 12% sodium dodecyl sulphate polyacrylamide gel (SDS-PAGE) for electrophoresis and then transferred to the PVDF membrane. Membranes were blocked with 5% (w/v) milk in TBS-T buffer (10 mM Tris-HCl, pH 7.5, 150 mM NaCl, 0.05% Tween-20) for 1 h and incubated with primary antibodies for 16 h at 4°C. The primary antibodies are as follows: SOD1 (1:2000, Santa Cruz Biotechnology), iNOS (1:1000, Santa Cruz Biotechnology), PDI (1:1000, Cedarlane). β -actin was used as a loading control (1:2000, Santa Cruz Biotechnology). Blots were washed three times in TBS-T buffer then probed with HRP-conjugated goat anti-rabbit or goat anti-mouse antibodies at 1: 2500 for 1 h at RT, and then developed using chemiluminescence (ECL) reagents (PerkinElmer). Quantification of band intensities was performed by densitometric analysis using quantity one (Bio-Rad).

4.2.8 Statistics

All data were tested using one-way analysis of variance (ANOVA) with Tukey's post hoc test. A p value of 0.05 or less was judged to be significant and results were expressed as mean \pm standard error of the mean (SEM).

4.3 Results

4.3.1 iNOS protein levels were up-regulated in the spinal cords of mutant SOD1 transgenic mice and increased with disease progression.

Spinal cord extracts from non-transgenic mice, wild-type SOD1 transgenic mice and mutant SOD1 transgenic mice (G93A and G37R) were analyzed by Western blotting and probed with iNOS antibodies. A band of immunoreactivity at 130 kDa was detected and it was consistent with the molecular weight of full-length iNOS protein [440,441]. Both G93A and G37R mutant SOD1 transgenic mice had greater levels of iNOS expression in the spinal cords compared with the non-transgenic mice and wild-type SOD1 transgenic mice (Fig.4-1 A). In non-transgenic and wild-type SOD1 transgenic mice, iNOS levels varied to some extent in different individual mice, probably due to individual variability between the mice. However, statistic analysis of data of three independent experiments using 6 mice in each group showed no significant difference in iNOS expression in the spinal cords of both non-transgenic mice and wild-type SOD1 transgenic mice (Fig.4-1 A). Furthermore, the iNOS levels in mutant transgenic mice were increased during disease progression. The levels of iNOS expression in G93A and G37R mutant SOD1 transgenic mice at disease end-stage reached an optical density of almost 3 and 2 folds respectively, compared with the average density from mice at the pre-symptomatic stage (Fig.4-1 C&D). However, there were no significant changes in iNOS expression levels in both non-transgenic mice and wild-type SOD1 transgenic mice in the course of development (Fig.4-1 B).

4.3.2 NO concentrations were increased in the spinal cords of mutant SOD1 transgenic mice and the NO production was up-regulated during disease progression

In order to measure the tissue concentrations of NO (measured nitrite concentration by Griess reagent), spinal cord extracts were prepared as described in the materials and methods section. The concentration of NO was significantly increased in mutant SOD1 transgenic mice (both G93A and G37R), as compared with the wild-type SOD1 transgenic mice and non-transgenic mice (Fig.4-2 A). Both non-transgenic mice and wild-type SOD1 transgenic mice did not produce significant alterations in the levels of NO in the course of development (Fig.2 B). Furthermore, with the progression of disease, the NO production was increased in the spinal cord tissues of mutant SOD1 transgenic mice, and reached a peak at disease end-stage (Fig.4-2 C&D). This up-regulation of NO levels as the disease progresses was statistically significant. This change correlated well with the increase in iNOS expression during disease progression. Compared with the wild-type SOD1 transgenic mice and non-transgenic mice, the mutant SOD1 transgenic mice had a higher net amount of NO production, which was probably due to the enhanced inflammation and gliosis with a concomitant increase in iNOS expression and iNOS-derived NO generation in the absence of nNOS due to motor neuron death.

4.3.3 PDI was increased and S-nitrosylated in the spinal cords of mutant transgenic mice, and up-regulation and S-nitrosylation of PDI developed as disease progresses

Quantitative Western blot analysis was employed to detect the PDI expression in the spinal cords of the mice model of ALS. PDI expression was nearly equivalent in the spinal cords of non-transgenic mice and wild-type SOD1 transgenic mice. However, in both G93A and G37R mutant SOD1 transgenic mice, PDI levels were significantly up-regulated, compared with the non-transgenic and wild-type SOD1 transgenic mice (Fig.4-3 B). PDI expression increased gradually with disease progression, and peaked at disease end-stage in mutant SOD1 transgenic mice, but the non-transgenic and wild-type SOD1 transgenic mice did not have variable expression of PDI in the course of development (Fig.4-3 C). The PDI expression levels in the spinal cords of G93A mutant SOD1 transgenic mice was nearly 3-fold greater at the end-stage of ALS than that at the pre-symptomatic stage (Fig.4-3 D). Similarly, PDI in the spinal cords of G37R mutant SOD1 transgenic mice at end-stage revealed a significant increase compared to that at the pre-symptomatic stage (Fig.4-3 E).

We investigated whether or not aberrant generation of NO through activation of iNOS mediated S-nitrosylation of PDI in mutant SOD1 transgenic mice occurred. Using a biotin-switch assay, we detected that S-nitrosylation of PDI occurred in ALS (Fig.4-3 B). The specificity of the biotinylation reaction was confirmed by almost no detection of S-nitrosylated PDI in the samples without treatment of ascorbate. Ascorbate is required to enhance the chemical decomposition of nitrosothiol groups required for reaction with the biotinylating reagent biotin-HPDP [442]. In addition, there was no detection of S-nitrosylated PDI in the absence of biotin-HPDP (Fig.4-3 A). Despite up-regulation of total PDI in mutant SOD1 transgenic mice, S-nitrosylated PDI levels were abundant in spinal cord tissue from end-stage G93A (Fig.4-3 D) and G37R (Fig.4-3 E) mutant SOD1

transgenic mice. However, SNO-PDI was virtually undetectable in the pre-symptomatic stage. This trend of SNO-PDI level consisted with the change of iNOS expression and NO level during the disease progression. In addition, barely any SNO-PDI was found in non-transgenic mice and wild-type SOD1 transgenic mice. To rule out the possibility that the detectable SNO-PDI in mutant SOD1 transgenic mice was not due to the up-regulation of total PDI expression, we deliberately increased total protein loading to enhance total PDI level in wild-type SOD1 mice group (Fig.3 A). However, we could not detect the presence of SNO-PDI in this group. Furthermore, in the mutant SOD1 transgenic mice group, with less manipulated total PDI levels due to less total protein loading, had detectable SNO-PDI. These data demonstrate that NO-mediated S-nitrosylation of PDI is a common feature of the mutant SOD1-linked transgenic mice [23], which is the most widely accepted mouse model of ALS.

4.3.4 Mutant SOD1 induced up-regulation of iNOS expression and NO generation.

To investigate whether or not mutant SOD1 expression would affect iNOS expression and NO generation, the human neuroblastoma SH-SY5Y cells were transiently transfected with vectors encoding either SOD1^{wt} or mutant SOD1^{G93A} tagged with EGFP. Control cells were not transfected with plasmids (Fig.4-4 A). Forty-eight hours after transfection, cells were harvested to determine the iNOS expression and NO production. Immunoblotting of cell lysates indicated that iNOS expression was unchanged in cells transfected with SOD1^{wt}, as compared with the control cells. In contrast, mutant SOD1^{G93A} expression in cells resulted in a significant increase in iNOS expression compared to both control cells and cells expressing SOD1^{wt} (Fig.4-4 B).

Furthermore, cells expressing mutant SOD1^{G93A} had much higher NO generation than control cells and cells with SOD1^{wt} expression (Fig.4-4 C). This result indicates that mutant SOD1 expression in cells triggers nitrosative stress, which results in increased iNOS expression and iNOS-derived NO generation.

4.3.5 Exposure of SH-SY5Y cells to SNOC triggered the SNO-PDI formation. Expression of mutant SOD1^{G93A} in SH-SY5Y cells induced the SNO-PDI formation, which was blocked by the NOS inhibitor NNA

To investigate whether exogenously generated NO can induce S-nitrosylation of PDI, NO donor SNOC was used as a reagent to transfer NO⁺ to cysteine thiols (Cys-SH) of the PDI's redox modulator sites. SH-SY5Y cells were exposed to freshly-prepared SNOC in various concentrations and decayed (old) SNOC and then subjected to the biotin-switch assay. Exposing the cells to SNOC resulted in SNO-PDI formation. Further increase in NO release from SNOC led to a marked increase in abundance of SNO-PDI. SNOC behaved in a dose-dependent manner (Fig.5-5 A). However, the control cells subjected to old SNOC didn't exhibit S-nitrosylation of PDI. Using the same conditions, we found that mutant SOD1^{G93A} expression induced SNO-PDI formation. Formation of S-nitrosylated PDI was observed only in cells expressing mutant SOD1^{G93A}, not in the control cells or cells with SOD1^{wt} expression; this reaction was suppressed by the NOS inhibitor NNA, which dramatically reduced the SNO-PDI formation. SNOC reinforced the SNO-PDI formation, as SNOC exposure promoted the SNO-PDI levels in mutant SOD1^{G93A} expressing cells (Fig.5-5 B). This result suggests that mutant SOD1^{G93A} induces S-nitrosylation of PDI probably results from up-regulation of iNOS expression

and NO generation, which can be manipulated by introducing NO donors or NOS inhibitors.

4.3.6 SNOC promoted and NNA suppressed the mutant SOD1 aggregates formation in transfected SH-SY5Y cells

To assess the effects of SNOC on mutant SOD1 aggregates, transfected SH-SY5Y cells were exposed to SNOC. The cells expressing SOD1^{wt} and the control cells showed a widespread fluorescence in the cytoplasm, whereas in the cells transfected with mutant SOD1^{G93A}, large and prominent cytoplasmic protein inclusions were observed (Fig.6-6 A). The proportion of cells containing inclusions was quantified. In the presence of SNOC, the mutant SOD1^{G93A} formed inclusions with increased frequency (Fig.6-6 B). The effect of SNOC was also monitored using a different assay for protein aggregation: detergent insolubility that is usually used for aggregated proteins including mutant SOD1^{G93A}. Mutant SOD1^{G93A} was consistently found to be enriched in the pellet fraction, whereas SOD1^{wt} was found in the soluble fraction (Fig.6-6 A). When the transfected cells were exposed to SNOC, there was a statistically significant increase in the amount of insoluble SOD1^{G93A} in the pellet (Fig.6-6 C). These results indicate that SNOC induces further formation of inclusion or aggregates of SOD1^{G93A} in the cells, which probably operate through the mechanism of S-nitrosylation of PDI. To further elucidate the importance of iNOS activation in SNO-PDI-related SOD1 aggregates formation, NNA was added to the medium on the day of transfection. NNA treatment inhibited the formation of SOD1^{G93A} inclusions in transfected cells (Fig.6 B). Furthermore, the level of insoluble SOD1^{G93A} in the pellet was reduced after NNA treatment, which inhibited NO generation (Fig.6-6 C).

4.4 Discussion

There are three subtypes of NOS in the nervous system. The two constitutive forms of NOS-neuronal (nNOS) and endothelial (eNOS)-are mainly sources of NO production. The third subtype-iNOS-as its name indicates, is induced by acute inflammatory stimuli. iNOS is induced mainly by reactive astrocytes and microglia cells in various neurodegenerative diseases. Once iNOS is expressed, it will produce neurotoxic amounts of NO chronically, without any requirement for further activation [322]. In ALS, increased tissue levels of NO in the lumbar spinal cord of mutant ALS transgenic mice are mainly produced by iNOS located in astrocytes, seeing as nNOS-positive motor neurons are depleted while iNOS-positive activated glial cells are increased in ALS mice [324]. Furthermore, pharmacological inhibition of iNOS shows the significant effects of delaying disease-onset and extending survival in ALS mice [328]. The findings of our study demonstrate that iNOS protein expression is up-regulated in the spinal cords of both G93A and G37R SOD1 mutant transgenic mice compared with non-transgenic mice and wild-type SOD1 transgenic mice. In addition, the level of iNOS increased during the progression of disease, and it reached a peak at the end-stage of ALS. These observations demonstrate that iNOS is involved in the causal mechanisms of motor neuron degeneration in ALS mice. The role of iNOS in the pathogenesis of ALS is less clear (than nNOS), probably because study on its effect is very controversial. For example, iNOS-knockout mice are protected against neuronal injury in several models of neurodegenerative diseases, including Alzheimer's disease [443] and Parkinson's disease [444]. In ALS, the G93A-high-mutant SOD1 mouse, iNOS gene deletion has a significantly prolonged survival [326]. However, a recent study of three different strains

of iNOS-knockout showed no effect of iNOS on the infarct size after transient focal brain ischemia [445]. This may suggest that iNOS is more likely to be toxic to chronic neurodegeneration, rather than to acute neuronal injury [321]. We focused on iNOS because earlier studies on ALS mice [326,446,447] and human patients [327] have indicated that this isoform of NOS could be vital in ALS, and its role in the neuropathology of ALS has been under-appreciated. The importance of iNOS comes from its properties that are different from eNOS and nNOS. Homodimeric iNOS is catalytically active when expressed and it is active for extended periods with a maximum of 10-fold greater than other NOS isoforms, generating a very high output of NO [325].

We also studied the concentrations of NO in the spinal cord extracts in mutant SOD1 transgenic mice (both G93A and G37R), wild-type SOD1 transgenic mice, and non-transgenic mice. As predicted, compared with the wild-type SOD1 transgenic mice and non-transgenic mice, the mutant SOD1 transgenic mice had a higher net amount of NO production, which was probably due to the increase in inflammation and gliosis with a concomitant up-regulation of iNOS expression. Furthermore, NO concentration was significantly increased in the spinal cord extracts of mutant SOD1 transgenic mice at end-stage of ALS. The up-regulation of NO level during disease progression presumably resulted from activation of astrocytes and microglia, which induced iNOS up-regulation in the spinal cords of mutant SOD1 transgenic mice. The unaltered NO levels in both non-transgenic mice and wild-type SOD1 transgenic mice indicated that the constitutive level of NO was probably due to nNOS residued in motor neurons. Our results imply an interesting connection between robust iNOS expression and excessive NO generation in mutant transgenic mice at end-stage of ALS. Up-regulation of iNOS may account for the

large amount of NO generation at disease end-stage. NO mediates cellular signaling pathways that regulate broad aspects of physiological processes. NO has been implicated in neurotransmission, synaptic plasticity, and neuromodulation in the central nervous system (CNS) [448]. Excessive generation of NO and its derivatives has also been implicated in the pathogenesis of neurodegenerative disorders [449]. For example, high levels of NO induce neuronal death by causing inhibition of mitochondrial cytochrome oxidase in neurons [450]. The inhibition of neuronal respiration leads to depolarization and glutamate release, followed by excitotoxicity via the NMDA receptor [451,452]. Normally, NO mediates the physiological and pathophysiological effects via stimulation of guanylate cyclase to form cyclic guanosine – 3',5'-monophosphate (cGMP) or through S-nitrosylation of regulatory protein thiol groups [453]. S-nitrosylation involves the covalent addition of a NO group to a critical cysteine thiol/sulfhydryl to form an S-nitrosothiol derivative. This S-nitrosylated modification can influence the function of a broad spectrum of proteins as well as the protein-protein interaction [454]. Our studies have found that PDI is S-nitrosylated in spinal cord tissues of end-stage mutant SOD1 transgenic mice (both G93A and G37R). However, the S-nitrosylated PDI was virtually undetectable in our pre-symptomatic-stage mice. In addition, in non-transgenic mice and wild-type SOD1 transgenic mice, there was no S-nitrosylation of PDI. This finding suggests that S-nitrosylation of PDI probably inactivates the normal properties of PDI and it may contribute to the pathogenesis of ALS. Consistent with this result, we also found that PDI expression levels at the end stage of disease were significantly up-regulated in spinal cords of both G93A and G37R SOD1 mutant transgenic mice as compared with the non-transgenic and wild-type transgenic mice. Similarly, a previous

study confirmed significant up-regulation of PDI expression at disease end stage in both G93A mutant mice and rats as compared to that of the non-transgenic controls [54]. However, there are some varieties of PDI expression at different disease stages in mutant transgenic rats relative to the corresponding non-transgenic rat. Ferri and colleagues found that PDI expression was up-regulated at the presymptomatic stage (8 weeks), but at 16 weeks and end stage, PDI levels were not significantly higher in the spinal cords of G93A mutant transgenic rats as compared to non-transgenic rats [455]. Another study showed that PDI levels in cerebrospinal fluid (CSF) of G93A mutant transgenic rats were most prominently elevated at the disease onset stage when compared with non-transgenic rats [58]. All these studies set the age-matched non-transgenic mice or rats as control. To examine the change of PDI expression during disease progression, absolute PDI levels were quantified as a ratio relative to the corresponding β -actin amounts at each stage. We found that the PDI level increased gradually with the progression of disease and peaked at disease end-stage in both G93A and G37R mutant transgenic mice. Even though the up-regulation of PDI represents an adaptive response to provide potential neuroprotection [373,374,418,420], NO-mediated S-nitrosylation of PDI probably affects its normal function and promotes aggregate formation. The formation of SOD1 aggregates in ALS was probably through destabilizing mutant SOD1 with reactive reduced cysteine residues [455]. Cysteine residues are crucial for SOD1 stability, and a non-physiological intermolecular disulfide bond between cysteine 6 and 111 in mutant SOD1 was found to be associated with mutant SOD1 aggregates' formation [456]. PDI may get involved in rearranging the cysteine residues of SOD1, and S-nitrosylation of PDI towards the end stage of ALS may facilitate the formation of non-physiological disulfide bonds and

promote SOD1 aggregates formation. This could be a possible explanation to the finding that cysteine-reduced SOD1 levels increased with disease progression and reach the peak at end stage in G93A mutant transgenic rats [455]. Furthermore, an association of PDI and mutant SOD1 aggregates was identified, seeing as high levels of PDI that recruit to abnormal inclusions were observed in both G93A transgenic mice and ALS patients [54,58]. In addition, PDI was found to be co-localized with SOD1 in neuronal cytoplasmic inclusions (NCIs) [457]. Given the chaperone activity of PDI, it is possible that PDI may interact with insoluble mutant SOD1 to form abnormal inclusions, this may partially explain the findings of other studies that PDI levels were not most prominently up-regulated at the disease end stage in mutant transgenic rat when compared to non-transgenic mice [58,455]. A greater portion of PDI may be associated with mutant SOD1 in abnormal inclusion at end stage of ALS, and then it cannot be detected in the soluble fraction of tissue lysates.

PDI is a ubiquitous, highly conserved redox enzyme from the thioredoxin superfamily, and it is mainly located in the ER [458]. During protein folding in the ER, PDI facilitates proper protein folding and helps to maintain the structural stability of the mature protein [417]. As a consequence, PDI is considered a molecular chaperone capable of stabilizing the correct folding of substrate proteins. It also facilitates ER-associated degradation of misfolded proteins [459]. Through interacting with the ER transmembrane protein Derlin-1, PDI is involved in retro-translocation of misfolded cholera toxin from the ER to the cytoplasm. [460]. As we know, aberrant protein folding and further protein aggregates are associated with various neurodegenerative diseases, including ALS. The accumulation of misfolded protein in the ER results in ER stress that

triggers the protective unfolded protein's response (UPR). The UPR entails the induction of chaperone molecules, the degradation of misfolded proteins, and inhibition of protein translation [461]. Prolonged ER stress can nonetheless lead to activation of apoptosis [462]. Studies involving pancreatic β cells, macrophages [463], and cerebellar granule cells [464] have demonstrated that NO can induce ER stress. However the molecular basis is not clear. Furthermore, although the involvement of NO in neurodegeneration has been widely accepted, the chemical relationship between nitrosative stress and formation of protein aggregates has remained obscure. Our findings indicate that S-nitrosylation of PDI may hold some of the answers to these questions. Studies have shown that excitotoxic activation of nNOS leads to excessive NO generation, which causes S-nitrosylation of the active-site thiols of PDI, inhibiting its isomerase and chaperone activities [421]. In this regard, NO blocks the protein's protective effect via S-nitrosylation of PDI, which leads to accumulation of misfolded and polyubiquitinated proteins, resulting in prolonged UPR activation, and thus persistent ER stress, which induces apoptosis. Our study showed that, when SH-SY5Y cells were expressing mutant SOD1^{G93A}, iNOS expression was significantly increased in compared with cells expressing SOD1^{wt}. This finding was relatively inconsistent with the previous study that had showed expressing SOD1^{wt} or mutant SOD1^{G93A} in NSC-34 cells did not alter iNOS expression, which remained at a constitutive level. This variation may be due to the controlled SOD1^{wt} or mutant SOD1^{G93A} expression in NSC-34 cells. In that study, the cell clones expressing low and similar amounts of various SOD1 proteins upon induction. The induced human SOD1 expression was lower than murine endogenous SOD1 expression; this low expression of human expression may not be extensive enough to

trigger the possible correlation between mutant SOD1 expression and iNOS expression. Furthermore, the increased iNOS level in mitochondria has been observed in G93A mutant transgenic mice and the deletion of iNOS gene significantly extended the survival of mice. However, the activity of iNOS is more crucial to its biological role in ALS pathogenesis. The effect of mutant SOD1 in alteration of iNOS activity was further investigated. We found that cells expressing mutant SOD1^{G93A} had much higher NO generation, and this increased NO generation could be reversed by the use of NNA (non-selective inhibitor of NOS) (data not shown). Consequently, ALS-linked SOD1 is highly associated with up-regulated iNOS expression and increased iNOS-derived NO generation. However, another enzyme responsible for NO production, nNOS, was found to be down-regulated in SH-SY5Y cells with mutant SOD1^{G93A} expression in a study [465]. The down-regulation of nNOS-derived NO production was also evidenced. It has been suggested that NO released from nNOS activity keeps iNOS inhibited under normal conditions. However, under pathophysiological conditions, down-regulation of nNOS is a necessary condition to promote the iNOS expression and the release of large amounts of NO [466]. For example, in a rat model of inflammatory bowel disease (IBD), nNOS downregulation could induce iNOS overexpression [467]. Our results could be in agreement with the hypothesis that downregulation of nNOS is associated with upregulation of iNOS in SH-SY5Y cells expressing mutant SOD1^{G93A}. However, the nNOS expression and the mechanism for the association between iNOS and nNOS will certainly deserve further investigation. We introduced the physiological NO donor, SNOC to provoke S-nitrosylation of PDI. The dose-dependent manner of SNOC-induced S-nitrosylation of PDI confirmed that PDI was S-nitrosylated by NO-related species. The

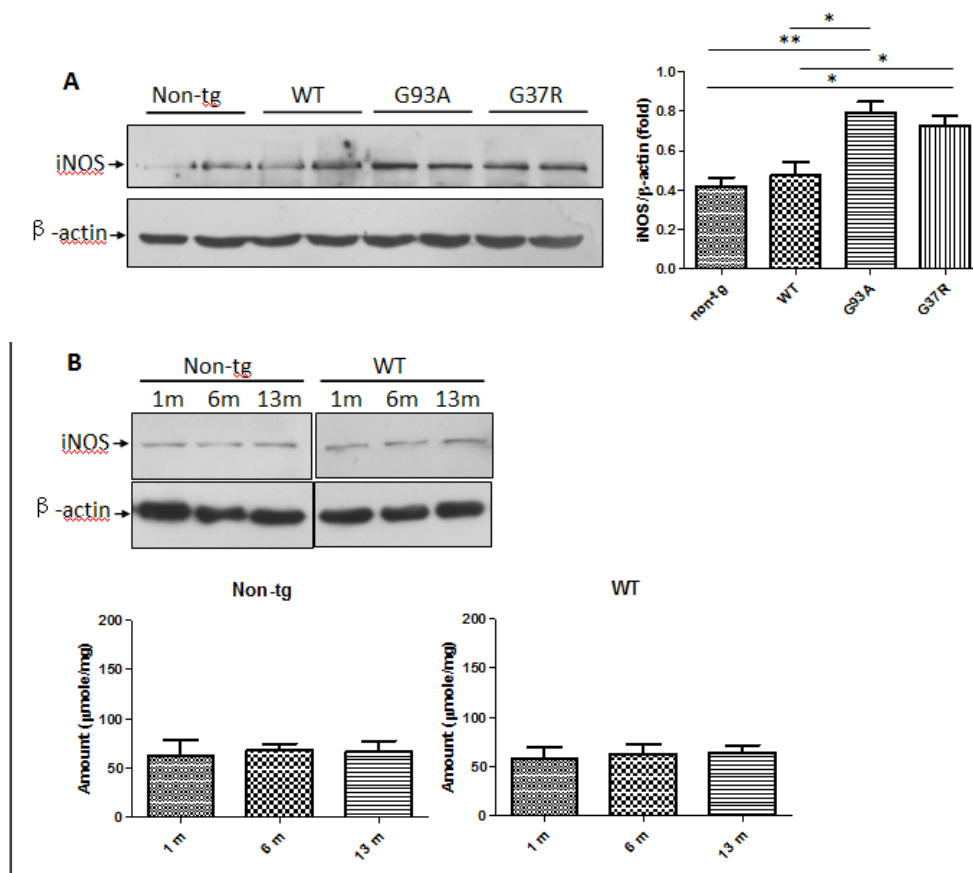
role of PDI in protecting against mutant protein aggregation in ALS is supported by various studies. For example, when mutant SOD1 expressing NSC-34 cells were treated with baccatin, an inhibitor of PDI, the formation of SOD1 inclusions was increased [54]. Another example was siRNA-mediated knockdown of PDI resulted in increased formation of mutant SOD1 inclusion in neuroblastoma cells [60]. However, the PDI up-regulation in ALS was not enough to protect against mutant SOD1 aggregate formation, since S-nitrosylation of PDI may affect its enzymatic activity and promote the aggregates formation. We found that NO-mediated S-nitrosylation of PDI was probably involved in the formation of mutant SOD1 aggregates, seeing as NO donor SNOC induced S-nitrosylation of PDI in a dose-dependent manner. Furthermore, the inclusions in mutant SOD1^{G93A} expressing cells were enhanced by SNOC. Our studies also showed that, with the use of NOS inhibitor NNA to suppress S-nitrosylation of PDI, the SOD1 inclusions were inhibited, and the level of insoluble mutant SOD1 in the pellet fraction was decreased as well. This finding indicates that in the cell model of ALS, manipulating the NO levels by using an NO donor or NOS inhibitor, affects the formation of S-nitrosylated PDI. S-nitrosylation of PDI may highly correlate with mutant SOD1 aggregates formation. Since S-nitrosylation of PDI could inhibit its chaperone activity in rearrangement of protein folding, allow the misfolded proteins to accumulate, and finally contribute to neuronal cell death. In addition, the subcellular redistribution of PDI has recently been implicated in the pathogenesis of ALS. Studies have demonstrated that the reticulon family of proteins can modulate PDI distribution. They found that reticulon overexpression causes a change of PDI localization, from a normal ER distribution to a less homogenous punctuate pattern [320]. In ALS mice, knocking down the expression of

the reticulon-4A, B proteins accelerate disease processes, possibly resulting from the prevention of reticulon-mediated PDI redistribution [320]. Furthermore, co-localized inclusions of PDI with mutant SOD1, and TAR DNA-binding protein 43kDa (TDP-43) have been found in ALS patients [457]. Under cellular stress, PDI may leave the ER and then accumulate with SOD1 or TDP-43 in the cytosol. PDI also accumulates in the swollen neuritis, the disturbance of axon transport was probably due to the loss of PDI function [457]. Another ALS-related protein, fused in sarcoma (FUS), is found to be associated with PDI. Mutant FUS inclusions in human ALS lumbar spinal cords are co-localized with PDI. Since FUS contains cysteine residues, similar to mutant SOD1 and mutant TDP-43, it may physically interact with PDI, and the chaperone function of PDI may have a protective role in refolding misfolded FUS protein. Overall, these findings indicate that posttranslational modifications and subcellular redistribution of PDI are involved in regulation of PDI's function in ALS, with potential implications for disease pathogenesis.

In summary, the current study examined the propensity of S-nitrosylated PDI contributing to the accumulation of mutant SOD1 aggregates in ALS. Since excessive production of NO derived from iNOS up-regulation is thought to be a contributing factor in ALS, our elucidation of an NO-mediated pathway to dysfunction of PDI by S-nitrosylation provides a mechanism link between the production of free radicals and aberrant protein accumulation in ALS. The outcome of this study shall open up new therapeutic approaches to prevent aberrant protein misfolding by targeted-prevention of nitrosylation of specific proteins such as PDI in the future. Moreover, enhancing the action of PDI may represent a novel strategy for the treatment of ALS.

Fig. 4.1 iNOS protein levels in the spinal cords of non-transgenic and SOD1 transgenic mice

A. Full-length iNOS protein is more enriched in the spinal cords of mutant SOD1 transgenic mice (both G93A and G37R) than in the age-matched non-transgenic mice and wild-type SOD1 transgenic mice (6 m). The densitometry of the iNOS-immunoreactive band increases significantly in mutant SOD1 transgenic mice. B. iNOS expression does not change during the lifetime of non-transgenic mice and wild-type SOD1 transgenic mice. C, D. iNOS expression in the spinal cords of G93A and G37R mutant transgenic mice is increased with the disease progression and reaches a peak at disease end-stage. Values represent the mean±S.E of 5 independent experiments; *, $p < 0.05$; **, $p < 0.01$ by one-way ANOVA with Tukey's post hoc test.



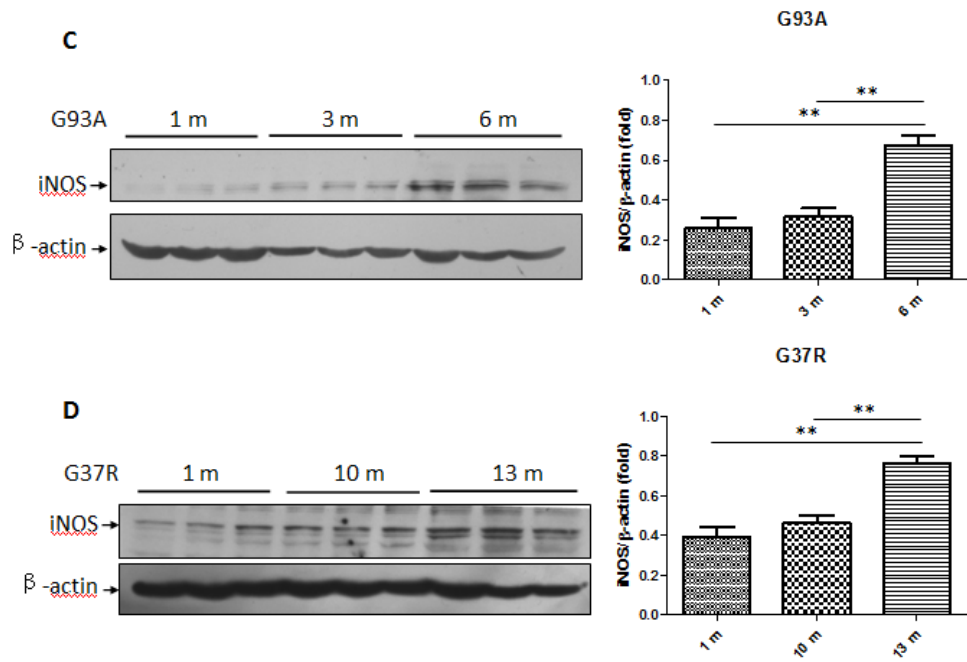


Fig. 4.2 The changes of NO levels in the spinal cords of non-transgenic and SOD1 transgenic mice

A. NO concentration increases significantly in the spinal cords of mutant SOD1 transgenic mice (both G93A and G37R) compared to that of the age-matched non-transgenic mice and wild-type SOD1 transgenic mice (6 m). B. NO production remains unchanged during the lifetime of non-transgenic mice and wild-type SOD1 transgenic mice. C, D. NO generation in the spinal cords of G93A and G37R mutant SOD1 transgenic mice increases significantly at disease end-stage, compared to the pre-symptomatic and onset stages. Given are the mean±S.E from 5 independent measurements; *, $p < 0.05$; **, $p < 0.01$; ***, $p < 0.001$ by one-way ANOVA with Tukey's post hoc test.

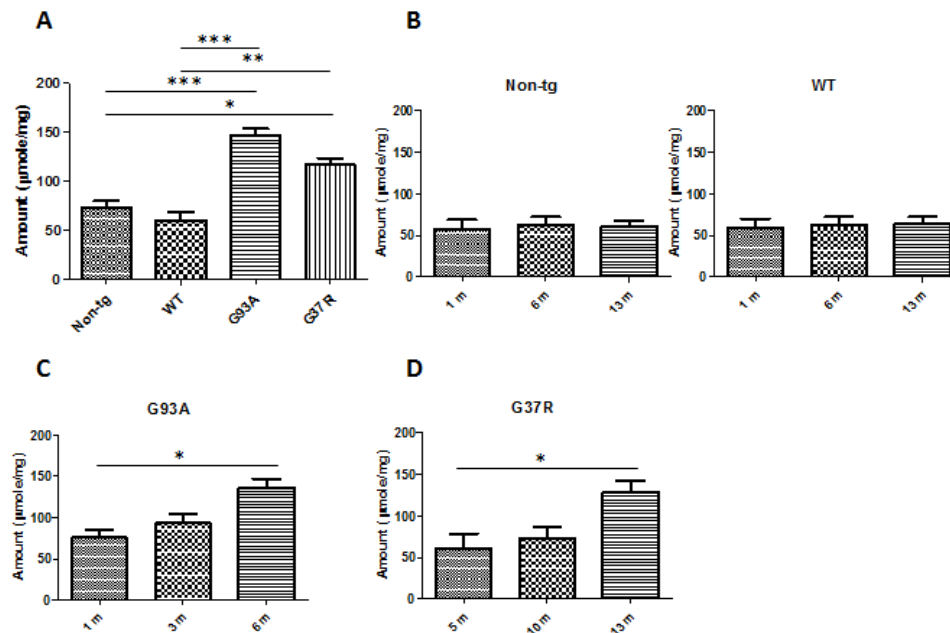
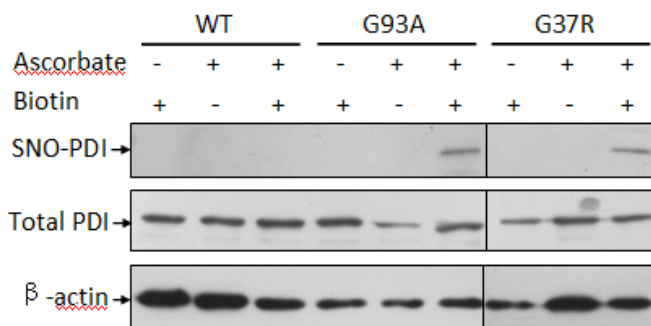


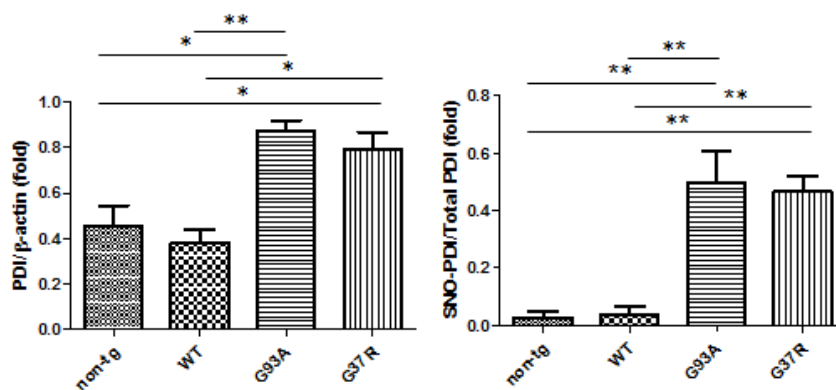
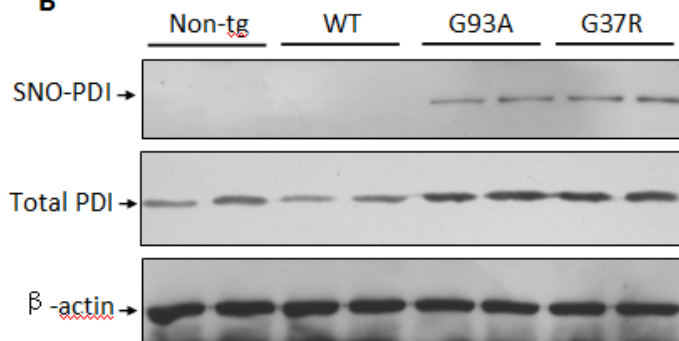
Fig. 4.3 Total PDI and SNO-PDI levels in the spinal cords of non-transgenic and SOD1 transgenic mice

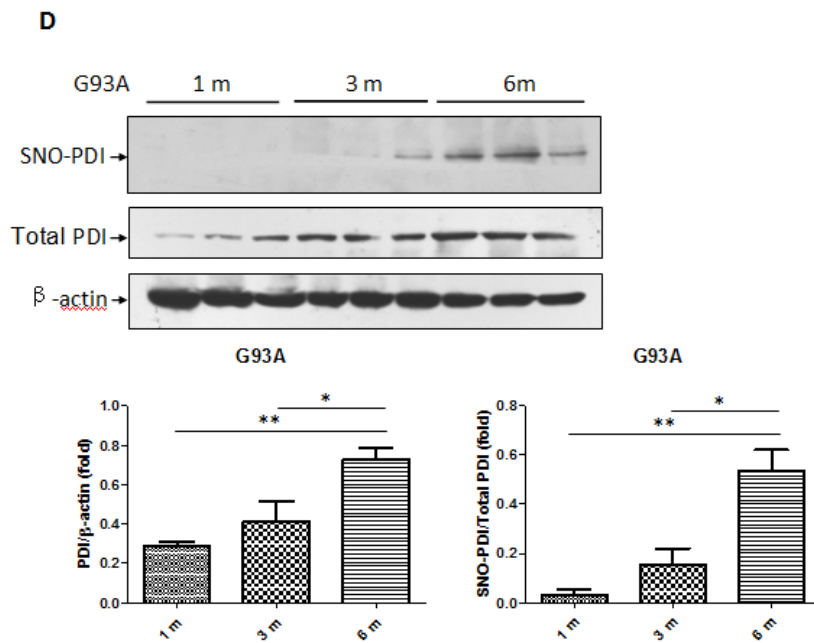
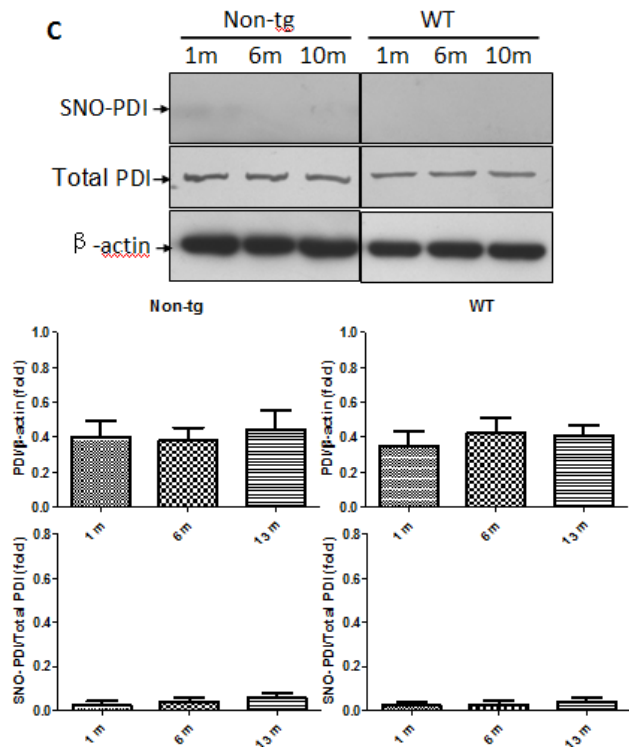
A. Without ascorbate or biotin-HPDP treatment, there is no SNO-PDI. B. PDI is up-regulated and S-nitrosylated in the spinal cords of mutant SOD1 transgenic mice (both G93A and G37R). C. There are no change of PDI expression and no S-nitrosylation of PDI during the lifetime of non-transgenic mice and wild-type SOD1 transgenic mice. D, E. PDI is increased and becoming S-nitrosylated with disease progression in both G93A and G37R SOD1 mutant transgenic mice. SNO-PDI level is much higher at disease end-stage than pre-symptomatic and onset stages, and this difference is significant in densitometric quantitation. Data is presented as mean±S.E.; *, $p < 0.05$ by one-way ANOVA with Tukey's post hoc test.

A



B





E

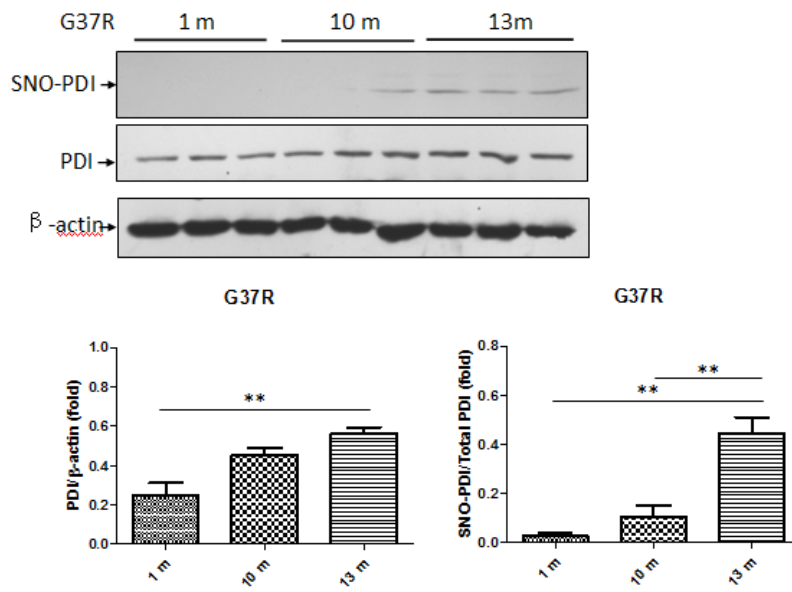


Fig. 4.4 The iNOS expression and NO generation in SH-SY5Y cells expressing SOD1^{wt} or mutant SOD1^{G93A}.

A. Cells transfected with SOD1^{wt} or SOD1^{G93A} have equivalent hSOD1-EGFP expression, compared with control cells without transfection. B. SH-SY5Y cells expressing SOD1^{G93A} have increased iNOS expression compared with control cells and cells expressing SOD1^{wt}. C. NO production from cells with SOD1^{G93A} expression is much higher than that from control cells or cells expressing SOD1^{wt}. Data is presented as mean±S.E.; *, $p < 0.05$ by one-way ANOVA with Tukey's post hoc test.

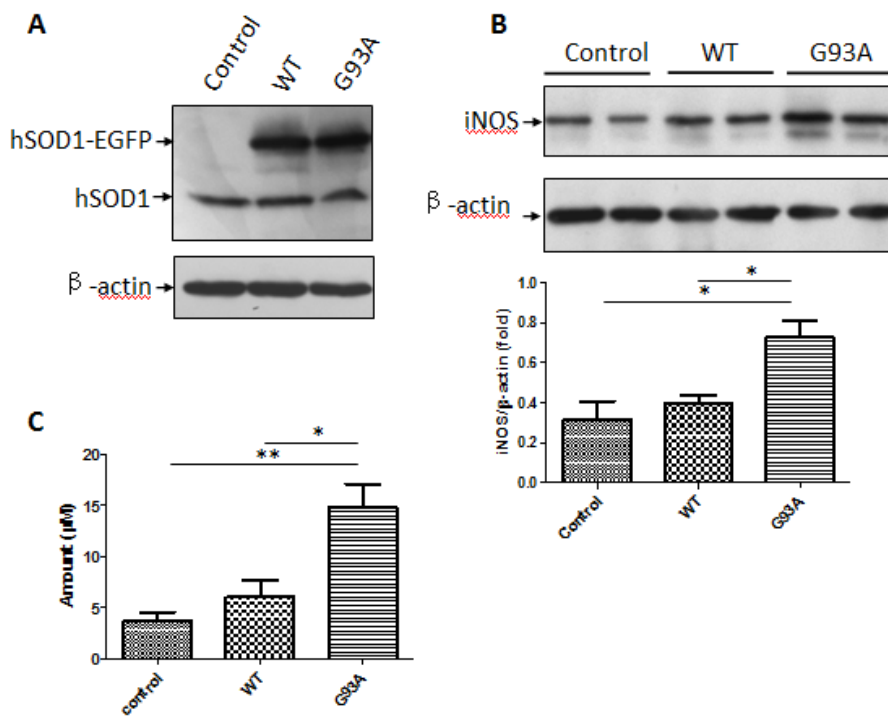


Fig. 4.5 Exogenous NO donor and mutant SOD1^{G93A} expression induce S-nitrosylation of PDI in SH-SY5Y cells.

A. Old SNOC has no effect on the SNO-PDI formation; the freshly prepared SNOC induces S-nitrosylation of PDI. The level of SNO-PDI is up-regulated with the increased concentration of SNOC. SNOC induces S-nitrosylation of PDI in a strongly and statistically significant dose-dependent manner, with the maximum effect seen in the concentration of 400 μ M. B. SH-SY5Y cells expression SOD1^{G93A} have SNO-PDI formation, not in cells expressing SOD1^{wt}. Exposing the cells with SOD1^{G93A} expression to SNOC (200 μ M) promotes the SNO-PDI formation; NNA (100 μ M) suppresses the SNO-PDI formation. Data is presented as mean \pm S.E.; *, $p < 0.05$ by one-way ANOVA with Tukey's post hoc test.

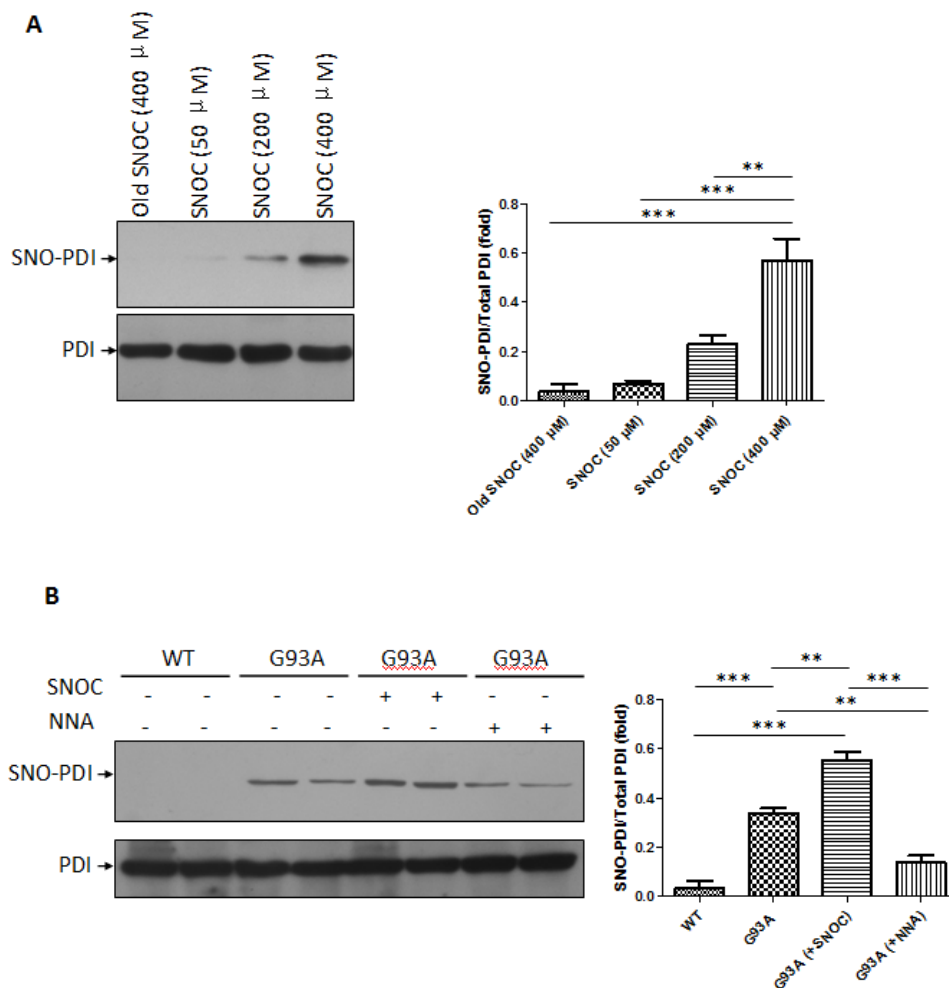
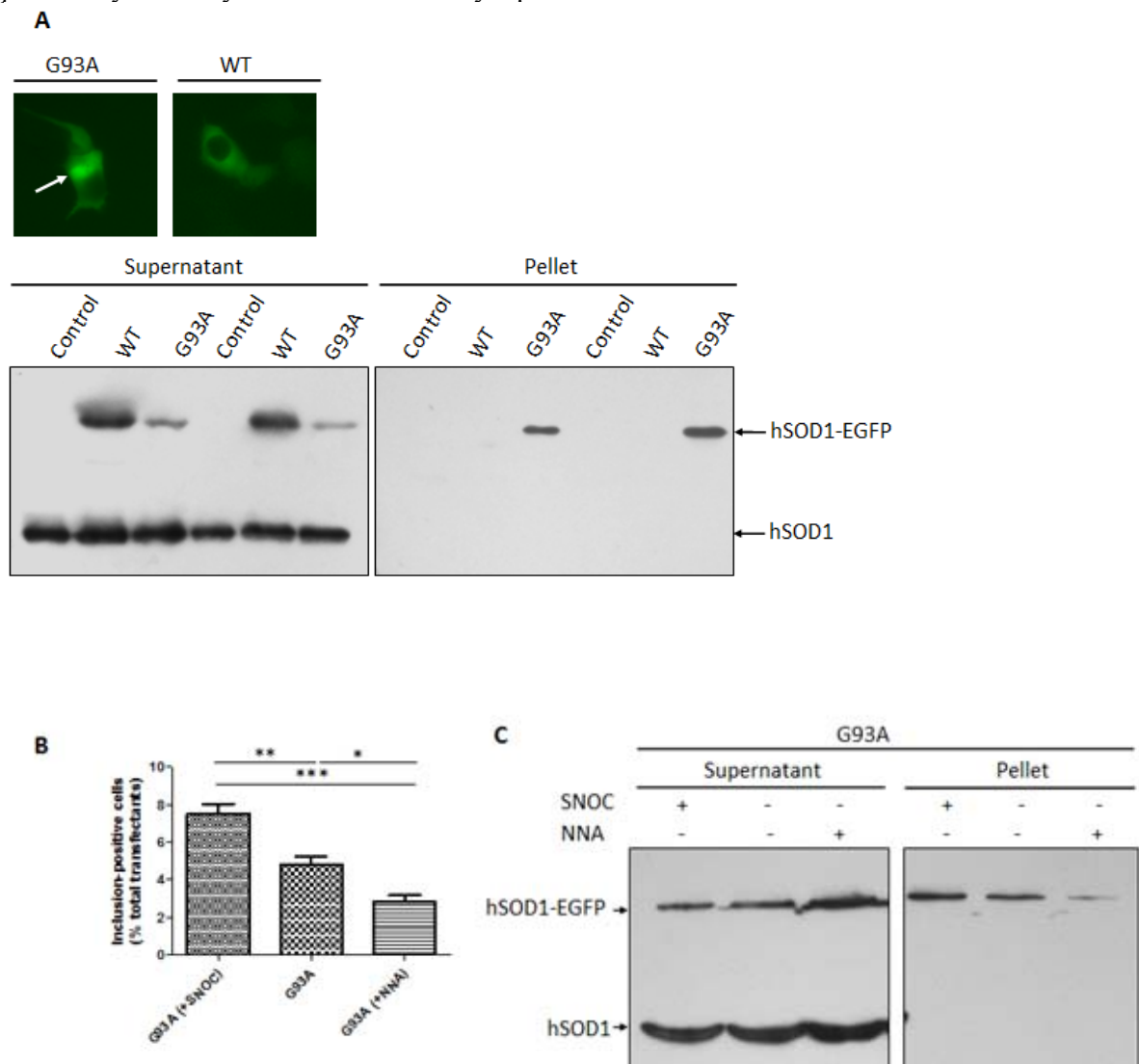


Fig. 4.6 The effect of SNOC and NNA on the SOD1 aggregates formation in transfected SH-SY5Y cells.

A. SH-SY5Y cells expressing SOD1^{G93A} have strong inclusion formation in the cytoplasm. EGFP-hSOD1 is clearly detectable in the pellet fraction of SH-SY5Y cells expressing SOD1^{G93A}. B. Exposing SOD1^{G93A} transfected cells to SNOC leads to a statistically significant increase in inclusion formation compared with the transfected cells without SNOC treatment; NNA treatment suppress inclusion formation in SOD1^{G93A} transfected cells. C. SNOC exposure increases EGFP-hSOD1 expression in pellet fractions of SOD1^{G93A} transfected cells; NNA treatment decreases EGFP-hSOD1 level in the insoluble pellet fraction of transfected cells. Data is presented as mean±S.E.; *, $p < 0.05$ by one-way ANOVA with Tukey's post hoc test.



Chapter 5. SOD1-linked ubiquitination and aggregation in astrocytes following OGD/reperfusion: a role of NO-mediated S-nitrosylation of protein disulfide isomerase in hypoxic/ischemic injury

5.1 Introduction

Brain ischemia/reperfusion injury is a major public health problem. It causes excitotoxicity, inflammation, cell death, and compensatory neurogenesis [468,469]. Neurons are more susceptible to hypoxic stress than astrocytes. They have fewer antioxidant mechanisms than astrocytes and rely mainly on the metabolic support from surrounding astrocytes [469,470,471]. It is proposed that brain ischemia/reperfusion injury is a consequence of the failure of astrocytes to support the essential needs of neurons. Dysfunction of astrocytes may lead to increasing neuronal death [469]. Any pathophysiological events that affect the function of astrocytes will compromise their neuronal supportive role. One detrimental event after ischemia/reperfusion injury is the dramatic increase in damaging free radicals; including nitric oxide (NO), superoxide, and peroxynitrite, both in astrocytes and neurons [472]. Expressions and activities of nitric oxide synthases (NOS) are enhanced in the experimental mouse model of cerebral ischemia/reperfusion injury. NO and its further oxidative products are generally implicated in the pathology of brain ischemia/reperfusion injury. There are three isoforms of mammalian NOS: neuronal NOS (nNOS), inducible NOS (iNOS), and endothelial NOS (eNOS). Although experimental brain ischemia/reperfusion injury leads to the up-regulation of all three NOS isoforms, their expression patterns differ both temporally and spatially. The induction of iNOS expression occurs much later than nNOS and eNOS, suggesting that iNOS contributes to relatively late injury [344]. iNOS-deficient mice

exhibit a significant reduction in infarct volume and attendant behavioural change after 48 h of hypoxic/ischemic injury [473,474]. Studies show that astrocytes are the cells mainly responsible for iNOS expression after ischemia/reperfusion injury [475]. Once iNOS is expressed following transient hypoxic/ischemic, it will promote the production of neurotoxic amounts of NO consecutively [346,476], with maximal levels after 24 h in the striatum and 48 h in the cortex, without any requirement for further activation [322].

Ischemia/reperfusion injury may impair chaperone function and ubiquitin-proteasomal degradation and lead to protein aggregation [477]. Studies show that ubiquitinated-protein aggregates can be visualized in cultured astrocytes after glucose deprivation [391]. Ischemia/reperfusion injury disrupts proper peptide folding in the endoplasmic reticulum (ER) and triggers ER stress and an unfolded protein response (UPR) [478]. Formation of these ubiquitinated-protein aggregates is one of the consequences of functional disturbance within the ER. Proper maturation and folding of native proteins rely on the activity of the ER chaperones and enzymes. Dysfunction of ER chaperone proteins can lead to protein misfolding and further aggregation, which will be recognized and ubiquitinated by the ubiquitin system through a series of ATP dependent reactions [479]. Protein disulfide isomerase (PDI), an ER chaperone, is critical for proper protein folding in the ER. PDI is responsible for facilitating disulfide bond formation, rearrangement reactions, and structural stability [417]. Copper-zinc superoxide dismutase (SOD1) is an intracellular homodimeric metalloprotein, which is stabilized by an intrasubunit disulfide bond between cysteine 57 and cysteine 146. Mutations in SOD1 protein promote the formation of disulfide-reduced monomers, which are prone to forming aggregates. Hence, modulation of disulfide bond formation may be important in

SOD1-linked aggregate formation. PDI was found to be associated with SOD1 in cellular and animal models of familial amyotrophic lateral sclerosis (FALS), a neurodegenerative disease affecting motor neurons. Furthermore, a biochemical interaction between PDI and SOD1 is implicated in the pathogenesis of FALS [54]. In many neurodegenerative disorders and cerebral ischemia, upregulation of PDI expression represents an adaptive response promoting protein refolding and may offer neuronal cell protection [373,420]. Recently, Uehara and colleagues [421] demonstrated that in Parkinson's disease and related neurodegenerative disorders, the NO-mediated S-nitrosylation of PDI inhibits PDI function, which leads to dysregulated protein folding, and consequently results in ER stress that promotes neuronal cell death. S-nitrosylation is an important biological reaction of NO and involves the covalent addition of NO to a cysteine thiol group of the protein to form S-nitrosothiols (RSNOs). This modification can affect many cellular processes and alter both protein function and protein-protein interactions [333].

In this study, we examined if the iNOS expression was correlated with NO-induced S-nitrosylation of PDI in cultured astrocytes following oxygen glucose deprivation (OGD)/reperfusion treatment. We also detected whether or not S-nitrosylation of PDI was associated with accumulation of ubiquitinated-protein aggregates. We report here that the OGD/reperfusion treatment of cultured astrocytes led to an increase in NO production that was accompanied by augmented iNOS protein expression. The expression of both PDI and SOD1 were adaptively up-regulated in response to ischemia/reperfusion injury and an interaction between these two proteins was identified in cultured astrocytes by using co-immunoprecipitation. Although total PDI expression was increased following OGD/reperfusion treatment, PDI was found to be S-nitrosylated by

ischemia/reperfusion-induced nitrosative stress. The formation of S-nitrosylated PDI (SNO-PDI) was detected in cultured astrocytes following OGD/reperfusion treatment, and the SNO-PDI level had a parallel relationship to the formation of ubiquitinated-protein aggregates. These aggregates were found to be co-localized with SOD1 protein, which was indicated to be an ubiquitinated protein in astrocytes under ischemia/reperfusion stress. Blocking NO generation with iNOS inhibitor 1400W significantly attenuated the formation of SNO-PDI and ubiquitinated-protein aggregates in cultured astrocytes following OGD/reperfusion treatment. We report here that, in cultured astrocytes, the up-regulation of iNOS after OGD/reperfusion promoted the NO-mediated S-nitrosylation of PDI. This modification of PDI may affect the chaperone activity of PDI and result in the formation of SOD1-linked ubiquitinated-protein aggregates in cultured astrocytes.

5.2 Materials and methods

5.2.1 Primary astrocyte culture

Primary astrocytes were taken from cerebral cortices of neonatal Wistar rats as described previously [480]. Cortices were harvested, while the meninges and blood vessels were removed. Tissues were digested in 0.25% Trypsin containing 0.1 EDTA at 37°C for 15 min, and passed through a nylon sieve (80 µm pore size). The cells were seeded in Dulbecco's modified Eagle's medium (DMEM) supplemented with heat-inactivated 10% fetal calf serum, 50 µg/ml penicillin, and 100 µg/ml streptomycin. Cultured cells were grown at 37°C in a humidified atmosphere with 5% CO₂. After 10

days, the microglia and oligodendrocyte progenitors were depleted through shaking. The remaining astrocytes were then detached by trypsinization and re-plated at a density of approximately 1×10^5 cells/ml for future experiments. The purity of astrocytes (>90%) was identified through immunohistochemical analysis with anti-glial fibrillary acidic protein (GFAP).

5.2.2 OGD/reperfusion and 1400W treatment

On the third day of subculture, astrocytes were subjected to OGD with Earl's Balanced Salt Solution (EBSS) medium (in mg/L: 6800 NaCl, 400 KCl, 264 CaCl₂·2H₂O, 200 MgCl₂·7H₂O, 2200 NaHCO₃, 140 NaH₂PO₄·H₂O, pH 7.2) and incubated in a hypoxic incubator filled with 1.5% O₂ and 5% CO₂ at the same time for 8 h. The oxygen level in the OGD solution decreased to about 2-3% after 60 min in the hypoxic incubator [481]. Then the cells were provided with a normal amount of oxygen and maintenance medium without glutamate to mimic *in vivo* reperfusion for up to 24 h. Normoxic control cells were incubated in 37°C with 5% CO₂ and atmospheric air in a buffer almost identical to EBSS except containing 5.5 mM glucose. iNOS inhibitor 1400W was prepared as concentrated stock solutions according to the manufacturer's instructions. The final concentrations of 1400W in media applied to astrocytes were as follows: 1, 10, and 50 μM. 1400W was added to culture medium 30 min prior to OGD exposure, and astrocytes were maintained in EBSS and maintenance medium during the treatment.

5.2.3 Measurement of NO level

The concentration of NO in the culture media was determined by the Griess reaction

with minor change [439]. Briefly, 40 μ l cell culture fluid, 10 μ l NADPH, and 40 μ l basal solution (0.03 M PBS, 1.25 mM glucose-6-phosphate, 400 U/L glucose-6-phosphate dehydrogenase, 200 U/L nitrate reductase) were incubated in a 96-well microtiter plate for 45 min at room temperature (RT). Next 50 μ l Griess reagent was added and the solution was incubated for 20 min in the dark at RT. Finally, the absorbance of the samples was measured at 540 nm. NO₂ concentrations were calculated from a standard curve of Sodium nitrite (NaNO₂).

5.2.4 Western blot and immunoprecipitation

Protein concentrations of cell lysates were determined by using the bicinchoninic acid (BCA) method (Pierce, Rockford). Samples (20 μ g) were loaded on 12% sodium dodecyl sulphate polyacrylamide gel (SDS-PAGE) for electrophoresis and then transferred to the PVDF membrane. Membranes were blocked with 5% (w/v) milk in TBS-T buffer (10 mM Tris-HCl, pH 7.5, 150 mM NaCl, 0.05% Tween-20) for 1 h and then incubated with primary antibodies for 16 h at 4°C; SOD1 (1:2000, Santa Cruz Biotechnology), iNOS (1:1000, Santa Cruz Biotechnology), PDI (1:1000, Cedarlane). β -actin was used as a internal control (1:2000, Santa Cruz Biotechnology). Blots were washed in TBS-T buffer three times, probed with HRP-conjugated goat anti-rabbit or goat anti-mouse antibodies at 1: 2500 for 1 h at RT, and then developed using chemiluminescence (ECL) reagents (PerkinElmer). Quantification of band intensities was performed by densitometric analysis using quantity one (Bio-Rad). Whole cell lysates (200 μ l) were incubated with 50 μ l of protein A-Sepharose CL-4B (Amersham Biosciences) for 30 min at 4°C with gentle rotation to remove IgG from the sample. The

beads were briefly spun down and precleared cell lysates transferred to fresh tubes. 30 μ l of 50% (w/v) protein A-Sepharose CL-4B in Tris buffer (50 mM Tris-HCl, pH 7.5, 0.02% (w/v) NaN₃) and anti-SOD1 or -PDI (1:750) antibodies were incubated with 100 μ l precleared cell lysates on a rotating wheel overnight at 4 °C. 20 μ g of total protein was incubated with the sepharose-antibody to capture the antibody-binding protein complexes. After centrifugation at 15,800 \times g for 1 min to remove the supernatant, the precipitate was washed three times in Tris buffer for 10 min each. Both the supernatant and the immunoprecipitate was mixed with a 2% (w/v) SDS sample loading buffer and used for SDS-PAGE and immunoblot following the methods described above..

5.2.5 Biotin-switch assay for detection of SNO-PDI

The cell lysates were prepared in HENC buffers (250 mM Hepes pH 7.5, 1 mM EDTA, 0.1 mM neocuproine, 0.4% CHAPS). Typically 1 mg of cell lysate was used. The Blocking buffer (2.5% SDS, 20 mM methyl methane thiosulphonate [MMTS] in HEN buffer) was mixed with the samples and incubated for 30 min at 50°C to block any free thiol groups. After removing excess MMTS by acetone precipitation, nitrosothiols were reduced to thiols with 1 mM ascorbate. The newly formed thiols were then linked with the sulphhydryl-specific biotinylating reagent *N*-[6-(biotinamido)hexyl]-3'-(2'-pyridyldithio) propionamide (Biotin-HPDP). The biotinylated proteins were pulled down with Streptavidin-agarose beads. Western blot analysis was then performed to detect the amount of PDI remaining in the samples [60].

5.2.6 Subcellular fractionation

Both the pellet and cytosolic fraction were prepared as described by Chen et al [384]. Briefly, cell lysates of cultured astrocytes were sonicated for 30 sec at 4°C in ice-cold lysis buffer (pH 7.6) containing (mM): 15 Tris-HCl, 1 dithiothreitol, 250 sucrose, 1 MgCl₂, 2.5 EDTA, 1 EGTA, 250 Na₃VO₄, 25 NaF, 2 sodium pyrophosphate, 0.5 phenylmethylsulfonyl fluoride (PMSF), plus 1 µg/mL pepstatin A, 5 µg/mL leupeptin, and 2.5 µg/mL aprotonin. Protein content in lysates was determined by BCA assay. Equal amounts of total cell lysate protein in each sample (0.5 mg) were centrifuged at 13,000 g in 4°C for 10 min. The pellet fractions were sonicated three times and washed for 1 h at 4°C with 2% Triton X-100 and 150 mM KCl in the ice-cold lysis buffer. After being centrifuged at 13,000 g in 4°C for 10 min, the pellet fraction containing the detergent/salt-insoluble aggregates was sonicated and re-dissolved in the lysis buffer for Western-blotting assay.

5.2.7 Double-immunofluorescence staining of ubiquitin and SOD1

Astrocytes on coverslips were fixed with 4% paraformaldehyde in PBS for 20 min. After being rinsed three times, cells were incubated with the blocking buffer (5% goat serum, 0.3% Triton X-100, and 1% bovine serum albumin in PBS) for 1 h, the coverslips were incubated with primary antibodies against ubiquitin (1:500) and SOD1 (1:1000) overnight at 4°C. After rinsing, coverslips were incubated with Alexa Fluor 488 anti-mouse IgG or 594 anti-rabbit IgG for 1 h at 37°C. Then hoeschest 33342 was added in order to stain the nuclei and the coverslips were mounted on the slides. The slides were imaged by an observer blind to treatments on a Zeiss Axiovert upright fluorescent microscope with identical exposure settings and identical post-acquisition processing for

each image.

Astrocytes on coverslips were fixed with 4% paraformaldehyde in PBS for 20 min. After being rinsed for three times, cells were incubated with the blocking buffer (5% goat serum, 0.3% Triton X-100, and 1% bovine serum albumin in PBS) for 1 h, the coverslips were incubated with primary antibodies against ubiquitin (1:500) and SOD1 (1:1000) overnight at 4°C. After rinsing, coverslips were incubated with Alexa Fluor 488 anti-mouse IgG or 594 anti-rabbit IgG for 1 h at 37°C. Then hoeschest 33342 was added to stain nuclei and the coverslips were mounted on the slides. The slides were imaged by an observer blind to treatments on a Zeiss Axiovert upright fluorescent microscope with identical exposure settings and identical post-acquisition processing for each image.

5.2.8 Statistics

Quantification of band intensities was performed by densitometric analysis using Quantity One® 1-D analysis software (Bio-Rad). The statistical calculations and graphing were performed using GraphPad Prism® software, version 5. All data was tested using one-way analysis of variance (ANOVA) with Tukey's post hoc test. A p value of 0.05 or less was judged to be significant. Results were expressed as mean ± SEM.

5.3 Results

5.3.1 OGD/reperfusion induces NO formation and iNOS protein expression

The cortical astrocyte culture was subjected to OGD for 8 h and then exposed to reperfusion for either 16 h or 24 h. The concentration of NO in the culture media and the

protein expression of iNOS were then determined. NO generation was slightly increased after OGD treatment. The increase of NO was exaggerated by the reperfusion treatment. NO concentration reached a maximal level at the latest time studied (OGD 8 h/reperfusion 24 h). A similar result was observed in the iNOS protein assay. Under normal circumstances, the iNOS expression was too low to be detected. After OGD treatment, the iNOS expression was up-regulated. Furthermore, the reperfusion treatment led to a dramatic increase of iNOS expression in reactive astrocytes compared with the control cells that were not treated. When iNOS protein expression was quantified, exposure to OGD/reperfusion induced a remarkable increase in the iNOS protein level, especially in astrocytes following OGD 8 h/reperfusion 24 h. These cells exhibited a significant increase of iNOS expression, about 2.5-fold as compared with the control (Fig. 5-1).

5.3.2 PDI and SOD1 are up-regulated after OGD/reperfusion treatment, and they were binding to each other

We investigated the changes in PDI and SOD1 expression levels following OGD/reperfusion treatment in cultured astrocytes. Cell lysates from astrocytes under various treatments were analyzed by immunoblot. Western blot analysis using anti-PDI monoclonal antibody treatment revealed an enhancement of PDI expression after OGD 8 h, which had reached a maximum by 24 h of reperfusion. A similar pattern was also observed in SOD1 expression. Immunoblot analyses confirmed an increased expression of SOD1 in cultured astrocytes when they were exposed to OGD for 8 h. In addition, reperfusion significantly induced appreciable SOD1 expression in these cells, yielding a

3-fold higher abundance of SOD1 protein in OGD 8 h/reperfusion 24 h group when compared with the control group. These results demonstrate that the elevation of PDI and SOD1 expression correlate well with the induction of iNOS in activated astrocytes following OGD/reperfusion treatment. We then used immunoprecipitation to examine the interaction between PDI and SOD1. Cell lysates from astrocytes under various treatments were subjected to immunoprecipitation using the anti-SOD1 antibody or anti-PDI antibodies. Western blot analysis of immunoprecipitated proteins revealed that PDI was co-precipitated by anti-SOD1 antibody and SOD1 was co-precipitated by the anti-PDI antibody. This result suggested a physical interaction between PDI and SOD1. Fainter PDI bands were observed in the OGD/reperfusion group after immunoprecipitation using the anti-SOD1 antibody. The up-regulated PDI after OGD/reperfusion treatment seemed not to bind any more SOD1 in the immunoprecipitation studies. The reverse experiment was also performed; the cell lysates were immunoprecipitated with anti-PDI antibody, followed by western blot with anti-SOD1 antibody. The SOD1 bands were observed, which were also more abundant in the control group (Fig. 5-2).

5.3.3 PDI is S-nitrosylated in astrocytes following OGD/reperfusion; this S-nitrosylation of PDI is blocked by iNOS inhibitor 1400W

We investigated whether or not aberrant generation of NO through activation of iNOS mediated S-nitrosylation of PDI resulted in reactive astrocytes following OGD/reperfusion. Using a biotin-switch assay, we identified that PDI was S-nitrosylated in cultured astrocytes after hypoxic/ischemic stress. The specificity of the biotinylation reaction was confirmed by no detection of SNO-PDI in the samples without treatment of

ascorbate. Ascorbate is required to enhance the chemical decomposition of nitrosothiol groups required for reacting with the biotinylating reagent biotin-HPDP [442]. In addition, no detection of SNO-PDI in the absence of biotin-HPDP also confirmed the specificity of the final streptavidin precipitation step of the assay. Despite the fact that total PDI levels were increased in astrocytes under OGD/reperfusion treatment, abundant SNO-PDI levels were detected in astrocytes following OGD 8 h/reperfusion 24 h treatment. However SNO-PDI was virtually undetectable in the control group and the OGD 8 h group. This trend of SNO-PDI level was consistent with the change of iNOS expression and NO level during the OGD/reperfusion process. To rule out the possibility that the detectable SNO-PDI in the OGD/reperfusion group was not due to the up-regulation of total PDI expression after OGD/reperfusion treatment, we deliberately increased total protein loading to enhance total PDI level in the control group. However, we could not detect the presence of SNO-PDI in the control group. Furthermore, in the OGD 8 h/reperfusion 24 h group, with manipulated less total PDI level due to less total protein loading had tectable SNO-PDI. This data demonstrates that NO-mediated S-nitrosylation of PDI is a characteristic feature of astrocytes in response to hypoxia/ischemic stress. To determine whether or not iNOS plays a role in the promotion of S-nitrosylated PDI formation, we pre-treated primary astrocytes cultures with the iNOS inhibitor 1400W for 30 min followed by OGD/reperfusion. As expected, 1400W pre-treatment strongly inhibited iNOS activity as demonstrated by dose-dependent suppression of NO production in reactive astrocytes. However the iNOS protein levels were not affected by 1400W. Immunoblot analysis of cell lysates revealed that NO-mediated formation of SNO-PDI following OGD/reperfusion treatment in astrocytes was significantly blocked by iNOS

inhibition, with the blockade behaving in a dose-dependent manner. These results suggest that iNOS signaling is involved in the SNO-PDI formation in astrocytes following OGD/reperfusion (Fig. 5-3).

5.3.4 OGD/reperfusion triggers formation of detergent/salt-insoluble ubiquitinated-protein aggregates, which is blocked by iNOS inhibitor 1400W

Protein aggregates have low solubility in a detergent/salt solution. We examined the formation of detergent/salt-insoluble ubiquitinated-protein aggregates in astrocytes under normoxic control conditions and after exposure to OGD/reperfusion. Under normal control conditions, the pellet fraction of astrocytes showed no or hardly any detectable ubiquitinated-protein aggregates. In contrast, during OGD/reperfusion treatment, there was a time-dependent accumulation of ubiquitinated-proteins in the pellets. The ubiquitinated-protein-smears ranged between 37 and 250 kDa as detected by a monoclonal anti-ubiquitin antibody. Since these proteins were detergent/salt-insoluble, they were considered to be protein aggregates. OGD led to a slight increase in ubiquitinated-protein aggregate formation. However, the difference between the OGD 8 h group and the control group did not reach statistical significance. The level of ubiquitinated-protein aggregates was further developed and reached approximately 6-fold at 16 h reperfusion; it remained significantly elevated at 24 h reperfusion, at which point it was about 8-fold as compared to the OGD 8 h group. These results suggest that OGD/reperfusion results in a progressive formation of ubiquitinated-protein aggregates. These aggregates may link to the formation of SNO-PDI in astrocytes. Since inhibiting the activity of iNOS through inhibitor 1400W led to the suppression of S-nitrosylation of

PDI, we hypothesized that while S-nitrosylation of PDI was blocked by 1400W, the formation of ubiquitinated-protein aggregates might be subsequently inhibited. We examined the changes of ubiquitinated-protein aggregate levels in astrocytes following OGD 8 h/reperfusion 24 h treatment when S-nitrosylation of PDI was inhibited by 1400W. In the presence of various concentrations of 1400W, the levels of ubiquitinated-protein aggregates were significantly decreased in a dose-dependent manner. This change of ubiquitinated-protein aggregates with the use of 1400W correlated well with the change of SNO-PDI formation (Fig. 5-4).

5.3.5 OGD/reperfusion induces re-distribution of ubiquitinated-protein, and co-localization of ubiquitin with SOD1 protein

Seeing as the monoclonal anti-ubiquitin antibody can recognize both free and conjugated ubiquitin, it was used to monitor both ubiquitin redistribution and formation. The normoxic control astrocytes showed even and diffuse immunoreactivity of ubiquitin with nuclear staining. In astrocytes subjected to OGD 8 h/reperfusion 16 h treatment, the diffuse distribution of free ubiquitin was absent; instead, the ubiquitin immunoreactivity changed into loss of nuclear staining and the appearance of aggregates throughout the cytoplasm. This punctuated ubiquitin in the peri-nuclear regions were considered to be the conjugated ubiquitin. With the use of 1400W to inhibit the S-nitrosylation of PDI, the punctuated staining of ubiquitin in the cytoplasm was less abundant when compared to those cells without 1400W treatment. To investigate whether this ubiquitin was conjugated to SOD1 protein, we examined localization of SOD1 under normal conditions and under conditions of OGD/reperfusion. Under normal conditions, SOD1 was

distributed in the nucleus and throughout the cytosol. However, following OGD 8 h/reperfusion 16 h, the SOD1 immunoreactivity was clustered near nuclei in addition to the nuclear distribution. Small SOD1-positive aggregates were seen in the cytoplasm of astrocytes following OGD 8 h/reperfusion 16 h. To further examine the ubiquitination of SOD1, we performed double immunostaining with anti-SOD1 and anti-ubiquitin antibodies. After OGD 8 h/reperfusion 16 h treatment, the cultured astrocytes were immunostained with anti-SOD1 and anti-ubiquitin antibodies. As a result, SOD1 aggregates induced by OGD 8 h/reperfusion 16 h were clearly co-localized with ubiquitin, suggesting the ubiquitination of the SOD1 protein (Fig. 5-5).

5.4 Discussion

Brain ischemia/reperfusion injury encompasses all cell types in the CNS, including neurons and astrocytes. Astrocytes are believed to play a fundamental role in the pathogenesis of neuronal death. The failure of astrocytes in supporting the essential needs of neurons constitutes a great threat for neuronal survival. The multifaceted and complex role of astrocytes in response to injury includes enhancing neuronal survival/regeneration and contributing to further injury [482,483]. Glial cells, including astrocytes, generate excessive amounts of NO as a result of the activation of iNOS, and NO can induce neuronal apoptosis in ischemia/reperfusion injury. However, the cellular and molecular mechanisms of neuronal death induced by excessive NO have not yet been clearly defined. Brain hypoxic/ischemic injury is associated with an obvious inflammatory reaction that results in the expression and release of several cytokines [484]. These important mediators activate the expression of iNOS in different cell types, including

glial cells in the CNS [485,486,487]. Interleukin-1 β (IL-1 β) and tumour necrosis factor (TNF α), which are significantly increased within a few hours of ischemia. IL-1 β and TNF α trigger transcriptional activation of the iNOS gene and then up-regulate iNOS expression [349,488]. Oxidative stress induced by ischemia might itself trigger the induction of iNOS. Moreover, the iNOS promoter contains a hypoxia response element, seeing as a specific pathway with regards to the hypoxia-inducible factor-1 α (HIF-1 α) pathway can be activated at the onset of ischemia [350]. Consequently, the NO generation persists. It is believed that NO produced by de novo expression of iNOS contributes to brain damage caused by hypoxic ischemia [489]. In the present study, we examined whether or not iNOS expression was enhanced in response to OGD/reperfusion in astrocytes. Consistent with previous research, OGD/reperfusion markedly elevated iNOS protein levels in cultured astrocytes. Our study first demonstrates that PDI is S-nitrosylated in cultured astrocytes following ischemia/reperfusion injury, and that this is highly associated with extensive generation of NO, which is induced by up-regulated iNOS expression. This finding suggests that S-nitrosylation of PDI probably inactivates the normal properties of PDI, and it may contribute to the pathogenesis of ischemia/reperfusion injury.

PDI is a ubiquitous, highly conserved redox enzyme from the thioredoxin superfamily, located mainly in the ER [458]. During protein folding in the ER, PDI facilitates proper protein folding and helps to maintain the structural stability of the mature protein [417]. As a consequence, PDI is considered to be a molecular chaperone capable of stabilizing the correct folding of substrate proteins. It also facilitates the ER-associated degradation of misfolded proteins [459]. PDI is involved in the

retro-translocation of misfolded cholera toxin from the ER to the cytoplasm by interacting with the ER transmembrane protein Derlin-1 [460]. In this study, we found that PDI expression was up-regulated in astrocytes following OGD/reperfusion. This result was consistent with previous studies that have indicated the up-regulation of PDI in astrocytes in response to hypoxia or transient forebrain ischemia in astrocytes [374]. Study of ischemic cardiomyopathy indicates that PDI is up-regulated in the viable peri-infarct myocardial region after infarction. This up-regulation of PDI led to a significant decrease in the rate of cardiomyocyte apoptosis [372]. All of this evidence put together indicates that the up-regulation of PDI in ischemia/reperfusion injury represents an adaptive response that promotes correct protein folding and offers potential protection to cells. However, detrimental generation of NO derived from iNOS induces S-nitrosylation of PDI; this posttranslational modification of PDI may attenuate its protective effects in ischemia/reperfusion injury.

As we know, ischemia-reperfusion causes accumulation of high-molecular weight ubiquitinated-proteins following forebrain ischemia [378]. These ubiquitinated-protein aggregates are visualized in cultured astrocytes following glucose deprivation/recovery [391]. They are clustered with co-translational chaperones, protein folding enzymes [381], subcellular structures [379], proteasomes [490], and stress granules [383]. These changes may contribute to ischemic dysfunction of astrocytes and lead to neuronal damage. The accumulation of misfolded protein in the ER results in ER stress that triggers the protective UPR. The UPR entails the induction of chaperone molecules, the degradation of misfolded proteins, and inhibition of protein translation [461]. Prolonged ER stress can nonetheless still lead to activation of apoptosis [462]. Studies done on pancreatic β cells,

macrophages [463], and cerebellar granule cells [464] have demonstrated that NO can also induce ER stress. However, the molecular basis of this remains unknown. Furthermore, although the involvement of NO in the pathology of brain ischemia/reperfusion injury has been widely accepted, the chemical relationship between nitrosative stress and formation of ubiquitinated-protein aggregates has remained obscure. Our findings indicate that S-nitrosylation of PDI may hold some of the answers to these questions. Studies have shown that in Parkinson's disease, excitotoxic activation of nNOS leads to excessive NO generation, which causes S-nitrosylation of the active-site thiols of PDI and inhibits its corresponding isomerase and chaperone activities [421]. In this regard, NO blocks the protein's protective effects via S-nitrosylation of PDI. S-nitrosylation of PDI leads to the accumulation of misfolded and polyubiquitinated proteins, and results in prolonged UPR activation. NO-mediated S-nitrosylation of PDI thus participates in persistent ER stress and the induction of apoptosis [421].

We further demonstrated that NO-mediated S-nitrosylation of PDI may take part in the formation of ubiquitinated-protein aggregates in cultured astrocytes following OGD/reperfusion, seeing as the aggregate's formation was blocked by the iNOS inhibitor 1400W, which could efficiently inhibit the S-nitrosylation of PDI. When cultured astrocytes were subjected to OGD/reperfusion, the cells formed smear detergent/salt-insoluble ubiquitinated-protein aggregates. Furthermore, diffuse free ubiquitin staining changed into punctuated staining within peri-nuclear regions. This conjugated ubiquitin with reduced cytosolic and nuclear free ubiquitin distribution was considered to be ubiquitinated-protein aggregates. The formation of these aggregates correlated well with the level of S-nitrosylation of PDI. With the use of 1400W to inhibit

the activity of iNOS, the generation of NO was consequently decreased, which subsequently led to down-regulation of SNO-PDI levels. With the inhibition of S-nitrosylation of PDI, the formation of ubiquitinated-protein aggregates was decreased, seeing as the detergent/salt-insoluble smear of ubiquitin in the pellet fraction was significantly reduced through the use of 1400W. This finding clearly demonstrates that blocking NO generation reduces the accumulation of ubiquitinated-protein aggregates. This blockade effect of 1400W may, result from reducing NO-mediated S-nitrosylation of PDI.

Free radicals contribute to neuronal death following hypoxic/ischemic brain injury. Not surprisingly, several studies have demonstrated that antioxidant treatment improves neuroprotection and recovery after brain injury [491,492,493]. SOD1 is an enzyme that detoxifies free radicals under normal physiologic conditions. SOD1 converts the superoxide anion into hydrogen peroxide, which is subsequently detoxified to water by glutathione peroxidase (GPX) or catalase [494]. Reperfusion following cerebral ischemia leads to an overproduction of free radicals and the consumption of endogenous antioxidants. Neurons are particularly vulnerable to free radical damage partially due to their relatively low levels of endogenous antioxidants. Studies have shown that non-neuronal cells may participate in free radical scavenging during ischemia/reperfusion [495]. One facet of reactive astrocytes in brain ischemia/reperfusion injury is the chronic secretion of antioxidants for neuronal protection and survival. SOD1 is one of the beneficial antioxidants produced by astrocytes. Prior studies using transgenic animal models have clearly established a beneficial role of SOD1 in adult ischemia/reperfusion injury [496]. Rodents overexpressing SOD1 have a much better outcome following head

injury [497]. In our study, the expression of SOD1 was up-regulated in cultured astrocytes following OGD/reperfusion. The increased expression of SOD1 may represent a protective response to ischemic stress that enhances the antioxidant ability. However, studies have shown that SOD1 overexpression offers no protection under OGD conditions in a hippocampal culture model of excitotoxic injury [498]. Our results regarding the S-nitrosylation of PDI in cultured astrocytes following OGD/reperfusion provides an explanation to this finding. First, SOD1 was shown to be one of the PDI molecular targets [306] in ischemic cardiomyopathy. Second, a physical interaction between SOD1 and PDI has been indicated in cultured cells in FALS [54]. PDI bound to both wild-type and mutant SOD1, and co-localized with intracellular aggregates of mutant SOD1. Inhibition of the activity of PDI with the use of bacitracin increases aggregate production [54]. In patients with amyotrophic lateral sclerosis (ALS), PDI was found to be co-localized with SOD1 in neuronal cytoplasmic inclusions (NCIs) [457]. In the present study, PDI and SOD1 were found to bind to one another in astrocyte cultures. Although PDI was up-regulated after OGD/reperfusion treatment, increased total PDI did not bind more SOD1. Instead, less PDI-SOD1 binding was detected after OGD/reperfusion treatment in immunoprecipitation. The possibility is, despite the induction of PDI after ischemia/reperfusion injury, the SNO-PDI could not bind to SOD1 as efficiently as normal PDI. In addition, SOD1 was ubiquitinated to form aggregates, and the insoluble SOD1 aggregates could not be detected in the soluble cell lysates used in the experiment. Some proportion of PDI was associated with SOD1 aggregates in the insoluble fraction of the cell lysates. We may envisage that PDI normally binds to SOD1 to form a disulfide-linked dimer. However, if PDI was S-nitrosylated, it could not bind to

SOD1 as efficiently; and the disulfide-reduced SOD1 would more easily form aggregates. The diffuse distribution of SOD1 within the cytosol and nucleus under normal conditions changed into punctuated peri-nuclear and nuclear distribution following treatment with OGD 8 h/reperfusion 16 h. This result suggests abnormal folding of SOD1 in the cytoplasm had occurred. The ubiquitin-proteasome system (UPS) is the major intracellular proteolytic mechanism that controls the degradation of misfolded/abnormal proteins [499]. The co-localization of SOD1 and ubiquitin indicates that the misfolded SOD1 is ubiquitinated for further degradation. .

In this study, we have successfully demonstrated for the first time that OGD/reperfusion treatment in cultured astrocytes leads to an excess amount of NO generation by iNOS up-regulation in response to stress induced by ischemia/reperfusion. This leads to the formation of ubiquitinated-protein aggregates, probably through the process of S-nitrosylation of PDI. Our elucidation of an NO-mediated pathway that causes dysfunction of PDI by S-nitrosylation provides a mechanistic link between free radical production and abnormal protein aggregation in brain ischemia/reperfusion-induced injury. NO-based therapeutic strategies may help to prevent aberrant protein misfolding by targeting disruption or prevention of nitrosylation of specific proteins such as PDI. These therapeutic strategies may help to improve the protective astrocytic activities in the future, thus enhancing neuronal survival, and improving the outcomes following brain ischemia/reperfusion injury.

Fig. 5.1 Effect of OGD/reperfusion treatment on NO production and iNOS protein production.

A. The changes of NO levels in cultured astrocytes following OGD/reperfusion as determined by Griess reagent. Following reperfusion, NO production increased gradually and reached a peak under the treatment of OGD 8h/reperfusion 24h. This increase was significant in comparison to all other groups. B. iNOS protein levels in cultured astrocytes following OGD/reperfusion as determined by Western blotting. Full-length iNOS protein (~130kDa) was more enriched in the OGD/reperfusion groups compared to the control group. OGD/reperfusion significantly induced greater levels of iNOS than in normal conditions. Five independent experiments were performed and data were analyzed in triplicate. Values were presented as mean±S.E.; *, $p < 0.05$; **, $p < 0.01$; ***, $p < 0.001$ by one-way ANOVA with Tukey's post hoc test.

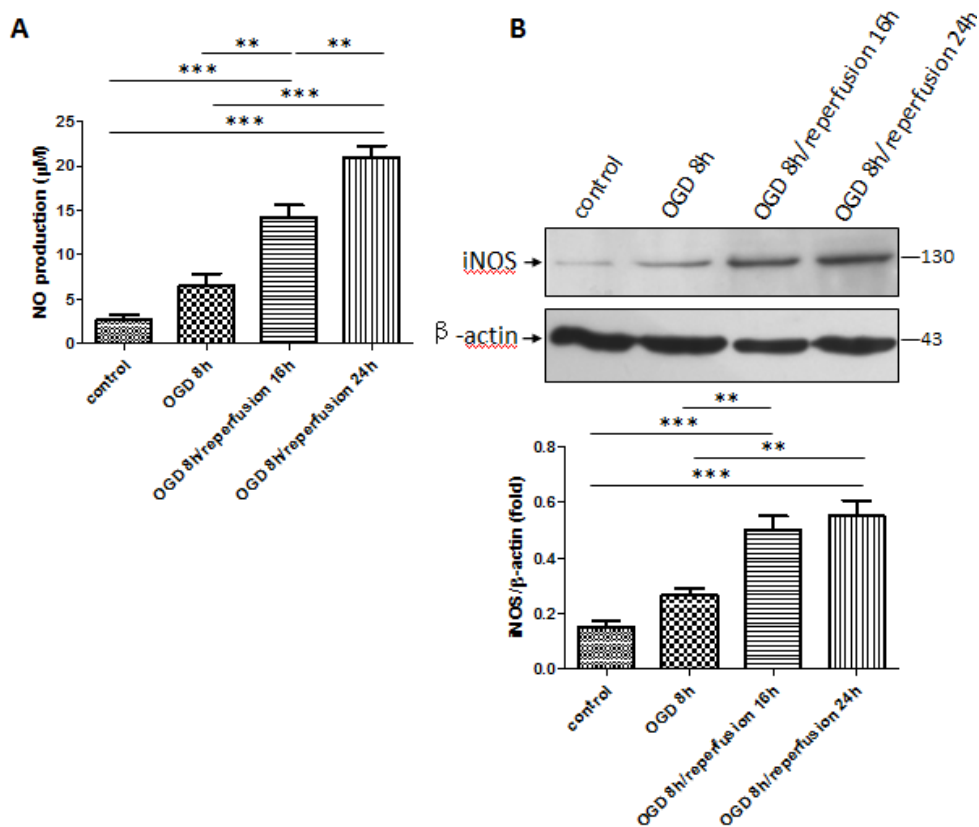


Fig. 5.2 Expressions of PDI and SOD1 protein and their correlations in cultured astrocytes following OGD/reperfusion

A. PDI expression in cultured astrocytes demonstrated an increasing trend in the process of reperfusion and peaked at OGD 8h/reperfusion 24h. B. SOD1 expression in cultured astrocytes was increased gradually during the process of OGD/reperfusion and reached a peak at OGD 8h/reperfusion 24h. C. The anti-SOD1 antibody co-precipitated PDI, and the anti-PDI antibody co-precipitated SOD1 in cultured astrocytes. Three separate immunoprecipitations were performed, and data in triplicate were analyzed. Data were presented as mean±S.E.; *, $p<0.05$; **, $p<0.01$; ***, $p<0.001$ by one-way ANOVA with Tukey's post hoc test.

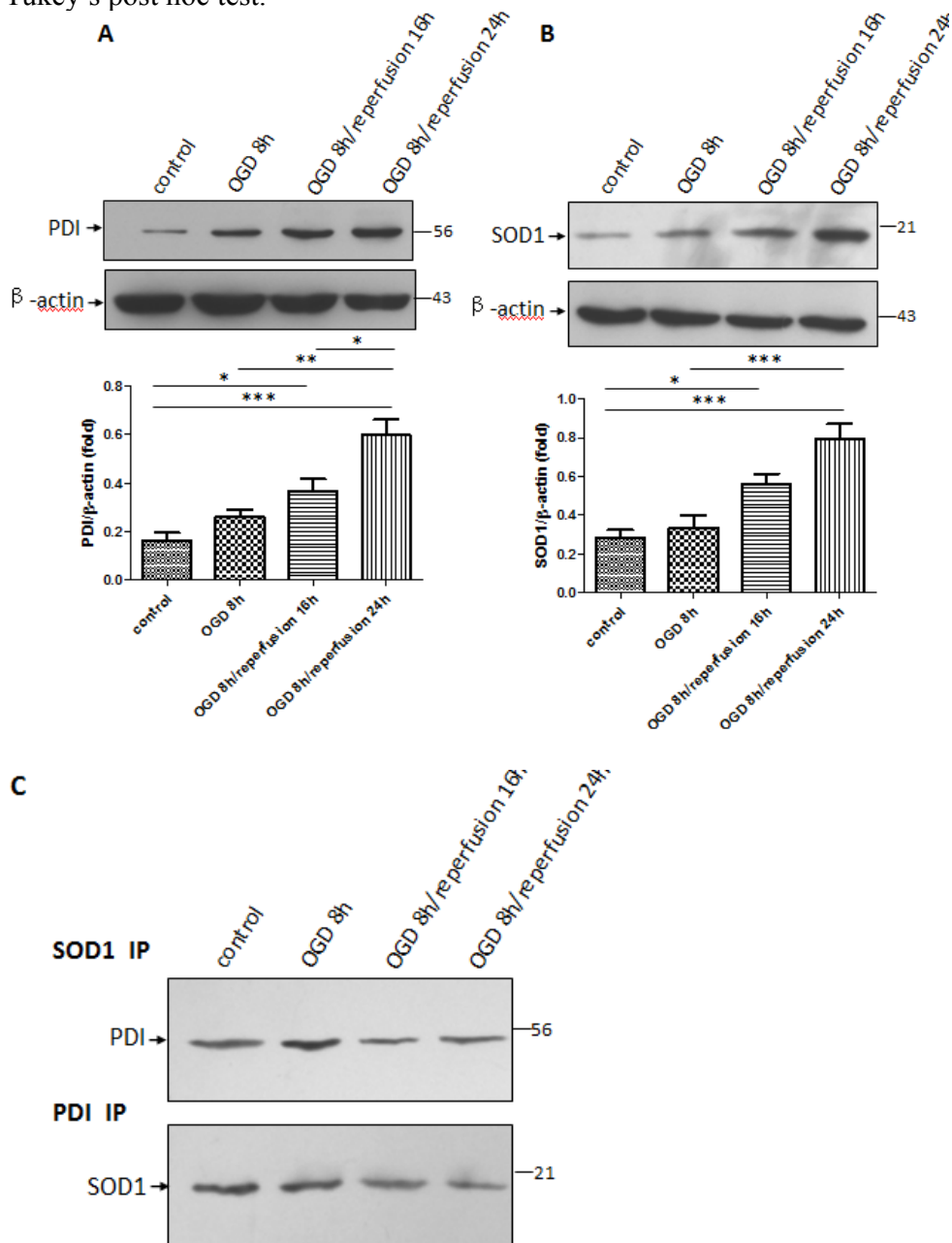
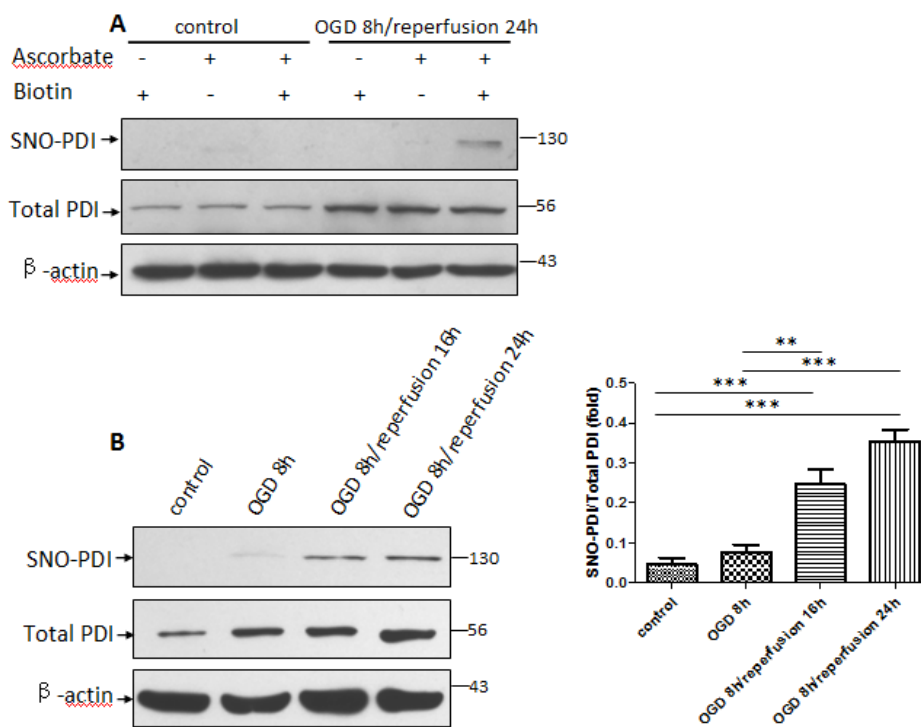


Fig. 5.3 S-nitrosylation of PDI in cultured astrocytes following OGD/reperfusion

A. In the presence of both ascorbate and biotin-HPDP, astrocytes following OGD 8h/reperfusion 24h treatment have detectable SNO-PDI, indicating the specificity of biotin-switch assay. B. PDI was S-nitrosylated in cultured astrocytes following OGD/reperfusion. Densitometric quantitation showed significant differences of SNO-PDI levels between the control group and the OGD/reperfusion groups. C. 1400W significantly inhibited NO production; the iNOS protein expression remained unaltered in cultured astrocytes following OGD 8h/reperfusion 24h. C. The cultured astrocytes were pretreated with various concentrations of iNOS inhibitor 1400W, which suppressed the S-nitrosylated PDI formation under OGD 8h/reperfusion 24h. The level of SNO-PDI was reduced with the increased concentration of 1400W (1, 10, and 50 μ M). Moreover, 1400W suppressed S-nitrosylation of PDI, with the maximum effect seen at the concentration of 50 μ M. Three independent experiments were performed in triplicate. Data were presented as mean \pm S.E.; *, $p < 0.05$; **, $p < 0.01$; ***, $p < 0.001$ by one-way ANOVA with Tukey's post hoc test.



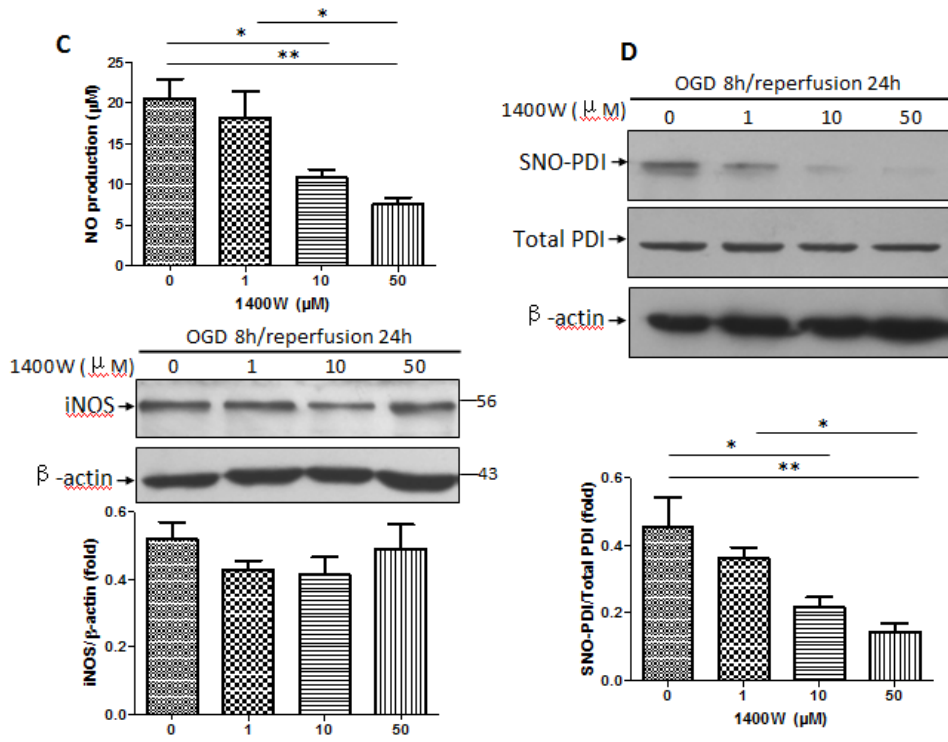


Fig. 5.4 The formation of detergent/salt-insoluble ubiquitinated-protein aggregates following OGD/reperfusion, and the inhibition effect of 1400W.

A. Protein smears ranging from 37 to 250 kDa were considered to be ubiquitinated proteins. Increased levels of detergent/salt-insoluble ubiquitinated-protein aggregates were observed in pellet fractions under OGD/reperfusion. This change was more pronounced in OGD 8h/reperfusion 24h group. 1400W inhibited the formation of ubiquitinated-protein aggregates in the insoluble pellet fraction, with the maximum effect seen at the concentration of 50 μ M. B. The ubiquitinated-protein aggregates were quantified using average intensity of protein smear, using β -actin as an internal control. Data from three independent experiments were presented as mean \pm S.E.; *, $p<0.05$; **, $p<0.01$; ***, $p<0.001$ by one-way ANOVA with Tukey's post hoc test.

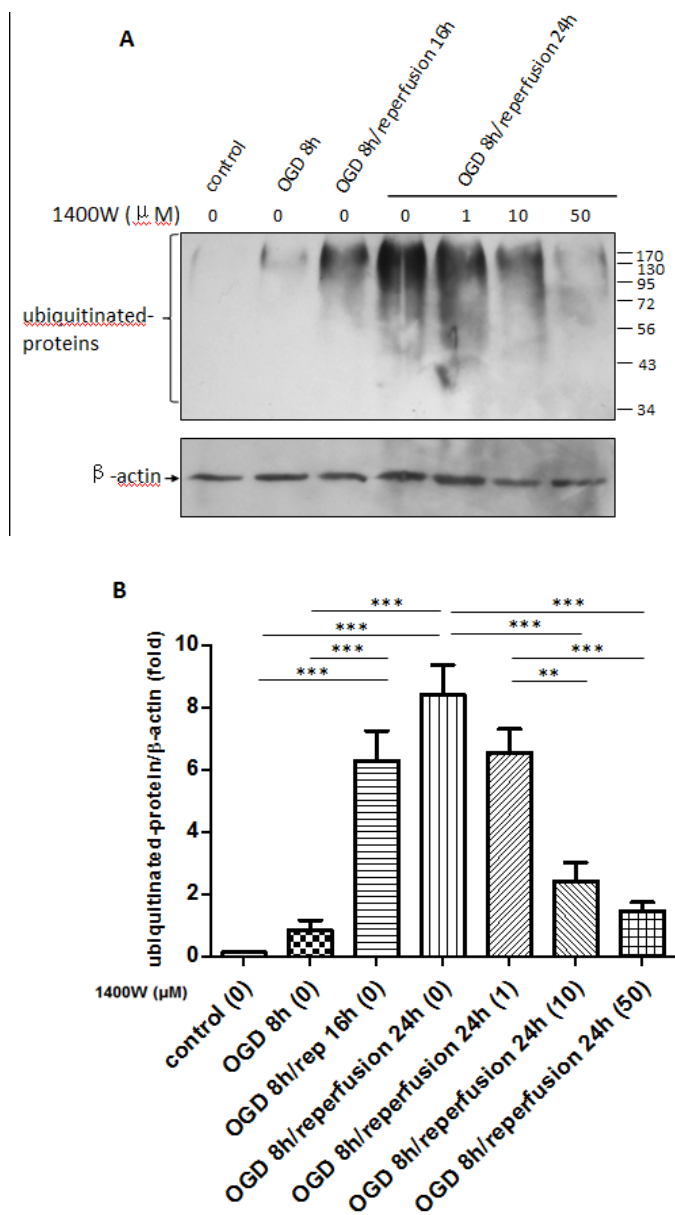
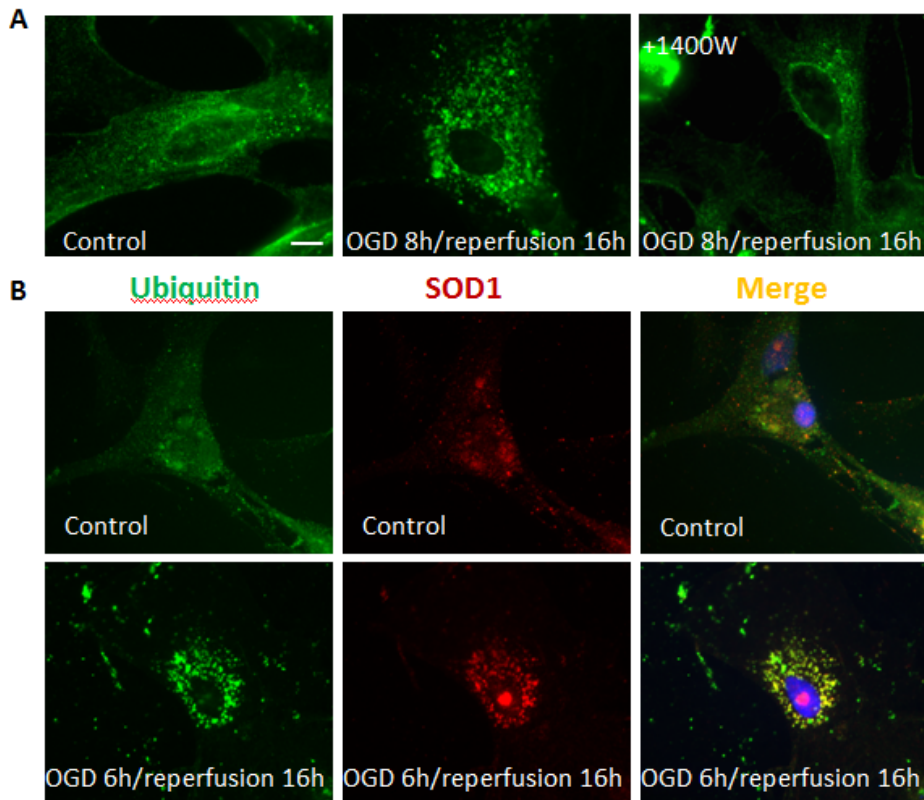


Fig. 5.5 The distribution of ubiquitin-conjugated proteins and localization of ubiquitin and SOD1 in cultured astrocytes following OGD/reperfusion by using immunostaining.

A. In normoxic control astrocytes, the ubiquitin immunoreactivity was diffuse and evenly distributed in cytoplasm and nucleus. Following OGD 8h/reperfusion 16h, the diffuse distribution of free ubiquitin lost nuclear staining and changed into clustered immunoreactivity near nucleus. 1400W attenuated the punctuated ubiquitin perinuclear distribution B. Co-localization of ubiquitin and SOD1 by using double-immunostaining. Ubiquitinated-protein aggregates were identified following OGD 8h/reperfusion 16h. Diffused SOD1 immunoreactivity changed into punctuated perinuclear-nuclear localization. Scale bar is 100 μ m. Green, ubiquitin immunosignals; red, SOD1 immunosignals; blue, nucleus staining with hoechst 33342.



Chapter 6. Discussion and Significance

The purpose of this thesis is to improve the understanding of how oxidative stress and nitrosative stress works as mechanisms of protein posttranslational modification, and to correlate this posttranslational modification with protein aggregates formation. This study contributes to determining the pathogenesis of aggregate-linked neurodegeneration in CNS disorders, such as ALS and cerebral ischemia. Further direction includes finding the therapeutic approaches to inhibit the protein aggregation by targeting the posttranslational modification. This study was divided into three distinct sets of experiments; the results were discussed separately. Although these three experiments are distinct, they are connected with each other and make up a whole picture. We will summarize the correlation of three components of this work. The strengths and limitations will also be identified. Finally, future work will be discussed.

6.1 Oxidative modification of SOD1 in protein aggregate formation in ALS

Oxidative stress is caused by the overwhelming generation of ROS and RNS, which shift the balance between oxidant generation and defense mechanisms against pro-oxidative conditions. Physiologically, in CNS diseases, the activation of glia cells and neuroinflammation is associated with ROS and RNS generation. More and more evidence supports the idea that oxidative stress is involved in neurodegenerative diseases. Oxidative overload in the neuronal micro-environment causes oxidation of lipids [500], proteins [501] and DNA [502] and generates many byproducts such as peroxides, alcohols, aldehydes, ketones, and cholesterol oxide [503]. ROS mediates oxidation of protein side-chains, which results in the introduction of hydroxyl groups or in the

generation of protein based carbonyls [504]. Carbonyl groups are introduced in proteins by oxidizing amino acid residue side-chain hydroxyls into ketone or aldehyde derivatives [505]. Carbonyl groups can also be introduced in proteins by direct oxidation of lysine, arginine, proline and threonine residues, or from the cleavage of peptide bonds by the α -amidation pathway or by the oxidation of glutamyl residues [506]. Measurement of protein carbonylation is thought to be a good estimate for the extent of oxidative damage of proteins associated with various conditions of oxidative stress [507,508,509].

A common pathological hallmark of multiple neurodegenerative diseases is the aberrant intracellular and extracellular deposition of self-aggregating misfolded proteins that form highly-ordered insoluble fibrils. Although the pathogenicity of protein aggregates remains uncertain [510], a causative link between the formation of protein aggregates and neurodegeneration has been established, which may occur as a result of the toxic action of substances produced during early phases. Soluble oligomers and protofibrillar derivatives of misfolded proteins may play a pathogenic role [511,512]. These abnormal protein aggregates can be produced by several events, including glycation/glycooxidation, modification of proteins by lipid peroxidation products, halogenations of amino acid residues, faulty posttranslational modifications, and oxidation and/or nitration of amino acid residues by ROS or RNS. However, the exact mechanisms of abnormal aggregates formation are not fully understood. Genetic and environmental factors (especially oxidative stress) contribute to these mechanisms. [513]. Aberrant proteins are the result of inherited or acquired amino acid substitution or damage. Aberrant proteins cannot fold correctly under oxidative modification; they become trapped in misfolded conformations. Growing evidence supports the hypothesis

that oxidative stress, combined with protein aggregation, triggers a cascade of events leading to cell death in multiple neurodegenerative diseases. Proteins modified by oxidative reactive species tend to form aggregates. Highly oxidized and cross-linked proteins may act as endogenous inhibitors of proteasomal activity. Since the proteasome represents the major proteolytic machinery for the removal of oxidized and misfolded protein [514], inhibition of the proteasome or decreasing proteasomal activity will result in an accumulation of abnormal proteins [515]. Therefore, timely removal of oxidatively damaged proteins is of critical importance to maintain normal cellular homeostasis and viability. If homeostasis is not restored, cells ultimately undergo apoptotic or necrotic cell death. To prevent cytotoxicity induced by oxidized proteins, normal proteasome-dependent degradation is essential for cells to cope with oxidative stress [516]. In a vicious cycle, proteasomal dysfunction can lead to decreased degradation of misfolded proteins; this results in the accumulation of oxidized proteins and subsequent protein aggregation. Protein aggregates can then feedback to further inhibit proteasome activities, stimulate ROS/RNS formation, and lead to cytotoxicity and human pathologies. Such phenomena have been implicated in many oxidative stress-associated disorders, including neurodegenerative diseases [517,518].

A broad spectrum of proteins reportedly go through oxidative modification. This modification leads to abnormal and damaged proteins and protein aggregation. As an example, SOD1 converts reactive oxygen to harmless water with its antioxidant activity. However, mutant SOD1 in ALS functions to gain a toxic property, not a loss of its enzymatic activity. One toxic property is the abnormal accumulation of mSOD1 aggregates. The accumulation of these abnormal protein aggregates leads to progressive

loss of motor neurons in an age-dependent manner. In Chapter 3 of this thesis, we focused on the oxidative modification of the cysteine residues of SOD1 in mechanism of mSOD1 aggregates formation. There are four cysteine residues in SOD1; they are Cys6, Cys57, Cys111 and Cys146. Only Cys111 exists in thiol state (-SH), and this is the main source for alkylation, providing thiolate anion (-S⁻) for oxidative modification. The presence of Cys111-peroxidized SOD1 in the spinal cord of G37R mutant SOD1 transgenic mice indicated that under genetic mutation and environmental oxidative stress, the thiol group (-SH) of Cys111 is oxidized to sulfonic acid (-SO₃H), detected by the specific anti-C111ox-SOD1 antibody. *In vitro* study also demonstrated that oxidative modification of Cys111 of mSOD1 could be induced by H₂O₂ in a dose-dependent manner. Interestingly, this oxidized SOD1 (Cys111-peroxidized SOD1) and mSOD1 are conformationally similar, seeing as both G93A mutation and Cys111 sulfonic acid moiety (-SO₃H) could induce the formation of conformational epitope. Furthermore, this oxidized SOD1 is detectable in the spinal cords of SALS patients [45], and correlates well with the formation of high molecular weight protein aggregates with the progression of ALS. The unique characteristic of this high molecular weight protein aggregates is its presence after being boiled in Laemmli's sample buffer (typically containing 0.1-2.0% SDS and 5% β-mercaptoethanol). Under this extremely reducing condition, all the disulfide-bonds are broken down, which indicates that the formation of this HMW protein aggregate does not rely on disulfide bond, but is mediated by covalently-linked oxidative modified SOD1 species. This result is consistent with another study which indicated that SOD1-containing oligomers may be partially held together by covalent bonds and contains covalently modified SOD1 species [177]. Furthermore, the involvement of

Cys111 of in aggregate formation was confirmed by the DSG cross-linking experiment. When Cys111 is mutated to serine, combined with G93A mutations, the formation of cross-linked HMW complexes decreases significantly compared to the single G93A mutation. However, when G86R mutant is overexpressed in mice, mice developed an ALS-like disease marked by hind-limb paralysis. Since mice lack cysteine in position 111, this mouse model indicates that Cys111 may not mediate all toxicity aspects of mSOD1 and may indicate that aberrant mSOD1 aggregation are partially mediated by the oxidative modification of Cys111.

6.2 S-nitrosylated modification of PDI in protein aggregates formation in ALS

Excessive generation of ROS/RNS, including superoxide anion (O_2^-) and nitric oxide (NO) contributes to neuronal cell injury and death in neurodegenerative diseases. NO participates in various cellular signaling pathways to regulate broad aspects of brain function, such as synaptic plasticity, normal developments, and neuronal cell death [519]. Over the past decade and a half, evidence has suggested that these effects are largely achieved by a reaction of NO termed S-nitrosylation. S-nitrosylation is a covalent reaction transferring a NO group to a reactive cysteine thiol (RSH), forming a S-nitrosothiol derivative (R-SNO) on target proteins. This modification is broadly identified in mammalian, plant, and microbial proteins; this modification is analogous to phosphorylation in regulating the biological activity of many proteins [520]. Interestingly, S-nitrosylation can mediate either protective or neurodestructive effects depending on the substrate proteins it is targeting. NO mediates neuroprotective effects through S-nitrosylation of NMDA receptors and caspases [521]. However, NO exerts neurotoxic

effects through forming S-nitrosylation or peroxynitrite of MMP-9 and GAPDH [522]. In addition, recent studies indicate that the excessive generation of NO-related species may play a key role in the process of protein misfolding and aggregation. Aberrant oxidative and nitrosative stress are implicated in chaperone and proteasomal dysfunction, leading to accumulation of aberrant protein aggregates. However, the exact molecular and pathogenic mechanisms underlying NO contributing to the aggregate formation is still unclear. S-nitrosylation of PDI regulates its isomerase and chaperone activities, contributing to protein misfolding and neurotoxicity in models of PD. Our studies in Chapter 4 also indicate that NO-mediated dysfunction of PDI by S-nitrosylation is involved in the abnormal accumulation of mSOD1 protein aggregates in ALS.

The accumulation of protein aggregates is an adaptive response to pathological stresses; these misfolded or otherwise abnormal proteins are produced even in healthy cells. However, under normal conditions, cells have mechanisms in quality control, including (1) molecular chaperones that help protein fold properly and reduce toxic aggregation, (2) the ubiquitin-proteasome system (UPS) that degrades misfolded proteins, (3) the unfolded protein response (UPR) that up-regulates the ER-resident chaperones to ameliorate the accumulation of unfolded or misfolded proteins, and (4) autophagy/lysosomal degradation that is responsible for the removal of large protein complexes [523,524]. Under pathological conditions, dysfunction of molecular chaperone or proteasome activities can lead to deposition and accumulation of aberrant protein aggregates. Several mutations in molecular chaperones or UPS-associated proteins are indicated in neurodegeneration. In PD, the ubiquitin E3 ligase parkin takes part in ubiquitin-proteasome-dependent degradation of misfolded proteins. However, several

mutations in parkin have been associated with Lewy body formation [525]. Aberrant accumulation of these proteins tightly links to the poor prognosis for the survival of dopaminergic neuron in PD. Just like the effects of mutations on parkin in familial PD, nitrosative and oxidative stress act as a potential causal factor for protein misfolding in sporadic PD in the absence of a genetic mutation. Actually, S-nitrosylation of parkin and further oxidation of parkin change its E3 ligase activity, thus inducing disruption of UPS function [526]. PDI was also S-nitrosylated modified in PD. PDI, located in the ER, facilitates proper protein folding by breaking disulfide bonds (reduction), introducing disulfide bonds into proteins (oxidation), and catalyzing thiol/disulfide exchange (isomerization). It functions to facilitate disulfide bond formation, rearrange the reaction, and maintain the structural stability of the mature protein. Furthermore, PDI is capable of stabilizing the correct folding of substrate proteins with its molecular chaperone activity. In several neurodegenerative diseases and in ischemic injuries, the PDI expression is up-regulated, which represents an adaptive response that promotes protein refolding. However, PD transgenic mouse studies have shown that excessive generation of NO can cause S-nitrosylation of the active-site thiols of PDI, suppressing its isomerase and chaperone activities. Consequently, S-nitrosylation of PDI partially takes a part in the accumulation of misfolded and polyubiquitinated proteins, which trigger prolonged UPR activation and persistent ER stress. Further studies also demonstrate that PDI is S-nitrosylated modified in the brains of sporadic AD and PD patients. These studies suggests that PDI gets S-nitrosylated under severe ER stress and that it is due to the posttranslational modification of PDI that turns its potential neuroprotective function into a neurodestructive role.

In Chapter 4 of this thesis, PDI was also found to be S-nitrosylated in the spinal cords of two strains of mSOD1 transgenic ALS mice, and S-nitrosylation of PDI inhibited PDI's isomerase and chaperone activities and compromised its up-regulation, which offered some degree of neuronal protection. Furthermore, S-nitrosylated modification of PDI is highly associated with high levels of iNOS expression and subsequently high levels of NO generation. This correlation was confirmed by the finding that NO-mediated S-nitrosylation of PDI was attenuated by the NOS inhibitor NNA treatment. Furthermore, S-nitrosylated modification of PDI is highly linked to the formation of mSOD1 aggregates. mSOD1 expression in SH-SY5Y cells promoted iNOS expression and NO generation, which triggered S-nitrosylation of PDI. Inhibiting S-nitrosylation of PDI with NOS inhibitor NNA attenuated mSOD1 aggregation. These results of S-nitrosylated modification of PDI in ALS are consistent with the previous work focusing on other neurodegenerative diseases. These results provide a mechanistic link between free radical production and abnormal protein accumulation. In addition, these findings have important implications for new therapeutic approaches targeting aberrant S-nitrosylated modification. These results also indicate that elucidation of this aberrant S-nitrosylated modification will help us attain a better understanding of the molecular mechanisms involved in NO-mediated neurodegeneration. S-nitrosylated modification of PDI may become a target for future treatment of neurodegenerative diseases.

6.3 S-nitrosylated modification of PDI in ubiquitinated-protein aggregates formation in cerebral ischemia

Emerging evidence suggests that cerebral ischemia can lead to protein misfolding and aggregation, resulting in overproduction of protein aggregate-associated organelles [527]. Protein aggregation was identified as an important factor resulting in ischemia-induced neuron death in 2000 by Hu et al. These combined results indicate that protein aggregation is one cause of neuron death. Moreover, evidence from studies on protein chemistry, molecular, and cellular biology indicates that certain proteins are susceptible to unfolding and forming aggregates. These studies also show that soluble oligomeric assemblies of misfolded proteins may cause cell injury or death. Protein aggregation was first identified in AD. Protein aggregation exists in more than 20 degenerative conditions affecting either the CNS or a variety of peripheral tissues. PD, Huntington's disease, Creutzfeldt-Jakob disease, cystic fibrosis, and Gaucher's disease are all included in these degenerative conditions [528]. Normally, the protein aggregates formation is triggered by various stresses; some of the newly synthesized proteins misfold and some of the already synthesized proteins unfold. Thus, the denatured proteins lose their normal three-dimensional structures. If this situation gets worse, it will expose the sticky hydrophobic subunits interiorly buried in the denatured proteins. The denatured proteins will tend to stick to one another to form cyto-toxic protein aggregates. The deposition of these protein aggregates is normally located in the cytosol or cellular membrane; mitochondrial and ER are also included. Thus, the subcellular normal activities are interfered with, leading to cell death. During cerebral ischemia, the ischemic stress can induce the conformational changes in proteins. Then the proteins lose their three dimensional conformation, expose hydrophobic residue, and turn into denatured proteins that stick to one another, precipitate, and form protein aggregates. To maintain

cellular function and integrity, the cells will initiate a series of mechanisms to eliminate or rescue the denatured and aggregated proteins. If the protein is badly damaged it will undergo degradation to block its cyto-toxic effects. The most common proteolytic machinery in the cell is ubiquitin-proteasomal system (UPS).

The presence of free radicals and the resulting oxidative stress and nitrosative stress have a multitude of modifying and destroying effects to various molecules and to proteins, which lead sooner or later to cellular dysfunction and diseases. To keep cells undamaged and functional, cells develop a large arsenal of defending and repairing mechanisms, including an anti-oxidative redox-system that detoxifies oxidants and the UPS, which degrades damaged, misfolded and mutant proteins. The central part of UPS is the proteasome itself. The second part is the ubiquitin machinery, which contains three different groups of enzymes that are required for ubiquitin binding and elongation to tag proteins for degradation. Impairments of the protein degradation pathways have been implicated in many human diseases, including cerebral ischemia. Proteasome activity is decreased after transient cerebral ischemia, which leads to accumulation of protein aggregates, containing proteasome. Proteasome activity reduction is an important pathological phenomenon that is associated with proteins aggregation and neuronal death in neurons injured by transient ischemia.

Besides UPS, chaperones rescue the abnormal proteins in cells. Chaperones are a functionally related group of proteins that control both initial protein folding and subsequent maintenance of proteins in the cell. The assistance of molecular chaperones is required in the process of folding *in vivo* [390]. Once the protein is already synthesized,

chaperones also play a role in a posttranslational quality control system and thus are required to maintain the proper conformation of proteins under the challenge of stress. Many factors are involved in protein unfolding and misfolding of proteins. The cells depend on chaperones to control and counteract the aggregation process by refolding the liberated polypeptides or their proteolysis. In this way, chaperones help to assemble and disassemble protein complexes and suppress protein aggregation.

Protein folding in the ER starts with cotranslational/translocationally modifications and continues with posttranslational modifications until the native protein structures are reached [273]. The ER harbours factors that assist proteins in their folding. These factors support the attachment or formation of protective and stabilizing covalent modifications. The formation of disulfide bonds is a key step in the maturation of the majority of the proteins that traffic through the ER. The conditions of the ER favour the protein-assisted formation of disulfide bonds. PDI, the ER chaperone, catalyzes these reactions by acting as electron acceptors in the oxidation reaction or electron donors for the converse reduction reaction. PDI can also isomerize disulfide bonds, helping proteins to obtain native disulfides by rearranging nonnative linkages. PDI contains CXXC motifs in thioredoxin domains and acts as both an oxidoreductase and a chaperone. PDI contains two catalytically active thioredoxin-like domains (TLD), termed *a* and *a'* which are divided by inactive TLD, termed *b* and *b'*. The crystal structure of yeast PDI shows that the four TLD form a twisted "U" shape [278]. The catalytically active domains are located at the top of the U across from each other. The two non-catalytic domains are localized to the inside surface of the U in an area enriched in hydrophobic residues. The hydrophobic surface is considered to take a part in binding misfolded structures and

positioning the substrate for the catalytic domains to act upon the substrate. PDI, with the catalytic CXXC motifs, acts to accelerate the formation and rearrangement of disulfide bonds. PDI also acts as a molecular chaperone that facilitates the fidelity of the protein folding reaction by suppressing nonproductive aggregate formation. PDI interacts with the substrate proteins to promote correct protein folding.

In Chapter 5 of this thesis, the ER chaperone PDI was shown to be modified by S-nitrosylation in cultured astrocytes after OGD/reperfusion, which is associated with the up-regulation of iNOS expression and NO generation. NO-mediated S-nitrosylation of PDI is highly associated with the formation of ubiquitinated-protein aggregates. This result indicates that the nitrosative stress mediated by NO triggers the abnormal protein folding in the ER, and that the accumulation of misfolded proteins in the ER initiates the ER stress and subsequently the protective UPR, which entails the induction of chaperone molecules. The up-regulation of PDI in response to cerebral ischemic injury represents an adaptive reaction of the UPR. However, if the nitrosative stress is too severe, it will cause the postranslational modification of the chaperones. For example, S-nitrosylation of PDI leads to the inhibition of the catalytic and chaperone activities. Once the chaperones lose their functions, it will not help to refold the misfolded proteins in the ER, which will progress to protein aggregates. These protein aggregates are governed by a regulatory protein in a process named “ubiquitination”, which is a posttranslational modification that promotes the recognition of substrates by the proteasome degradation machinery [529]. The ubiquitin (Ub) molecule is an 8-kDa protein that covalently attaches itself to specific substrates through the action of Ub ligases, tagging the protein for destruction by proteasomes. This process is crucial for the maintenance of cellular homeostasis [530]. In

response to protein misfolding, cells attempt to refold the protein or promote its ubiquitination for proteasomal degradation. Failure in the adjustment of misfolded proteins can lead to their accumulation in aggregates, which are rich in Ub. Such ubiquitin-positive protein aggregates are a hallmark of many degenerative diseases. The aggregates in cultured astrocytes after OGD/reperfusion in this study are also ubiquitin-positive, with a punctuated pattern in the peri-nuclear regions. The relationship of S-nitrosylation of PDI and ubiquitinated-protein aggregates was confirmed by the using of the iNOS inhibitor 1400W. Once the activity of iNOS was inhibited by 1400W, the NO generaton was consequently decreased, which led to down-regulation of the PDI S-nitrosylation level. Meanwhile, the formation of ubiquitinated-protein aggregates was reduced as well. We believe that the protective effect of 1400W on aggregates formation partially resulted from reducing NO-mediated S-nitrosylation of PDI. Furthermore, the ubiquitinated-protein aggregates were co-localized with SOD1, which is a PDI molecular target in ischemic cardiomyopathy. PDI, with its catalytic function, helps to correct disulfide linking of SOD1. Once PDI was modified by S-nitrosylation, its activity in promoting correct disulfide linking of SOD1 was compromised, SOD1 probably went through misfolding and aggregation, and finally was identified by UPS for degradation. We demonstrate for the first time that PDI is S-nitrosylated in cultured astrocytes following OGD/reperfusion, and the formation of ubiquitinated-protein aggregates is partially induced by NO-mediated S-nitrosylation of PDI. Preventing protein aggregation will be a new target of research in the field of brain ischemia. The NO-based therapeutic strategies may help to prevent aberrant protein misfolding and aggregation by targeted disruption of nitrosylation of some specific proteins, such as PDI.

6.4 Limitations and strengths

6.4.1 Limitations

One limitation of studies presented in this thesis is the use of the biotin-switch method to detect the S-nitrosylated proteins [531]. S-nitrosylation of protein—the covalent adduction of a nitroso group to a cysteine thiol side chain, is an important posttranslational modification that has profound effects on protein function. To date, over 200 different proteins have been identified as being by S-nitrosylation. In addition, aberrant S-nitrosylation is implicated in several disease states, including tumour initiation and growth, neurodegenerative diseases, cerebral ischemia, and malignant hyperthermia [532]. There are some technical difficulties in detecting the endogenously S-nitrosylated proteins. The S-NO bond is highly labile and redox sensitive, thus it is lost easily or gained artificially during sample preparation. Furthermore, the detectable levels of endogenously S-nitrosylated protein in cells are so low that overlap the limits of detection of currently available assays [533]. The biotin-switch technique (BST) introduced by Jaffrey et al [534] has proven to be a sensitive and specific method of measuring low levels of endogenous protein S-nitrosylation. The BST consists of three principal steps (1) “blocking” free cysteine thiols by S-methylthiolation with MMTS (a reactive thiosulfonate); (2) converting of S-NOs to thiols (S-H) via transnitrosation with ascorbate; and (3) in situ “labeling” by S-biotinylation of the nascent thiols with biotin-HPDP, a reactive mixed disulfide of biotin. The degree of biotinylation (and thus S-nitrosylation) is determined by either anti-biotin immunoblotting or streptavidin pull-down followed by immunoblotting for the protein(s) of interest. Despite its widespread use, the validity of

this technique has been challenged by some groups. Each step contains potential sources of error; for example, incomplete blocking of free thiols by MMTS can initiate false positives [535]. In addition, the ascorbic-dependent false-positive signals are generated in the presence of indirect sunlight but not when the samples are shielded from sunlight [536,537]. Performing the assay in the dark can avoid this problem. Another concern is that if BST is sensitive enough to distinguish between S-nitrosylated proteins and S-oxidized or S-glutathionylated proteins [537]. However, several studies have confirmed that BST preferentially detects S-nitrosylated proteins as opposed to S-oxidized or S-glutathionylated proteins [535,538]. During the sample preparation, extra attention should be paid to several steps. First, it is imperative to keep each sample containing equivalent protein inputs, seeing as the protein samples are subjected to multiple acetone precipitation steps and washes. To avoid this problem, we performed SDS-PAGE on the biotinylated material before avidin pulldown. The blocking step is a technical challenge, because some protein thiols can be resistant to complete blocking. When protein thiols are resistant to complete blocking, the result will be a high level of SNO-independent biotinylation. To avoid this problem, we applied a reverse strategy to omit the degree of blocking, which can attenuate a true SNO signal. Other strategies include lengthening the blocking reaction to improve efficiency and increasing ascorbic acid concentrations to improve the sensitivity of the assay. Like phosphorylation, S-nitrosylation is a rapidly reversible and precisely targeted posttranslational modification. Unlike phosphorylation, S-nitrosylation is a redox-sensitive and labile protein modification. Therefore, the detection of endogenous S-nitrosylation is technically more challenging than detecting stable protein modifications just like phosphorylation. Although BST is the most reliable

methods for detecting S-nitrosylation nowadays, technical advances that facilitate the detection and quantification of protein S-nitrosylation are required in the future to help us fully understand the role of S-nitrosylation in physical and pathological conditions. Based on these requirements, high sequence coverage and a sensitive mass spectrometric technique are needed in the detection and localization of posttranslational modifications, such as oxidative modification and S-nitrosylation.

More advanced mass spectrometric techniques and affinity chromatography methods (immobilized metal affinity chromatography and modification site-specific antibodies) have enlarged our knowledge on the modified proteins, as well as types of modification. Furthermore, using quantitative mass spectrometry, we can figure out the physiological relevance of a posttranslational modification by identifying the quantitative changes of the modified protein under physical or pathological conditions [539]. Taken together, with advancements in mass spectrometry and new methods of isolating and enriching posttranslationally modified proteins, we can analyze posttranslationally modified proteins as well as the site and type of modification. The physiological and pathophysiological relevance of these posttranslational modifications will be studied in the future.

6.4.2 Strengths

The major strength of this study was the analysis of the effects of oxidative stress/nitrosative stress in process of protein posttranslational modification. I extended the research from the neurodegenerative disease ALS to cerebral ischemia, established

the association between free radical generation and protein aggregation, and confirmed the function of protein posttranslational modification in this process.

In the case of SOD1, we found that the formation of disulfide-bond independent mSOD1 aggregates is mediated by Cys111 posttranslational oxidative modification. We tried to figure out the role of Cys111 oxidative modification on protein aggregation by mSOD1. Modification of amino acid residues, especially the oxidative modification induced by oxidative stress, can be a crucial factor that enhances the misfolding of mSOD1. SOD1-positive inclusion bodies are present in the spinal cords of FALS and mSOD1 transgenic mice. This finding indicates that mSOD1 is conformationally misfolded and subject to aggregation. This abnormal protein accumulation in neurons impairs multiple cellular functions and leads to neuronal toxicity. Cys111 is located on the edge of the dimer interface of each subunit. The oxidative modification of Cys111 interrupts the conformational dimer contact at the interface stereochemically and induces the dissociation of SOD1. Molecular dynamics simulation of SOD1 implies that Cys111 is critical for the residue interaction network in the protein. Modification of Cys111 is likely to affect the dimer interface through the network and may disrupt their coupled motions. Supporting that, in this study, we found that oxidative modification of Cys111 is involved in the aggregation process of mSOD1. Further studies will be required to clarify the detailed mechanism of oxidative modification of Cys111 mediating neurotoxicity in ALS.

In the case of PDI, it is associated with condition of ER. ER in young and healthy cells can cope with newly imported or damaged proteins generated after mildstress.

However, if the stress is too severe, a number of misfolded protein sensors will induce a range of protective genes, including folding chaperones as well as genes coding for antioxidants. In this study, we found that the expression of SOD1 and PDI protein was up-regulated under oxidative/nitrosative stress. Especially, PDI can be inactivated by S-nitrosylated modification mediated by NO in diseased conditions, such as ALS and ischemic/hypoxic injury. This will lead to inhibition of reduction and/or redistribution of protein disulfides and aggravation of ER stress. This was the first study to investigate the effects of excessive generation of NO via iNOS up-regulation in mechanism of protein aggregation in ALS and cerebral ischemia. NO is free diffusible, it can migrate to ER and trigger S-nitrosylated modification of proteins, such as PDI. We found S-nitrosylation of PDI can be the intermediary agent in the pathway of NO-triggered protein aggregation. PDI is supposed to provide neuroprotection against the severe ER stress; but NO-mediated S-nitrosylation of PDI makes it lose its isomerase and chaperone activity, which is highly associated with the formation of protein aggregates in pathological conditions.

6.5 Conclusions

In summary, oxidative/nitrosative stress induces posttranslational modifications of proteins, which contributes to the formation of protein aggregates. Excessive production of ROS and RNS is involved in multiple diseased conditions, such as ALS and cerebral ischemia. Here we described a molecular mechanism involving oxidative modification of SOD1 and S-nitrosylation of PDI that links free radicals production and abnormal protein aggregation to neuronal cell injury. These findings have important implications for new

therapeutic approaches targeting aberrant posttranslational modification pathways induced by oxidative stress/nitrosative stress.

6.6 Future directions

Within the ER, PDI functions to catalyze the proper folding and assembly of proteins. Accumulation of misfolded proteins is a hallmark of multiple neurodegenerative diseases, such as ALS. It is also implicated as a causative factor in a variety of neurodegenerative conditions, such as cerebral ischemia. The present study has demonstrated that PDI is S-nitrosylated by excessive NO in the pathological conditions. An extension of the project is to test the hypothesis that S-nitrosylation of PDI is partially associated with protein misfolding and aggregation, and this is due to the loss of the isomerase and the chaperone-like activities of PDI. To determine whether S-nitrosylation affects PDI function, we will perform assays to detect PDI enzymatic activity.

Furthermore, we will investigate the effect of S-nitrosylated PDI on neuronal death after ER stress and proteasome inhibition (resulting in the accumulation of polyubiquitinated proteins that cannot be degraded by the proteasome) induced by overexpressing of mSOD1 and ischemic/hypoxic injury. We will use SH-SY5Y cells and cultured astrocytes, because they can resist the direct NO-induced damage under conditions of formation of S-nitrosylated PDI. Using MAP2 staining to assess injury or retraction of neuronal processes, and Ub staining to evaluate the accumulation of ubiquitinated-proteins, we will examine if NO impairs the protective role of PDI through S-nitrosylation. We will study this effect along protein aggregates formation and neurotoxicity-associated cell death.

NO, as an important free radical, has received a great deal of attention in the past several decades. Particularly, the reaction of NO with protein cysteine residues that results in S-nitrosylation is believed to be critical for cellular physiological and pathological functions. A number of proteins have been identified as targets for S-nitrosylation. S-nitrosylation is thought to regulate protein activity and function. Previously, it has been hard to establish whether or not S-nitrosylation of these proteins is associated with endogenous NO activity under normal conditions or diseased conditions. This difficulty is due to the technical limitations in detecting S-nitrosylation. To date, the biotin switch method is the most popular method used to detect and isolate S-nitrosylated proteins from tissue or cell extracts. The biotin-switch assay method involves three chemical transformation steps that selectively convert unstable S-nitrosothiols (SNO) to stable biotin conjugates. Recently, some important improvements have been made to this technique to facilitate the better identification of S-nitrosylation of proteins. Microarray-based assay is the most important improvement [540]. We will apply this method to address the limitations of the original biotin switch method, which is biased toward the identification of abundant proteins. We will use an anti-biotin antibody and fluorescently labeled secondary antibody to label and analyze S-nitrosylated proteins on microarrays. The advantages of this method include relative quantification of SNO-reactivity across a proteome and assessment the effects of multiple S-nitrosylation reagents and cofactors.

Reference

1. Logroscino G, Traynor BJ, Hardiman O, Chio A, Mitchell D, et al. (2010) Incidence of amyotrophic lateral sclerosis in Europe. *Journal of neurology, neurosurgery, and psychiatry* 81: 385-390.
2. Beghi E, Millul A, Micheli A, Vitelli E, Logroscino G, et al. (2007) Incidence of ALS in Lombardy, Italy. *Neurology* 68: 141-145.
3. Forbes RB, Colville S, Swingler RJ, Scottish ALSMNDR (2004) The epidemiology of amyotrophic lateral sclerosis (ALS/MND) in people aged 80 or over. *Age and ageing* 33: 131-134.
4. Duffy JR, Peach RK, Strand EA (2007) Progressive apraxia of speech as a sign of motor neuron disease. *American journal of speech-language pathology / American Speech-Language-Hearing Association* 16: 198-208.
5. Ravits J, Paul P, Jorg C (2007) Focality of upper and lower motor neuron degeneration at the clinical onset of ALS. *Neurology* 68: 1571-1575.
6. Amoiridis G, Tsimoulis D, Ameridou I (2008) Clinical, electrophysiologic, and pathologic evidence for sensory abnormalities in ALS. *Neurology* 71: 779.
7. Isaacs JD, Dean AF, Shaw CE, Al-Chalabi A, Mills KR, et al. (2007) Amyotrophic lateral sclerosis with sensory neuropathy: part of a multisystem disorder? *Journal of neurology, neurosurgery, and psychiatry* 78: 750-753.
8. Lomen-Hoerth C, Murphy J, Langmore S, Kramer JH, Olney RK, et al. (2003) Are amyotrophic lateral sclerosis patients cognitively normal? *Neurology* 60: 1094-1097.
9. Ringholz GM, Appel SH, Bradshaw M, Cooke NA, Mosnik DM, et al. (2005) Prevalence and patterns of cognitive impairment in sporadic ALS. *Neurology* 65: 586-590.
10. Siddique T, Lalani I (2002) Genetic aspects of amyotrophic lateral sclerosis. *Advances in neurology* 88: 21-32.
11. Rosen DR (1993) Mutations in Cu/Zn superoxide dismutase gene are associated with familial amyotrophic lateral sclerosis. *Nature* 364: 362.
12. Neumann M, Sampathu DM, Kwong LK, Truax AC, Micsenyi MC, et al. (2006) Ubiquitinated TDP-43 in frontotemporal lobar degeneration and amyotrophic lateral sclerosis. *Science (New York, N Y)* 314: 130-133.
13. Kabashi E, Valdmanis PN, Dion P, Spiegelman D, McConkey BJ, et al. (2008) TARDBP mutations in individuals with sporadic and familial amyotrophic lateral sclerosis. *Nature genetics* 40: 572-574.
14. Maekawa S, Leigh PN, King A, Jones E, Steele JC, et al. (2009) TDP-43 is consistently co-localized with ubiquitinated inclusions in sporadic and Guam amyotrophic lateral sclerosis but not in familial amyotrophic lateral sclerosis with and without SOD1 mutations. *Neuropathology : official journal of the Japanese Society of Neuropathology* 29: 672-683.
15. Sreedharan J, Blair IP, Tripathi VB, Hu X, Vance C, et al. (2008) TDP-43 mutations in familial and sporadic amyotrophic lateral sclerosis. *Science (New York, N Y)* 319: 1668-1672.
16. Kwiatkowski TJ, Jr., Bosco DA, Leclerc AL, Tamrazian E, Vanderburg CR, et al.

- (2009) Mutations in the FUS/TLS gene on chromosome 16 cause familial amyotrophic lateral sclerosis. *Science (New York, N Y)* 323: 1205-1208.
17. Greenway MJ, Andersen PM, Russ C, Ennis S, Cashman S, et al. (2006) ANG mutations segregate with familial and 'sporadic' amyotrophic lateral sclerosis. *Nature genetics* 38: 411-413.
 18. Iida A, Hosono N, Sano M, Kamei T, Oshima S, et al. (2012) Optineurin mutations in Japanese amyotrophic lateral sclerosis. *Journal of neurology, neurosurgery, and psychiatry* 83: 233-235.
 19. Kiernan MC, Vucic S, Cheah BC, Turner MR, Eisen A, et al. (2011) Amyotrophic lateral sclerosis. *Lancet* 377: 942-955.
 20. DeJesus-Hernandez M, Mackenzie IR, Boeve BF, Boxer AL, Baker M, et al. (2011) Expanded GGGGCC hexanucleotide repeat in noncoding region of C9ORF72 causes chromosome 9p-linked FTD and ALS. *Neuron* 72: 245-256.
 21. Renton AE, Majounie E, Waite A, Simon-Sanchez J, Rollinson S, et al. (2011) A hexanucleotide repeat expansion in C9ORF72 is the cause of chromosome 9p21-linked ALS-FTD. *Neuron* 72: 257-268.
 22. Barber SC, Mead RJ, Shaw PJ (2006) Oxidative stress in ALS: a mechanism of neurodegeneration and a therapeutic target. *Biochimica et biophysica acta* 1762: 1051-1067.
 23. Turner BJ, Talbot K (2008) Transgenics, toxicity and therapeutics in rodent models of mutant SOD1-mediated familial ALS. *Progress in neurobiology* 85: 94-134.
 24. Subramaniam JR, Lyons WE, Liu J, Bartnikas TB, Rothstein J, et al. (2002) Mutant SOD1 causes motor neuron disease independent of copper chaperone-mediated copper loading. *Nature neuroscience* 5: 301-307.
 25. Harraz MM, Marden JJ, Zhou W, Zhang Y, Williams A, et al. (2008) SOD1 mutations disrupt redox-sensitive Rac regulation of NADPH oxidase in a familial ALS model. *The Journal of clinical investigation* 118: 659-670.
 26. Shaw PJ, Ince PG, Falkous G, Mantle D (1995) Oxidative damage to protein in sporadic motor neuron disease spinal cord. *Annals of neurology* 38: 691-695.
 27. Shibata N, Nagai R, Uchida K, Horiuchi S, Yamada S, et al. (2001) Morphological evidence for lipid peroxidation and protein glycoxidation in spinal cords from sporadic amyotrophic lateral sclerosis patients. *Brain research* 917: 97-104.
 28. Fitzmaurice PS, Shaw IC, Kleiner HE, Miller RT, Monks TJ, et al. (1996) Evidence for DNA damage in amyotrophic lateral sclerosis. *Muscle & nerve* 19: 797-798.
 29. Mitsumoto H, Santella RM, Liu X, Bogdanov M, Zipprich J, et al. (2008) Oxidative stress biomarkers in sporadic ALS. *Amyotrophic lateral sclerosis : official publication of the World Federation of Neurology Research Group on Motor Neuron Diseases* 9: 177-183.
 30. Andrus PK, Fleck TJ, Gurney ME, Hall ED (1998) Protein oxidative damage in a transgenic mouse model of familial amyotrophic lateral sclerosis. *Journal of neurochemistry* 71: 2041-2048.
 31. Miana-Mena FJ, Gonzalez-Mingot C, Larrode P, Munoz MJ, Olivan S, et al. (2011) Monitoring systemic oxidative stress in an animal model of amyotrophic lateral sclerosis. *Journal of neurology* 258: 762-769.
 32. Ferraiuolo L, Kirby J, Grierson AJ, Sendtner M, Shaw PJ (2011) Molecular pathways of motor neuron injury in amyotrophic lateral sclerosis. *Nature reviews*

- Neurology 7: 616-630.
33. Vargas MR, Johnson DA, Sirkis DW, Messing A, Johnson JA (2008) Nrf2 activation in astrocytes protects against neurodegeneration in mouse models of familial amyotrophic lateral sclerosis. *The Journal of neuroscience : the official journal of the Society for Neuroscience* 28: 13574-13581.
 34. Sarlette A, Krampfl K, Grothe C, Neuhoff Nv, Dengler R, et al. (2008) Nuclear erythroid 2-related factor 2-antioxidative response element signaling pathway in motor cortex and spinal cord in amyotrophic lateral sclerosis. *Journal of neuropathology and experimental neurology* 67: 1055-1062.
 35. Cassina P, Cassina A, Pehar M, Castellanos R, Gandelman M, et al. (2008) Mitochondrial dysfunction in SOD1G93A-bearing astrocytes promotes motor neuron degeneration: prevention by mitochondrial-targeted antioxidants. *The Journal of neuroscience : the official journal of the Society for Neuroscience* 28: 4115-4122.
 36. Ito H, Wate R, Zhang J, Ohnishi S, Kaneko S, et al. (2008) Treatment with edaravone, initiated at symptom onset, slows motor decline and decreases SOD1 deposition in ALS mice. *Experimental neurology* 213: 448-455.
 37. Piao Y-S, Wakabayashi K, Kakita A, Yamada M, Hayashi S, et al. (2003) Neuropathology with clinical correlations of sporadic amyotrophic lateral sclerosis: 102 autopsy cases examined between 1962 and 2000. *Brain pathology (Zurich, Switzerland)* 13: 10-22.
 38. Wegorzewska I, Baloh RH (2011) TDP-43-based animal models of neurodegeneration: new insights into ALS pathology and pathophysiology. *Neuro-degenerative diseases* 8: 262-274.
 39. Groen EJM, van Es MA, van Vught PWJ, Spliet WGM, van Engelen-Lee J, et al. (2010) FUS mutations in familial amyotrophic lateral sclerosis in the Netherlands. *Archives of neurology* 67: 224-230.
 40. Ince PG, Tomkins J, Slade JY, Thatcher NM, Shaw PJ (1998) Amyotrophic lateral sclerosis associated with genetic abnormalities in the gene encoding Cu/Zn superoxide dismutase: molecular pathology of five new cases, and comparison with previous reports and 73 sporadic cases of ALS. *Journal of neuropathology and experimental neurology* 57: 895-904.
 41. Gros-Louis F, Soucy G, Lariviere R, Julien J-P (2010) Intracerebroventricular infusion of monoclonal antibody or its derived Fab fragment against misfolded forms of SOD1 mutant delays mortality in a mouse model of ALS. *Journal of neurochemistry* 113: 1188-1199.
 42. Ezzi SA, Lariviere R, Urushitani M, Julien J-P (2010) Neuronal over-expression of chromogranin A accelerates disease onset in a mouse model of ALS. *Journal of neurochemistry* 115: 1102-1111.
 43. Chia R, Tattum MH, Jones S, Collinge J, Fisher EMC, et al. (2010) Superoxide dismutase 1 and tgSOD1 mouse spinal cord seed fibrils, suggesting a propagative cell death mechanism in amyotrophic lateral sclerosis. *PloS one* 5: e10627.
 44. Munch C, Bertolotti A (2011) Self-propagation and transmission of misfolded mutant SOD1: prion or prion-like phenomenon? *Cell cycle (Georgetown, Tex)* 10: 1711.
 45. Bosco DA, Morfini G, Karabacak NM, Song Y, Gros-Louis F, et al. (2010) Wild-type and mutant SOD1 share an aberrant conformation and a common pathogenic

- pathway in ALS. *Nature neuroscience* 13: 1396-1403.
46. Verkhratsky A (2005) Physiology and pathophysiology of the calcium store in the endoplasmic reticulum of neurons. *Physiological reviews* 85: 201-279.
 47. Verkhratsky A (2004) Endoplasmic reticulum calcium signaling in nerve cells. *Biological research* 37: 693-699.
 48. Grosskreutz J, Van Den Bosch L, Keller BU (2010) Calcium dysregulation in amyotrophic lateral sclerosis. *Cell calcium* 47: 165-174.
 49. Lautenschlaeger J, Prell T, Grosskreutz J (2012) Endoplasmic reticulum stress and the ER mitochondrial calcium cycle in amyotrophic lateral sclerosis. *Amyotrophic lateral sclerosis : official publication of the World Federation of Neurology Research Group on Motor Neuron Diseases* 13: 166-177.
 50. Sasaki S (2010) Endoplasmic reticulum stress in motor neurons of the spinal cord in sporadic amyotrophic lateral sclerosis. *Journal of neuropathology and experimental neurology* 69: 346-355.
 51. Tobisawa S, Hozumi Y, Arawaka S, Koyama S, Wada M, et al. (2003) Mutant SOD1 linked to familial amyotrophic lateral sclerosis, but not wild-type SOD1, induces ER stress in COS7 cells and transgenic mice. *Biochemical and biophysical research communications* 303: 496-503.
 52. Wate R, Ito H, Zhang JH, Ohnishi S, Nakano S, et al. (2005) Expression of an endoplasmic reticulum-resident chaperone, glucose-regulated stress protein 78, in the spinal cord of a mouse model of amyotrophic lateral sclerosis. *Acta neuropathologica* 110: 557-562.
 53. Kikuchi H, Almer G, Yamashita S, Guegan C, Nagai M, et al. (2006) Spinal cord endoplasmic reticulum stress associated with a microsomal accumulation of mutant superoxide dismutase-1 in an ALS model. *Proceedings of the National Academy of Sciences of the United States of America* 103: 6025-6030.
 54. Atkin JD, Farg MA, Turner BJ, Tomas D, Lysaght JA, et al. (2006) Induction of the unfolded protein response in familial amyotrophic lateral sclerosis and association of protein-disulfide isomerase with superoxide dismutase 1. *The Journal of biological chemistry* 281: 30152-30165.
 55. Jaiswal MK, Keller BU (2009) Cu/Zn superoxide dismutase typical for familial amyotrophic lateral sclerosis increases the vulnerability of mitochondria and perturbs Ca²⁺ homeostasis in SOD1G93A mice. *Molecular pharmacology* 75: 478-489.
 56. Langou K, Moumen A, Pellegrino C, Aebischer J, Medina I, et al. (2010) AAV-mediated expression of wild-type and ALS-linked mutant VAPB selectively triggers death of motoneurons through a Ca²⁺-dependent ER-associated pathway. *Journal of neurochemistry* 114: 795-809.
 57. Chakrabarti A, Chen AW, Varner JD (2011) A review of the mammalian unfolded protein response. *Biotechnology and bioengineering* 108: 2777-2793.
 58. Atkin JD, Farg MA, Walker AK, McLean C, Tomas D, et al. (2008) Endoplasmic reticulum stress and induction of the unfolded protein response in human sporadic amyotrophic lateral sclerosis. *Neurobiology of disease* 30: 400-407.
 59. Ilieva EV, Ayala V, Jove M, Dalfo E, Cacabelos D, et al. (2007) Oxidative and endoplasmic reticulum stress interplay in sporadic amyotrophic lateral sclerosis. *Brain : a journal of neurology* 130: 3111-3123.

60. Walker AK, Farg MA, Bye CR, McLean CA, Horne MK, et al. (2010) Protein disulphide isomerase protects against protein aggregation and is S-nitrosylated in amyotrophic lateral sclerosis. *Brain : a journal of neurology* 133: 105-116.
61. Kalmar B, Novoselov S, Gray A, Cheetham ME, Margulis B, et al. (2008) Late stage treatment with arimocloleol delays disease progression and prevents protein aggregation in the SOD1 mouse model of ALS. *Journal of neurochemistry* 107: 339-350.
62. Wang L, Popko B, Roos RP (2011) The unfolded protein response in familial amyotrophic lateral sclerosis. *Human molecular genetics* 20: 1008-1015.
63. Jung C, Higgins CMJ, Xu Z (2002) A quantitative histochemical assay for activities of mitochondrial electron transport chain complexes in mouse spinal cord sections. *Journal of neuroscience methods* 114: 165-172.
64. Mattiazzi M, D'Aurelio M, Gajewski CD, Martushova K, Kiaei M, et al. (2002) Mutated human SOD1 causes dysfunction of oxidative phosphorylation in mitochondria of transgenic mice. *The Journal of biological chemistry* 277: 29626-29633.
65. Menzies FM, Cookson MR, Taylor RW, Turnbull DM, Chrzanowska-Lightowler ZMA, et al. (2002) Mitochondrial dysfunction in a cell culture model of familial amyotrophic lateral sclerosis. *Brain : a journal of neurology* 125: 1522-1533.
66. Rizzardini M, Lupi M, Mangolini A, Babetto E, Ubezio P, et al. (2006) Neurodegeneration induced by complex I inhibition in a cellular model of familial amyotrophic lateral sclerosis. *Brain research bulletin* 69: 465-474.
67. Son M, Leary SC, Romain N, Pierrel F, Winge DR, et al. (2008) Isolated cytochrome c oxidase deficiency in G93A SOD1 mice overexpressing CCS protein. *The Journal of biological chemistry* 283: 12267-12275.
68. Cousse E, De Smet P, Bogaert E, Elens I, Van Damme P, et al. (2011) G37R SOD1 mutant alters mitochondrial complex I activity, Ca²⁺ uptake and ATP production. *Cell calcium* 49: 217-225.
69. Browne SE, Yang L, DiMauro J-P, Fuller SW, Licata SC, et al. (2006) Bioenergetic abnormalities in discrete cerebral motor pathways presage spinal cord pathology in the G93A SOD1 mouse model of ALS. *Neurobiology of disease* 22: 599-610.
70. Tradewell ML, Cooper LA, Minotti S, Durham HD (2011) Calcium dysregulation, mitochondrial pathology and protein aggregation in a culture model of amyotrophic lateral sclerosis: mechanistic relationship and differential sensitivity to intervention. *Neurobiology of disease* 42: 265-275.
71. Barber SC, Shaw PJ (2010) Oxidative stress in ALS: key role in motor neuron injury and therapeutic target. *Free radical biology & medicine* 48: 629-641.
72. Cozzolino M, Pesaresi MG, Amori I, Crosio C, Ferri A, et al. (2009) Oligomerization of mutant SOD1 in mitochondria of motoneuronal cells drives mitochondrial damage and cell toxicity. *Antioxidants & redox signaling* 11: 1547-1558.
73. Sotelo-Silveira JR, Lepanto P, Elizondo V, Horjales S, Palacios F, et al. (2009) Axonal mitochondrial clusters containing mutant SOD1 in transgenic models of ALS. *Antioxidants & redox signaling* 11: 1535-1545.
74. Ferri A, Fiorenzo P, Nencini M, Cozzolino M, Pesaresi MG, et al. (2010) Glutaredoxin 2 prevents aggregation of mutant SOD1 in mitochondria and abolishes its toxicity. *Human molecular genetics* 19: 4529-4542.

75. Israelson A, Arbel N, Da Cruz S, Ilieva H, Yamanaka K, et al. (2010) Misfolded mutant SOD1 directly inhibits VDAC1 conductance in a mouse model of inherited ALS. *Neuron* 67: 575-587.
76. Shoshan-Barmatz V, Ben-Hail D (2012) VDAC, a multi-functional mitochondrial protein as a pharmacological target. *Mitochondrion* 12: 24-34.
77. Szabadkai G, Bianchi K, Varnai P, De Stefani D, Wieckowski MR, et al. (2006) Chaperone-mediated coupling of endoplasmic reticulum and mitochondrial Ca²⁺ channels. *The Journal of cell biology* 175: 901-911.
78. Shoshan-Barmatz V, De Pinto V, Zweckstetter M, Raviv Z, Keinan N, et al. (2010) VDAC, a multi-functional mitochondrial protein regulating cell life and death. *Molecular aspects of medicine* 31: 227-285.
79. Bilsland LG, Nirmalanathan N, Yip J, Greensmith L, Duchen MR (2008) Expression of mutant SOD1 in astrocytes induces functional deficits in motoneuron mitochondria. *Journal of neurochemistry* 107: 1271-1283.
80. Zhou H, Huang C, Chen H, Wang D, Landel CP, et al. (2010) Transgenic rat model of neurodegeneration caused by mutation in the TDP gene. *PLoS genetics* 6: e1000887.
81. Bordet T, Buisson B, Michaud M, Drouot C, Galea P, et al. (2007) Identification and characterization of cholest-4-en-3-one, oxime (TRO19622), a novel drug candidate for amyotrophic lateral sclerosis. *The Journal of pharmacology and experimental therapeutics* 322: 709-720.
82. Clement AM, Nguyen MD, Roberts EA, Garcia ML, Boillee S, et al. (2003) Wild-type nonneuronal cells extend survival of SOD1 mutant motor neurons in ALS mice. *Science (New York, N Y)* 302: 113-117.
83. Papadeas ST, Kraig SE, O'Banion C, Lepore AC, Maragakis NJ (2011) Astrocytes carrying the superoxide dismutase 1 (SOD1G93A) mutation induce wild-type motor neuron degeneration in vivo. *Proceedings of the National Academy of Sciences of the United States of America* 108: 17803-17808.
84. Turner MR, Cagnin A, Turkheimer FE, Miller CCJ, Shaw CE, et al. (2004) Evidence of widespread cerebral microglial activation in amyotrophic lateral sclerosis: an [¹¹C](R)-PK11195 positron emission tomography study. *Neurobiology of disease* 15: 601-609.
85. Lasiene J, Yamanaka K (2011) Glial cells in amyotrophic lateral sclerosis. *Neurology research international* 2011: 718987.
86. Gowing G, Philips T, Van Wijmeersch B, Audet J-N, Dewil M, et al. (2008) Ablation of proliferating microglia does not affect motor neuron degeneration in amyotrophic lateral sclerosis caused by mutant superoxide dismutase. *The Journal of neuroscience : the official journal of the Society for Neuroscience* 28: 10234-10244.
87. Weydt P, Yuen EC, Ransom BR, Moller T (2004) Increased cytotoxic potential of microglia from ALS-transgenic mice. *Glia* 48: 179-182.
88. Xiao Q, Zhao W, Beers DR, Yen AA, Xie W, et al. (2007) Mutant SOD1(G93A) microglia are more neurotoxic relative to wild-type microglia. *Journal of neurochemistry* 102: 2008-2019.
89. Boillee S, Yamanaka K, Lobsiger CS, Copeland NG, Jenkins NA, et al. (2006) Onset and progression in inherited ALS determined by motor neurons and microglia.

- Science (New York, N Y) 312: 1389-1392.
90. Wang L, Sharma K, Grisotti G, Roos RP (2009) The effect of mutant SOD1 dismutase activity on non-cell autonomous degeneration in familial amyotrophic lateral sclerosis. *Neurobiology of disease* 35: 234-240.
 91. Beers DR, Henkel JS, Xiao Q, Zhao W, Wang J, et al. (2006) Wild-type microglia extend survival in PU.1 knockout mice with familial amyotrophic lateral sclerosis. *Proceedings of the National Academy of Sciences of the United States of America* 103: 16021-16026.
 92. Zhao W, Beers DR, Henkel JS, Zhang W, Urushitani M, et al. (2010) Extracellular mutant SOD1 induces microglial-mediated motoneuron injury. *Glia* 58: 231-243.
 93. Van Damme P, Bogaert E, Dewil M, Hersmus N, Kiraly D, et al. (2007) Astrocytes regulate GluR2 expression in motor neurons and their vulnerability to excitotoxicity. *Proceedings of the National Academy of Sciences of the United States of America* 104: 14825-14830.
 94. Nagai M, Re DB, Nagata T, Chalazonitis A, Jessell TM, et al. (2007) Astrocytes expressing ALS-linked mutated SOD1 release factors selectively toxic to motor neurons. *Nature neuroscience* 10: 615-622.
 95. Pehar M, Cassina P, Vargas MR, Castellanos R, Viera L, et al. (2004) Astrocytic production of nerve growth factor in motor neuron apoptosis: implications for amyotrophic lateral sclerosis. *Journal of neurochemistry* 89: 464-473.
 96. Lepore AC, Rauck B, Dejea C, Pardo AC, Rao MS, et al. (2008) Focal transplantation-based astrocyte replacement is neuroprotective in a model of motor neuron disease. *Nature neuroscience* 11: 1294-1301.
 97. Ohnishi S, Ito H, Suzuki Y, Adachi Y, Wate R, et al. (2009) Intra-bone marrow-bone marrow transplantation slows disease progression and prolongs survival in G93A mutant SOD1 transgenic mice, an animal model mouse for amyotrophic lateral sclerosis. *Brain research* 1296: 216-224.
 98. Vercelli A, Mereuta OM, Garbossa D, Muraca G, Mareschi K, et al. (2008) Human mesenchymal stem cell transplantation extends survival, improves motor performance and decreases neuroinflammation in mouse model of amyotrophic lateral sclerosis. *Neurobiology of disease* 31: 395-405.
 99. Wong M, Martin LJ (2010) Skeletal muscle-restricted expression of human SOD1 causes motor neuron degeneration in transgenic mice. *Human molecular genetics* 19: 2284-2302.
 100. Riddoch-Contreras J, Yang S-Y, Dick JRT, Goldspink G, Orrell RW, et al. (2009) Mechano-growth factor, an IGF-I splice variant, rescues motoneurons and improves muscle function in SOD1(G93A) mice. *Experimental neurology* 215: 281-289.
 101. Heath PR, Shaw PJ (2002) Update on the glutamatergic neurotransmitter system and the role of excitotoxicity in amyotrophic lateral sclerosis. *Muscle & nerve* 26: 438-458.
 102. Shaw PJ, Forrest V, Ince PG, Richardson JP, Wastell HJ (1995) CSF and plasma amino acid levels in motor neuron disease: elevation of CSF glutamate in a subset of patients. *Neurodegeneration : a journal for neurodegenerative disorders, neuroprotection, and neuroregeneration* 4: 209-216.
 103. Milanese M, Zappettini S, Onofri F, Musazzi L, Tardito D, et al. (2011) Abnormal

- exocytotic release of glutamate in a mouse model of amyotrophic lateral sclerosis. *Journal of neurochemistry* 116: 1028-1042.
104. Guo Y, Duan W, Li Z, Huang J, Yin Y, et al. (2010) Decreased GLT-1 and increased SOD1 and HO-1 expression in astrocytes contribute to lumbar spinal cord vulnerability of SOD1-G93A transgenic mice. *FEBS letters* 584: 1615-1622.
 105. van Zundert B, Peuscher MH, Hynynen M, Chen A, Neve RL, et al. (2008) Neonatal neuronal circuitry shows hyperexcitable disturbance in a mouse model of the adult-onset neurodegenerative disease amyotrophic lateral sclerosis. *The Journal of neuroscience : the official journal of the Society for Neuroscience* 28: 10864-10874.
 106. Bensimon G, Lacomblez L, Meininger V (1994) A controlled trial of riluzole in amyotrophic lateral sclerosis. ALS/Riluzole Study Group. *The New England journal of medicine* 330: 585-591.
 107. Cheah BC, Vucic S, Krishnan AV, Kiernan MC (2010) Riluzole, neuroprotection and amyotrophic lateral sclerosis. *Current medicinal chemistry* 17: 1942-1199.
 108. Ghoddoussi F, Galloway MP, Jambekar A, Bame M, Needleman R, et al. (2010) Methionine sulfoximine, an inhibitor of glutamine synthetase, lowers brain glutamine and glutamate in a mouse model of ALS. *Journal of the neurological sciences* 290: 41-47.
 109. Bilsland LG, Sahai E, Kelly G, Golding M, Greensmith L, et al. (2010) Deficits in axonal transport precede ALS symptoms in vivo. *Proceedings of the National Academy of Sciences of the United States of America* 107: 20523-20528.
 110. De Vos KJ, Chapman AL, Tennant ME, Manser C, Tudor EL, et al. (2007) Familial amyotrophic lateral sclerosis-linked SOD1 mutants perturb fast axonal transport to reduce axonal mitochondria content. *Human molecular genetics* 16: 2720-2728.
 111. Perlson E, Jeong G-B, Ross JL, Dixit R, Wallace KE, et al. (2009) A switch in retrograde signaling from survival to stress in rapid-onset neurodegeneration. *The Journal of neuroscience : the official journal of the Society for Neuroscience* 29: 9903-9917.
 112. Pun S, Santos AF, Saxena S, Xu L, Caroni P (2006) Selective vulnerability and pruning of phasic motoneuron axons in motoneuron disease alleviated by CNTF. *Nature neuroscience* 9: 408-419.
 113. Fischer LR, Culver DG, Tennant P, Davis AA, Wang M, et al. (2004) Amyotrophic lateral sclerosis is a distal axonopathy: evidence in mice and man. *Experimental neurology* 185: 232-240.
 114. Gitcho MA, Baloh RH, Chakraverty S, Mayo K, Norton JB, et al. (2008) TDP-43 A315T mutation in familial motor neuron disease. *Annals of neurology* 63: 535-538.
 115. Vance C, Rogelj B, Hortobagyi T, De Vos KJ, Nishimura AL, et al. (2009) Mutations in FUS, an RNA processing protein, cause familial amyotrophic lateral sclerosis type 6. *Science (New York, N Y)* 323: 1208-1211.
 116. Igaz LM, Kwong LK, Lee EB, Chen-Plotkin A, Swanson E, et al. (2011) Dysregulation of the ALS-associated gene TDP-43 leads to neuronal death and degeneration in mice. *The Journal of clinical investigation* 121: 726-738.
 117. Polymenidou M, Lagier-Tourenne C, Hutt KR, Huelga SC, Moran J, et al. (2011) Long pre-mRNA depletion and RNA missplicing contribute to neuronal

- vulnerability from loss of TDP-43. *Nature neuroscience* 14: 459-468.
118. Chang Y, Kong Q, Shan X, Tian G, Ilieva H, et al. (2008) Messenger RNA oxidation occurs early in disease pathogenesis and promotes motor neuron degeneration in ALS. *PloS one* 3: e2849.
 119. Volkening K, Leystra-Lantz C, Yang W, Jaffee H, Strong MJ (2009) Tar DNA binding protein of 43 kDa (TDP-43), 14-3-3 proteins and copper/zinc superoxide dismutase (SOD1) interact to modulate NFL mRNA stability. Implications for altered RNA processing in amyotrophic lateral sclerosis (ALS). *Brain research* 1305: 168-182.
 120. Ferraiuolo L, Heath PR, Holden H, Kasher P, Kirby J, et al. (2007) Microarray analysis of the cellular pathways involved in the adaptation to and progression of motor neuron injury in the SOD1 G93A mouse model of familial ALS. *The Journal of neuroscience : the official journal of the Society for Neuroscience* 27: 9201-9219.
 121. Kirby J, Halligan E, Baptista MJ, Allen S, Heath PR, et al. (2005) Mutant SOD1 alters the motor neuronal transcriptome: implications for familial ALS. *Brain : a journal of neurology* 128: 1686-1706.
 122. Bartel DP (2004) MicroRNAs: genomics, biogenesis, mechanism, and function. *Cell* 116: 281-297.
 123. Gregory RI, Yan K-P, Amuthan G, Chendrimada T, Doratotaj B, et al. (2004) The Microprocessor complex mediates the genesis of microRNAs. *Nature* 432: 235-240.
 124. Williams AH, Valdez G, Moresi V, Qi X, McAnally J, et al. (2009) MicroRNA-206 delays ALS progression and promotes regeneration of neuromuscular synapses in mice. *Science (New York, N Y)* 326: 1549-1554.
 125. Van Den Bosch L (2011) Genetic rodent models of amyotrophic lateral sclerosis. *J Biomed Biotechnol* 2011: 348765.
 126. Joyce PI, Fratta P, Fisher EM, Acevedo-Arozena A (2011) SOD1 and TDP-43 animal models of amyotrophic lateral sclerosis: recent advances in understanding disease toward the development of clinical treatments. *Mamm Genome* 22: 420-448.
 127. Gurney ME, Pu H, Chiu AY, Dal Canto MC, Polchow CY, et al. (1994) Motor neuron degeneration in mice that express a human Cu,Zn superoxide dismutase mutation. *Science* 264: 1772-1775.
 128. Jonsson PA, Graffmo KS, Andersen PM, Brannstrom T, Lindberg M, et al. (2006) Disulphide-reduced superoxide dismutase-1 in CNS of transgenic amyotrophic lateral sclerosis models. *Brain* 129: 451-464.
 129. Gould TW, Buss RR, Vinsant S, Prevet D, Sun W, et al. (2006) Complete dissociation of motor neuron death from motor dysfunction by Bax deletion in a mouse model of ALS. *J Neurosci* 26: 8774-8786.
 130. Pun S, Santos AF, Saxena S, Xu L, Caroni P (2006) Selective vulnerability and pruning of phasic motoneuron axons in motoneuron disease alleviated by CNTF. *Nat Neurosci* 9: 408-419.
 131. Fischer LR, Culver DG, Tennant P, Davis AA, Wang M, et al. (2004) Amyotrophic lateral sclerosis is a distal axonopathy: evidence in mice and man. *Exp Neurol* 185: 232-240.

132. Filali M, Lalonde R, Rivest S (2011) Sensorimotor and cognitive functions in a SOD1(G37R) transgenic mouse model of amyotrophic lateral sclerosis. *Behav Brain Res* 225: 215-221.
133. Deng HX, Shi Y, Furukawa Y, Zhai H, Fu R, et al. (2006) Conversion to the amyotrophic lateral sclerosis phenotype is associated with intermolecular linked insoluble aggregates of SOD1 in mitochondria. *Proc Natl Acad Sci U S A* 103: 7142-7147.
134. Luche RM, Maiwald R, Carlson EJ, Epstein CJ (1997) Novel mutations in an otherwise strictly conserved domain of CuZn superoxide dismutase. *Mol Cell Biochem* 168: 191-194.
135. Ferri A, Cozzolino M, Crosio C, Nencini M, Casciati A, et al. (2006) Familial ALS-superoxide dismutases associate with mitochondria and shift their redox potentials. *Proc Natl Acad Sci U S A* 103: 13860-13865.
136. Wang J, Xu G, Borchelt DR (2006) Mapping superoxide dismutase 1 domains of non-native interaction: roles of intra- and intermolecular disulfide bonding in aggregation. *J Neurochem* 96: 1277-1288.
137. Kotulska K, LePecheur M, Marcol W, Lewin-Kowalik J, Larysz-Brysz M, et al. (2006) Overexpression of copper/zinc-superoxide dismutase in transgenic mice markedly impairs regeneration and increases development of neuropathic pain after sciatic nerve injury. *J Neurosci Res* 84: 1091-1097.
138. Jaarsma D (2006) Swelling and vacuolisation of mitochondria in transgenic SOD1-ALS mice: a consequence of supranormal SOD1 expression? *Mitochondrion* 6: 48-49; author reply 50-41.
139. Shaw PJ, Eggett CJ (2000) Molecular factors underlying selective vulnerability of motor neurons to neurodegeneration in amyotrophic lateral sclerosis. *Journal of neurology* 247 Suppl 1: I17-27.
140. Whitney NP, Peng H, Erdmann NB, Tian C, Monaghan DT, et al. (2008) Calcium-permeable AMPA receptors containing Q/R-unedited GluR2 direct human neural progenitor cell differentiation to neurons. *FASEB J* 22: 2888-2900.
141. Williams TL, Day NC, Ince PG, Kamboj RK, Shaw PJ (1997) Calcium-permeable alpha-amino-3-hydroxy-5-methyl-4-isoxazole propionic acid receptors: a molecular determinant of selective vulnerability in amyotrophic lateral sclerosis. *Annals of neurology* 42: 200-207.
142. Ince P, Stout N, Shaw P, Slade J, Hunziker W, et al. (1993) Parvalbumin and calbindin D-28k in the human motor system and in motor neuron disease. *Neuropathology and applied neurobiology* 19: 291-299.
143. Saxena S, Cabuy E, Caroni P (2009) A role for motoneuron subtype-selective ER stress in disease manifestations of FALS mice. *Nature neuroscience* 12: 627-636.
144. Kirby J, Ning K, Ferraiuolo L, Heath PR, Ismail A, et al. (2011) Phosphatase and tensin homologue/protein kinase B pathway linked to motor neuron survival in human superoxide dismutase 1-related amyotrophic lateral sclerosis. *Brain : a journal of neurology* 134: 506-517.
145. Rothstein JD, Patel S, Regan MR, Haenggeli C, Huang YH, et al. (2005) Beta-lactam antibiotics offer neuroprotection by increasing glutamate transporter expression. *Nature* 433: 73-77.
146. Hargitai J, Lewis H, Boros I, Racz T, Fiser A, et al. (2003) Bimoclolmol, a heat

- shock protein co-inducer, acts by the prolonged activation of heat shock factor-1. *Biochemical and biophysical research communications* 307: 689-695.
147. Kieran D, Kalmar B, Dick JRT, Riddoch-Contreras J, Burnstock G, et al. (2004) Treatment with arimoclomol, a coinducer of heat shock proteins, delays disease progression in ALS mice. *Nature medicine* 10: 402-405.
 148. Raoul C, Abbas-Terki T, Bensadoun J-C, Guillot S, Haase G, et al. (2005) Lentiviral-mediated silencing of SOD1 through RNA interference retards disease onset and progression in a mouse model of ALS. *Nature medicine* 11: 423-428.
 149. Smith RA, Miller TM, Yamanaka K, Monia BP, Condon TP, et al. (2006) Antisense oligonucleotide therapy for neurodegenerative disease. *The Journal of clinical investigation* 116: 2290-2296.
 150. Wang H, Ghosh A, Baigude H, Yang C-S, Qiu L, et al. (2008) Therapeutic gene silencing delivered by a chemically modified small interfering RNA against mutant SOD1 slows amyotrophic lateral sclerosis progression. *The Journal of biological chemistry* 283: 15845-15852.
 151. Danzeisen R, Schwalenstoecker B, Gillardon F, Buerger E, Krzykalla V, et al. (2006) Targeted antioxidative and neuroprotective properties of the dopamine agonist pramipexole and its nondopaminergic enantiomer SND919CL2x [(+)-2-amino-4,5,6,7-tetrahydro-6-L-propylamino-benzothiazole dihydrochloride]. *The Journal of pharmacology and experimental therapeutics* 316: 189-199.
 152. Kalra S, Genge A, Arnold DL (2003) A prospective, randomized, placebo-controlled evaluation of corticoneuronal response to intrathecal BDNF therapy in ALS using magnetic resonance spectroscopy: feasibility and results. *Amyotrophic lateral sclerosis and other motor neuron disorders : official publication of the World Federation of Neurology, Research Group on Motor Neuron Diseases* 4: 22-26.
 153. Zheng C, Nennesmo I, Fadeel B, Hentzer J-I (2004) Vascular endothelial growth factor prolongs survival in a transgenic mouse model of ALS. *Annals of neurology* 56: 564-567.
 154. Storkebaum E, Lambrechts D, Dewerchin M, Moreno-Murciano M-P, Appelmans S, et al. (2005) Treatment of motoneuron degeneration by intracerebroventricular delivery of VEGF in a rat model of ALS. *Nature neuroscience* 8: 85-92.
 155. Mazzini L, Mareschi K, Ferrero I, Vassallo E, Oliveri G, et al. (2008) Stem cell treatment in Amyotrophic Lateral Sclerosis. *Journal of the neurological sciences* 265: 78-83.
 156. Martinez HR, Gonzalez-Garza MT, Moreno-Cuevas JE, Caro E, Gutierrez-Jimenez E, et al. (2009) Stem-cell transplantation into the frontal motor cortex in amyotrophic lateral sclerosis patients. *Cytotherapy* 11: 26-34.
 157. Deda H, Inci MC, Kurekci AE, Sav A, Kayihan K, et al. (2009) Treatment of amyotrophic lateral sclerosis patients by autologous bone marrow-derived hematopoietic stem cell transplantation: a 1-year follow-up. *Cytotherapy* 11: 18-25.
 158. Cadena SM, Tomkinson KN, Monnell TE, Spaitis MS, Kumar R, et al. (2010) Administration of a soluble activin type IIB receptor promotes skeletal muscle growth independent of fiber type. *Journal of applied physiology (Bethesda, Md : 1985)* 109: 635-642.
 159. Jokic N, Gonzalez de Aguilar J-L, Pradat P-F, Dupuis L, Echaniz-Laguna A, et al.

- (2005) Nogo expression in muscle correlates with amyotrophic lateral sclerosis severity. *Annals of neurology* 57: 553-556.
160. Jokic N, Gonzalez de Aguilar J-L, Dimou L, Lin S, Fergani A, et al. (2006) The neurite outgrowth inhibitor Nogo-A promotes denervation in an amyotrophic lateral sclerosis model. *EMBO reports* 7: 1162-1167.
 161. Milani P, Gagliardi S, Cova E, Cereda C (2011) SOD1 Transcriptional and Posttranscriptional Regulation and Its Potential Implications in ALS. *Neurology research international* 2011: 458427.
 162. Furukawa Y, O'Halloran TV (2006) Posttranslational modifications in Cu,Zn-superoxide dismutase and mutations associated with amyotrophic lateral sclerosis. *Antioxidants & redox signaling* 8: 847-867.
 163. Valentine JS, Doucette PA, Zittin Potter S (2005) Copper-zinc superoxide dismutase and amyotrophic lateral sclerosis. *Annual review of biochemistry* 74: 563-593.
 164. Culotta VC, Yang M, O'Halloran TV (2006) Activation of superoxide dismutases: putting the metal to the pedal. *Biochimica et biophysica acta* 1763: 747-758.
 165. Arnesano F, Banci L, Bertini I, Martinelli M, Furukawa Y, et al. (2004) The unusually stable quaternary structure of human Cu,Zn-superoxide dismutase 1 is controlled by both metal occupancy and disulfide status. *The Journal of biological chemistry* 279: 47998-48003.
 166. Thornton JM (1981) Disulphide bridges in globular proteins. *Journal of molecular biology* 151: 261-287.
 167. Requejo R, Hurd TR, Costa NJ, Murphy MP (2010) Cysteine residues exposed on protein surfaces are the dominant intramitochondrial thiol and may protect against oxidative damage. *The FEBS journal* 277: 1465-1480.
 168. Andersen PM (2006) Amyotrophic lateral sclerosis associated with mutations in the CuZn superoxide dismutase gene. *Current neurology and neuroscience reports* 6: 37-46.
 169. Pasinelli P, Brown RH (2006) Molecular biology of amyotrophic lateral sclerosis: insights from genetics. *Nature reviews Neuroscience* 7: 710-723.
 170. Lill CM, Abel O, Bertram L, Al-Chalabi A (2011) Keeping up with genetic discoveries in amyotrophic lateral sclerosis: the ALSod and ALSGene databases. *Amyotrophic lateral sclerosis : official publication of the World Federation of Neurology Research Group on Motor Neuron Diseases* 12: 238-249.
 171. Conforti FL, Magariello A, Mazzei R, Sprovieri T, Patitucci A, et al. (2004) Abnormally high levels of SOD1 mRNA in a patient with amyotrophic lateral sclerosis. *Muscle & nerve* 29: 610-611.
 172. Jiang Y-M, Yamamoto M, Kobayashi Y, Yoshihara T, Liang Y, et al. (2005) Gene expression profile of spinal motor neurons in sporadic amyotrophic lateral sclerosis. *Annals of neurology* 57: 236-251.
 173. Wang X-S, Simmons Z, Liu W, Boyer PJ, Connor JR (2006) Differential expression of genes in amyotrophic lateral sclerosis revealed by profiling the post mortem cortex. *Amyotrophic lateral sclerosis : official publication of the World Federation of Neurology Research Group on Motor Neuron Diseases* 7: 201-210.
 174. Gagliardi S, Cova E, Davin A, Guareschi S, Abel K, et al. (2010) SOD1 mRNA expression in sporadic amyotrophic lateral sclerosis. *Neurobiology of disease* 39: 198-203.

175. Cova E, Cereda C, Galli A, Curti D, Finotti C, et al. (2006) Modified expression of Bcl-2 and SOD1 proteins in lymphocytes from sporadic ALS patients. *Neuroscience letters* 399: 186-190.
176. Forsberg K, Jonsson PA, Andersen PM, Bergemalm D, Graffmo KS, et al. (2010) Novel antibodies reveal inclusions containing non-native SOD1 in sporadic ALS patients. *PloS one* 5: e11552.
177. Gruzman A, Wood WL, Alpert E, Prasad MD, Miller RG, et al. (2007) Common molecular signature in SOD1 for both sporadic and familial amyotrophic lateral sclerosis. *Proc Natl Acad Sci U S A* 104: 12524-12529.
178. Watanabe M, Dykes-Hoberg M, Culotta VC, Price DL, Wong PC, et al. (2001) Histological evidence of protein aggregation in mutant SOD1 transgenic mice and in amyotrophic lateral sclerosis neural tissues. *Neurobiol Dis* 8: 933-941.
179. Rothstein JD (2009) Current hypotheses for the underlying biology of amyotrophic lateral sclerosis. *Ann Neurol* 65 Suppl 1: S3-9.
180. Howland DS, Liu J, She Y, Goad B, Maragakis NJ, et al. (2002) Focal loss of the glutamate transporter EAAT2 in a transgenic rat model of SOD1 mutant-mediated amyotrophic lateral sclerosis (ALS). *Proc Natl Acad Sci U S A* 99: 1604-1609.
181. Jonsson PA, Ernhill K, Andersen PM, Bergemalm D, Brannstrom T, et al. (2004) Minute quantities of misfolded mutant superoxide dismutase-1 cause amyotrophic lateral sclerosis. *Brain* 127: 73-88.
182. Wang J, Slunt H, Gonzales V, Fromholt D, Coonfield M, et al. (2003) Copper-binding-site-null SOD1 causes ALS in transgenic mice: aggregates of non-native SOD1 delineate a common feature. *Hum Mol Genet* 12: 2753-2764.
183. Reaume AG, Elliott JL, Hoffman EK, Kowall NW, Ferrante RJ, et al. (1996) Motor neurons in Cu/Zn superoxide dismutase-deficient mice develop normally but exhibit enhanced cell death after axonal injury. *Nat Genet* 13: 43-47.
184. Bruijn LI, Houseweart MK, Kato S, Anderson KL, Anderson SD, et al. (1998) Aggregation and motor neuron toxicity of an ALS-linked SOD1 mutant independent from wild-type SOD1. *Science* 281: 1851-1854.
185. Urushitani M, Ezzi SA, Matsuo A, Tooyama I, Julien JP (2008) The endoplasmic reticulum-Golgi pathway is a target for translocation and aggregation of mutant superoxide dismutase linked to ALS. *FASEB J* 22: 2476-2487.
186. Damiano M, Starkov AA, Petri S, Kipiani K, Kiaei M, et al. (2006) Neural mitochondrial Ca²⁺ capacity impairment precedes the onset of motor symptoms in G93A Cu/Zn-superoxide dismutase mutant mice. *J Neurochem* 96: 1349-1361.
187. Urushitani M, Nakamizo T, Inoue R, Sawada H, Kihara T, et al. (2001) N-methyl-D-aspartate receptor-mediated mitochondrial Ca(2+) overload in acute excitotoxic motor neuron death: a mechanism distinct from chronic neurotoxicity after Ca(2+) influx. *J Neurosci Res* 63: 377-387.
188. Vande Velde C, Miller TM, Cashman NR, Cleveland DW (2008) Selective association of misfolded ALS-linked mutant SOD1 with the cytoplasmic face of mitochondria. *Proc Natl Acad Sci U S A* 105: 4022-4027.
189. Inoue H, Tsukita K, Iwasato T, Suzuki Y, Tomioka M, et al. (2003) The crucial role of caspase-9 in the disease progression of a transgenic ALS mouse model. *EMBO J* 22: 6665-6674.
190. Reyes NA, Fisher JK, Austgen K, VandenBerg S, Huang EJ, et al. (2010) Blocking

- the mitochondrial apoptotic pathway preserves motor neuron viability and function in a mouse model of amyotrophic lateral sclerosis. *J Clin Invest* 120: 3673-3679.
191. Zhu YB, Sheng ZH (2011) Increased axonal mitochondrial mobility does not slow amyotrophic lateral sclerosis (ALS)-like disease in mutant SOD1 mice. *J Biol Chem* 286: 23432-23440.
 192. Ahtoniemi T, Jaronen M, Keksa-Goldsteine V, Goldsteins G, Koistinaho J (2008) Mutant SOD1 from spinal cord of G93A rats is destabilized and binds to inner mitochondrial membrane. *Neurobiol Dis* 32: 479-485.
 193. Goldsteins G, Keksa-Goldsteine V, Ahtoniemi T, Jaronen M, Arens E, et al. (2008) Deleterious role of superoxide dismutase in the mitochondrial intermembrane space. *J Biol Chem* 283: 8446-8452.
 194. Magrane J, Hervias I, Henning MS, Damiano M, Kawamata H, et al. (2009) Mutant SOD1 in neuronal mitochondria causes toxicity and mitochondrial dynamics abnormalities. *Hum Mol Genet* 18: 4552-4564.
 195. Kikuchi H, Almer G, Yamashita S, Guegan C, Nagai M, et al. (2006) Spinal cord endoplasmic reticulum stress associated with a microsomal accumulation of mutant superoxide dismutase-1 in an ALS model. *Proc Natl Acad Sci U S A* 103: 6025-6030.
 196. Urushitani M, Sik A, Sakurai T, Nukina N, Takahashi R, et al. (2006) Chromogranin-mediated secretion of mutant superoxide dismutase proteins linked to amyotrophic lateral sclerosis. *Nat Neurosci* 9: 108-118.
 197. Nishitoh H, Kadowaki H, Nagai A, Maruyama T, Yokota T, et al. (2008) ALS-linked mutant SOD1 induces ER stress- and ASK1-dependent motor neuron death by targeting Derlin-1. *Genes & development* 22: 1451-1464.
 198. Tobisawa S, Hozumi Y, Arawaka S, Koyama S, Wada M, et al. (2003) Mutant SOD1 linked to familial amyotrophic lateral sclerosis, but not wild-type SOD1, induces ER stress in COS7 cells and transgenic mice. *Biochem Biophys Res Commun* 303: 496-503.
 199. Lafon-Cazal M, Adjali O, Galeotti N, Poncet J, Jouin P, et al. (2003) Proteomic analysis of astrocytic secretion in the mouse. Comparison with the cerebrospinal fluid proteome. *J Biol Chem* 278: 24438-24448.
 200. Turner BJ, Atkin JD, Farg MA, Zang DW, Rembach A, et al. (2005) Impaired extracellular secretion of mutant superoxide dismutase 1 associates with neurotoxicity in familial amyotrophic lateral sclerosis. *J Neurosci* 25: 108-117.
 201. Nagai M, Re DB, Nagata T, Chalazonitis A, Jessell TM, et al. (2007) Astrocytes expressing ALS-linked mutated SOD1 release factors selectively toxic to motor neurons. *Nat Neurosci* 10: 615-622.
 202. Di Giorgio FP, Boulting GL, Bobrowicz S, Eggan KC (2008) Human embryonic stem cell-derived motor neurons are sensitive to the toxic effect of glial cells carrying an ALS-causing mutation. *Cell Stem Cell* 3: 637-648.
 203. Di Giorgio FP, Carrasco MA, Siao MC, Maniatis T, Eggan K (2007) Non-cell autonomous effect of glia on motor neurons in an embryonic stem cell-based ALS model. *Nat Neurosci* 10: 608-614.
 204. Zhao W, Xie W, Xiao Q, Beers DR, Appel SH (2006) Protective effects of an anti-inflammatory cytokine, interleukin-4, on motoneuron toxicity induced by

- activated microglia. *J Neurochem* 99: 1176-1187.
205. Liu HN, Sanelli T, Horne P, Piore EP, Strong MJ, et al. (2009) Lack of evidence of monomer/misfolded superoxide dismutase-1 in sporadic amyotrophic lateral sclerosis. *Ann Neurol* 66: 75-80.
 206. Zetterstrom P, Andersen PM, Brannstrom T, Marklund SL (2011) Misfolded superoxide dismutase-1 in CSF from amyotrophic lateral sclerosis patients. *J Neurochem* 117: 91-99.
 207. Johnston JA, Dalton MJ, Gurney ME, Kopito RR (2000) Formation of high molecular weight complexes of mutant Cu, Zn-superoxide dismutase in a mouse model for familial amyotrophic lateral sclerosis. *Proc Natl Acad Sci U S A* 97: 12571-12576.
 208. Wang J, Xu G, Li H, Gonzales V, Fromholt D, et al. (2005) Somatodendritic accumulation of misfolded SOD1-L126Z in motor neurons mediates degeneration: alphaB-crystallin modulates aggregation. *Hum Mol Genet* 14: 2335-2347.
 209. Watanabe Y, Yasui K, Nakano T, Doi K, Fukada Y, et al. (2005) Mouse motor neuron disease caused by truncated SOD1 with or without C-terminal modification. *Brain Res Mol Brain Res* 135: 12-20.
 210. Koyama S, Arawaka S, Chang-Hong R, Wada M, Kawanami T, et al. (2006) Alteration of familial ALS-linked mutant SOD1 solubility with disease progression: its modulation by the proteasome and Hsp70. *Biochem Biophys Res Commun* 343: 719-730.
 211. Niwa J, Ishigaki S, Hishikawa N, Yamamoto M, Doyu M, et al. (2002) Dofin ubiquitylates mutant SOD1 and prevents mutant SOD1-mediated neurotoxicity. *J Biol Chem* 277: 36793-36798.
 212. Urushitani M, Kurisu J, Tateno M, Hatakeyama S, Nakayama K, et al. (2004) CHIP promotes proteasomal degradation of familial ALS-linked mutant SOD1 by ubiquitinating Hsp/Hsc70. *J Neurochem* 90: 231-244.
 213. Bruijn LI, Miller TM, Cleveland DW (2004) Unraveling the mechanisms involved in motor neuron degeneration in ALS. *Annu Rev Neurosci* 27: 723-749.
 214. Storkebaum E, Lambrechts D, Dewerchin M, Moreno-Murciano MP, Appelmans S, et al. (2005) Treatment of motoneuron degeneration by intracerebroventricular delivery of VEGF in a rat model of ALS. *Nat Neurosci* 8: 85-92.
 215. Liu J, Lillo C, Jonsson PA, Vande Velde C, Ward CM, et al. (2004) Toxicity of familial ALS-linked SOD1 mutants from selective recruitment to spinal mitochondria. *Neuron* 43: 5-17.
 216. Pasinelli P, Belford ME, Lennon N, Bacskai BJ, Hyman BT, et al. (2004) Amyotrophic lateral sclerosis-associated SOD1 mutant proteins bind and aggregate with Bcl-2 in spinal cord mitochondria. *Neuron* 43: 19-30.
 217. Molnar KS, Karabacak NM, Johnson JL, Wang Q, Tiwari A, et al. (2009) A common property of amyotrophic lateral sclerosis-associated variants: destabilization of the copper/zinc superoxide dismutase electrostatic loop. *J Biol Chem* 284: 30965-30973.
 218. Wang Q, Johnson JL, Agar NY, Agar JN (2008) Protein aggregation and protein instability govern familial amyotrophic lateral sclerosis patient survival. *PLoS Biol* 6: e170.
 219. Shibata N, Asayama K, Hirano A, Kobayashi M (1996) Immunohistochemical study

- on superoxide dismutases in spinal cords from autopsied patients with amyotrophic lateral sclerosis. *Developmental neuroscience* 18: 492-498.
220. Rakhit R, Cunningham P, Furtos-Matei A, Dahan S, Qi X-F, et al. (2002) Oxidation-induced misfolding and aggregation of superoxide dismutase and its implications for amyotrophic lateral sclerosis. *The Journal of biological chemistry* 277: 47551-47556.
 221. Crow JP, Sampson JB, Zhuang Y, Thompson JA, Beckman JS (1997) Decreased zinc affinity of amyotrophic lateral sclerosis-associated superoxide dismutase mutants leads to enhanced catalysis of tyrosine nitration by peroxynitrite. *Journal of neurochemistry* 69: 1936-1944.
 222. Elam JS, Taylor AB, Strange R, Antonyuk S, Doucette PA, et al. (2003) Amyloid-like filaments and water-filled nanotubes formed by SOD1 mutant proteins linked to familial ALS. *Nature structural biology* 10: 461-467.
 223. Hough MA, Grossmann JG, Antonyuk SV, Strange RW, Doucette PA, et al. (2004) Dimer destabilization in superoxide dismutase may result in disease-causing properties: structures of motor neuron disease mutants. *Proceedings of the National Academy of Sciences of the United States of America* 101: 5976-5981.
 224. Rakhit R, Crow JP, Lepock JR, Kondejewski LH, Cashman NR, et al. (2004) Monomeric Cu,Zn-superoxide dismutase is a common misfolding intermediate in the oxidation models of sporadic and familial amyotrophic lateral sclerosis. *The Journal of biological chemistry* 279: 15499-15504.
 225. Rodriguez JA, Shaw BF, Durazo A, Sohn SH, Doucette PA, et al. (2005) Destabilization of apoprotein is insufficient to explain Cu,Zn-superoxide dismutase-linked ALS pathogenesis. *Proceedings of the National Academy of Sciences of the United States of America* 102: 10516-10521.
 226. Aoki M, Ogasawara M, Matsubara Y, Narisawa K, Nakamura S, et al. (1993) Mild ALS in Japan associated with novel SOD mutation. *Nature genetics* 5: 323-324.
 227. Juneja T, Pericak-Vance MA, Laing NG, Dave S, Siddique T (1997) Prognosis in familial amyotrophic lateral sclerosis: progression and survival in patients with glu100gly and ala4val mutations in Cu,Zn superoxide dismutase. *Neurology* 48: 55-57.
 228. Oztug Durer ZA, Cohlberg JA, Dinh P, Padua S, Ehrenclou K, et al. (2009) Loss of metal ions, disulfide reduction and mutations related to familial ALS promote formation of amyloid-like aggregates from superoxide dismutase. *PloS one* 4: e5004.
 229. Bruns CK, Kopito RR (2007) Impaired post-translational folding of familial ALS-linked Cu, Zn superoxide dismutase mutants. *The EMBO journal* 26: 855-866.
 230. Furukawa Y, O'Halloran TV (2005) Amyotrophic lateral sclerosis mutations have the greatest destabilizing effect on the apo- and reduced form of SOD1, leading to unfolding and oxidative aggregation. *The Journal of biological chemistry* 280: 17266-17274.
 231. Doyle KM, Kennedy D, Gorman AM, Gupta S, Healy SJM, et al. (2011) Unfolded proteins and endoplasmic reticulum stress in neurodegenerative disorders. *Journal of cellular and molecular medicine* 15: 2025-2039.
 232. Deng HX, Shi Y, Furukawa Y, Zhai H, Fu R, et al. (2006) Conversion to the

- amyotrophic lateral sclerosis phenotype is associated with intermolecular linked insoluble aggregates of SOD1 in mitochondria. *Proceedings of the National Academy of Sciences of the United States of America* 103: 7142-7147.
233. Furukawa Y, Fu R, Deng HX, Siddique T, O'Halloran TV (2006) Disulfide cross-linked protein represents a significant fraction of ALS-associated Cu, Zn-superoxide dismutase aggregates in spinal cords of model mice. *Proceedings of the National Academy of Sciences of the United States of America* 103: 7148-7153.
 234. Cozzolino M, Amori I, Pesaresi MG, Ferri A, Nencini M, et al. (2008) Cysteine 111 affects aggregation and cytotoxicity of mutant Cu,Zn-superoxide dismutase associated with familial amyotrophic lateral sclerosis. *The Journal of biological chemistry* 283: 866-874.
 235. Niwa J, Yamada S, Ishigaki S, Sone J, Takahashi M, et al. (2007) Disulfide bond mediates aggregation, toxicity, and ubiquitylation of familial amyotrophic lateral sclerosis-linked mutant SOD1. *The Journal of biological chemistry* 282: 28087-28095.
 236. Furukawa Y, Fu R, Deng H-X, Siddique T, O'Halloran TV (2006) Disulfide cross-linked protein represents a significant fraction of ALS-associated Cu, Zn-superoxide dismutase aggregates in spinal cords of model mice. *Proceedings of the National Academy of Sciences of the United States of America* 103: 7148-7153.
 237. Karch CM, Borchelt DR (2008) A limited role for disulfide cross-linking in the aggregation of mutant SOD1 linked to familial amyotrophic lateral sclerosis. *The Journal of biological chemistry* 283: 13528-13537.
 238. Kawamata H, Manfredi G (2008) Different regulation of wild-type and mutant Cu,Zn superoxide dismutase localization in mammalian mitochondria. *Hum Mol Genet* 17: 3303-3317.
 239. Karch CM, Prudencio M, Winkler DD, Hart PJ, Borchelt DR (2009) Role of mutant SOD1 disulfide oxidation and aggregation in the pathogenesis of familial ALS. *Proceedings of the National Academy of Sciences of the United States of America* 106: 7774-7779.
 240. Ferri A, Cozzolino M, Crosio C, Nencini M, Casciati A, et al. (2006) Familial ALS-superoxide dismutases associate with mitochondria and shift their redox potentials. *Proceedings of the National Academy of Sciences of the United States of America* 103: 13860-13865.
 241. Urushitani M, Kurisu J, Tsukita K, Takahashi R (2002) Proteasomal inhibition by misfolded mutant superoxide dismutase 1 induces selective motor neuron death in familial amyotrophic lateral sclerosis. *J Neurochem* 83: 1030-1042.
 242. Uchida K, Kawakishi S (1994) Identification of oxidized histidine generated at the active site of Cu,Zn-superoxide dismutase exposed to H₂O₂. Selective generation of 2-oxo-histidine at the histidine 118. *The Journal of biological chemistry* 269: 2405-2410.
 243. Ezzi SA, Urushitani M, Julien JP (2007) Wild-type superoxide dismutase acquires binding and toxic properties of ALS-linked mutant forms through oxidation. *J Neurochem* 102: 170-178.
 244. Kurahashi T, Miyazaki A, Suwan S, Isobe M (2001) Extensive investigations on

- oxidized amino acid residues in H₂O₂-treated Cu,Zn-SOD protein with LC-ESI-Q-TOF-MS, MS/MS for the determination of the copper-binding site. *J Am Chem Soc* 123: 9268-9278.
245. Zhang H, Andrekopoulos C, Joseph J, Chandran K, Karoui H, et al. (2003) Bicarbonate-dependent peroxidase activity of human Cu,Zn-superoxide dismutase induces covalent aggregation of protein: intermediacy of tryptophan-derived oxidation products. *The Journal of biological chemistry* 278: 24078-24089.
 246. Oeda T, Shimohama S, Kitagawa N, Kohno R, Imura T, et al. (2001) Oxidative stress causes abnormal accumulation of familial amyotrophic lateral sclerosis-related mutant SOD1 in transgenic *Caenorhabditis elegans*. *Hum Mol Genet* 10: 2013-2023.
 247. Bendotti C, Marino M, Cheroni C, Fontana E, Crippa V, et al. (2011) Dysfunction of constitutive and inducible ubiquitin-proteasome system in amyotrophic lateral sclerosis: Implication for protein aggregation and immune response. *Prog Neurobiol*.
 248. Sullivan PG, Rabchevsky AG, Keller JN, Lovell M, Sodhi A, et al. (2004) Intrinsic differences in brain and spinal cord mitochondria: Implication for therapeutic interventions. *J Comp Neurol* 474: 524-534.
 249. Cleveland DW (1996) Neuronal growth and death: order and disorder in the axoplasm. *Cell* 84: 663-666.
 250. Williamson TL, Cleveland DW (1999) Slowing of axonal transport is a very early event in the toxicity of ALS-linked SOD1 mutants to motor neurons. *Nature neuroscience* 2: 50-56.
 251. Jacob C, Holme AL, Fry FH (2004) The sulfinic acid switch in proteins. *Org Biomol Chem* 2: 1953-1956.
 252. Woo HA, Jeong W, Chang TS, Park KJ, Park SJ, et al. (2005) Reduction of cysteine sulfinic acid by sulfiredoxin is specific to 2-cys peroxiredoxins. *The Journal of biological chemistry* 280: 3125-3128.
 253. Choi J, Rees HD, Weintraub ST, Levey AI, Chin LS, et al. (2005) Oxidative modifications and aggregation of Cu,Zn-superoxide dismutase associated with Alzheimer and Parkinson diseases. *The Journal of biological chemistry* 280: 11648-11655.
 254. Fink RC, Scandalios JG (2002) Molecular evolution and structure--function relationships of the superoxide dismutase gene families in angiosperms and their relationship to other eukaryotic and prokaryotic superoxide dismutases. *Arch Biochem Biophys* 399: 19-36.
 255. Fukuhara R, Tezuka T, Kageyama T (2002) Structure, molecular evolution, and gene expression of primate superoxide dismutases. *Gene* 296: 99-109.
 256. de Beus MD, Chung J, Colon W (2004) Modification of cysteine 111 in Cu/Zn superoxide dismutase results in altered spectroscopic and biophysical properties. *Protein Sci* 13: 1347-1355.
 257. Wilcox KC, Zhou L, Jordon JK, Huang Y, Yu Y, et al. (2009) Modifications of superoxide dismutase (SOD1) in human erythrocytes: a possible role in amyotrophic lateral sclerosis. *The Journal of biological chemistry* 284: 13940-13947.
 258. Redler RL, Wilcox KC, Proctor EA, Fee L, Caplow M, et al. (2011)

- Glutathionylation at Cys-111 induces dissociation of wild type and FALS mutant SOD1 dimers. *Biochemistry* 50: 7057-7066.
259. Ferri A, Fiorenzo P, Nencini M, Cozzolino M, Pesaresi MG, et al. (2010) Glutaredoxin 2 prevents aggregation of mutant SOD1 in mitochondria and abolishes its toxicity. *Hum Mol Genet* 19: 4529-4542.
 260. Watanabe S, Nagano S, Duce J, Kiaei M, Li QX, et al. (2007) Increased affinity for copper mediated by cysteine 111 in forms of mutant superoxide dismutase 1 linked to amyotrophic lateral sclerosis. *Free Radic Biol Med* 42: 1534-1542.
 261. Fujiwara N, Nakano M, Kato S, Yoshihara D, Ookawara T, et al. (2007) Oxidative modification to cysteine sulfonic acid of Cys111 in human copper-zinc superoxide dismutase. *The Journal of biological chemistry* 282: 35933-35944.
 262. Teilum K, Smith MH, Schulz E, Christensen LC, Solomentsev G, et al. (2009) Transient structural distortion of metal-free Cu/Zn superoxide dismutase triggers aberrant oligomerization. *Proceedings of the National Academy of Sciences of the United States of America* 106: 18273-18278.
 263. Gruzman A, Wood WL, Alpert E, Prasad MD, Miller RG, et al. (2007) Common molecular signature in SOD1 for both sporadic and familial amyotrophic lateral sclerosis. *Proceedings of the National Academy of Sciences of the United States of America* 104: 12524-12529.
 264. Kabashi E, Valdmanis PN, Dion P, Rouleau GA (2007) Oxidized/misfolded superoxide dismutase-1: the cause of all amyotrophic lateral sclerosis? *Annals of neurology* 62: 553-559.
 265. Casoni F, Basso M, Massignan T, Gianazza E, Cheroni C, et al. (2005) Protein nitration in a mouse model of familial amyotrophic lateral sclerosis: possible multifunctional role in the pathogenesis. *The Journal of biological chemistry* 280: 16295-16304.
 266. Furukawa Y, Torres AS, O'Halloran TV (2004) Oxygen-induced maturation of SOD1: a key role for disulfide formation by the copper chaperone CCS. *The EMBO journal* 23: 2872-2881.
 267. Ezzi SA, Urushitani M, Julien J-P (2007) Wild-type superoxide dismutase acquires binding and toxic properties of ALS-linked mutant forms through oxidation. *Journal of neurochemistry* 102: 170-178.
 268. Rakhit R, Robertson J, Vande Velde C, Horne P, Ruth DM, et al. (2007) An immunological epitope selective for pathological monomer-misfolded SOD1 in ALS. *Nature medicine* 13: 754-759.
 269. Bosco DA, Morfini G, Karabacak NM, Song Y, Gros-Louis F, et al. (2010) Wild-type and mutant SOD1 share an aberrant conformation and a common pathogenic pathway in ALS. *Nature neuroscience* 13: 1396-1403.
 270. Pelham HR (1990) The retention signal for soluble proteins of the endoplasmic reticulum. *Trends Biochem Sci* 15: 483-486.
 271. Hatahet F, Ruddock LW (2009) Protein disulfide isomerase: a critical evaluation of its function in disulfide bond formation. *Antioxidants & redox signaling* 11: 2807-2850.
 272. Reinhardt C, von Bruhl M-L, Manukyan D, Grahl L, Lorenz M, et al. (2008) Protein disulfide isomerase acts as an injury response signal that enhances fibrin generation via tissue factor activation. *The Journal of clinical investigation* 118:

- 1110-1122.
273. Hebert DN, Molinari M (2007) In and out of the ER: protein folding, quality control, degradation, and related human diseases. *Physiological reviews* 87: 1377-1408.
 274. Wang CC, Tsou CL (1993) Protein disulfide isomerase is both an enzyme and a chaperone. *FASEB journal : official publication of the Federation of American Societies for Experimental Biology* 7: 1515-1517.
 275. Appenzeller-Herzog C, Ellgaard L (2008) The human PDI family: versatility packed into a single fold. *Biochimica et biophysica acta* 1783: 535-548.
 276. Hatahet F, Ruddock LW (2007) Substrate recognition by the protein disulfide isomerases. *The FEBS journal* 274: 5223-5234.
 277. Klappa P, Ruddock LW, Darby NJ, Freedman RB (1998) The b' domain provides the principal peptide-binding site of protein disulfide isomerase but all domains contribute to binding of misfolded proteins. *The EMBO journal* 17: 927-935.
 278. Tian G, Xiang S, Noiva R, Lennarz WJ, Schindelin H (2006) The crystal structure of yeast protein disulfide isomerase suggests cooperativity between its active sites. *Cell* 124: 61-73.
 279. Hirano N, Shibasaki F, Kato H, Sakai R, Tanaka T, et al. (1994) Molecular cloning and characterization of a cDNA for bovine phospholipase C-alpha: proposal of redesignation of phospholipase C-alpha. *Biochemical and biophysical research communications* 204: 375-382.
 280. Jessop CE, Watkins RH, Simmons JJ, Tasab M, Bulleid NJ (2009) Protein disulphide isomerase family members show distinct substrate specificity: P5 is targeted to BiP client proteins. *Journal of cell science* 122: 4287-4295.
 281. Elliott JG, Oliver JD, High S (1997) The thiol-dependent reductase ERp57 interacts specifically with N-glycosylated integral membrane proteins. *The Journal of biological chemistry* 272: 13849-13855.
 282. Oliver JD, van der Wal FJ, Bulleid NJ, High S (1997) Interaction of the thiol-dependent reductase ERp57 with nascent glycoproteins. *Science (New York, N Y)* 275: 86-88.
 283. Maattanen P, Kozlov G, Gehring K, Thomas DY (2006) ERp57 and PDI: multifunctional protein disulfide isomerases with similar domain architectures but differing substrate-partner associations. *Biochem Cell Biol* 84: 881-889.
 284. Park B, Lee S, Kim E, Cho K, Riddell SR, et al. (2006) Redox regulation facilitates optimal peptide selection by MHC class I during antigen processing. *Cell* 127: 369-382.
 285. LaMantia ML, Lennarz WJ (1993) The essential function of yeast protein disulfide isomerase does not reside in its isomerase activity. *Cell* 74: 899-908.
 286. Park S-W, Zhen G, Verhaeghe C, Nakagami Y, Nguyenvu LT, et al. (2009) The protein disulfide isomerase AGR2 is essential for production of intestinal mucus. *Proceedings of the National Academy of Sciences of the United States of America* 106: 6950-6955.
 287. Hosoda A, Tokuda M, Akai R, Kohno K, Iwawaki T (2010) Positive contribution of ERdj5/JPDI to endoplasmic reticulum protein quality control in the salivary gland. *The Biochemical journal* 425: 117-125.
 288. Braakman I, Bulleid NJ (2011) Protein folding and modification in the mammalian endoplasmic reticulum. *Annu Rev Biochem* 80: 71-99.

289. Mezghrani A, Fassio A, Benham A, Simmen T, Braakman I, et al. (2001) Manipulation of oxidative protein folding and PDI redox state in mammalian cells. *EMBO J* 20: 6288-6296.
290. Zito E, Melo EP, Yang Y, Wahlander A, Neubert TA, et al. (2010) Oxidative protein folding by an endoplasmic reticulum-localized peroxiredoxin. *Mol Cell* 40: 787-797.
291. Hatahet F, Ruddock LW (2009) Protein disulfide isomerase: a critical evaluation of its function in disulfide bond formation. *Antioxid Redox Signal* 11: 2807-2850.
292. Wilkinson B, Gilbert HF (2004) Protein disulfide isomerase. *Biochim Biophys Acta* 1699: 35-44.
293. Wang C, Yu J, Huo L, Wang L, Feng W, et al. (2012) Human protein-disulfide isomerase is a redox-regulated chaperone activated by oxidation of domain a'. *J Biol Chem* 287: 1139-1149.
294. Tsai B, Rodighiero C, Lencer WI, Rapoport TA (2001) Protein disulfide isomerase acts as a redox-dependent chaperone to unfold cholera toxin. *Cell* 104: 937-948.
295. Malhotra JD, Kaufman RJ (2007) The endoplasmic reticulum and the unfolded protein response. *Semin Cell Dev Biol* 18: 716-731.
296. Essex DW (2009) Redox control of platelet function. *Antioxid Redox Signal* 11: 1191-1225.
297. Fenouillet E, Barbouche R, Jones IM (2007) Cell entry by enveloped viruses: redox considerations for HIV and SARS-coronavirus. *Antioxid Redox Signal* 9: 1009-1034.
298. Gilbert J, Ou W, Silver J, Benjamin T (2006) Downregulation of protein disulfide isomerase inhibits infection by the mouse polyomavirus. *J Virol* 80: 10868-10870.
299. Cheng HJ, Lei HY, Lin CF, Luo YH, Wan SW, et al. (2009) Anti-dengue virus nonstructural protein 1 antibodies recognize protein disulfide isomerase on platelets and inhibit platelet aggregation. *Mol Immunol* 47: 398-406.
300. Uehara T, Nakamura T, Yao D, Shi ZQ, Gu Z, et al. (2006) S-nitrosylated protein-disulphide isomerase links protein misfolding to neurodegeneration. *Nature* 441: 513-517.
301. Cheng H, Wang L, Wang CC (2010) Domain a' of protein disulfide isomerase plays key role in inhibiting alpha-synuclein fibril formation. *Cell Stress Chaperones* 15: 415-421.
302. Riedel M, Goldbaum O, Schwarz L, Schmitt S, Richter-Landsberg C (2010) 17-AAG induces cytoplasmic alpha-synuclein aggregate clearance by induction of autophagy. *PLoS One* 5: e8753.
303. Shashidharan P, Sandu D, Potla U, Armata IA, Walker RH, et al. (2005) Transgenic mouse model of early-onset DYT1 dystonia. *Hum Mol Genet* 14: 125-133.
304. Honjo Y, Ito H, Horibe T, Takahashi R, Kawakami K (2010) Protein disulfide isomerase-immunopositive inclusions in patients with Alzheimer disease. *Brain Res* 1349: 90-96.
305. Tanaka S, Uehara T, Nomura Y (2000) Up-regulation of protein-disulfide isomerase in response to hypoxia/brain ischemia and its protective effect against apoptotic cell death. *J Biol Chem* 275: 10388-10393.
306. Toldo S, Severino A, Abbate A, Baldi A (2011) The role of PDI as a survival factor in cardiomyocyte ischemia. *Methods in enzymology* 489: 47-65.

307. Schroder M, Kaufman RJ (2005) ER stress and the unfolded protein response. *Mutat Res* 569: 29-63.
308. Lai E, Teodoro T, Volchuk A (2007) Endoplasmic reticulum stress: signaling the unfolded protein response. *Physiology (Bethesda, Md)* 22: 193-201.
309. Vembar SS, Brodsky JL (2008) One step at a time: endoplasmic reticulum-associated degradation. *Nature reviews Molecular cell biology* 9: 944-957.
310. Shen X, Zhang K, Kaufman RJ (2004) The unfolded protein response--a stress signaling pathway of the endoplasmic reticulum. *Journal of chemical neuroanatomy* 28: 79-92.
311. Kato H, Sakaki K, Mihara K (2006) Ubiquitin-proteasome-dependent degradation of mammalian ER stearoyl-CoA desaturase. *Journal of cell science* 119: 2342-2353.
312. Kieran D, Woods I, Villunger A, Strasser A, Prehn JHM (2007) Deletion of the BH3-only protein puma protects motoneurons from ER stress-induced apoptosis and delays motoneuron loss in ALS mice. *Proceedings of the National Academy of Sciences of the United States of America* 104: 20606-20611.
313. Hetz C, Thielen P, Matus S, Nassif M, Court F, et al. (2009) XBP-1 deficiency in the nervous system protects against amyotrophic lateral sclerosis by increasing autophagy. *Genes & development* 23: 2294-2306.
314. Nakagawa T, Zhu H, Morishima N, Li E, Xu J, et al. (2000) Caspase-12 mediates endoplasmic-reticulum-specific apoptosis and cytotoxicity by amyloid-beta. *Nature* 403: 98-103.
315. Oh YK, Shin KS, Yuan J, Kang SJ (2008) Superoxide dismutase 1 mutants related to amyotrophic lateral sclerosis induce endoplasmic stress in neuro2a cells. *Journal of neurochemistry* 104: 993-1005.
316. Nishimura AL, Mitne-Neto M, Silva HC, Richieri-Costa A, Middleton S, et al. (2004) A mutation in the vesicle-trafficking protein VAPB causes late-onset spinal muscular atrophy and amyotrophic lateral sclerosis. *Am J Hum Genet* 75: 822-831.
317. Massignan T, Casoni F, Basso M, Stefanazzi P, Biasini E, et al. (2007) Proteomic analysis of spinal cord of presymptomatic amyotrophic lateral sclerosis G93A SOD1 mouse. *Biochemical and biophysical research communications* 353: 719-725.
318. Tsuda H, Han SM, Yang Y, Tong C, Lin YQ, et al. (2008) The amyotrophic lateral sclerosis 8 protein VAPB is cleaved, secreted, and acts as a ligand for Eph receptors. *Cell* 133: 963-977.
319. Walker AK (2010) Protein disulfide isomerase and the endoplasmic reticulum in amyotrophic lateral sclerosis. *The Journal of neuroscience : the official journal of the Society for Neuroscience* 30: 3865-3867.
320. Yang YS, Harel NY, Strittmatter SM (2009) Reticulon-4A (Nogo-A) redistributes protein disulfide isomerase to protect mice from SOD1-dependent amyotrophic lateral sclerosis. *The Journal of neuroscience : the official journal of the Society for Neuroscience* 29: 13850-13859.
321. Brown GC (2010) Nitric oxide and neuronal death. *Nitric oxide : biology and chemistry / official journal of the Nitric Oxide Society* 23: 153-165.
322. Saha RN, Pahan K (2006) Regulation of inducible nitric oxide synthase gene in glial

- cells. *Antioxidants & redox signaling* 8: 929-947.
323. Pannu R, Singh I (2006) Pharmacological strategies for the regulation of inducible nitric oxide synthase: neurodegenerative versus neuroprotective mechanisms. *Neurochemistry international* 49: 170-182.
 324. Lee J, Ryu H, Kowall NW (2009) Differential regulation of neuronal and inducible nitric oxide synthase (NOS) in the spinal cord of mutant SOD1 (G93A) ALS mice. *Biochemical and biophysical research communications* 387: 202-206.
 325. Lowenstein CJ, Padalko E (2004) iNOS (NOS2) at a glance. *Journal of cell science* 117: 2865-2867.
 326. Martin LJ, Liu Z, Chen K, Price AC, Pan Y, et al. (2007) Motor neuron degeneration in amyotrophic lateral sclerosis mutant superoxide dismutase-1 transgenic mice: mechanisms of mitochondriopathy and cell death. *The Journal of comparative neurology* 500: 20-46.
 327. Phul RK, Shaw PJ, Ince PG, Smith ME (2000) Expression of nitric oxide synthase isoforms in spinal cord in amyotrophic lateral sclerosis. *Amyotrophic lateral sclerosis and other motor neuron disorders : official publication of the World Federation of Neurology, Research Group on Motor Neuron Diseases* 1: 259-267.
 328. Chen K, Northington FJ, Martin LJ (2010) Inducible nitric oxide synthase is present in motor neuron mitochondria and Schwann cells and contributes to disease mechanisms in ALS mice. *Brain structure & function* 214: 219-234.
 329. Sasaki S, Warita H, Abe K, Iwata M (2001) Inducible nitric oxide synthase (iNOS) and nitrotyrosine immunoreactivity in the spinal cords of transgenic mice with a G93A mutant SOD1 gene. *Journal of neuropathology and experimental neurology* 60: 839-846.
 330. Kiaei M, Kipiani K, Chen J, Calingasan NY, Beal MF (2005) Peroxisome proliferator-activated receptor-gamma agonist extends survival in transgenic mouse model of amyotrophic lateral sclerosis. *Experimental neurology* 191: 331-336.
 331. Martin LJ (2010) Mitochondrial pathobiology in Parkinson's disease and amyotrophic lateral sclerosis. *Journal of Alzheimer's disease : JAD* 20 Suppl 2: S335-356.
 332. Martin LJ (2010) Mitochondrial and Cell Death Mechanisms in Neurodegenerative Diseases. *Pharmaceuticals (Basel)* 3: 839-915.
 333. Hess DT, Matsumoto A, Kim S-O, Marshall HE, Stamler JS (2005) Protein S-nitrosylation: purview and parameters. *Nature reviews Molecular cell biology* 6: 150-166.
 334. Hara MR, Snyder SH (2007) Cell signaling and neuronal death. *Annual review of pharmacology and toxicology* 47: 117-141.
 335. Gu Z, Kaul M, Yan B, Kridel SJ, Cui J, et al. (2002) S-nitrosylation of matrix metalloproteinases: signaling pathway to neuronal cell death. *Science (New York, N Y)* 297: 1186-1190.
 336. Yao D, Gu Z, Nakamura T, Shi Z-Q, Ma Y, et al. (2004) Nitrosative stress linked to sporadic Parkinson's disease: S-nitrosylation of parkin regulates its E3 ubiquitin ligase activity. *Proceedings of the National Academy of Sciences of the United States of America* 101: 10810-10814.
 337. Wagner SRt, Lanier WL (1994) Metabolism of glucose, glycogen, and high-energy

- phosphates during complete cerebral ischemia. A comparison of normoglycemic, chronically hyperglycemic diabetic, and acutely hyperglycemic nondiabetic rats. *Anesthesiology* 81: 1516-1526.
338. Dirnagl U, Iadecola C, Moskowitz MA (1999) Pathobiology of ischaemic stroke: an integrated view. *Trends in neurosciences* 22: 391-397.
 339. Maiti P, Singh SB, Ilavazhagan G (2010) Nitric oxide system is involved in hypobaric hypoxia-induced oxidative stress in rat brain. *Acta histochemica* 112: 222-232.
 340. Kumar A, Mittal R, Khanna HD, Basu S (2008) Free radical injury and blood-brain barrier permeability in hypoxic-ischemic encephalopathy. *Pediatrics* 122: e722-727.
 341. Rodrigo J, Fernandez AP, Serrano J, Peinado MA, Martinez A (2005) The role of free radicals in cerebral hypoxia and ischemia. *Free radical biology & medicine* 39: 26-50.
 342. Holtz ML, Craddock SD, Pettigrew LC (2001) Rapid expression of neuronal and inducible nitric oxide synthases during post-ischemic reperfusion in rat brain. *Brain research* 898: 49-60.
 343. Huang Z, Huang PL, Ma J, Meng W, Ayata C, et al. (1996) Enlarged infarcts in endothelial nitric oxide synthase knockout mice are attenuated by nitro-L-arginine. *Journal of cerebral blood flow and metabolism : official journal of the International Society of Cerebral Blood Flow and Metabolism* 16: 981-987.
 344. Murphy S (2000) Production of nitric oxide by glial cells: regulation and potential roles in the CNS. *Glia* 29: 1-13.
 345. Forster C, Clark HB, Ross ME, Iadecola C (1999) Inducible nitric oxide synthase expression in human cerebral infarcts. *Acta Neuropathol* 97: 215-220.
 346. Lerouet D, Beray-Berthet V, Palmier B, Plotkine M, Margail I (2002) Changes in oxidative stress, iNOS activity and neutrophil infiltration in severe transient focal cerebral ischemia in rats. *Brain research* 958: 166-175.
 347. Zhu DY, Deng Q, Yao HH, Wang DC, Deng Y, et al. (2002) Inducible nitric oxide synthase expression in the ischemic core and penumbra after transient focal cerebral ischemia in mice. *Life Sci* 71: 1985-1996.
 348. Schroeter M, Kury P, Jander S (2003) Inflammatory gene expression in focal cortical brain ischemia: differences between rats and mice. *Brain Res Mol Brain Res* 117: 1-7.
 349. Lopez-Figueroa MO, Day HE, Lee S, Rivier C, Akil H, et al. (2000) Temporal and anatomical distribution of nitric oxide synthase mRNA expression and nitric oxide production during central nervous system inflammation. *Brain research* 852: 239-246.
 350. Matrone C, Pignataro G, Molinaro P, Irace C, Scorziello A, et al. (2004) HIF-1alpha reveals a binding activity to the promoter of iNOS gene after permanent middle cerebral artery occlusion. *Journal of neurochemistry* 90: 368-378.
 351. Ezquer ME, Valdez SR, Seltzer AM (2006) Inflammatory responses of the substantia nigra after acute hypoxia in neonatal rats. *Experimental neurology* 197: 391-398.
 352. Parmentier S, Bohme GA, Lerouet D, Damour D, Stutzmann JM, et al. (1999) Selective inhibition of inducible nitric oxide synthase prevents ischaemic brain injury. *British journal of pharmacology* 127: 546-552.

353. Iadecola C, Ross ME (1997) Molecular pathology of cerebral ischemia: delayed gene expression and strategies for neuroprotection. *Annals of the New York Academy of Sciences* 835: 203-217.
354. Parmentier-Batteur S, Bohme GA, Lerouet D, Zhou-Ding L, Beray V, et al. (2001) Antisense oligodeoxynucleotide to inducible nitric oxide synthase protects against transient focal cerebral ischemia-induced brain injury. *Journal of cerebral blood flow and metabolism : official journal of the International Society of Cerebral Blood Flow and Metabolism* 21: 15-21.
355. Loihl AK, Whalen S, Campbell IL, Mudgett JS, Murphy S (1999) Transcriptional activation following cerebral ischemia in mice of a promoter-deleted nitric oxide synthase-2 gene. *J Biol Chem* 274: 8844-8849.
356. Iadecola C, Zhang F, Casey R, Nagayama M, Ross ME (1997) Delayed reduction of ischemic brain injury and neurological deficits in mice lacking the inducible nitric oxide synthase gene. *J Neurosci* 17: 9157-9164.
357. Egea J, Martin-de-Saavedra MD, Parada E, Romero A, Del Barrio L, et al. (2012) Galantamine elicits neuroprotection by inhibiting iNOS, NADPH oxidase and ROS in hippocampal slices stressed with anoxia/reoxygenation. *Neuropharmacology* 62: 1082-1090.
358. Chang C-C, Wang Y-H, Chern C-M, Liou K-T, Hou Y-C, et al. (2011) Prodigiosin inhibits gp91(phox) and iNOS expression to protect mice against the oxidative/nitrosative brain injury induced by hypoxia-ischemia. *Toxicology and applied pharmacology* 257: 137-147.
359. Chern C-M, Liou K-T, Wang Y-H, Liao J-F, Yen J-C, et al. (2011) Andrographolide inhibits PI3K/AKT-dependent NOX2 and iNOS expression protecting mice against hypoxia/ischemia-induced oxidative brain injury. *Planta medica* 77: 1669-1679.
360. Lu Q, Xia N, Xu H, Guo L, Wenzel P, et al. (2011) Betulinic acid protects against cerebral ischemia-reperfusion injury in mice by reducing oxidative and nitrosative stress. *Nitric oxide : biology and chemistry / official journal of the Nitric Oxide Society* 24: 132-138.
361. Srivastava AK, Kalita J, Dohare P, Ray M, Misra UK (2009) Studies of free radical generation by neurons in a rat model of cerebral venous sinus thrombosis. *Neuroscience letters* 450: 127-131.
362. Bolanos JP, Herrero-Mendez A, Fernandez-Fernandez S, Almeida A (2007) Linking glycolysis with oxidative stress in neural cells: a regulatory role for nitric oxide. *Biochemical Society transactions* 35: 1224-1227.
363. Li S, Wang W, Wang C, Tang Y-Y (2010) Possible involvement of NO/NOS signaling in hippocampal amyloid-beta production induced by transient focal cerebral ischemia in aged rats. *Neuroscience letters* 470: 106-110.
364. Pei DS, Sun YF, Song YJ (2009) S-nitrosylation of PTEN Involved in ischemic brain injury in rat hippocampal CA1 region. *Neurochem Res* 34: 1507-1512.
365. Chen SC, Huang B, Liu YC, Shyu KG, Lin PY, et al. (2008) Acute hypoxia enhances proteins' S-nitrosylation in endothelial cells. *Biochem Biophys Res Commun* 377: 1274-1278.
366. Thuerauf DJ, Marcinko M, Gude N, Rubio M, Sussman MA, et al. (2006) Activation of the unfolded protein response in infarcted mouse heart and hypoxic cultured

- cardiac myocytes. *Circulation research* 99: 275-282.
367. Okada K-i, Minamino T, Tsukamoto Y, Liao Y, Tsukamoto O, et al. (2004) Prolonged endoplasmic reticulum stress in hypertrophic and failing heart after aortic constriction: possible contribution of endoplasmic reticulum stress to cardiac myocyte apoptosis. *Circulation* 110: 705-712.
 368. Myoishi M, Hao H, Minamino T, Watanabe K, Nishihira K, et al. (2007) Increased endoplasmic reticulum stress in atherosclerotic plaques associated with acute coronary syndrome. *Circulation* 116: 1226-1233.
 369. Dickhout JG, Colgan SM, Lhotak S, Austin RC (2007) Increased endoplasmic reticulum stress in atherosclerotic plaques associated with acute coronary syndrome: a balancing act between plaque stability and rupture. *Circulation* 116: 1214-1216.
 370. Tian F, Zhou X, Wikstrom J, Karlsson H, Sjolund H, et al. (2009) Protein disulfide isomerase increases in myocardial endothelial cells in mice exposed to chronic hypoxia: a stimulatory role in angiogenesis. *American journal of physiology Heart and circulatory physiology* 297: H1078-1086.
 371. Graven KK, Molvar C, Roncarati JS, Klahn BD, Lowrey S, et al. (2002) Identification of protein disulfide isomerase as an endothelial hypoxic stress protein. *American journal of physiology Lung cellular and molecular physiology* 282: L996-1003.
 372. Severino A, Campioni M, Straino S, Salloum FN, Schmidt N, et al. (2007) Identification of protein disulfide isomerase as a cardiomyocyte survival factor in ischemic cardiomyopathy. *Journal of the American College of Cardiology* 50: 1029-1037.
 373. Ko HS, Uehara T, Nomura Y (2002) Role of ubiquilin associated with protein-disulfide isomerase in the endoplasmic reticulum in stress-induced apoptotic cell death. *The Journal of biological chemistry* 277: 35386-35392.
 374. Tanaka S, Uehara T, Nomura Y (2000) Up-regulation of protein-disulfide isomerase in response to hypoxia/brain ischemia and its protective effect against apoptotic cell death. *The Journal of biological chemistry* 275: 10388-10393.
 375. Hwang IK, Yoo K-Y, Kim DW, Han BH, Kang T-C, et al. (2005) Protein disulfide isomerase immunoreactivity and protein level changes in neurons and astrocytes in the gerbil hippocampal CA1 region following transient ischemia. *Neuroscience letters* 375: 117-122.
 376. DeGracia DJ, Montie HL (2004) Cerebral ischemia and the unfolded protein response. *Journal of neurochemistry* 91: 1-8.
 377. Nardai G, Stadler K, Papp E, Korcsmaros T, Jakus J, et al. (2005) Diabetic changes in the redox status of the microsomal protein folding machinery. *Biochemical and biophysical research communications* 334: 787-795.
 378. Hu BR, Janelidze S, Ginsberg MD, Busto R, Perez-Pinzon M, et al. (2001) Protein aggregation after focal brain ischemia and reperfusion. *Journal of cerebral blood flow and metabolism : official journal of the International Society of Cerebral Blood Flow and Metabolism* 21: 865-875.
 379. Hu BR, Martone ME, Jones YZ, Liu CL (2000) Protein aggregation after transient cerebral ischemia. *The Journal of neuroscience : the official journal of the Society for Neuroscience* 20: 3191-3199.

380. Liu C, Gao Y, Barrett J, Hu B (2010) Autophagy and protein aggregation after brain ischemia. *Journal of neurochemistry* 115: 68-78.
381. Liu CL, Ge P, Zhang F, Hu BR (2005) Co-translational protein aggregation after transient cerebral ischemia. *Neuroscience* 134: 1273-1284.
382. Zhang F, Liu CL, Hu BR (2006) Irreversible aggregation of protein synthesis machinery after focal brain ischemia. *Journal of neurochemistry* 98: 102-112.
383. DeGracia DJ, Rudolph J, Roberts GG, Rafols JA, Wang J (2007) Convergence of stress granules and protein aggregates in hippocampal cornu ammonis 1 at later reperfusion following global brain ischemia. *Neuroscience* 146: 562-572.
384. Chen X, Kintner DB, Baba A, Matsuda T, Shull GE, et al. (2010) Protein aggregation in neurons following OGD: a role for Na⁺ and Ca²⁺ ionic dysregulation. *Journal of neurochemistry* 112: 173-182.
385. Gregersen N, Bolund L, Bross P (2005) Protein misfolding, aggregation, and degradation in disease. *Molecular biotechnology* 31: 141-150.
386. Markossian KA, Kurganov BI (2004) Protein folding, misfolding, and aggregation. Formation of inclusion bodies and aggresomes. *Biochemistry Biokhimiia* 69: 971-984.
387. Kopito RR (2000) Aggresomes, inclusion bodies and protein aggregation. *Trends in cell biology* 10: 524-530.
388. Bukau B, Weissman J, Horwich A (2006) Molecular chaperones and protein quality control. *Cell* 125: 443-451.
389. Chaudhuri TK, Paul S (2006) Protein-misfolding diseases and chaperone-based therapeutic approaches. *The FEBS journal* 273: 1331-1349.
390. Liberek K, Lewandowska A, Zietkiewicz S (2008) Chaperones in control of protein disaggregation. *The EMBO journal* 27: 328-335.
391. Giffard RG, Xu L, Zhao H, Carrico W, Ouyang Y, et al. (2004) Chaperones, protein aggregation, and brain protection from hypoxic/ischemic injury. *The Journal of experimental biology* 207: 3213-3220.
392. Liu C, Chen S, Kamme F, Hu BR (2005) Ischemic preconditioning prevents protein aggregation after transient cerebral ischemia. *Neuroscience* 134: 69-80.
393. Ge P-F, Luo T-F, Zhang J-Z, Chen D-W, Luan Y-X, et al. (2008) Ischemic preconditioning induces chaperone hsp70 expression and inhibits protein aggregation in the CA1 neurons of rats. *Neuroscience bulletin* 24: 288-296.
394. Friedlander RM (2003) Apoptosis and caspases in neurodegenerative diseases. *N Engl J Med* 348: 1365-1375.
395. Barbeito LH, Pehar M, Cassina P, Vargas MR, Peluffo H, et al. (2004) A role for astrocytes in motor neuron loss in amyotrophic lateral sclerosis. *Brain Res Brain Res Rev* 47: 263-274.
396. Cleveland DW, Rothstein JD (2001) From Charcot to Lou Gehrig: deciphering selective motor neuron death in ALS. *Nat Rev Neurosci* 2: 806-819.
397. Andersen PM, Sims KB, Xin WW, Kiely R, O'Neill G, et al. (2003) Sixteen novel mutations in the Cu/Zn superoxide dismutase gene in amyotrophic lateral sclerosis: a decade of discoveries, defects and disputes. *Amyotroph Lateral Scler Other Motor Neuron Disord* 4: 62-73.
398. Cleveland DW (1999) From Charcot to SOD1: mechanisms of selective motor neuron death in ALS. *Neuron* 24: 515-520.

399. Ross CA, Poirier MA (2005) Opinion: What is the role of protein aggregation in neurodegeneration? *Nature reviews Molecular cell biology* 6: 891-898.
400. Kurahashi T, Miyazaki A, Suwan S, Isobe M (2001) Extensive investigations on oxidized amino acid residues in H₂O₂-treated Cu,Zn-SOD protein with LC-ESI-Q-TOF-MS, MS/MS for the determination of the copper-binding site. *Journal of the American Chemical Society* 123: 9268-9278.
401. Di Noto L, Whitson LJ, Cao X, Hart PJ, Levine RL (2005) Proteasomal degradation of mutant superoxide dismutases linked to amyotrophic lateral sclerosis. *The Journal of biological chemistry* 280: 39907-39913.
402. Makmura L, Hamann M, Areopagita A, Furuta S, Munoz A, et al. (2001) Development of a sensitive assay to detect reversibly oxidized protein cysteine sulfhydryl groups. *Antioxidants & redox signaling* 3: 1105-1118.
403. Zhang F, Strom A-L, Fukada K, Lee S, Hayward LJ, et al. (2007) Interaction between familial amyotrophic lateral sclerosis (ALS)-linked SOD1 mutants and the dynein complex. *The Journal of biological chemistry* 282: 16691-16699.
404. Parge HE, Hallewell RA, Tainer JA (1992) Atomic structures of wild-type and thermostable mutant recombinant human Cu,Zn superoxide dismutase. *Proceedings of the National Academy of Sciences of the United States of America* 89: 6109-6113.
405. Jacob C, Holme AL, Fry FH (2004) The sulfinic acid switch in proteins. *Organic & biomolecular chemistry* 2: 1953-1956.
406. Urushitani M, Kurisu J, Tsukita K, Takahashi R (2002) Proteasomal inhibition by misfolded mutant superoxide dismutase 1 induces selective motor neuron death in familial amyotrophic lateral sclerosis. *Journal of neurochemistry* 83: 1030-1042.
407. Strom A-L, Shi P, Zhang F, Gal J, Kilty R, et al. (2008) Interaction of amyotrophic lateral sclerosis (ALS)-related mutant copper-zinc superoxide dismutase with the dynein-dynactin complex contributes to inclusion formation. *The Journal of biological chemistry* 283: 22795-22805.
408. Tiwari A, Xu Z, Hayward LJ (2005) Aberrantly increased hydrophobicity shared by mutants of Cu,Zn-superoxide dismutase in familial amyotrophic lateral sclerosis. *The Journal of biological chemistry* 280: 29771-29779.
409. Calabrese V, Cornelius C, Stella AMG, Calabrese EJ (2010) Cellular stress responses, mitostress and carnitine insufficiencies as critical determinants in aging and neurodegenerative disorders: role of hormesis and vitagenes. *Neurochemical research* 35: 1880-1915.
410. Krishnan U, Son M, Rajendran B, Elliott JL (2006) Novel mutations that enhance or repress the aggregation potential of SOD1. *Molecular and cellular biochemistry* 287: 201-211.
411. Son M, Puttaparthi K, Kawamata H, Rajendran B, Boyer PJ, et al. (2007) Overexpression of CCS in G93A-SOD1 mice leads to accelerated neurological deficits with severe mitochondrial pathology. *Proceedings of the National Academy of Sciences of the United States of America* 104: 6072-6077.
412. Deng H-X, Shi Y, Furukawa Y, Zhai H, Fu R, et al. (2006) Conversion to the amyotrophic lateral sclerosis phenotype is associated with intermolecular linked insoluble aggregates of SOD1 in mitochondria. *Proceedings of the National Academy of Sciences of the United States of America* 103: 7142-7147.

413. Goldsteins G, Keksa-Goldsteine V, Ahtoniemi T, Jaronen M, Arens E, et al. (2008) Deleterious role of superoxide dismutase in the mitochondrial intermembrane space. *The Journal of biological chemistry* 283: 8446-8452.
414. Ripps ME, Huntley GW, Hof PR, Morrison JH, Gordon JW (1995) Transgenic mice expressing an altered murine superoxide dismutase gene provide an animal model of amyotrophic lateral sclerosis. *Proceedings of the National Academy of Sciences of the United States of America* 92: 689-693.
415. Deng HX, Hentati A, Tainer JA, Iqbal Z, Cayabyab A, et al. (1993) Amyotrophic lateral sclerosis and structural defects in Cu,Zn superoxide dismutase. *Science (New York, N Y)* 261: 1047-1051.
416. Doucette PA, Whitson LJ, Cao X, Schirf V, Demeler B, et al. (2004) Dissociation of human copper-zinc superoxide dismutase dimers using chaotrope and reductant. Insights into the molecular basis for dimer stability. *The Journal of biological chemistry* 279: 54558-54566.
417. Lyles MM, Gilbert HF (1991) Catalysis of the oxidative folding of ribonuclease A by protein disulfide isomerase: dependence of the rate on the composition of the redox buffer. *Biochemistry* 30: 613-619.
418. Conn KJ, Gao W, McKee A, Lan MS, Ullman MD, et al. (2004) Identification of the protein disulfide isomerase family member PDIP in experimental Parkinson's disease and Lewy body pathology. *Brain research* 1022: 164-172.
419. Rao RV, Bredesen DE (2004) Misfolded proteins, endoplasmic reticulum stress and neurodegeneration. *Current opinion in cell biology* 16: 653-662.
420. Hetz C, Russelakis-Carneiro M, Walchli S, Carboni S, Vial-Knecht E, et al. (2005) The disulfide isomerase Grp58 is a protective factor against prion neurotoxicity. *The Journal of neuroscience : the official journal of the Society for Neuroscience* 25: 2793-2802.
421. Uehara T, Nakamura T, Yao D, Shi Z-Q, Gu Z, et al. (2006) S-nitrosylated protein-disulphide isomerase links protein misfolding to neurodegeneration. *Nature* 441: 513-517.
422. Nakamura T, Lipton SA (2010) Preventing Ca²⁺-mediated nitrosative stress in neurodegenerative diseases: possible pharmacological strategies. *Cell calcium* 47: 190-197.
423. De Palma C, Falcone S, Panzeri C, Radice S, Bassi MT, et al. (2008) Endothelial nitric oxide synthase overexpression by neuronal cells in neurodegeneration: a link between inflammation and neuroprotection. *Journal of neurochemistry* 106: 193-204.
424. Uehara T (2007) Accumulation of misfolded protein through nitrosative stress linked to neurodegenerative disorders. *Antioxidants & redox signaling* 9: 597-601.
425. Arciello M, Capo CR, Cozzolino M, Ferri A, Nencini M, et al. (2010) Inactivation of cytochrome c oxidase by mutant SOD1s in mouse motoneuronal NSC-34 cells is independent from copper availability but is because of nitric oxide. *Journal of neurochemistry* 112: 183-192.
426. Beers DR, Zhao W, Liao B, Kano O, Wang J, et al. (2011) Neuroinflammation modulates distinct regional and temporal clinical responses in ALS mice. *Brain, behavior, and immunity* 25: 1025-1035.
427. Glass CK, Saijo K, Winner B, Marchetto MC, Gage FH (2010) Mechanisms

- underlying inflammation in neurodegeneration. *Cell* 140: 918-934.
428. McGeer PL, McGeer EG (2002) Inflammatory processes in amyotrophic lateral sclerosis. *Muscle & nerve* 26: 459-470.
 429. Di Giorgio FP, Carrasco MA, Siao MC, Maniatis T, Eggan K (2007) Non-cell autonomous effect of glia on motor neurons in an embryonic stem cell-based ALS model. *Nature neuroscience* 10: 608-614.
 430. Yamanaka K, Chun SJ, Boillee S, Fujimori-Tonou N, Yamashita H, et al. (2008) Astrocytes as determinants of disease progression in inherited amyotrophic lateral sclerosis. *Nature neuroscience* 11: 251-253.
 431. Bal-Price A, Brown GC (2001) Inflammatory neurodegeneration mediated by nitric oxide from activated glia-inhibiting neuronal respiration, causing glutamate release and excitotoxicity. *The Journal of neuroscience : the official journal of the Society for Neuroscience* 21: 6480-6491.
 432. Brown GC, Bal-Price A (2003) Inflammatory neurodegeneration mediated by nitric oxide, glutamate, and mitochondria. *Molecular neurobiology* 27: 325-355.
 433. Ludolph AC, Bendotti C, Blaugrund E, Chio A, Greensmith L, et al. (2010) Guidelines for preclinical animal research in ALS/MND: A consensus meeting. *Amyotrophic lateral sclerosis : official publication of the World Federation of Neurology Research Group on Motor Neuron Diseases* 11: 38-45.
 434. Lobsiger CS, Boillee S, McAlonis-Downes M, Khan AM, Feltri ML, et al. (2009) Schwann cells expressing dismutase active mutant SOD1 unexpectedly slow disease progression in ALS mice. *Proceedings of the National Academy of Sciences of the United States of America* 106: 4465-4470.
 435. Liu J, Shinobu LA, Ward CM, Young D, Cleveland DW (2005) Elevation of the Hsp70 chaperone does not effect toxicity in mouse models of familial amyotrophic lateral sclerosis. *Journal of neurochemistry* 93: 875-882.
 436. Schutz B, Reimann J, Dumitrescu-Ozimek L, Kappes-Horn K, Landreth GE, et al. (2005) The oral antidiabetic pioglitazone protects from neurodegeneration and amyotrophic lateral sclerosis-like symptoms in superoxide dismutase-G93A transgenic mice. *The Journal of neuroscience : the official journal of the Society for Neuroscience* 25: 7805-7812.
 437. Matsumoto A, Okada Y, Nakamichi M, Nakamura M, Toyama Y, et al. (2006) Disease progression of human SOD1 (G93A) transgenic ALS model rats. *Journal of neuroscience research* 83: 119-133.
 438. Turner BJ, Atkin JD, Farg MA, Zang DW, Rembach A, et al. (2005) Impaired extracellular secretion of mutant superoxide dismutase 1 associates with neurotoxicity in familial amyotrophic lateral sclerosis. *The Journal of neuroscience : the official journal of the Society for Neuroscience* 25: 108-117.
 439. Lee J, Ryu H, Ferrante RJ, Morris SM, Jr., Ratan RR (2003) Translational control of inducible nitric oxide synthase expression by arginine can explain the arginine paradox. *Proceedings of the National Academy of Sciences of the United States of America* 100: 4843-4848.
 440. Heneka MT, Feinstein DL (2001) Expression and function of inducible nitric oxide synthase in neurons. *Journal of neuroimmunology* 114: 8-18.
 441. Mungrue IN, Bredt DS, Stewart DJ, Husain M (2003) From molecules to mammals: what's NOS got to do with it? *Acta physiologica Scandinavica* 179: 123-135.

442. Jaffrey SR, Erdjument-Bromage H, Ferris CD, Tempst P, Snyder SH (2001) Protein S-nitrosylation: a physiological signal for neuronal nitric oxide. *Nature cell biology* 3: 193-197.
443. Nathan C, Calingasan N, Nezezon J, Ding A, Lucia MS, et al. (2005) Protection from Alzheimer's-like disease in the mouse by genetic ablation of inducible nitric oxide synthase. *The Journal of experimental medicine* 202: 1163-1169.
444. Dehmer T, Lindenau J, Haid S, Dichgans J, Schulz JB (2000) Deficiency of inducible nitric oxide synthase protects against MPTP toxicity in vivo. *Journal of neurochemistry* 74: 2213-2216.
445. Pruss H, Prass K, Ghaeni L, Milosevic M, Muselmann C, et al. (2008) Inducible nitric oxide synthase does not mediate brain damage after transient focal cerebral ischemia in mice. *Journal of cerebral blood flow and metabolism : official journal of the International Society of Cerebral Blood Flow and Metabolism* 28: 526-539.
446. Almer G, Vukosavic S, Romero N, Przedborski S (1999) Inducible nitric oxide synthase up-regulation in a transgenic mouse model of familial amyotrophic lateral sclerosis. *Journal of neurochemistry* 72: 2415-2425.
447. Sasaki S, Shibata N, Iwata M (2001) Neuronal nitric oxide synthase immunoreactivity in the spinal cord in amyotrophic lateral sclerosis. *Acta neuropathologica* 101: 351-357.
448. Garthwaite J, Boulton CL (1995) Nitric oxide signaling in the central nervous system. *Annual review of physiology* 57: 683-706.
449. Calabrese V, Bates TE, Stella AM (2000) NO synthase and NO-dependent signal pathways in brain aging and neurodegenerative disorders: the role of oxidant/antioxidant balance. *Neurochemical research* 25: 1315-1341.
450. Brown GC, Cooper CE (1994) Nanomolar concentrations of nitric oxide reversibly inhibit synaptosomal respiration by competing with oxygen at cytochrome oxidase. *FEBS letters* 356: 295-298.
451. Jekabsone A, Neher JJ, Borutaite V, Brown GC (2007) Nitric oxide from neuronal nitric oxide synthase sensitises neurons to hypoxia-induced death via competitive inhibition of cytochrome oxidase. *Journal of neurochemistry* 103: 346-356.
452. Golde S, Chandran S, Brown GC, Compston A (2002) Different pathways for iNOS-mediated toxicity in vitro dependent on neuronal maturation and NMDA receptor expression. *Journal of neurochemistry* 82: 269-282.
453. Isaacs AM, Senn DB, Yuan M, Shine JP, Yankner BA (2006) Acceleration of amyloid beta-peptide aggregation by physiological concentrations of calcium. *The Journal of biological chemistry* 281: 27916-27923.
454. Hara MR, Agrawal N, Kim SF, Cascio MB, Fujimuro M, et al. (2005) S-nitrosylated GAPDH initiates apoptotic cell death by nuclear translocation following Siah1 binding. *Nature cell biology* 7: 665-674.
455. Ahtoniemi T, Jaronen M, Keksa-Goldsteine V, Goldsteins G, Koistinaho J (2008) Mutant SOD1 from spinal cord of G93A rats is destabilized and binds to inner mitochondrial membrane. *Neurobiology of disease* 32: 479-485.
456. Niwa J-i, Yamada S-i, Ishigaki S, Sone J, Takahashi M, et al. (2007) Disulfide bond mediates aggregation, toxicity, and ubiquitylation of familial amyotrophic lateral sclerosis-linked mutant SOD1. *The Journal of biological chemistry* 282: 28087-28095.

457. Honjo Y, Kaneko S, Ito H, Horibe T, Nagashima M, et al. (2011) Protein disulfide isomerase-immunopositive inclusions in patients with amyotrophic lateral sclerosis. *Amyotrophic lateral sclerosis : official publication of the World Federation of Neurology Research Group on Motor Neuron Diseases* 12: 444-450.
458. Noiva R (1999) Protein disulfide isomerase: the multifunctional redox chaperone of the endoplasmic reticulum. *Seminars in cell & developmental biology* 10: 481-493.
459. Lee S-O, Cho K, Cho S, Kim I, Oh C, et al. (2010) Protein disulphide isomerase is required for signal peptide peptidase-mediated protein degradation. *The EMBO journal* 29: 363-375.
460. Moore P, Bernardi KM, Tsai B (2010) The Ero1alpha-PDI redox cycle regulates retro-translocation of cholera toxin. *Molecular biology of the cell* 21: 1305-1313.
461. Zhang K, Kaufman RJ (2006) The unfolded protein response: a stress signaling pathway critical for health and disease. *Neurology* 66: S102-109.
462. Xu W, Liu L, Charles IG, Moncada S (2004) Nitric oxide induces coupling of mitochondrial signalling with the endoplasmic reticulum stress response. *Nature cell biology* 6: 1129-1134.
463. Gotoh T, Mori M (2006) Nitric oxide and endoplasmic reticulum stress. *Arteriosclerosis, thrombosis, and vascular biology* 26: 1439-1446.
464. He J, Kang H, Yan F, Chen C (2004) The endoplasmic reticulum-related events in S-nitrosoglutathione-induced neurotoxicity in cerebellar granule cells. *Brain research* 1015: 25-33.
465. Aquilano K, Rotilio G, Ciriolo MR (2003) Proteasome activation and nNOS down-regulation in neuroblastoma cells expressing a Cu,Zn superoxide dismutase mutant involved in familial ALS. *J Neurochem* 85: 1324-1335.
466. Qu XW, Wang H, De Plaen IG, Rozenfeld RA, Hsueh W (2001) Neuronal nitric oxide synthase (NOS) regulates the expression of inducible NOS in rat small intestine via modulation of nuclear factor kappa B. *FASEB J* 15: 439-446.
467. Porras M, Martin MT, Torres R, Vergara P (2006) Cyclical upregulated iNOS and long-term downregulated nNOS are the bases for relapse and quiescent phases in a rat model of IBD. *Am J Physiol Gastrointest Liver Physiol* 290: G423-430.
468. Farkas O, Povlishock JT (2007) Cellular and subcellular change evoked by diffuse traumatic brain injury: a complex web of change extending far beyond focal damage. *Progress in brain research* 161: 43-59.
469. Greve MW, Zink BJ (2009) Pathophysiology of traumatic brain injury. *The Mount Sinai journal of medicine, New York* 76: 97-104.
470. Shih AY, Johnson DA, Wong G, Kraft AD, Jiang L, et al. (2003) Coordinate regulation of glutathione biosynthesis and release by Nrf2-expressing glia potently protects neurons from oxidative stress. *The Journal of neuroscience : the official journal of the Society for Neuroscience* 23: 3394-3406.
471. Sagara JI, Miura K, Bannai S (1993) Maintenance of neuronal glutathione by glial cells. *Journal of neurochemistry* 61: 1672-1676.
472. Cherian L, Goodman JC, Robertson CS (2000) Brain nitric oxide changes after controlled cortical impact injury in rats. *Journal of neurophysiology* 83: 2171-2178.
473. Iadecola C, Zhang F, Casey R, Nagayama M, Ross ME (1997) Delayed reduction of

- ischemic brain injury and neurological deficits in mice lacking the inducible nitric oxide synthase gene. *The Journal of neuroscience : the official journal of the Society for Neuroscience* 17: 9157-9164.
474. Loihl AK, Whalen S, Campbell IL, Mudgett JS, Murphy S (1999) Transcriptional activation following cerebral ischemia in mice of a promoter-deleted nitric oxide synthase-2 gene. *The Journal of biological chemistry* 274: 8844-8849.
475. Gibson CL, Coughlan TC, Murphy SP (2005) Glial nitric oxide and ischemia. *Glia* 50: 417-426.
476. Zhu D-Y, Deng Q, Yao H-H, Wang D-C, Deng Y, et al. (2002) Inducible nitric oxide synthase expression in the ischemic core and penumbra after transient focal cerebral ischemia in mice. *Life sciences* 71: 1985-1996.
477. DeGracia DJ, Hu BR (2007) Irreversible translation arrest in the reperfused brain. *Journal of cerebral blood flow and metabolism : official journal of the International Society of Cerebral Blood Flow and Metabolism* 27: 875-893.
478. Groenendyk J, Michalak M (2005) Endoplasmic reticulum quality control and apoptosis. *Acta biochimica Polonica* 52: 381-395.
479. Hershko A, Ciechanover A (1998) The ubiquitin system. *Annual review of biochemistry* 67: 425-479.
480. Hu J, Castets F, Guevara JL, Van Eldik LJ (1996) S100 beta stimulates inducible nitric oxide synthase activity and mRNA levels in rat cortical astrocytes. *The Journal of biological chemistry* 271: 2543-2547.
481. Beck J, Lenart B, Kintner DB, Sun D (2003) Na-K-Cl cotransporter contributes to glutamate-mediated excitotoxicity. *The Journal of neuroscience : the official journal of the Society for Neuroscience* 23: 5061-5068.
482. Sofroniew MV (2009) Molecular dissection of reactive astrogliosis and glial scar formation. *Trends in neurosciences* 32: 638-647.
483. Sofroniew MV, Vinters HV (2010) Astrocytes: biology and pathology. *Acta neuropathologica* 119: 7-35.
484. Rothwell NJ, Relton JK (1993) Involvement of cytokines in acute neurodegeneration in the CNS. *Neuroscience and biobehavioral reviews* 17: 217-227.
485. Galea E, Feinstein DL, Reis DJ (1992) Induction of calcium-independent nitric oxide synthase activity in primary rat glial cultures. *Proceedings of the National Academy of Sciences of the United States of America* 89: 10945-10949.
486. Simmons ML, Murphy S (1993) Cytokines regulate L-arginine-dependent cyclic GMP production in rat glial cells. *The European journal of neuroscience* 5: 825-831.
487. Simmons ML, Murphy S (1992) Induction of nitric oxide synthase in glial cells. *Journal of neurochemistry* 59: 897-905.
488. Schroeter M, Kury P, Jander S (2003) Inflammatory gene expression in focal cortical brain ischemia: differences between rats and mice. *Brain research Molecular brain research* 117: 1-7.
489. Moro MA, Cardenas A, Hurtado O, Leza JC, Lizasoain I (2004) Role of nitric oxide after brain ischaemia. *Cell calcium* 36: 265-275.
490. Ge P, Luo Y, Liu CL, Hu B (2007) Protein aggregation and proteasome dysfunction after brain ischemia. *Stroke; a journal of cerebral circulation* 38: 3230-3236.

491. Chung RS, Penkowa M, Dittmann J, King CE, Bartlett C, et al. (2008) Redefining the role of metallothionein within the injured brain: extracellular metallothioneins play an important role in the astrocyte-neuron response to injury. *The Journal of biological chemistry* 283: 15349-15358.
492. Leung YKJ, Pankhurst M, Dunlop SA, Ray S, Dittmann J, et al. (2010) Metallothionein induces a regenerative reactive astrocyte phenotype via JAK/STAT and RhoA signalling pathways. *Experimental neurology* 221: 98-106.
493. Tsuru-Aoyagi K, Potts MB, Trivedi A, Pfankuch T, Raber J, et al. (2009) Glutathione peroxidase activity modulates recovery in the injured immature brain. *Annals of neurology* 65: 540-549.
494. Sugawara T, Chan PH (2003) Reactive oxygen radicals and pathogenesis of neuronal death after cerebral ischemia. *Antioxidants & redox signaling* 5: 597-607.
495. Wilson JX (1997) Antioxidant defense of the brain: a role for astrocytes. *Canadian journal of physiology and pharmacology* 75: 1149-1163.
496. Chan PH, Kawase M, Murakami K, Chen SF, Li Y, et al. (1998) Overexpression of SOD1 in transgenic rats protects vulnerable neurons against ischemic damage after global cerebral ischemia and reperfusion. *The Journal of neuroscience : the official journal of the Society for Neuroscience* 18: 8292-8299.
497. Pineda JA, Aono M, Sheng H, Lynch J, Wellons JC, et al. (2001) Extracellular superoxide dismutase overexpression improves behavioral outcome from closed head injury in the mouse. *Journal of neurotrauma* 18: 625-634.
498. Zemlyak I, Nimon V, Brooke S, Moore T, McLaughlin J, et al. (2006) Gene therapy in the nervous system with superoxide dismutase. *Brain research* 1088: 12-18.
499. Zheng Q, Li J, Wang X (2009) Interplay between the ubiquitin-proteasome system and autophagy in proteinopathies. *International journal of physiology, pathophysiology and pharmacology* 1: 127-142.
500. Adibhatla RM, Hatcher JF (2010) Lipid oxidation and peroxidation in CNS health and disease: from molecular mechanisms to therapeutic opportunities. *Antioxid Redox Signal* 12: 125-169.
501. Bochkov VN, Oskolkova OV, Birukov KG, Levonen AL, Binder CJ, et al. (2010) Generation and biological activities of oxidized phospholipids. *Antioxid Redox Signal* 12: 1009-1059.
502. Sedelnikova OA, Redon CE, Dickey JS, Nakamura AJ, Georgakilas AG, et al. (2010) Role of oxidatively induced DNA lesions in human pathogenesis. *Mutat Res* 704: 152-159.
503. Ferrari R, Guardigli G, Mele D, Percoco GF, Ceconi C, et al. (2004) Oxidative stress during myocardial ischaemia and heart failure. *Current pharmaceutical design* 10: 1699-1711.
504. Davies MJ (2005) The oxidative environment and protein damage. *Biochimica et biophysica acta* 1703: 93-109.
505. Berlett BS, Stadtman ER (1997) Protein oxidation in aging, disease, and oxidative stress. *The Journal of biological chemistry* 272: 20313-20316.
506. Dalle-Donne I, Aldini G, Carini M, Colombo R, Rossi R, et al. (2006) Protein carbonylation, cellular dysfunction, and disease progression. *Journal of cellular and molecular medicine* 10: 389-406.

507. Levine RL, Williams JA, Stadtman ER, Shacter E (1994) Carbonyl assays for determination of oxidatively modified proteins. *Methods in enzymology* 233: 346-357.
508. Smith MA, Sayre LM, Anderson VE, Harris PL, Beal MF, et al. (1998) Cytochemical demonstration of oxidative damage in Alzheimer disease by immunochemical enhancement of the carbonyl reaction with 2,4-dinitrophenylhydrazine. *The journal of histochemistry and cytochemistry : official journal of the Histochemistry Society* 46: 731-735.
509. Korolainen MA, Nyman TA, Nyysönen P, Hartikainen ES, Pirttilä T (2007) Multiplexed proteomic analysis of oxidation and concentrations of cerebrospinal fluid proteins in Alzheimer disease. *Clinical chemistry* 53: 657-665.
510. Tyedmers J, Mogk A, Bukau B (2010) Cellular strategies for controlling protein aggregation. *Nat Rev Mol Cell Biol* 11: 777-788.
511. Klein WL, Stine WB, Jr., Teplow DB (2004) Small assemblies of unmodified amyloid beta-protein are the proximate neurotoxin in Alzheimer's disease. *Neurobiology of aging* 25: 569-580.
512. Roy S, Zhang B, Lee VMY, Trojanowski JQ (2005) Axonal transport defects: a common theme in neurodegenerative diseases. *Acta neuropathologica* 109: 5-13.
513. Williams A (2002) Defining neurodegenerative diseases. *BMJ (Clinical research ed)* 324: 1465-1466.
514. Lee BH, Lee MJ, Park S, Oh DC, Elsassner S, et al. (2010) Enhancement of proteasome activity by a small-molecule inhibitor of USP14. *Nature* 467: 179-184.
515. Jung T, Catalgol B, Grune T (2009) The proteasomal system. *Molecular aspects of medicine* 30: 191-296.
516. Seifert U, Bialy LP, Ebstein F, Bech-Otschir D, Voigt A, et al. (2010) Immunoproteasomes preserve protein homeostasis upon interferon-induced oxidative stress. *Cell* 142: 613-624.
517. Ciechanover A, Brundin P (2003) The ubiquitin proteasome system in neurodegenerative diseases: sometimes the chicken, sometimes the egg. *Neuron* 40: 427-446.
518. Dahlmann B (2007) Role of proteasomes in disease. *BMC Biochem* 8 Suppl 1: S3.
519. Nakamura T, Lipton SA (2011) Redox modulation by S-nitrosylation contributes to protein misfolding, mitochondrial dynamics, and neuronal synaptic damage in neurodegenerative diseases. *Cell Death Differ* 18: 1478-1486.
520. Nakamura T, Lipton SA (2011) S-nitrosylation of critical protein thiols mediates protein misfolding and mitochondrial dysfunction in neurodegenerative diseases. *Antioxid Redox Signal* 14: 1479-1492.
521. Calabrese V, Mancuso C, Calvani M, Rizzarelli E, Butterfield DA, et al. (2007) Nitric oxide in the central nervous system: neuroprotection versus neurotoxicity. *Nat Rev Neurosci* 8: 766-775.
522. Nakamura T, Lipton SA (2007) S-Nitrosylation and uncompetitive/fast off-rate (UFO) drug therapy in neurodegenerative disorders of protein misfolding. *Cell Death Differ* 14: 1305-1314.
523. Vabulas RM, Raychaudhuri S, Hayer-Hartl M, Hartl FU (2010) Protein folding in the cytoplasm and the heat shock response. *Cold Spring Harb Perspect Biol* 2:

- a004390.
524. Dantuma NP, Lindsten K (2010) Stressing the ubiquitin-proteasome system. *Cardiovasc Res* 85: 263-271.
 525. Winklhofer KF, Tatzelt J, Haass C (2008) The two faces of protein misfolding: gain- and loss-of-function in neurodegenerative diseases. *EMBO J* 27: 336-349.
 526. Meng F, Yao D, Shi Y, Kabakoff J, Wu W, et al. (2011) Oxidation of the cysteine-rich regions of parkin perturbs its E3 ligase activity and contributes to protein aggregation. *Mol Neurodegener* 6: 34.
 527. Ge P, Luo Y, Liu CL, Hu B (2007) Protein aggregation and proteasome dysfunction after brain ischemia. *Stroke* 38: 3230-3236.
 528. Stefani M, Dobson CM (2003) Protein aggregation and aggregate toxicity: new insights into protein folding, misfolding diseases and biological evolution. *Journal of molecular medicine (Berlin, Germany)* 81: 678-699.
 529. Wong E, Cuervo AM (2010) Integration of clearance mechanisms: the proteasome and autophagy. *Cold Spring Harb Perspect Biol* 2: a006734.
 530. Glickman MH, Ciechanover A (2002) The ubiquitin-proteasome proteolytic pathway: destruction for the sake of construction. *Physiological reviews* 82: 373-428.
 531. Jaffrey SR, Snyder SH (2001) The biotin switch method for the detection of S-nitrosylated proteins. *Sci STKE* 2001: pl1.
 532. Mannick JB, Schonhoff CM (2008) Measurement of protein S-nitrosylation during cell signaling. *Methods Enzymol* 440: 231-242.
 533. Forrester MT, Foster MW, Benhar M, Stamler JS (2009) Detection of protein S-nitrosylation with the biotin-switch technique. *Free Radic Biol Med* 46: 119-126.
 534. Jaffrey SR, Erdjument-Bromage H, Ferris CD, Tempst P, Snyder SH (2001) Protein S-nitrosylation: a physiological signal for neuronal nitric oxide. *Nat Cell Biol* 3: 193-197.
 535. Forrester MT, Foster MW, Stamler JS (2007) Assessment and application of the biotin switch technique for examining protein S-nitrosylation under conditions of pharmacologically induced oxidative stress. *J Biol Chem* 282: 13977-13983.
 536. Huang B, Chen C (2006) An ascorbate-dependent artifact that interferes with the interpretation of the biotin switch assay. *Free Radic Biol Med* 41: 562-567.
 537. Gladwin MT, Wang X, Hogg N (2006) Methodological vexation about thiol oxidation versus S-nitrosation -- a commentary on "An ascorbate-dependent artifact that interferes with the interpretation of the biotin-switch assay". *Free Radic Biol Med* 41: 557-561.
 538. Hara MR, Agrawal N, Kim SF, Cascio MB, Fujimuro M, et al. (2005) S-nitrosylated GAPDH initiates apoptotic cell death by nuclear translocation following Siah1 binding. *Nat Cell Biol* 7: 665-674.
 539. Kerner J, Lee K, Hoppel CL (2011) Post-translational modifications of mitochondrial outer membrane proteins. *Free Radic Res* 45: 16-28.
 540. Wang H, Xian M (2011) Chemical methods to detect S-nitrosation. *Curr Opin Chem Biol* 15: 32-37.

